Microbiological, Geochemical and Hydrologic Processes Controlling Uranium Mobility: An Integrated Field Scale Subsurface Research Challenge Site at Rifle, Colorado

February 2011 to January 2012

Annual Report to the
U.S. Department of Energy
Office of Science, Subsurface Biogeochemistry Research Program

P.E. Long, Principal Investigator and Director

February 2012
Prepared for the U.S. Department of Energy

By

Lawrence Berkeley National Laboratory
Berkeley, California

Acknowledgment

This work was supported by the Director, Office of Science, Office of Biological and Environmental Research, Environmental Remediation Sciences Program, under Contract No. DE-AC02-05CH11231 between Lawrence Berkeley National Laboratory and the U.S. Department of Energy.

Microbiological, Geochemical and Hydrologic Processes Controlling Uranium Mobility: An Integrated Field-Scale Subsurface Research Challenge Site at Rifle, Colorado
Annual Report: February 2011 – January 2012

Principal Investigator:
Philip E. Long, Lawrence Berkeley National Laboratory (LBNL)

Co-Principal Investigators (FY 2011 Funding):
Jill Banfield, University of California Berkeley ($250,000) – perform genomic analysis of column and field-derived samples and oversee interactions and exchange of data and samples with all labs, especially the PNNL and ORNL proteomics facilities.

Darrell P. Chandler, Akonni Biosystems (no new funding provided in FY-2011) – develop, manufacture, apply, and distribute 16S, mRNA, and protein microarrays to assess the *in situ* metabolic status of the subsurface microbial community.

James A. Davis, LBNL ($~250,000, funding provided both through the U.S. Geological Survey and LBNL) - quantify U(VI) geochemistry under bioreduced conditions including the development of models, perform batch and column uranium experiments, and measure U(VI) sorption and desorption in the field.

Bob Hettich and Nathan VerBerkmoes, ORNL ($131,000) - conduct proteome measurements including high resolution MS and MS/MS measurements to characterize complex protein mixtures with a focus on microbial communities and associated bioinformatics for data mining / dissemination.

Peter R. Jaffe, Princeton University ($176,000) – supervise the design and implementation of the biogeochemical column experiments including *ex situ* and *in situ* columns for assessing post-biostimulation microbial community and uranium dynamics.

Lee J. Kerkhof, Rutgers University ($131,473 of FY-2010 funding was largely expended in FY-2011) - oversee the molecular techniques for activity measurements including stable isotope probing experiments with ^{13}C, DNA extractions, amplifications, TRFLP characterization of target genes, and data analysis. FY-2010 funds were not provided to Rutgers University until early in FY-2011.

Ravi K. Kukkadapu, PNNL ($100,000) - apply various spectroscopic techniques, particularly Fe-specific ^{57}Fe Mössbauer spectroscopy, to understand the role of bioavailable Fe-phase(s) on uranium bioremediation.

Mary Lipton, PNNL ($255,760) – perform proteomic characterization of environmental microbial systems including the high throughput proteomics pipeline and informatics support.

Aaron Peacock, Microbial Insights (no new funding provided in FY-2011) - develop sampling methods and molecular tools for the quantitative analysis of complex microbial communities in contaminated soils, sediments and groundwater. Note: Dr. Peacock is now employed in national security research. He will continue to devote a fraction of his time to the Rifle IFRC, particularly on the La Quinta Experiments.

Kenneth H. Williams, LBNL ($450,000, partially supported James A. Davis after he moved to LBNL from the U.S. Geological Survey) - coordinate all research done at LBNL and participate in laboratory- and field-scale geophysical data collection, analysis and interpretation. He also assists in project coordination and data dissemination to the research team.

Steven B. Yabusaki, PNNL ($186,000) - perform coupled multifluid flow and multicomponent biogeochemical reactive transport in laboratory and field settings to develop a predictive understanding of uranium mobility under bioreduced conditions.

(Note: Funding for FY 2011 was $3.0 M plus ~$0.56 M of carryover from FY 2010. FY 2011 funds not provided to Co-Principal Investigators were provided to DOE-Grand Junction for site operations and drilling or used for site characterization/project management. Approximately $25K was used for drilling specifically to support the SLAC SFA's need for naturally reduced sediment from Rifle.)

Key Collaborators:
Derek Lovley, University of Massachusetts; SBR project title: *In silico*-reactive transport model coupling. Dr. Lovley leads the metagenomic analysis effort and the analysis and interpretation of gene expression during *in situ* biostimulation experiments. Dr. Lovley also collaborates on metagenomic and gene expression analysis of samples from Rifle IFRC experiments.

Susan Hubbard (Lead), LBNL SFA, Focus on effect of mineral precipitation on hydrologic and geochemical properties during and after biostimulation and on modeling of naturally reduced zones.

John Bargar (Lead) SLAC SFA, Field-based approach for estimating remobilization rates for biogenic U(IV) under *in situ* conditions. Use of *in situ* columns for assessing redox status of U during field experiments.

Robert Smith, PI for SBR project on "Microbially Facilitated Calcite Precipitation for Immobilization of Strontium-90 and Other Trace Metals in the Subsurface." Fieldwork for this project is now conducted at the Rifle IFRC.

Kirk Hatfield, PI, University of Florida, "U flux estimation using passive flux meters."

Other collaborators:

Tim Scheibe, SCIDAC Project, *Geobacter* behavior in individual pores as part of the *In silico*-reactive transport model coupling.

John Zachara, Jim Fredrickson, PNNL SFA and the Hanford 300 Area IFRC, Collaborations for 2011 focused on a comparison of the Rifle and 300 Area sites. Product is a paper submitted in late January 2012 on the comparison.

Linda Figueroa and James Ranville, Colorado School of Mines, Organic carbon and colloid chemistry. Dr. Ranville also is a co-PI on the uranium cycling project (see below).

Brent Peyton, PI for SBR project on "Mobility of Source Zone Heavy Metals and Radionuclides: The Mixed Roles of Fermentative Activity on Fate and Transport of U and Cr" (Montana State University). Brent Peyton and Brandy Stewart are collaborating with Peter Nico (LBNL) to examine near-surface bioreduction of U in seeps adjacent to the Rifle IFRC.

Jill Banfield, Department of Earth and Planetary Science, University of California, Berkeley (PI); Luis Comolli, Life Science Divison, LBNL, Steven Singer, Physical and Life Sciences Directorate, LBNL, are (Co-PI's); SBR project title: "3D reconstruction of biological organization and mineralization in sediment attached biofilms during uranium bioremediation." Birgit Luef, LBNL, participated in specialized field sampling for microscopy as part of both the Super 8 and Best Western Experiments. This project has also provided cryoEM for other Rifle IFRC related experiments including Janet Leavitt/Steve Cabaniss (redox status uranium sorbed to cells) and Roberto Orellana/Janet Leavitt/Derek Lovley (redox status of uranium in contact with *Geobacter* with and without pilin genes).

Andreas Kemna, Adrián Flores Orozco, University of Bonn, Bonn, Germany. Collaboration on complex resistivity imaging to infer biogeochemical processes.

Brad Tebo, Oregon Health and Sciences University, Portland, Oregon; SBR Project title: Potential for oxidation of U(VI) by Mn oxides and cycling of Mn and other cations during water table rise and fall at the Rifle IFRC.

Phillipe Van Cappellen, (Georgia Tech, Atlanta, GA, now at University of Waterloo) SBR project title: "Mineral Solubility and Free Energy Controls on Microbial Reaction Kinetics: Application to Contaminant Transport in the Subsurface" will use Rifle-relevant microorganisms for laboratory studies of microbial reaction kinetics, data that will significantly aid reactive transport modeling.

Yi Lu, (UIUC) Assessing groundwater samples from the Rifle IFRC with a range of U concentrations to test a catalytic DNA hand-held uranium analysis device.

*Clara Chan, University of Delaware. SBR Project title: "The Effects of Fe- and S-oxidizing Microorganisms on Post-biostimulation Permeability Reduction and Oxidative Processes at the Rifle IFRC Site"

*Michael Hochella, Virginia Tech. SBR Project Title: "Biotic controls on uranium sequestration and release by framboidal pyrite in bioreduced sediments"

*Kristina Keating, Rutgers University. SBR Project title: "Integrated geophysical measurements for bioremediation monitoring: combining spectral induced polarization, nuclear magnetic resonance and magnetic methods"

*Derek Lovley, University of Massachusetts. SBR Project title: "Microbe-Electrode Interactions in the Subsurface: Estimating Rates of Anaerobic Respiration, Real-Time Monitoring of Electron Donor Availability, and a Novel In Situ Uranium Bioremediation Strategy"

*Craig Lundstrom, and Tom Johnson, University of Illinois, Urbana-Champaign. SBR Project title: "Development of U isotope fractionation as an indicator of U(VI) reduction in uranium plumes" This project is working closely with the LBNL SFA (Susan Hubbard and Mark Conrad) to share data and to perform uranium isotopic analyses in a way to maximize the amount of information obtained.

*Brian Mailloux, Barnard College. SBR Project title: "Uranium Cycling in Conjunction with Other Redox Sensitive Elements"

*Barbara Methé- JCVI, Mary Lipton- PNNL, Krishna Mahadevan- University of Toronto. Genomic Science and Technology for Energy and the Environment project title: "The Study of Microbial Environmental Processes Related to the Natural Attenuation of Uranium at the Rifle Site using Systems-level Biology"

*David Walsh, Vista Clara, Inc. SBR Project title: "Low Cost *In-Situ* NMR Technologies for Monitoring Biological and Geochemical Processes in the Subsurface" (National Laboratory Collaborator, Ken Williams, LBNL for a Small Business Innovation Research (SBIR) Phase I project).

Light source spectroscopy/tomography:
Activities that use national synchrotron light sources for determining a range of chemical and physical properties of Rifle IFRC sediments continue. Current activities are as follows:

SSRL-Bargar (U concentration and redox status and a field-based approach for estimating remobilization rates for biogenic U(IV) under *in situ* conditions among other experiments. Activities are described below under *"SLAC-SFA Collaborative experiments"*). The Rifle IFRC has also fostered SSRL use by Janet Leavitt/Steve Cabaniss (redox status uranium sorbed to cells) and Roberto Orellana/Janet Leavitt/Derek Lovley (redox status of uranium in contact with *Geobacter* with and without pilin genes).

APS-Kemner (Kukkadapu, Qafoku, Pearce et al., sulfide U concentration and U redox status)

Advanced Light Source-Nico (Hubbard, et al., grain tomography/surface chemistry, colloid issue)

The Rifle IFRC coordinates these activities to help ensure optimal use of light sources by Rifle IFRC co-PI's and collaborators.

* Denotes new collaborating projects initiated in FY-2011.

Contents

Figures

Tables

Project Status: A Five-Year Perspective

Research at the Integrated Field-Scale Subsurface Research Challenge Site (IFRC) at Rifle, Colorado continues to address knowledge gaps in (a) geochemical and microbial controls on stimulated U(VI) bioreduction, (b) U(VI) sorption under reducing conditions, (c) post-biostimulation U(VI) stability and removal, and (d) rates of natural U(VI) bioreduction. The overall goal of the project is to develop a mechanistic understanding of the hydrologic, microbiological and geochemical processes controlling uranium mobility; targeting new knowledge that can be translated into scientifically defensible flow and reactive transport process models. Work at the Rifle IFRC focuses on field and laboratory experiments combining uranium sorption-desorption with biostimulation via acetate amendment. Field experiments utilize novel proteogenomics, stable isotope probing, chip arrays, uranium isotopes, and biogeophysical monitoring techniques to link microbial metabolic status and biogeochemical processes controlling uranium reduction during *in situ* electron donor amendment at the field scale. During 2011, the project focused a portion of its research effort on assessing the metabolic potential of the alluvial aquifer at Rifle. This effort will enhance understanding of both the mechanisms controlling the persistence of the U plume and organic carbon cycling across the floodplain at Rifle.

As we enter the 6th year of the project, we have completed 8 field experiments and an increasing number of column and batch experiments. Figure 1 shows the completed and planned field experiments through 2012 (planning for field research at Rifle beyond 2012 is currently in progress—see page 4). During 2011 we completed a biostimulation/desorption experiment ("Best Western") that successfully compared desorption of U(VI) solely from an abiotic bicarbonate amendment with desorption stemming from bicarbonate increases of microbial origin occurring during acetate amendment. The experimental results matched our expectations well based on prior experiments, and we anticipate that the results will significantly improve our understanding of biotic versus abiotic processes impacting our models of uranium behavior during biostimulation of alluvial aquifers. The "Best Western" field experiment also enabled us to acquire temporally dense, microbial size-differentiated, proteogenomic data at a single location under conditions of a second biostimulation with acetate. In addition, we were able to quantify speciation-dependent arsenic release accompanying prolonged sulfate reducing conditions and the concomitant microbial response.

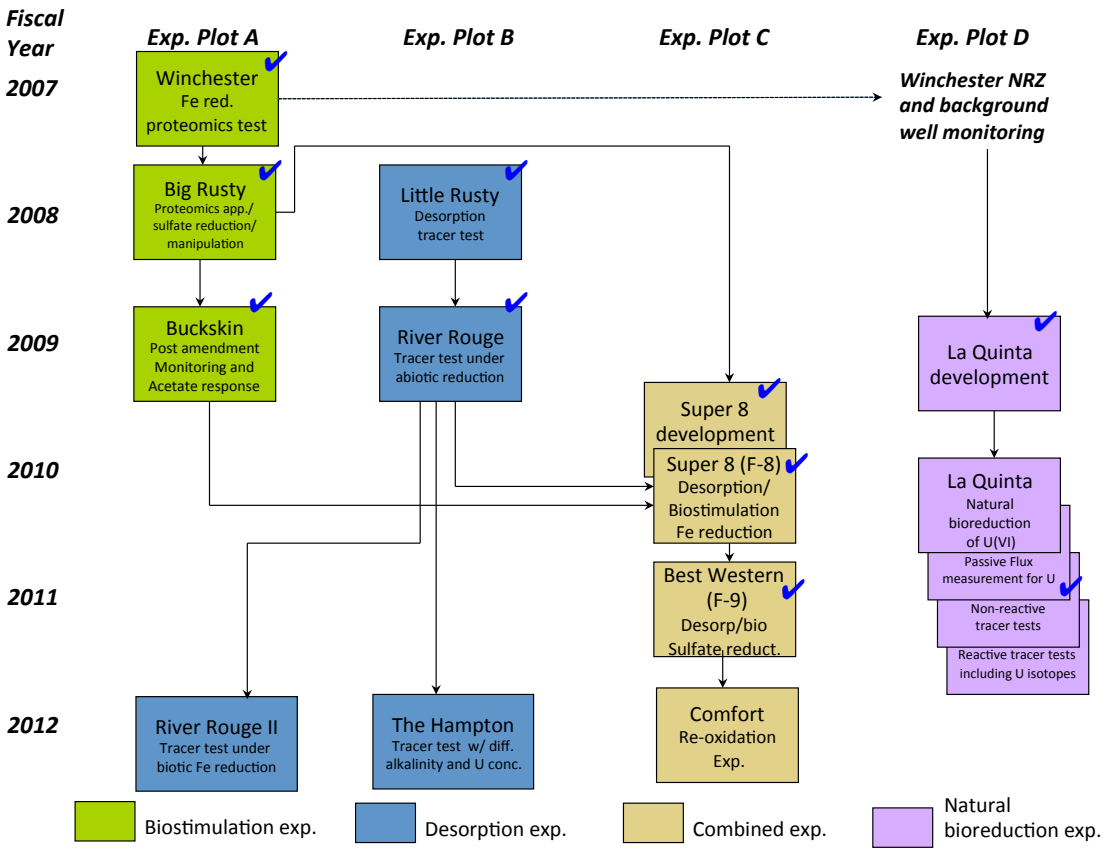

Figure 1. Current schedule and plan for field experiments at the Rifle IFRC. Checked experiments or activities have been completed.

Previous field-scale electron donor amendment experiments at the Rifle IFRC have demonstrated that uranium concentrations can be decreased in groundwater to levels below the U.S. Environmental Protection Agency's maximum contaminant level (MCL) for drinking water (0.126 μM). During three successive summer experiments - Winchester (2007), Big Rusty (2008), and Buckskin (2009) - acetate was added to the aquifer to stimulate the activity of dissimilatory metal reducing bacteria capable of reductively immobilizing uranium. The three experiments were conducted within the same flow cell; however, they differed in the length of injection (31, 110, and 36 days), the maximum concentration of acetate injected (5-30 mM *in situ* concentration), and the extent to which iron reduction (Winchester) or sulfate reduction (Big Rusty and Buckskin) was the predominant metabolic process. In all cases, rapid removal of U(VI) from groundwater occurred at calcium concentrations (~5 mM) and carbonate alkalinities (~8 meq/L) where Ca-UO_2-CO_3 ternary complexes were the predominant uranyl species, suggesting that such complexes do not impede the U(VI) removal process over the timescales studied here. By increasing acetate concentrations in excess of available sulfate (~10 mM), low U(VI) concentrations (50-100 nM) were achieved for extended periods of time (>140 days). Where acetate delivery was restricted due to upgradient consumption or changes in hydrological flow properties, U(VI) concentrations rebounded in a manner remarkably consistent between experiments. In portions of the aquifer where high acetate loadings were sustained, however, U(VI) concentrations remained at levels significantly below upgradient (i.e. background) values. Such prolonged U(VI) removal in the absence of

acetate injection is consistent with previous observations at the Rifle site and likely related to a combination of biotic and abiotic (e.g. sorption or reductive immobilization by mineral surfaces, such as FeS, FeS_2, F_3O_4, etc.) processes. Post-biostimulation monitoring has also been completed to assess the relative importance of these processes by use of novel *in situ* sediment columns.

In collaboration with Lawrence Berkeley National Laboratory's Sustainable Systems Science Focus Area (SFA; Susan Hubbard, PI), reactive transport modeling and the use of various stable isotopes to interpret biostimulation experiments for the Rifle IFRC has progressed well over the past three years. Model processes continue to incorporate new information from both microbiological and biogeochemical datasets. We successfully completed a 3-D model of experimental plot A, which produced improved matches with biogeochemical analytical results. The full range of Rifle IFRC field experiments, including Super 8 and Best Western, experiments will serve as "ground truth" for the predictive modeling capabilities developed in this project and by other reactive transport modelers around the world.

The SLAC SFA (John Bargar, PI) continues to work closely with the Rifle IFRC team to conduct experiments to directly measure *in situ* dissolution rates for biogenic uraninite and to deploy *in situ* columns that enable us to conduct light source spectroscopic measurements on Rifle sediments by enhancing the uranium concentration in the columns with no release of uranium to the environment. Both types of experiments are significantly improving our understanding of solid-phase geochemistry during biostimulation without the cost of drilling to obtain subsurface sediments. Various configurations of *in situ* columns have worked well in a variety of applications and are now widely used in Rifle IFRC field experiments.

The Rifle IFRC also continues to attract new collaborators and to work successfully with existing collaborators. New collaborating SBR Projects initiated in FY-2011 include a diverse list of research topics, all well integrated with Rifle IFRC goals and objectives (see pages *iv* and *v*). These projects are largely lead by university researchers and significantly leverage and supplement the research directly funded by the Rifle IFRC. Research topics range from geophysics, to biogeochemistry to new sensors, to metagenomics, each focused on a particular aspect of the subsurface of Rifle about which we need a deeper understanding.

The Rifle IFRC is now poised to complete analysis of prior field experiments, and conduct selected field experiments with focused objectives relating to U reoxidation and sorption behavior in 2012. At the same time, we will continue our assessment of both the metabolic potential and the U plume persistence across the site. Looking forward, we will also transition the Rifle IFRC to focus on the role that organic carbon plays in driving biogeochemical cycles and microbial community function within the naturally heterogeneous Rifle floodplain. Uranium plume dynamics will provide one metric for assessing our understanding. Although the subsurface science community has focused heavily on investigating biogeochemical reactions, the significance of degradation of organic carbon and its potential impact on plume behavior or microbial community functioning has only recently emerged. This research effort will be developed in close coordination with the LBNL SFA and will continue to leverage on and extend metagenomic investments at the Rifle Site, including our JGI community sequencing project and the Barbara Methé et al. Genomic Science project, both focused on systems-level biological processes impacting natural attenuation. To our knowledge, this would be the first coordinated attempt to quantify the metabolic potential of an entire ecosystem, which requires an understanding of the underlying genetic, biochemical, and physiological basis of microbial activity in the context of floodplain-wide fluxes and biogeochemical processes that occur within the heterogeneous subsurface. With the infrastructure and molecular to flood-plain scale research emphasis at the Rifle Site, we envision that the Rifle IFRC will continue to serve as a resource for US and international scientists interested in subsurface biogeochemistry and environmental molecular microbiology, including organic and inorganic carbon cycling and flux to the atmosphere and the Colorado River.

Major Accomplishments: Last 12 months

Summary

The Rifle IFRC continued to make excellent progress during the last 12 months. As noted above, a key field experiment (Best Western) was performed during 2011 as a logical follow-on to the Super 8 field experiment preformed in 2010. In the Super 8 experiment, we successfully combined desorption and bioreduction and deployed a number of novel tracer techniques to enhance our ability to interpret the biogeochemistry of the experiment. In the Best Western experiment, we used the same experimental plot (Plot C) as was used for Super 8. The overarching objective of the Best Western field experiment was to compared the impacts of abiotic vs. biotic increases in alkalinity and to assess the mass of the sorbed pool of U(VI) at Rifle at the field scale. Both of these objectives were met. Preliminary analysis of the data indicate that the underlying biogeochemical data sets were obtained that will support a mechanistic understanding of the underlying processes, including remarkable insight into previously unrecognized microbial processes taking place during acetate amendment of the subsurface for a second time.

We also made exceptional progress in the analysis of metagenomic data from earlier biostimulation experiments. Broadly, these experiments were designed to explore the response of microbial communities to changes in the resources around them. Intensive DNA sequencing applied to sediment and groundwater samples from these experiments has revealed that the subsurface hosts a remarkable diversity of organisms, many from lineages either known only from rRNA sequencing or completely unknown. Motivated by these and related findings, we secured from JGI terabase-scale sequencing to be applied to a series of background aquifer sediment samples. This study has been initiated, and will make it possible to predict capacities unique to specific organisms of interest, and to design, test, and validate these predictions via tailored *in situ* amendments to the Rifle aquifer. This will enable development of knowledge-based strategies for environmental manipulation and further our understanding of microbial pathways associated with carbon, nitrogen and nutrient cycling.

Another area of important scientific progress is the use of coupled reactive transport and *in silico* microbial models to predict protein expression in the subsurface during biostimulation and to directly compare that prediction to field observations. This work builds on the research of Lovley et al (2009). In these simulations, the assessment of the *in silico* model for *Geobacter metallireducens in silico* under a range of concentrations for electron donors, terminal electron acceptors, nutrients, and biomass can be considered the first step in refining (1) the model, (2) our understanding of *Geobacter* physiology, and (3) our conceptualization of nutrient (e.g., ammonium) availability. In the future we expect to expand the simulations to include multiple *in silico* models and to establish feedback between observed and predicted proteomes.

Selected accomplishments are summarized below and described in more detail under the section entitled "Description of Results During the Last 12 months by Individual Experiments and Subtasks."

Uranium Desorption and Biostimulation Experiment II (Best Western)

The "Best Western" field experiment, was aimed at understanding metabolic pathways under conditions of a second stimulation by electron donor amendment and the impact of prolonged bicarbonate injection on metal oxyanion (U, As, V, Se, Mo) mobility. The overarching objectives of the "Best Western" field experiment were threefold: (1) acquisition of temporally dense, size-dependent proteogenomic data at a single location under conditions of a second stimulation; (2) replication and extension of the "Little Rusty" [2008] and "Super 8" [2010] uranium (U) desorption experiments but designed to enable direct comparison of desorption associated with acetate amendment (and associated reductive U immobilization) with desorption associated soley with abiotic bicarbonate amendment; (3) quantification

of speciation-dependent arsenic release accompanying prolonged sulfate reducing conditions and the concomitant microbial response.

Early breakthrough of acetate corresponded to an initial increase in Fe(II) concentrations related to the onset of microbial iron reduction and stimulation of metal reducing bacteria, such as members of the *Geobacteraceae*, as observed during previous experiments at the site. Additionally, elevated Fe(II) concentration may partially result from the onset of microbial sulfate reduction and the abiotic reduction of Fe(III) minerals by aqueous sulfide. As observed repeatedly at the site, removal of sulfate from groundwater tied to the activity of sulfate reducing bacteria is non-stoichiometric with respect to the amount of aqueous sulfide produced. This results from the multiple sinks for aqueous sulfide within the aquifer, including precipitation of metal sulfides (e.g. FeS) and reduction of ferric oxide minerals, yielding Fe(II), elemental sulfur, and (perhaps) polysulfide and thiosulfate. For the first time, concentrations of thiosulfate were quantified during acetate amendment at Rifle, with production patterns mimicking those of aqueous sulfide, albeit at lower absolute concentration.

Dissolved gas measurements were made during and after the amendment period in four wells (CU01, CD01, CD04, and CD18). Acetate levels fell below detection at CD04 by 28-November-2011; groundwater CH_4 concentrations persisted at levels ranging from 10-100μM, falling from a maximum value of ca. 150μM on 23-November-2011. The presence of CH_4 in groundwater indicates the onset of methanogenesis during "Best Western" and the inferred presence of Archaeal biomarkers in the proteogenomic samples.

The length of sodium bicarbonate injection during "Best Western" exceeded all previous such injections at Rifle, enabling refinement of multi-rate mass transfer models describing uranium (U) desorption from diffusion-limited domains, such as those associated with fine-grained sediments. Additionally, bicarbonate injection during "Best Western" was not associated with spatially overlapping acetate injection, as occurred during the "Super 8" experiment. Rather, the bicarbonate-induced desorption of U and other metal oxyanions was allowed to proceed to its maximum extent over the course of 92 days. As observed during "Super 8," the most labile fraction of U desorbed rapidly, with U concentrations increasing by two- to four-fold within 7-10 days of bicarbonate reaching a given well location. Uranium desorption continued over the 92-day injection period at progressively lower rates. These results provide direct input to models for U desorption as a remedial strategy.

During the "Best Western" experiment, a follow-up series of samples were recovered from well CD-01, the same well from which "Super 8" biomass samples had been collected. To date, DNA has been extracted from all filters and we intend to submit 10 time points (2 from 2010 and 8 from 2011) for community sequencing. This sequencing will include all filters (1.2, 0.2, and 0.1 μm) for each time point in order to minimize size bias and capture the overall diversity of the planktonic biomass. Metagenomic reconstructions will underpin both community proteomic and transcriptomic efforts planned for Spring 2012. Initial results clearly show the relationship between microbe size and preponderance of species present in the planktonic phase, at least during a second stimulation such as "Best Western." This is the first time such size-fractionated observations have been made. Proteogenomics studies planned for 2012 will enable us to clearly establish community and metabolic changes that occurred as the "Best Western" experiment proceeded with broad implications for manipulation of the subsurface metabolic potential of alluvial aquifers.

Proteogenomic results from Big Rusty and Buckskin Experiments

Over the past year, intensive DNA sequencing applied to sediment and groundwater samples from prior field experiments has revealed that the subsurface hosts an almost unimaginable diversity of organisms, many from lineages either known only from rRNA sequencing or completely unknown. For example, in

a single pilot study of a series of three groundwater samples from "Big Rusty" (Arthur, Cristobal, and Dolly, ACD), we have recovered 49 near-complete genomes from five enigmatic phyla (Bacterial Candidate Divisions (CD)); two of the five phyla appear to be more diverse than the *Proteobacterial* phylum. Remarkably, metabolic analysis of the CD genomes indicates the predominance of obligate fermentation-based metabolism. One lineage has novel hydrogenases normally affiliated with Archaea, two others encode a novel Archaeal-like RuBisCO type previously unknown in Bacteria, and all encode genes such as glycoside hydrolases involved in carbon compound breakdown. In addition, dozens of genomes of Bacteria from known and divergent lineages with capacities for aerobic and anaerobic respiration were recovered, a finding that highlights the range of metabolic potential resident in the aquifer. These results, described in more detail below, will now be integrated into the overall biogeochemical status of the aquifer during biostimulation and the total data set used to formulate a fundamental predictive capability for the effect of perturbations on an alluvial aquifer. These results will be particularly import in predicting changes in U concentration in response to climate change, facilitating accurate long-term forecasting of natural attenuation of contaminants.

Uranium Redox Status and Bonding During Biostimulation

In-well sediment column experiments were initiated by collaborator John Bargar (SLAC) and collaborators in the SLAC SFA in July 2009 in conjunction with the "Buckskin" acetate-stimulated bioremediation experiment.

During 2011, Rifle IFRC key collaborator John Bargar (SLAC) and collaborators in the SLAC Science focus area performed XAS, XRM and SEM measurements on sediments harvested in the fall of 2010 from in-well sediment columns incorporated into the "Super 8" experiment. These results have led to two significant discoveries. First, XRM and SEM-EDS measurements reveal major difference in the sediment geochemistry depending on the specific conditions of *in situ* columns. Sediments exposed only to Fe reducing conditions do not exhibit grain coatings, and uranium cannot be detected in XRM and SEM-EDS measurements of these samples. These observations suggest that the U(IV) accumulated in the iron-reduced sediments is spread out among the sediment grains. In contrast, columns in which U amendment was initiated after the onset of sulfate-reducing conditions exhibit sulfide-rich grain coatings also enriched in U similar to those observed in the 2009 experiment. FeS is present as Fe:S stoichiometric ratios of 1:1. As observed in our earlier studies, U generally is not correlated with Fe or S on the scale of a few microns within the coatings. The second major observation is somewhat surprising; U L_{II}-edge EXAFS are similar in all sediments regardless of biogeochemical regime, and specifically are consistent with U(IV) bound to biomass. These observations suggest that U(IV) bioreduction mechanisms are ***dominant and similar*** under all conditions observed. Further analyses are in progress, including metagenomic analyses of these same sediments by the Banfield group. This will enable the linkage of specific U distribution, solid-phase biogeochemical products, and groundwater biogeochemistry with microbial populations and their metabolic processes.

Floodplain-wide assessment of plume stability

During 2010 a subtask was initiated in response to the observed persistence of the uranium groundwater plume and the need for a scientific assessment of the sources of uranium in groundwater at the Rifle IFRC. Underlying this subtask are four hypotheses to explain the persistence of the U(VI) plume:

A. Downward flux of U from the vadose zone that is entrained into the aquifer during times of high water table associated with high runoff in the Colorado River
B. Mobilization of reduced U from naturally bioreduced zones
C. Slow oxidation of U(IV) dispersed through the saturated zone
D. Influx of natural background U(VI) from upgradient groundwater recharge

During 2011, we made significant progress in constraining Hypothesis A. In the spring of 2011, the runoff in the Colorado River was the greater than it had been in nearly 30 years, creating an unusual opportunity to observe the impact of rising water table to U concentrations in the aquifer. To assess the role of the vadose zone as a possible U source, we collected both pumped and bailed samples from twelve wells across the Rifle floodplain. Bailed samples were collected at the top of the water table in each well. Pumped samples were collected in the normal fashion from a tube at mid-aquifer depth, using slow purge after the bailed samples were collected. Only two of the twelve wells exhibit greater U concentration in bailed samples than in pumped samples and those differences are relatively minor. All other wells either are nearly the same for bailed versus pumped samples or the pumped samples have higher U concentrations. Hence, even under conditions of extended water table rise, U concentrations do not increase in the upper parts of the aquifer. This contrasts with observations at the Hanford Site (300 Area IFRC) where a rising water table results in marked U concentration increases in bailed samples at least for some wells. We take this as strong evidence that the vadoze zone is not a dominant source of U that is capable of sustaining the U plume across the Rifle flood plain.

Reactive Transport Modeling

Key progress on numerical simulations made in 2011 was the integration of the Sun et al. (2009) *Geobacter metallireducens in silico* model into the eSTOMP coupled process subsurface simulator. The *in silico* model mechanistically represents 697 intracellular and 51 environmental exchange reactions. The system of reactions is driven by external fluxes of acetate, Fe(III), and ammonium uptake from the eSTOMP reactive transport routines. The flux balance approach assumes that intracellular reactions rapidly equilibrate to extracellular changes. This allows the system of physico-chemically constrained reaction fluxes to be solved using a linear programming approach (CPLEX) optimized for maximum biomass growth. Calculated mass fluxes (e.g., Fe(II), biomass, bicarbonate, H+, NH4+) are scaled by dry weight equivalent (gdw) of biomass, which then become source terms in eSTOMP. The incorporation of the unabridged *in silico* model specification into a large-scale subsurface flow and reactive transport simulator is unprecedented and requires supercomputing resources to address the modeled complexity. Computational effort in eSTOMP has increased 10 fold with the inclusion of the *in silico* model. This particular application to the 2008 "Big Rusty" field experiment was run with 1024 cores on the massively parallel Chinook computer housed and operated at The Environmental Molecular Sciences Laboratory (EMSL).

As of this point in time, 180 of the 637 *G. metallireducens* genes detected in planktonic biomass samples from the 2008 "Big Rusty" field experiment have been associated with *in silico* model reactions. The number of predicted *in silico* model reactions in specific COG (clusters of orthologous groups) categories can now be compared with the number of proteins detected in those same categories. While there are COGs with proteomic activity that are not represented by *in silico* model predicted reactions, the model does appear to match the field proteomics for the metabolic pathways related to respiration (i.e., central metabolism) particularly well.

The assessment of the *Geobacter metallireducens in silico* model under a range of concentrations for electron donors, terminal electron acceptors, nutrients, and biomass can be considered the first step in refining (1) the model, (2) our understanding of *Geobacter* physiology, and (3) our conceptualization of nutrient (e.g., ammonium) availability. We will now focus on simulation of the 2010 and 2011 biostimulation experiments where the analysis of more planktonic biomass samples over longer time periods for a wider range of conditions will provide new knowledge and a rigorous test of the *in silico* models. *In silico* models are under development for other important microorganisms (e.g., *Desulfobacterales*) and we anticipate future simulations that will include multiple interacting *in silico* models requiring even higher levels of computational performance. Increasing availability of metagenomic data from the Rifle site will allow a wider range of important organisms to be considered

with varying degrees of proteomically annotated physiology. Since it is probable that many of these organisms may not be available for experimentation in pure culture, alternatives to fully specified genome-scale *in silico* models need to be explored. Ultimately, the field proteome, metagenome, and biogeochemistry will provide a basis for refining mechanistic genome-specific metabolic models beyond the initial foundation of pure culture microcosm/chemostat experiments.

Field Infrastructure and Health & Safety

Field experimental results cannot be obtained without the site infrastructure including the site trailer, real-time measurement of tank volumes, injection well heads, and key geochemical parameters as well as new experimental plots installed to enable current and future experiments. During 2011, we enhanced Experimental Plot C with two new wells for the "Best Western" experiment. In addition to the existing mix of well types and geophysical monitoring electrodes, the two new wells added to our ability to geophysically interrogate the injection zone.

The field trailer continues to be vital for performing on-site geochemical and microbiologic sampling and analyses, notably sampling for proteomics and assembly of *in situ* column and related experiments. We improved the trailer interior during 2011, providing additional bench and storage space to support, for example, dissolved gas measurements. Figure 2 is a high-resolution aerial photo taken in August 2009 showing the location of most of the wells on the site (red and blue dots) and the site configuration including the location of the Experimental Plot C, the site of the "Best Western" experiment. We also added new monitoring wells at selected locations on the floodplain (not shown). Construction of these wells was partially supported by DOE-Legacy Management, indicating their strong interest in science outcomes from the Rifle IFRC.

Ken Williams, LBNL, continues to perform the role of Field Site Manager in addition to his roles as Co-PI and Associate Director of the Rifle IFRC, reporting to work at the site along with a field assistant. This arrangement is now crucial to the success of the Rifle IFRC, ensuring that health and safety requirements are met and that all operations at the site are conducted efficiently and effectively.

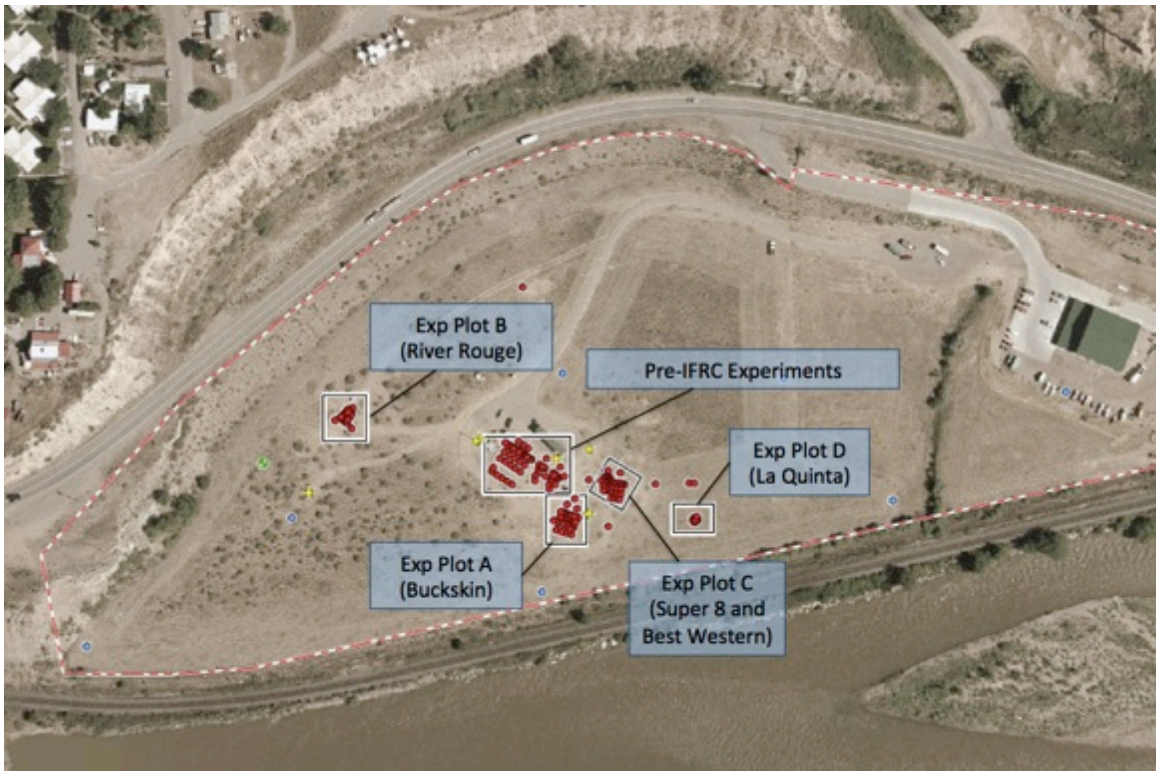

Figure 2. Rifle IFRC map showing locations of Rifle IFRC field experiments through 2011. The large green roofed building on the right is the City of Rifle Maintenance Facility.

On October 1, 2011 we began a transition of the management of the Rifle IFRC to Lawrence Berkeley National Laboratory (LBNL). This transition was completed in early January 2012 after a complete review and re-issue of the documents governing the operation of the site, including the health and safety plan. The principal advantage of managing the Rifle IFRC from LBNL is closer integration with the LBNL Sustainable System Science Focus Area. In addition, we have been able to increase operational effectiveness by utilizing the LBNL system of buildings and sites and by requiring that scientists working at the site enroll as LBNL Affiliates. This enables us to track both chemical management and personnel training within the LBNL management system, enhancing environmental and safety performance.

Description of Results During the Last 12 months by Individual Experiments and Subtasks

Subtasks that were actively pursued during the last 12 months are described in each of the sections below.

Subtask Big Rusty (F-5, F-7)

Primarily designed to replicate and expand the proteogenomic studies initiated during Winchester (2007) (including a period of low acetate), the "Big Rusty" field experiment involved a significantly longer period of acetate injection (110 days) designed to study the impact of extensive and prolonged sulfate reduction

The major results from the "Big Rusty" experiment were described in the 2008 and 2009 annual reports and continue to be published in various peer-reviewed journals (see publications section at the end of this report). Interpretation of the metagenomic and proteomic data from the Big Rusty experiment made excellent scientific progress in 2011 and is expected to result in a high-impact journal publication in 2012.

Proteogenomics of Big Rusty Samples

Microbial community samples (A, C and D) were collected 5, 7, and 10 days after the start of addition of acetate to the Rifle, Colorado aquifer in August, 2008 as part of the "Big Rusty" experiment (Wrighton et al., in prep.). From each groundwater sample, we recovered microbial cells that passed through the 1.2 μm filter to be retained on the 0.2 μm filter. Consequently, our analyses target smaller cells, not the entire planktonic consortia (see section on "Super 8" microbiology results). The sample was preserved on site for DNA extraction and for mass-spectrometry-based protein identification to verify the activity of organisms *in situ*.

Illumina sequence datasets from DNA extracted from each sample (A, C, and D) were assembled individually using Abyss, then co-assembled using an iterative application of the Velvet software. 16S rRNA gene reconstruction from Illumina reads was performed using EMIRGE (Miller et al. 2010) and confirmed by 16S rRNA clone library analysis. Both 16S rRNA gene sequence and phylogenetically informative gene analyses indicated that the communities were Bacterial (there was no indication of Archaea or Eukarya).

Our analyses focused primarily on the co-assembled ACD dataset because it provided better coverage of the many organisms present in more than one sample. Genome fragments > 5 kb were binned (assigned to an organism), primarily using their tetranucleotide sequence composition analyzed using emergent self-organizing map-based analysis (ESOM). Because the relative abundances of many organisms changed over the time series, we used the ratio of sampling in D vs. A to assist in defining bins. In total, 87 genome clusters were identified (Figure 3). Organism identity was assigned to genome bins based on phylogenetic analysis and by linking the 16S rRNA sequences to genome fragments. In total we extensively sampled 79 bacterial and 8 phage/plasmid genomes.

Our first analyses efforts focused on the genomes from the Candidate Division bacteria, as these organisms are only known based on single gene (16S rRNA) sequences. Here, we report partial and near-complete genomes for twenty one members of Candidate Division (CD) OD1, nineteen of OP11, six alternatively coded genomes, five of which are affiliated with BD1-5, and three that represent a new lineage (Table 1). These CD bacteria have a cell wall containing peptidoglycan, but lack membrane characteristics of Gram-negative Bacteria. All are obligate fermenters, and one OD1 group has novel archaeal-type hydrogenases that may reduce elemental sulfur (Figure 4). Proteomic results validate CD

bacteria are active and using a fermentative lifestyle, with cryptic growth by these organisms responsible for resource turnover decoupled from acetate amendment and external terminal electron acceptors in the aquifer.

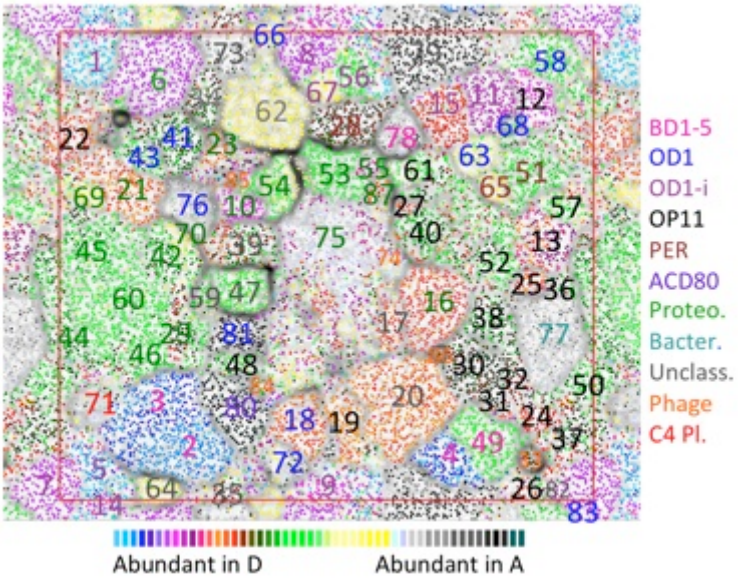

Figure 3. Binning of metagenomic data. Emergent self-organizing map for all contigs > 5 kb, build using tetranucleotide frequency information. Superimposed color indicates the relative abundance of the genome fragment in the D vs. A samples (see SOM). Fragments of 2 – 5 kb in length were binned by superimposing their tetranucleotide composition onto the map built using 5 kb fragments.

Table 1. Summary indicating the number of genomes recovered from five novel lineages. Estimated genes/genome is based on the number of genes per genome bin, corrected based on a completeness value.

	Number genomes	% Complete	Bins with >1 genome	Genomes > 90%	Genomes > 50%	Estimated genes/genome	GC content (average)
OD1	21	75 ± 24 %	0	10	18	1353 ± 350	0.38 ± 0.04
OP11	19	67 ± 26 %	5	3	15	1364 ± 252	0.39 ± 0.05
BD1-5	5	93 ± 3%	0	5	5	1540 ± 222	0.34 ± 0.07
PER	3	80 ± 17%	0	2	3	1666 ± 221	0.39 ± 0.05
ACD80	1	95	0	1	1	1301	0.33

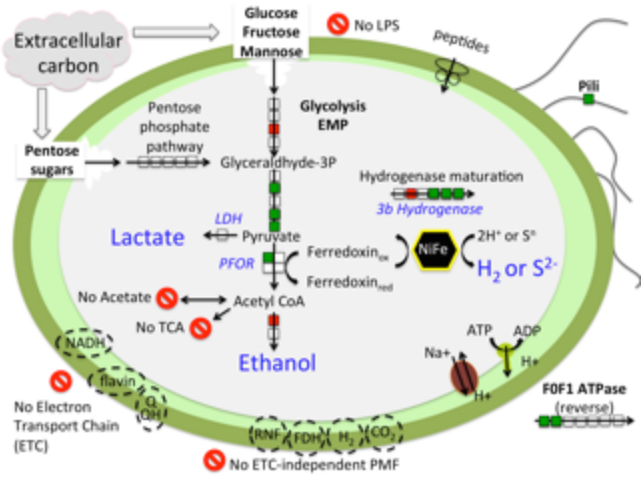

Figure 4. Genome-centered modeling recapitulated pathways for organic carbon flow in the Candidate Division (CD) Bacterium, OD1_i. Boxes denote genes in a pathway: white boxes are genes detected in OD1_i genomes, green boxes are peptides detected from OD1_i *in situ* community proteomics, while red boxes denote genes which could not be identified in genomic data. Proteomics confirmed the enzymes for the degradation of complex carbon (not acetate) leading to hydrogen production and ATP generation were expressed from CD bacteria during iron reduction in 2008.

Our continued research efforts are dedicated to understanding the network of both biological and abiotic interactions occurring in the aquifer. To this effect we are also characterizing the non-CD organisms, which were mainly affiliated with the *Proteobacteria*, though members of the *Bacteriodetes*, *Spirochaetes*, and *Chloroflexi.* Metabolic capabilities among the non-CD bacteria were highly varied. CD-produced fermentation products (hydrogen, acetate, ethanol) could fuel respiratory organisms including iron (*Geobacter*) and sulfate reducing bacteria (*Desulfotalea*-like). Proteomics confirmed the co-occurrence of dissimilatory sulfate reduction with the activity of iron reducing bacteria, suggesting biogenic sulfide may contribute to the abiotic reduction of iron in the aquifer. Functionally redundant pathways for aerobic and nitrate-reducing metabolisms were also confirmed by proteomics (Figure 5). Other metabolic capacities include the degradation of chlorinated and complex hydrocarbons. Together our results from both CD and non-CD bacteria demonstrate the utility of short-read sequencing for detailed genome-centric metabolic profiling of diverse subsurface assemblages. Results have significant implications for cycling of organic carbon in aquifers under both biostimulated and background conditions.

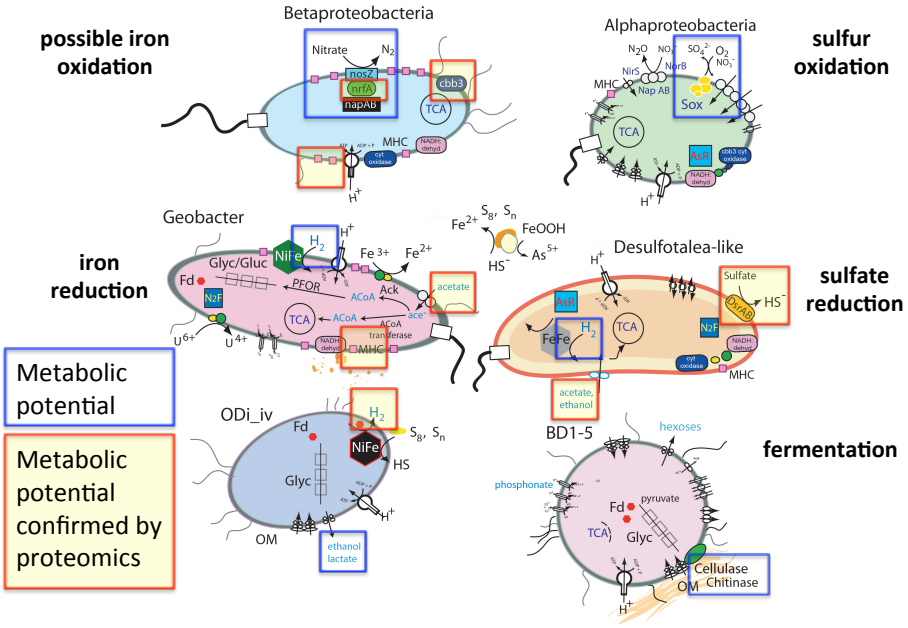

Figure 5. Genomic and proteomic reconstruction reveal trophic cascade occurs during secondary stimulation. At the primary level, complex organic matter is fermented to yield acetate, ethanol, and hydrogen. Fermentative end products can fuel the respiratory activities of heterotrophic iron, sulfate and nitrate reducing bacteria. Proteomics confirmed the presence of nrfA, dsrAB, and multi-heme cytochromes during all iron reducing time points suggesting these metabolisms may co-occur during secondary stimulation. In addition the reduced metabolic products from respiratory organisms might also serve as electron donors for sulfur and iron oxidizing organisms. Blue boxes are confirmed metabolic genes identified by metagenomic analyses, while red boxes filled with yellow are metagenomic properties that were confirmed by in situ proteomics.

We also performed deeper proteome measurements of Arthur, Crisotobal, and Dolly (ACD). These three samples have significant importance to the proteogenomic research effort, as they represent the first combined deep metagenome and metaproteome sample set. The goal was to enhance the proteome dataset by matching to the most relevant genome datasets and thereby provide deep coverage of not only *Geobacter* proteins but also low abundance microbial components of the community. The nearly complete genomes discussed above can be directly verified at the protein level by the proteomics group if deep enough peptide and spectral coverage can be obtained on these low abundance microbes. In the previous year, ORNL used a 2D-LC-MS/MS approach with an LTQ-Orbitrap mass spectrometer to analyze all 28 groundwater samples from 4 different collection wells spanning time from iron reduction to sulfate reduction from the 2008 gallery. During 2011, next generation Orbitrap instruments have become available and installed at ORNL. In particular, the new hybrid LTQ-Orbitrap Velos Mass Spectrometer provides noticeably enhanced qualitative and quantitative performance. The dual-trap hardware provides an increased speed of mass measurement, which equates to increased spectra collection and thus increased peptide and protein assignments (~2-3x increase for complex proteomes). However, while the increased ion transmission provides increased sensitivity, it was found to be less reproducible and robust compared to the original LTQ-Orbitrap. Due to the great potential of these instruments for the Rifle project, we have focused our research effort on improving robust performance by a unique ion switching

technique so that we feel we can now maintain peak performance across larger datasets. To test the ability of the next generation instruments to provide deeper and wider proteome coverage of Rifle groundwater communities, we re-analyzed ACD, since these samples are the focus of deep metagenomic sequencing. We processed the samples as before, and used the same genomic database for analyses. The results are listed in Table 2.

Table 2. Proteomic results from re-analysis of ACD

Database: JCVI_Scaff_metagenome_geo7					
Sample Name	**Instrument Type**	**Proteins**	**Peptides**	**Spectra**	**Trypsin Spectra**
Arthur	LTQ Orbi	2600	7594	20408	203
Cristobal	LTQ Orbi	2805	8465	16604	177
Dolly	LTQ Orbi	N/A	N/A	N/A	N/A
Arthur	Velos Orbi	4092	12381	29287	122
Cristobal	Velos Orbi	4008	10769	31487	202
Dolly	Velos Orbi	5933	17165	31472	231

These results clearly show the increased depth of the Velos measurements, as nearly twice as many proteins and spectra were identified relative to the LTQ runs. To enhance the coverage of the lower abundance members, we are currently re-processing these samples via an enhanced digestion method designed for small biomass samples, and will measure these samples on the newest version of these Velos instruments, which is the Velos Orbitrap Elite.

We are also re-analyzing the proteome datasets with different combinations of metagenomic data and *Geobacter* isolate datasets, to help provide the genomic group with direct feedback on the quality of the metagenomic databases. This iterative analysis of metagenome and metaproteome data is a powerful way to help guide and optimize the creation of the metagenomic databases. Currently we have searched the ACD metaproteomes with 6 different builds of metagenomic/isolate databases. All the data is provided in a timely manner and is posted on an accessible website for the entire Rifle group.
https://compbio.ornl.gov/mspipeline/ersp_rifle/Groundwater_2008_Velos/status.html

Subtask River Rouge (F-6; Tracer test under reducing conditions without biostimulation)

The River Rouge field experiment was performed in Experimental Plot B from August 29 to September 27, 2009. The goals of this experiment were to (1) determine the effect of Fe(II) on U(VI) sorption, (2) determine the level of Fe(II) sorption to sediments *in situ*, and (3) investigate the possibility of abiotic reduction of U(VI) by Fe(II). In order to achieve these goals, a series of injections of ~45μM $FeSO_4$ were performed in a single row of multi-level sampling (MLS) wells. This was followed by injection of a pulse of groundwater containing deuterium as a conservative tracer in 3 multi-level sampling wells upgradient of the Fe-reducing zone to allow us to track geochemical changes in groundwater, particularly dissolved U(VI), as it passed through the Fe-reducing zone. In order to understand the results of the River Rouge Experiment we continued laboratory experiments on selected Rifle IFRC sediments during 2011, focusing on *Fe(II) Uptake by Rifle Sediment and Abiotic U(VI) Reduction.* Here we report updated results from those experiments.

Background. Previous studies indicate that when Fe(II) is added to aqueous suspensions of Fe(III) oxide phases, the Fe(II) is oxidized at the mineral surface to Fe(III). It is commonly thought that the electron is transferred to the interior of the mineral. This phenomenon has been shown to occur on a wide variety of

Fe(III) phases, including ferrihydrite, magnetite (non-stoichiometric), goethite, hematite, and lepidocrocite [*Gorski and Scherer*, 2009; *Pedersen et al.*, 2005; *Williams and Scherer*, 2004]. Fe(II) oxidation on a Fe-free clay mineral (synthetic montmorillonite) has also been demonstrated – in this case the authors hypothesized that H^+ was the electron acceptor, producing H_2 that is closely associated with the mineral surface along with the oxidized Fe(III) [*Gehin et al.*, 2007]. In many cases, concomitant with the uptake and oxidation of Fe(II) by Fe(III)-minerals, recrystallization of the mineral occurs (i.e. ferrihydrite converted to goethite, lepidocrocite, or magnetite) [*Boland et al.*, 2011; *Hansel et al.*, 2005; *Jones et al.*, 2009; *Pedersen et al.*, 2005; *Stewart et al.*, 2009; *Yee et al.*, 2006]. Due to its position on the redox ladder, one would expect Fe(II) to be oxidized by Mn-oxides as well [*Postma*, 1985].

Thus, Fe(II) uptake by common soil and sediment minerals, particularly Fe(III) and Mn(IV)-containing minerals, cannot be expected to be described as a simple adsorption process like other non-redox active metals (e.g. Ni^{2+}, Zn^{2+}). [*Handler et al.*, 2009] described Fe(II) reaction with goethite nano-rods as a 'conveyer belt' of electrons, with adsorption and oxidation of Fe(II) on one crystal face and dissolution of Fe(III) and release of Fe(II) on another crystal face. After an initial uptake of Fe(II) by goethite over several hours, aqueous Fe(II) concentrations remained constant for 30 days; however, exchange of aqueous Fe(II) with structural Fe(III) continued as evidenced by complete isotopic equilibrium between the solution and solid phase. In their work on magnetite, Gorski and Scherer (2009) demonstrated that Fe(II) uptake by magnetite continued until the magnetite became completely stoichiometric with respect to the Fe(II)-Fe(III) ratio. [*Larese-Casanova and Scherer*, 2006] demonstrated that oxidation of Fe(II) on hematite continued until a monolayer surface coating of oxidized Fe was achieved, after which additional Fe(II) taken up by the solid remained as sorbed Fe(II).

A number of laboratory studies have demonstrated that U(VI) can be abiotically reduced by Fe-oxides and clay minerals in the presence of Fe(II) [*Behrends and Van Cappellen*, 2005; *Boland et al.*, 2011; *Chakraborty et al.*, 2010; *Jeon et al.*, 2005; *Liger et al.*, 1999], as well as by Fe(II) bearing minerals such as magnetite and green rust [*Ilton et al.*, 2006; *Ilton et al.*, 2009; *Jeon et al.*, 2005; *O'Loughlin et al.*, 2003]. In addition, [*Boyanov et al.*, 2007] demonstrated U(VI) reduction by Fe(II) adsorbed onto carboxyl-functionalized polystyrene microspheres at pH 8.4, while no reaction occurred at pH 7.5. While previous investigations have demonstrated that while thermodynamically feasible, reaction between aqueous Fe(II) and U(VI) (i.e. in homogenous solution) is not observed [*Liger et al.*, 1999], more recently [*Du et al.*, 2011] claimed that the reaction did conform to thermodynamic predictions. The relative importance of abiotic U(VI) reduction pathways compared to biologically mediated reduction in natural sediments and under field-relevant conditions has been rarely studied. Jeon et al. (2005) studied several natural solids and only found appreciable abiotic U(VI) reduction occurring on solids with extremely high Fe contents (18-35 wt % Fe).

The goals of this study are to determine the Fe(II) uptake and oxidation capacity of Rifle sediments and potential geochemical constraints on abiotic U(VI) reduction by Fe(II) added to the sediments. Bioremediation of U-contaminated aquifer sediments at the Rifle IFRC field site through injection of an electron donor (acetate) results in precipitation of U(IV) mineral phases under both Fe(III) and sulfate reducing conditions. The relative contributions of biotic (direct enzymatic reduction) and abiotic (U(VI)-Fe(II) reaction) pathways of U(VI) reduction in the Rifle aquifer are currently unknown and are important for both the modeling of biostimulation experiments and optimization of bioremediation approaches.

Fe(II) Uptake and Transformation Experiments performed at pH 8.3 in TRIZMA buffered systems resulted in 100% uptake of Fe(II) (data not shown). Fe(II) uptake increases with increasing pH, as well as with increasing Fe(II) concentration, which is consistent with previous studies on Fe(III) mineral phases (i.e. [*Dixit and Hering*, 2006; *Jeon et al.*, 2001; *Liger et al.*, 1999]). It should be noted that at pH 8.3, the samples were oversaturated with respect to $Fe(OH)_2$ above 0.55 mM. The presence of 5 mM Ca lowered Fe(II) uptake in the pH buffered systems at both pH 7.2 and 8.3. This is likely a result of competition

between Ca and Fe(II) for exchange/sorption sites on sediment minerals. In the case of the pH 7.2 samples, the addition of Ca resulted in uptake isotherms that very closely resembled the unbuffered RAGW system. The RAGW contained 5 mM Ca as well as 5 mM Mg, both of which may compete with Fe(II) for sorption sites.

Figure 6 shows the amount of Fe(II) recovered by FerAc and HCl extractions. In general, the fraction of Fe(II) recovered in the FerAc extraction increased with Fe(II) loading and was higher at pH 8.3 than at pH 7.2. 47-89% of the Fe(II) added was recovered by the sequential FerAc and HCl extractions throughout the entire range of conditions studied. At higher Fe(II) loadings (>6 μmol/g), greater than 82% was recovered.

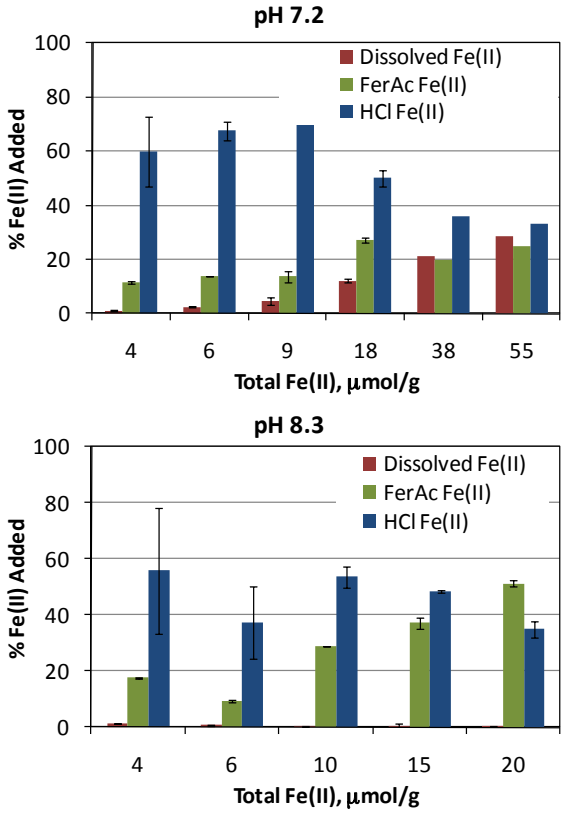

Figure 6. The percentage of Fe(II) present in the dissolved phase is and Fe(II) extracted from sediments by FerAc (2 mM ferrozine, 2 M ammonium acetate, 2 hr) and HCl (0.5 M HCl, 20 hr) extractions at pH 7.2 and 8.3. Each point shows the average and standard deviation of 2 replicate samples.

Mossbauer analysis at room temperature and 12 K was performed on a number of samples treated with ^{57}Fe(II). Figure 7 shows Mossbauer spectra from the background sediment along with fits of the data. The sediments contain a total of 2.43 weight% Fe, corresponding to approximately 9.2 μmol/g ^{57}Fe based on the natural abundance of ^{57}Fe. The Fe mineralogy is dominated by Fe-bearing clays (i.e. smectites and chlorites) which contain both Fe(II) (31-34%) and Fe(III) (21-26%), followed by Al-substituted goethite (21%), hematite (14%), magnetite (6%), and ilmenite (1-2%). This Fe mineralogy is similar to that observed in other samples from the Rifle site [*Komlos et al.*, 2008]. In addition, there is some evidence of ferrihydrite (~5%) which can be deduced by comparison of the room temperature and 12 K spectra. Mossbauer spectra of sediment reacted with 7.3 and 39 μmol/g ^{57}Fe are shown in Figure 8. The presence

of a broad sextet in the 12 K spectra of the 7.3 μmol/g ^{57}Fe sample indicates that nearly 100 % of the added ^{57}Fe(II) was oxidized to ^{57}Fe(III). However, the oxidized product does not resemble the hematite, lepidocrocite, or large particle goethite and magnetite which are present in the background sediment sample. In many studies on the reaction of Fe(II) with pure Fe oxides (goethite, magnetite), the oxidized product resembles the structure of the sorbent mineral phase [*Gorski and Scherer*, 2009; *Handler et al.*, 2009]. The fact that we did not observe this suggests that goethite and magnetite were probably not the predominant phases with which the ^{57}Fe(II) reacted. At the higher ^{57}Fe(II) loading (39 μmol/g), only 55% of the added ^{57}Fe(II) was oxidized to Fe(III). Table 3 shows a summary of the fraction of ^{57}Fe(II) oxidized at each ^{57}Fe(II) loading as analyzed by Mossbauer. At pH 8.3, slightly less ^{57}Fe(II) was oxidized (94%) compared to pH 7.2 (100%).

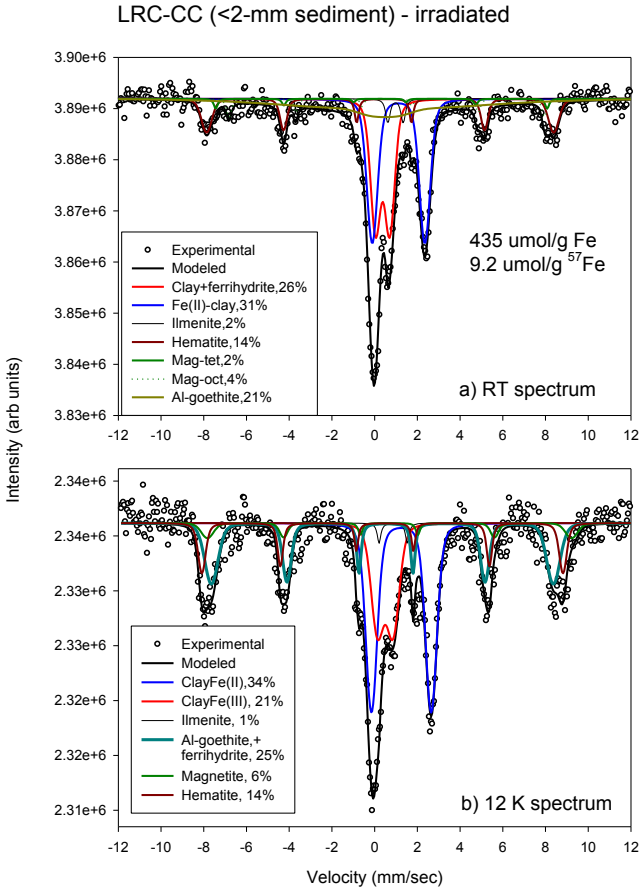

Figure 7. Mossbauer spectra and fit of background sediment at room temperature (A) and 12 K (B).

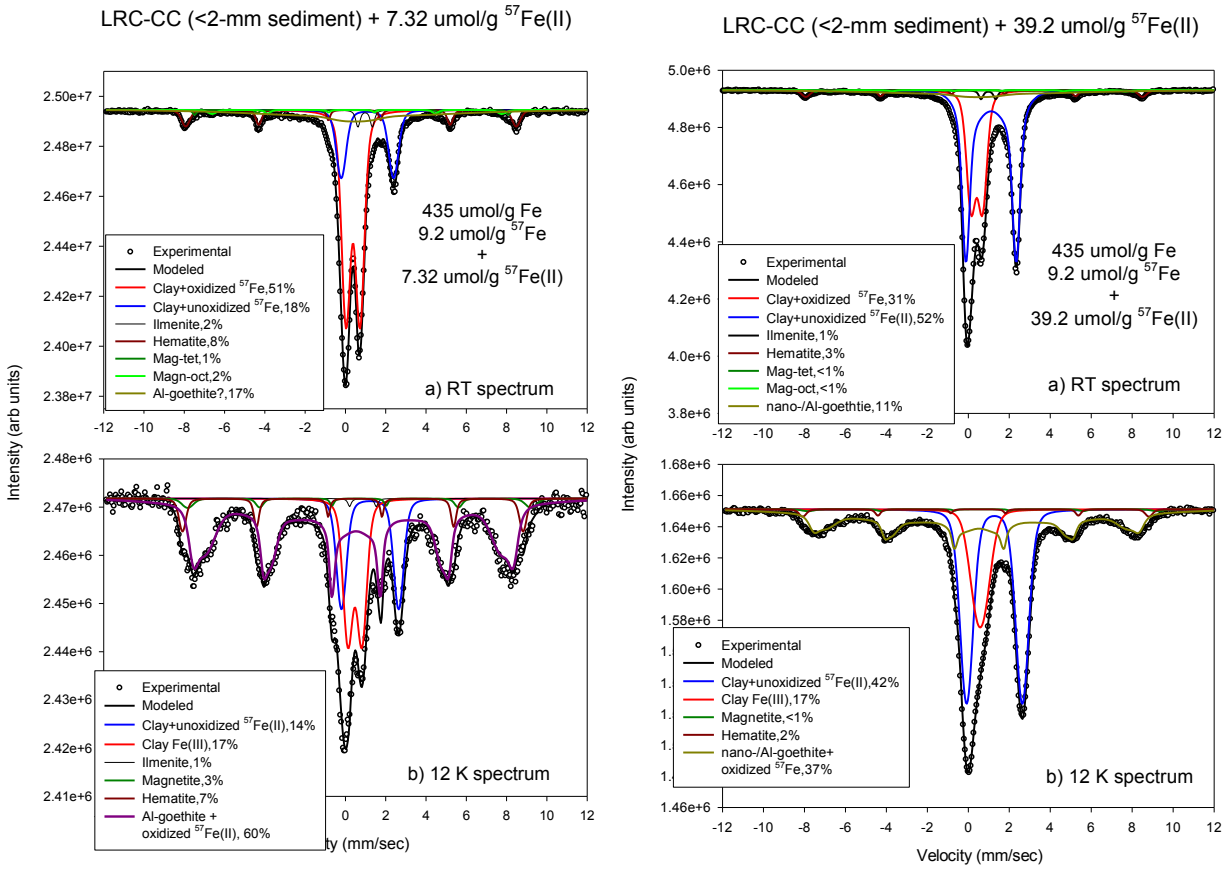

Figure 8. Mossbauer spectra and fits of ^{57}Fe(II) treated sediment at room temperature (A) and 12 K (B). Sediment containing 7.3 μmol/g ^{57}Fe(II) is shown in the left panel and sediment containing 39 μmol/g ^{57}Fe(II) is shown in the right panel. Experiments were performed at pH 7.2 and reacted for 1 week.

Table 3. Fraction of added ^{57}Fe(II) oxidized to ^{57}Fe(III) as observed by Mossbauer. Samples were reacted for 24 hr.

pH	pCO_2, %	^{57}Fe(II) loading, μmol/g	^{57}Fe(II) oxidized, %
7.2	0	7	100
7.2	0	13	89
7.2	0	39	55
8.3	0	7	94
7.2	3.5	7	100

One sample was reacted under a 3.5% CO_2 atmosphere at pH 7.2 and analyzed by Mossbauer spectrometry to determine whether siderite precipitation occurred. The siderite saturation index for this sample was 1.77. If siderite precipitation occurred and the dissolved Fe(II) concentration reached equilibrium with siderite, one would expect 98.3% of the Fe(II) to precipitate as siderite. However, no evidence of siderite precipitation was observed in the Mossbauer spectra; the spectra were similar to the samples prepared in the absence of CO_2.

Abiotic Reduction of U(VI). The effect of Fe(II) addition on U(VI) uptake onto sediment was studied in pH 7.2 and pH 8.3 buffered solutions in the presence of 400 ppm CO_2 (Figure 9 and Table 4). At pH 7.2 there was no observable effect of Fe(II) on U(VI) uptake, in part because there was 99% U(VI) uptake even in the absence of Fe(II). However, at pH 8.3 U(VI) uptake onto the sediments increased with increasing Fe(II) addition. At the highest Fe(II) concentration (5.6 mM), U(VI) uptake was equal at pH 7.2 and 8.3. At both pH values, U(VI) reduction to U(IV) was observed by XANES, with the extent of reduction increasing with increasing Fe(II) concentration (Table 4 and Figure 10). While greater levels of U(VI) reduction were observed at pH 8.3 compared to pH 7.2, it appears that this effect may be due to the greater uptake of Fe(II) onto sediments at higher pH. For example, 18% of solid phase U was present as U(IV) at pH 7.2 and 8.3 for similar Fe(II) loadings (40.7 and 37.6 μmol/g, respectively).

A greater amount of U(VI) reduction was observed in the absence of CO_2 compared to the presence of 400 ppm CO_2 (Table 4 and Figure 10). For example, at pH 8.3, we observed 54% U(IV) in the absence of CO_2 and 36% U(IV) in the presence of 400 ppm CO_2 for Fe(II) loadings of 54.8 and 56.1 μmol/g, respectively. Experiments performed in the absence of CO_2 were oversaturated with respect to U(VI) mineral phases (e.g., schoepite), while the experiments performed in the presence of 400 ppm CO_2 were undersaturated with respect to all U(VI) mineral phases.

Table 4. XANES fitting results for U(VI) and Fe(II) reacted samples. Samples were reacted for one week under sterile conditions.

pH[a]	pCO_2, atm	Total Fe(II) added, mM	Fe(II) on solid, μmol/g	U on solid, μmol/g	Fraction U(IV)	Fraction U(VI)
7.2 (7.2)	0	0	0	0.99	0.04	0.96
7.2 (NM[b])	0	0.75	7.3	0.99	0.00	1.00
7.2 (7.0)	0	5.7	17.3	0.98	0.44	0.56
8.3 (8.2)	0	0	0	0.91	0.01	0.99
8.3 (NM)	0	0.75	7.3	0.90	0.06	0.93
8.3 (7.8)	0	5.7	54.8	0.93	0.54	0.46
7.2 (7.1)	400	0	0	0.50	0.05	0.96
7.2 (7.1)	400	0.75	7.2	0.49	0.06	0.95
7.2 (7.1)	400	1.41	12.8	0.49	0.04	0.96
7.2 (7.0)	400	2.78	23.4	0.50	0.12	0.89
7.2 (7.0)	400	3.75	29.7	0.49	0.12	0.88
7.2 (6.9)	400	5.59	40.7	0.49	0.18	0.83
8.3 (8.2)	400	0	0	0.42	0.09	0.93
8.3 (8.1)	400	0.75	7.4	0.44	0.07	0.95
8.3 (8.1)	400	1.40	14.0	0.45	0.11	0.91
8.3 (8.0)	400	2.80	27.7	0.47	0.18	0.83
8.3 (8.0)	400	3.78	37.6	0.48	0.18	0.82
8.3 (7.9)	400	5.60	56.1	0.50	0.36	0.65

[a]pH values at the end of experiment are listed in parentheses
[b]NM=not measured

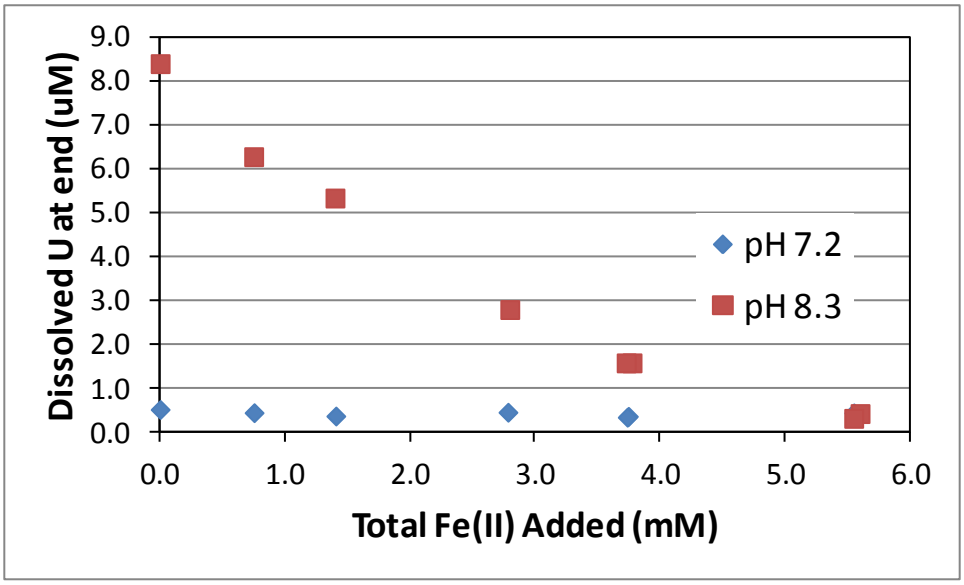

Figure 9. The effect of Fe(II) addition on U(VI) uptake onto carbonate-free LRC sediments. Experiments were performed in pH buffered solutions in the presence of 400 ppm CO_2 and an initial U(VI) concentration of 50 μM. Samples were reacted for one week under sterile conditions.

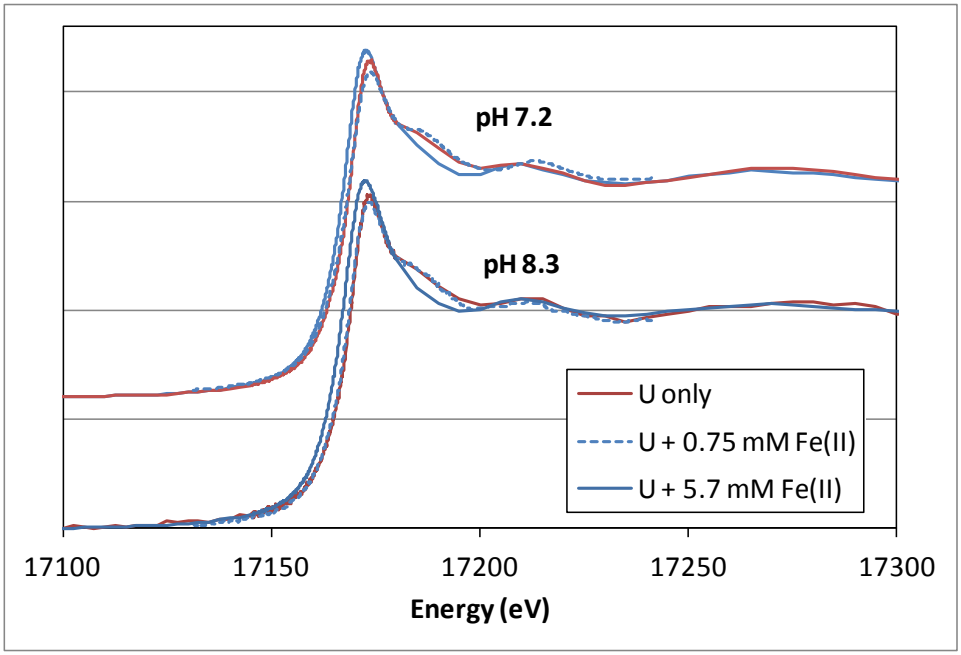

Figure 10. XANES analysis of carbonate-free LRC samples reacted with 100 μM U(VI) and Fe(II) in pH buffered solutions and in the absence of CO_2. Samples were reacted for 7 days under sterile conditions.

Subtask Buckskin (F-7A Biostimulation experiment to assess residual acetate impact and results of multi-year acetate amendment)

During three successive summer experiments, "Winchester" (2007), "Big Rusty" (2008), and "Buckskin" (2009), acetate was added to the aquifer to stimulate the activity of dissimilatory metal reducing bacteria capable of reductively immobilizing uranium. The three experiments were conducted within the same flow cell (see Experimental Plot A); however, they differed in the length of injection (31, 110, and 36 days), the maximum concentration of acetate injected (5-30 mM *in situ* concentration), and the extent to which iron reduction ("Winchester") or sulfate reduction ("Big Rusty" and "Buckskin") was the predominant metabolic process (Table 5). In all cases, rapid removal of U(VI) from groundwater occurred at calcium concentrations (5 mM) and carbonate alkalinities (8 meq/L) where $Ca\text{-}UO_2\text{-}CO_3$ ternary complexes were the predominant uranyl species. Complete consumption of acetate and increased alkalinity (>30 meq/L) occurred accompanying the onset of sulfate reduction.

Table 5. Experimental timeframe for the "Winchester" and "Big Rusty" field experiments; the groundwater flush periods are denoted by an absence of acetate and bromide.

Experiment [year]	Elapsed Time [days]	Acetate* [mM]	Bromide* [mM]
Winchester [2007][a]	0-12	50	20
	12-18	--	--
	18-31	50	20
Big Rusty [2008][b]	0-15	50	13
	15-24	--	--
	24-38	50	13
	38-110	150	13
Buckskin [2009][c]	0-36	150	13

*Concentrations represent stock tank values; an average dilution factor of 1:10 accompanied injection into the aquifer

[a]Start date 08-Aug-2007; [b]Start date 20-July-2008; [c]Start date 22-July-2009

As part of the "Buckskin" (2009) experiment, *in situ* sediment columns were deployed (*Handley et al., in prep.*). To ascertain the sediment-associated community response to acetate amendment during sulfate reduction, we incubated freshly excavated sediment within flow-through columns in well P104. Acetate-amended groundwater was pumped up through the columns for one month at a pore water velocity of approximately 1 m/day. Injection commenced July 22nd, and columns were removed August 18th. Acetate was maintained in excess of microbiological requirements (Figure 11). The onset of sulfate reduction was rapid, occurring within 4 days of the experiment start date. Under first-year stimulation conditions sulfate reduction occurs after one month of amendment.

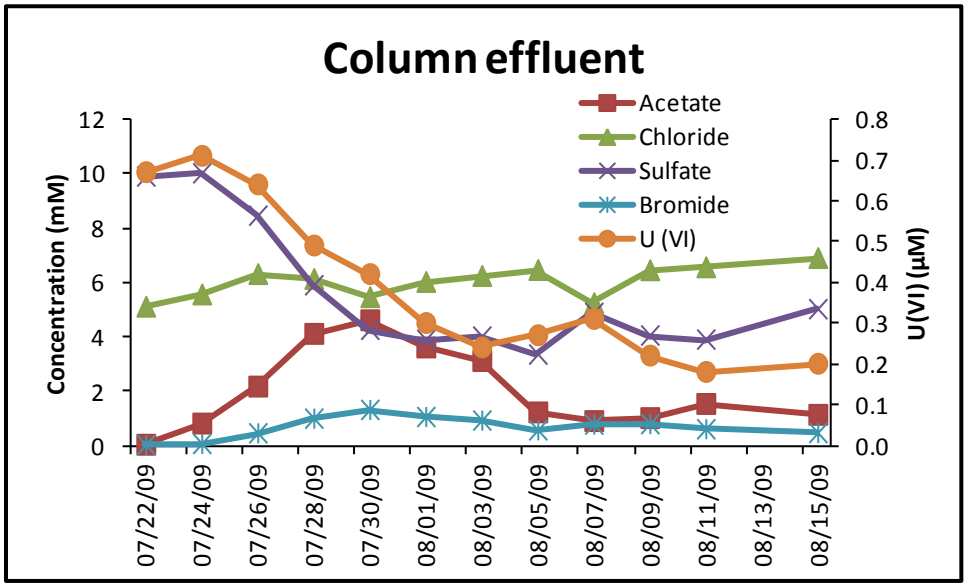

Figure 11. Geochemical data collected throughout the experiment. The column sediment represents an extension of the amended aquifer, and little difference was observed between geochemical values obtain directly from the well, and those in the column. Biological data confirm activity in the column.

Sediment was flash frozen upon collection in order to preserve the community and pool of expressed enzymes. Genomic DNA extracted from the community was first sequenced via the longer-read, higher-error 454 platform, and then also via the shorter-read, higher-accuracy Illumina platform following successful application of this technology in the reconstruction of community genomes from groundwater collected in 2008. 454 sequencing generated 4 Mb of 400 bp reads (with 1 kb mate-pairs), while Illumina sequencing generated 7 Gb of 120 bp paired-end reads. 454 reads were assembled into longer sequences (contigs) using Newbler. Illumina reads were assembled using iterative (taxa-abundance specific) Velvet followed by reference genome-guided Velvet assembly. The short Illumina reads were found to assembled as well as 454 reads, but provided fewer sequencing errors, and greater community coverage.

Using Illumina data, we were able to reconstruct near-complete genomes for relatives of *Desulfobacter* (Deltaproteobacteria), *Sulfurovum* and *Sulfurimonas* (Epsilonproteobacteria), CFB (Cytophaga-Flavobacterium-Bacteroidetes) group, and *Clostridium* (Firmicutes). Fragmentary genomic datasets were also obtained for *Desulfuromonadales*-like Deltaproteobacteria, closely related to *Geobacter* and *Desulfuromonas* species, and other bacteria. Contigs were assigned to genomic bins using multiple parameters, including tetranucleotide mapping, and the phylogenetic relationship of taxa to other known organisms was determined using reconstructed 16S rRNA sequences (Figure 12). Assessment of sequence length and core gene copy number indicates we have multiple genomes for organisms related to *Desulfobacter*, *Sulfurimonas* and the CFB group.

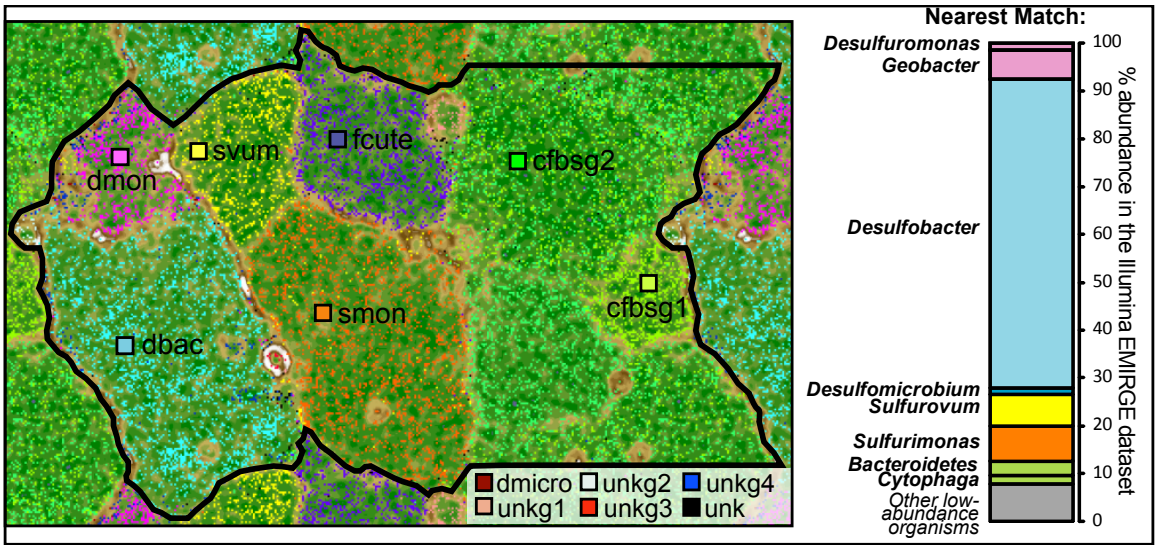

Figure 12. RHS: Emergent Self Organizing Map (ESOM) of tetranucleotide frequencies, distinguishing contigs into genomic clusters. LHS: Relative abundances of taxa, based on 16S rRNA reconstructions using the EMIRGE (Expectation Maximization Iterative Reconstruction of Genes from the Environment) method (Miller *et al*., 2011). Taxa shown by EMIRGE actually represent operation taxonomic units containing taxa with >97% 16S rRNA gene similarity.

Metagenomic data were used to identify proteomic data obtained from the same sample using LC-MS-MS. The majority of proteins identified by mass spectrometry derived from *Desulfobacter*-like species, and indicate the role of this organism in sulfate reduction (Dsr and APS), nitrogen-fixation (Nif) and acetate utilization (forward TCA cycle; Figure 13). Proteogenomic data also indicate that *Desulfuromonadales* and CFB group bacteria also contribute to carbon cycling via the TCA cycle proteins. *Desulfuromonadales* are known to do this in the forward direction, producing CO_2. Genes identified for CFB group bacteria also suggest they could generate CO_2 as a byproduct of acetate consumption, although expression of the full pathway is incomplete, either owing to their low abundance, or due to incomplete use of the TCA cycle. Interestingly, proteomic data show that sulfide was partially re-oxidized by Epsilonproteobacteria through nitrate-dependent sulfur oxidation (using Nap, Nir, Nos and Sox) and CO_2 fixed using the reverse TCA cycle.

In summary, high-levels of carbon amendment aimed to stimulate anaerobic heterotrophy led to carbon fixation in co-dependent chemoautotrophs. These results show that excess input of energy and carbon in the form of acetate activated syntrophic interactions involve organisms that use either the forward or reverse tricarboxylic acid (TCA) cycle. Results also have implications for understanding complex ecosystem behavior, and show that high levels of organic carbon supplementation can expand the range of microbial functionalities accessible for ecosystem manipulation.

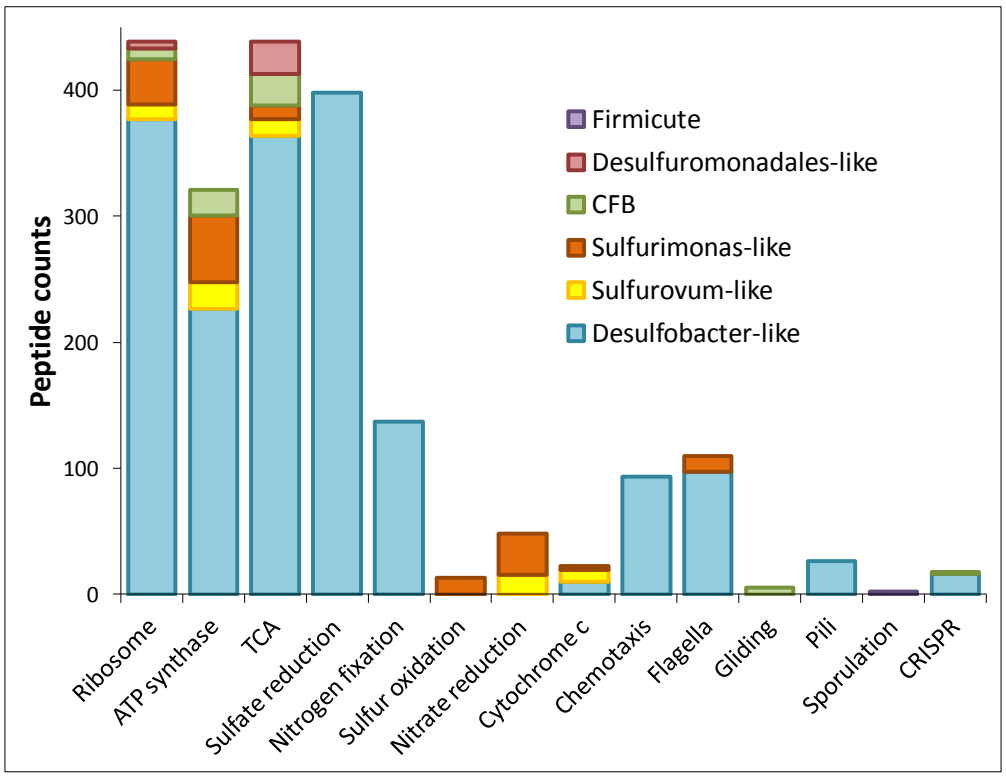

Figure 13. Peptide counts denoting expression of enzymes for some key functions**.**

Hydrologic Testing of Experimental Plot A Injection Wells. As reported in PNNL (2009, 4th quarter FY2009 report), the distribution of hydraulic conductivity at the Plot A well gallery indicated a significant reduction in permeability in the line of injection wells between the 2008 "Big Rusty" pre- and post-experiment slug-test results. The reduction in hydraulic conductivity between the pre- and post-experiment results ranged between ~1 to ~4 log cycles. More detailed information regarding this reduction in hydraulic conductivity can be found in PNNL (2009). In November 2010, slug tests were performed in a few selected Plot A injection wells to assess the long-term persistence of the zone of permeability reduction along the line of injection wells. Slug tests were conducted in wells G-51, G-53, G-56, and G-60 and the results indicate that the zone of reduced permeability continued to persist, even after ~730 days (~2 years) since the "Big Rusty" experiment ended and ~1 year after the "Buckskin experiment" (Figure 14). However, the wells that showed the greatest permeability reduction (i.e., wells G-51 and G-56) during the "Big Rusty" experiment exhibited a permeability rebound of ~1 to ~2 log cycles. The wells showing a lower permeability reduction (i.e., wells G-53 and G-60) during the "Big Rusty" experiment continued to decrease long after the experiment ended. Hydraulic conductivities at these four injection wells ranged from 0.005 to 0.081 m/day, ~2 years after the experiment ended, and show lower variability than the 2008 post-experiment results. Slug-test results for background well U-01 are shown in Figure 14 for comparison. These Experimental Plot A injection wells were slug tested in January 2012 to continue to assess the persistence of the zone of permeability reduction.

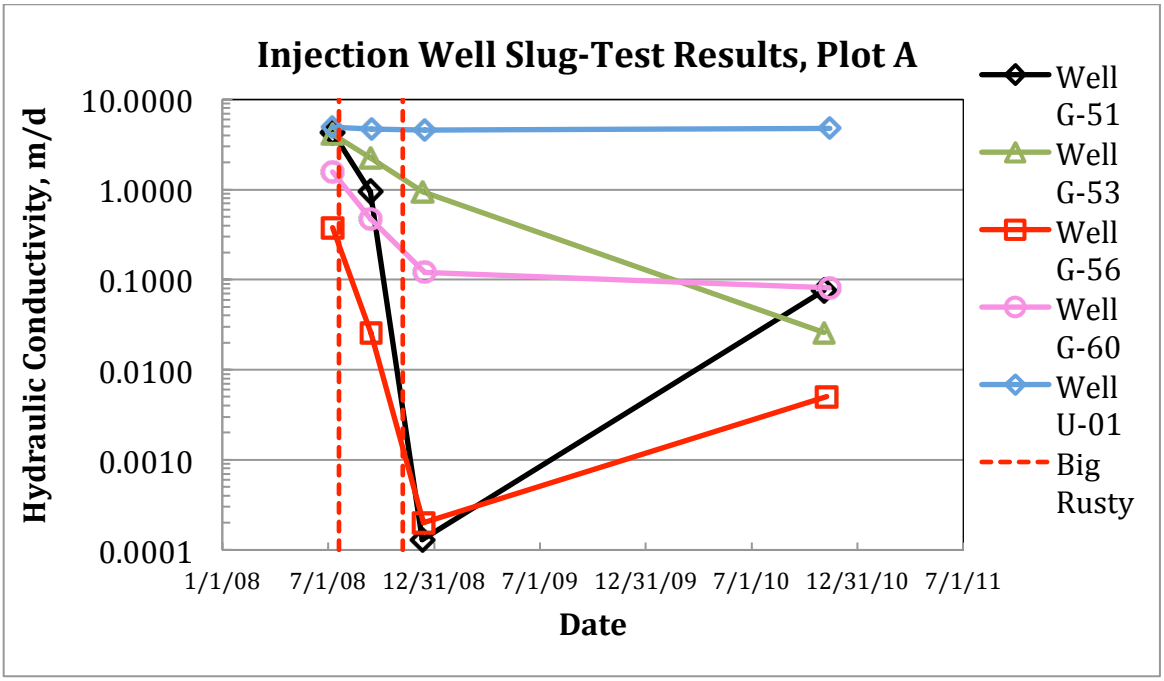

Figure 14. Hydraulic Conductivity in Selected Injection Wells from Experimental Plot A.

Column Experiments to assess well bore and formation clogging during biostimulation.
We are continuing our long-term column experiment to link changes in biomass and mineralogy due to biostimulation to changes in permeability. This experiment was reported in the September 2011 report and new results are discussed here. These results might be the first effort to show the importance of Archaea at Rifle. The experiments are being coordinated closely with Ken Williams (LBNL) and Li Li (Penn State). Li Li will be using the very detailed temporal and special data to conduct geochemical modeling during biostimulation.

We built 7 columns that allow for dissolved species sampling and pressure change measurements along their vertical axis, and the experiment has been running now for approximately 9 months. One column is equipped with electrodes to determine the induced polarization (IP) and link this to changes in permeability and to IP measurements that have been conducted at Rifle during previous biostimulation experiments. The IP method involves injection of variable frequency currents into the ground and the measurement of resulting voltage potentials via electrodes located above and below the ground surface. Variations in the phase and magnitude of the applied and measured potentials determine the frequency-dependent electrical properties of the subsurface. IP measurements are collected weekly and sent to Yuxin Wu (PNNL) for processing.
Figure 15 shows the column with the induced polarization probes, and Figure 16 shows the setup of all columns in the constant temperature incubator. The column with the IP electrodes will be the very last one sacrificed, so IP measurements can be taken throughout the duration of the experiment.

Figure 15. Column with electrodes for induced polarization measurements.

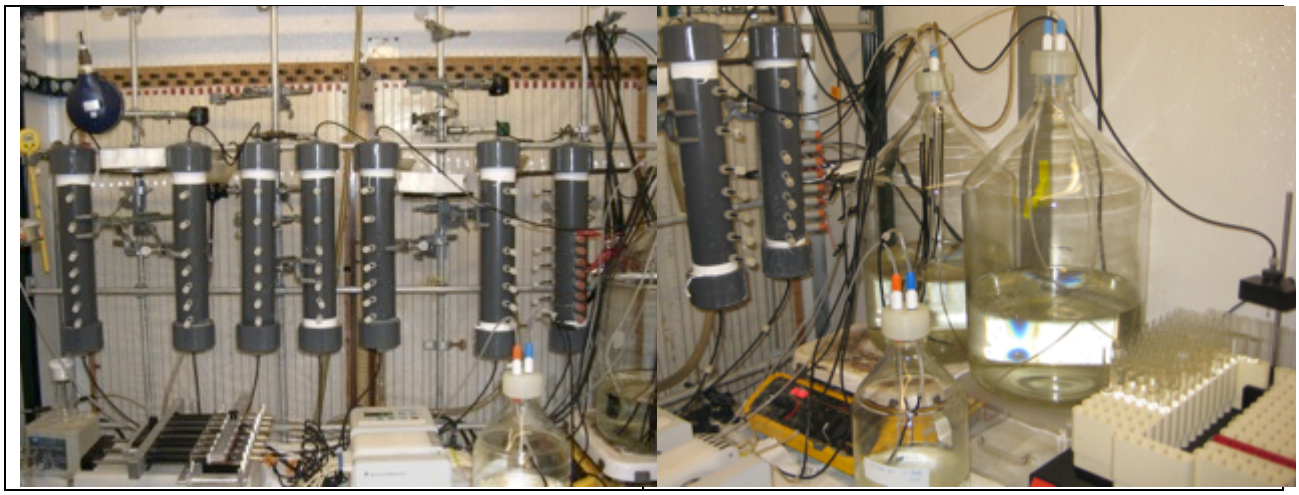

Figure 16. Left: Experimental setup for linking biostimulation to changes in permeability under Rifle conditions. Right: Fractional collection system (lower right side).

Since the first 100 days of stimulation have not shown a significant change in permeability (as indicated by changes in pressure under constant flow, Figure 17), we increased the acetate concentration from 3 mM to 12 mM, and have by now operated the columns under this higher acetate regime for an additional 150 days.

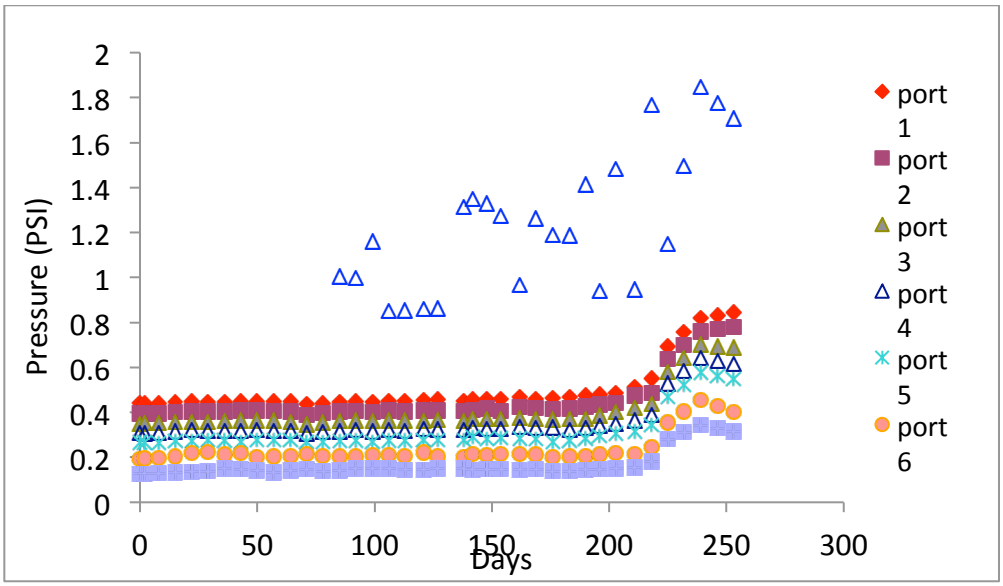

Figure 17. Pressure along the longitudinal axis of a column vs. time.

So far two columns have been sacrificed, one after 95 days of biostimulation and one after 207 days of biostimulation. Sediment samples from the first column that were sacrificed (t = 95 days) were sent to Microbial Insights for microbial characterization. Of interest is that even at this early point in time, methanogens consist of the largest biomass by at least two orders of magnitude (Figure 18). Sediments were also sent to LBNL for detailed geochemical analyses. Samples from the second column are being preserved at -80 C for future analyses. Iron analyses from the sediment of the two columns that have been sacrificed are shown in Figure 19. Consistent with our previous findings, Fe(II) levels in the sediment keep increasing even while the columns are operation under very active sulfate reduction.

Water samples along the longitudinal axis of the columns are being taken at weekly intervals and the first batch (~ 200 days) have been sent to LBNL to be analyzed for multiple ionic species and alkalinity in order to determine what chemical species are precipitating where and at what time. These analyses were started at LBNL late the week of January 16, and we should have at least partial results by the time the next report is due.

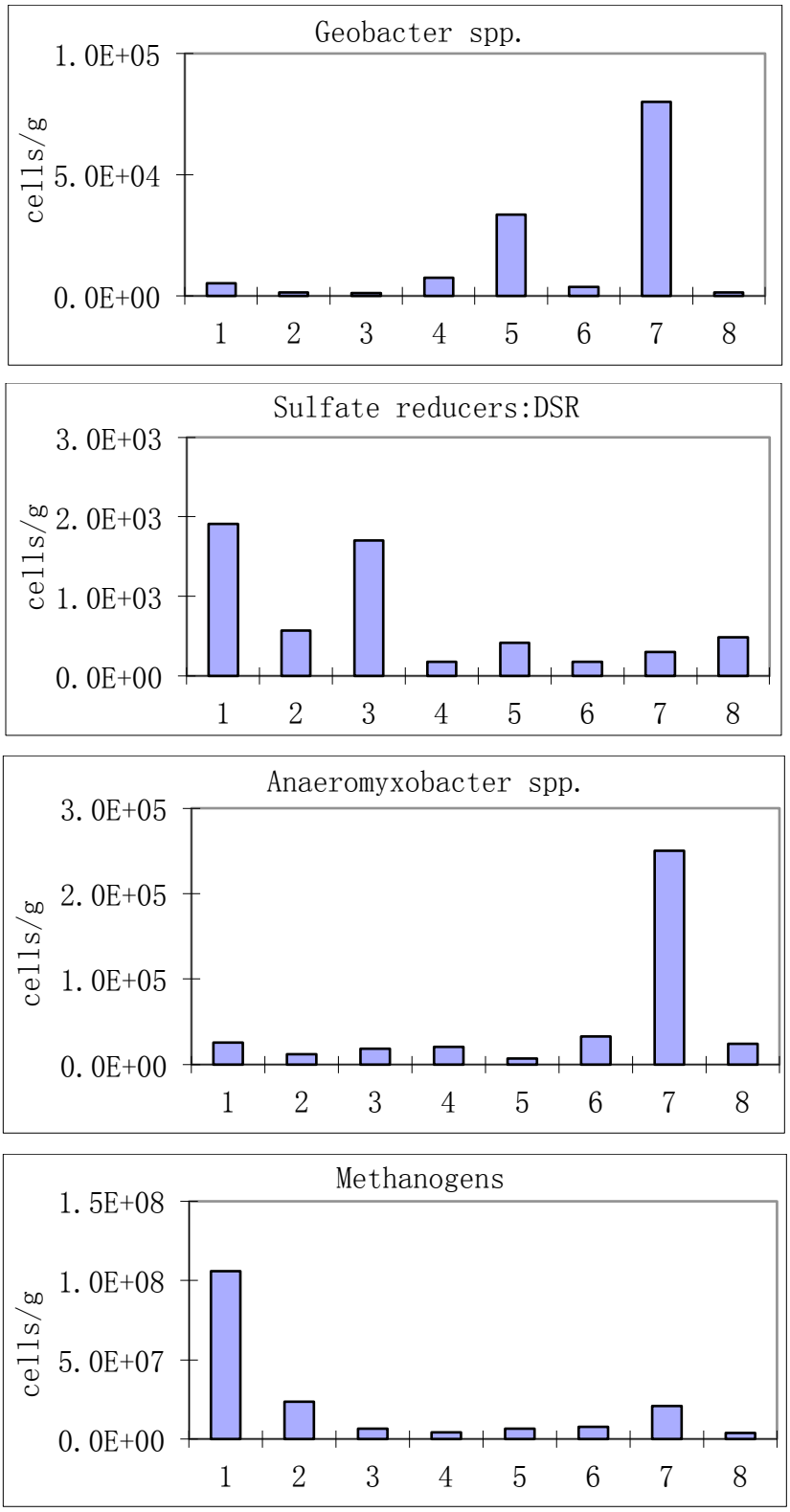

Figure 18. Bacterial numbers in column 1 after 95 days of operation. Note: Sample 1 was collected near the influent and 8 near effluent.

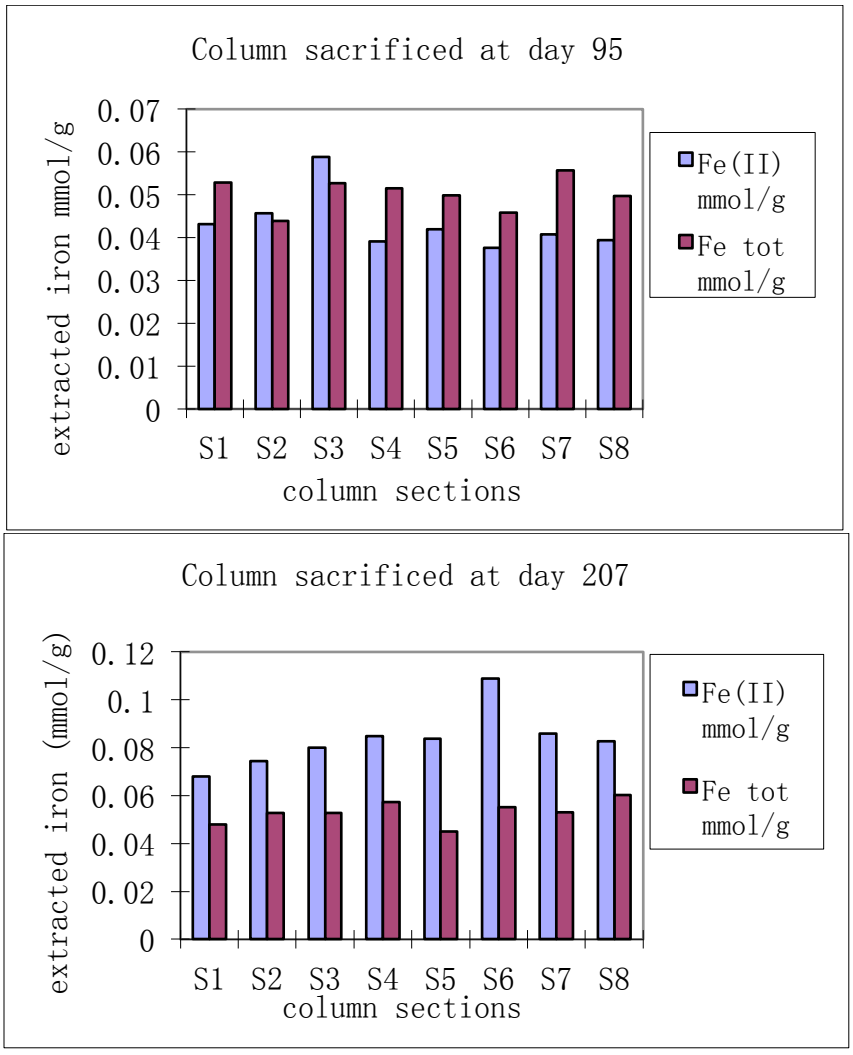

Figure 19. Fe in the sediments of the columns that have been sacrificed. Note: In column 1 Fe(total) < Fe(II). Per iron extraction protocol for Rifle IFRC, 0.5N HCl is used for Fe(II) extraction, 0.25N hydroxylamine in 0.25N HCl is used for total iron extraction. It seems in this case, 0.25N HCl extraction was not as efficient as the 0.5N HCl extraction.

Even though acetate levels were increased, there was not much of a change in permeability over the following 120 days of biostimulation (see Figure 17). Figure 20 shows that acetate consumption has been increasing gradually with time and that it is still increasing, hence even after 250 days of stimulation the system is not at "steady state". Similarly, dissolved inorganic carbon in the column effluent has not stabilized so far (Figure 21), nor the non-purgeable organic carbon (Figure 22). Figure 23 shows that sulfate was completely consumed after 50 days of implementing the higher influent acetate levels.

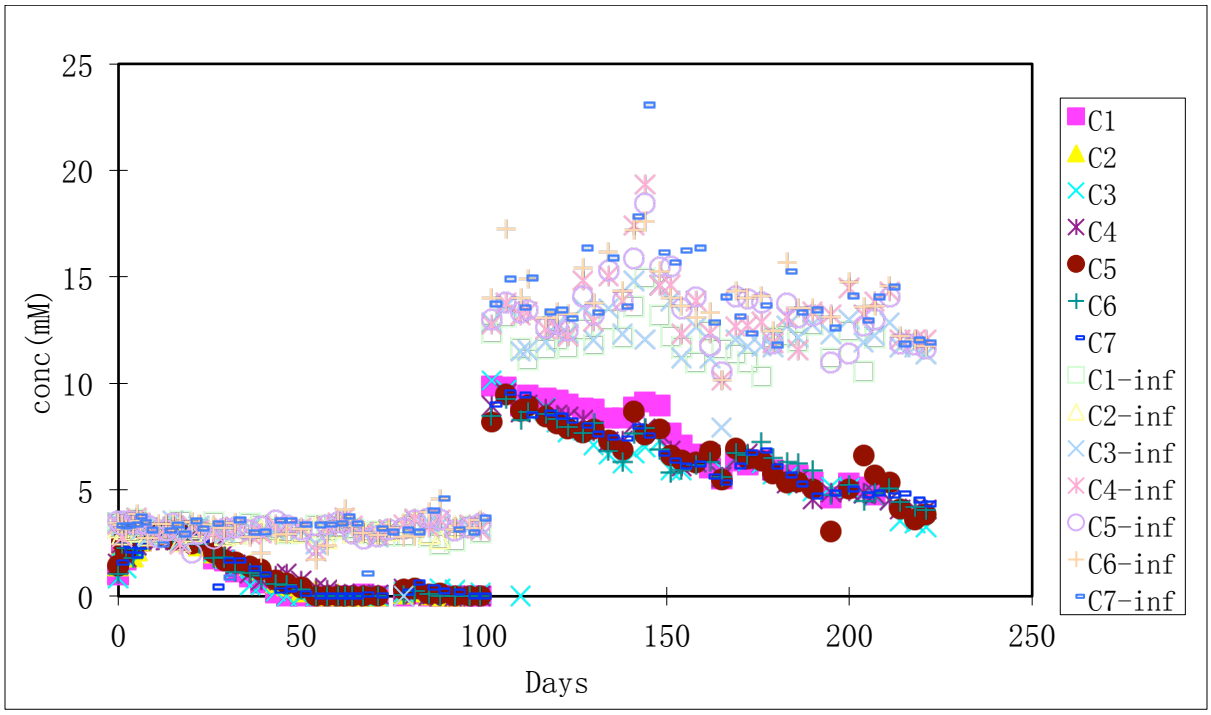

Figure 20. Influent and effluent acetate concentration vs. time.

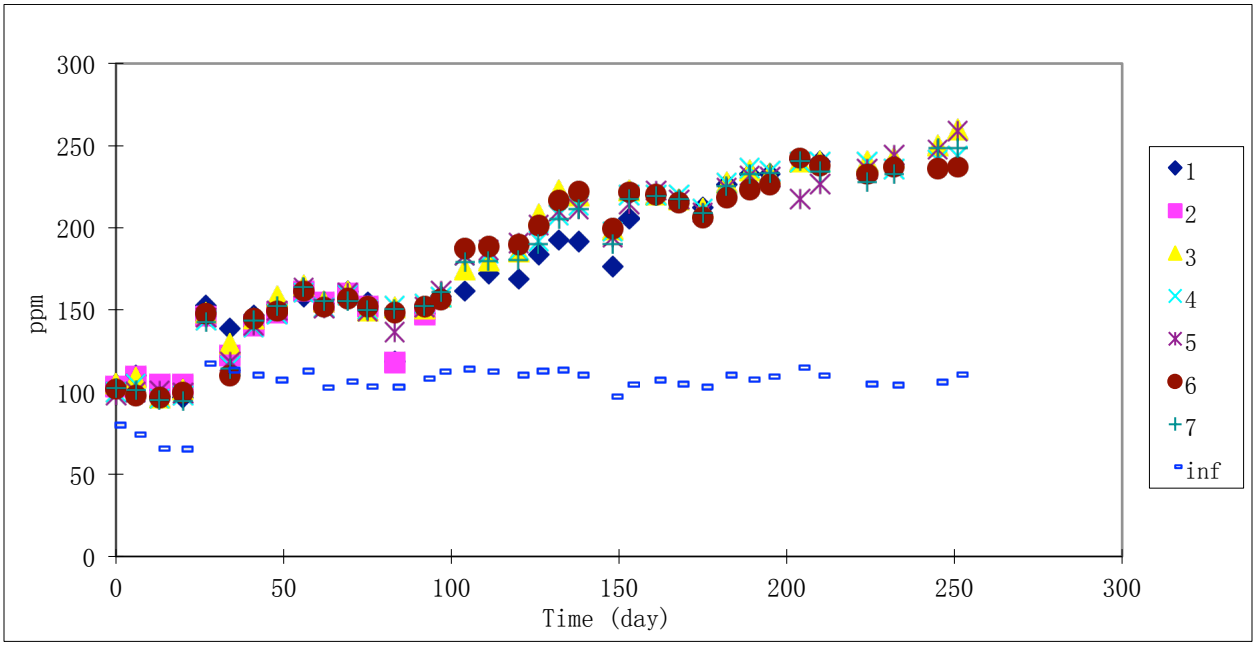

Figure 21. Influent and effluent dissolved inorganic carbon concentration vs. time.

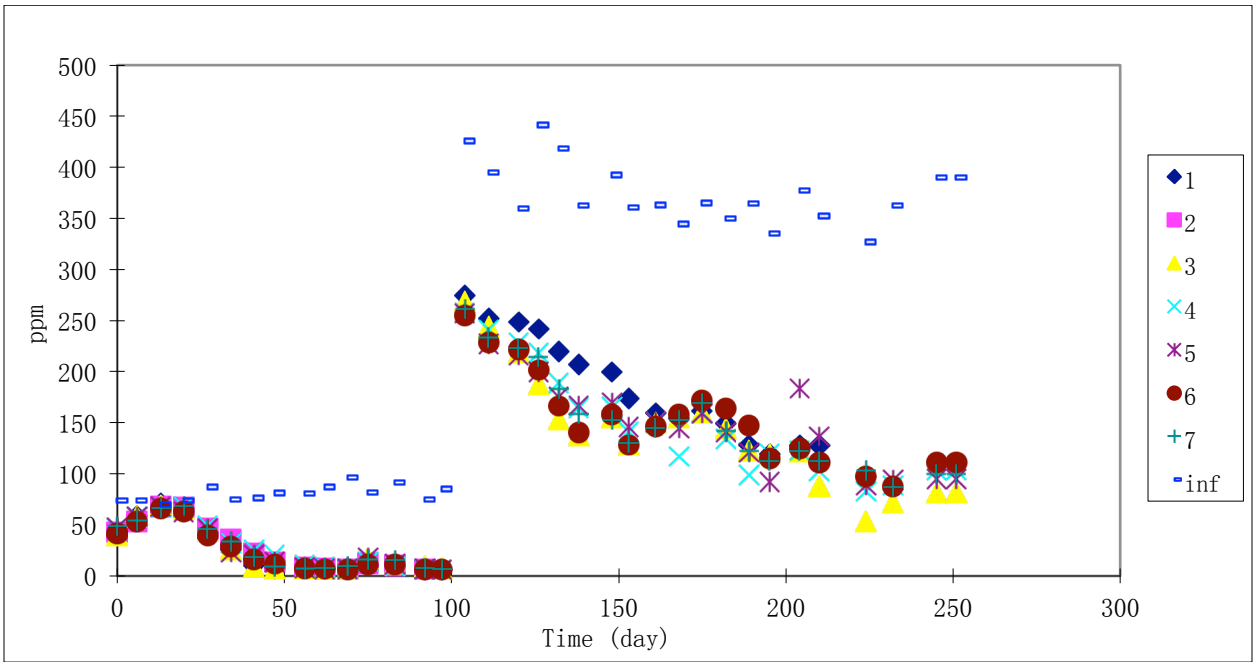

Figure 22. Influent and effluent non-purgeable organic carbon concentration vs. time.

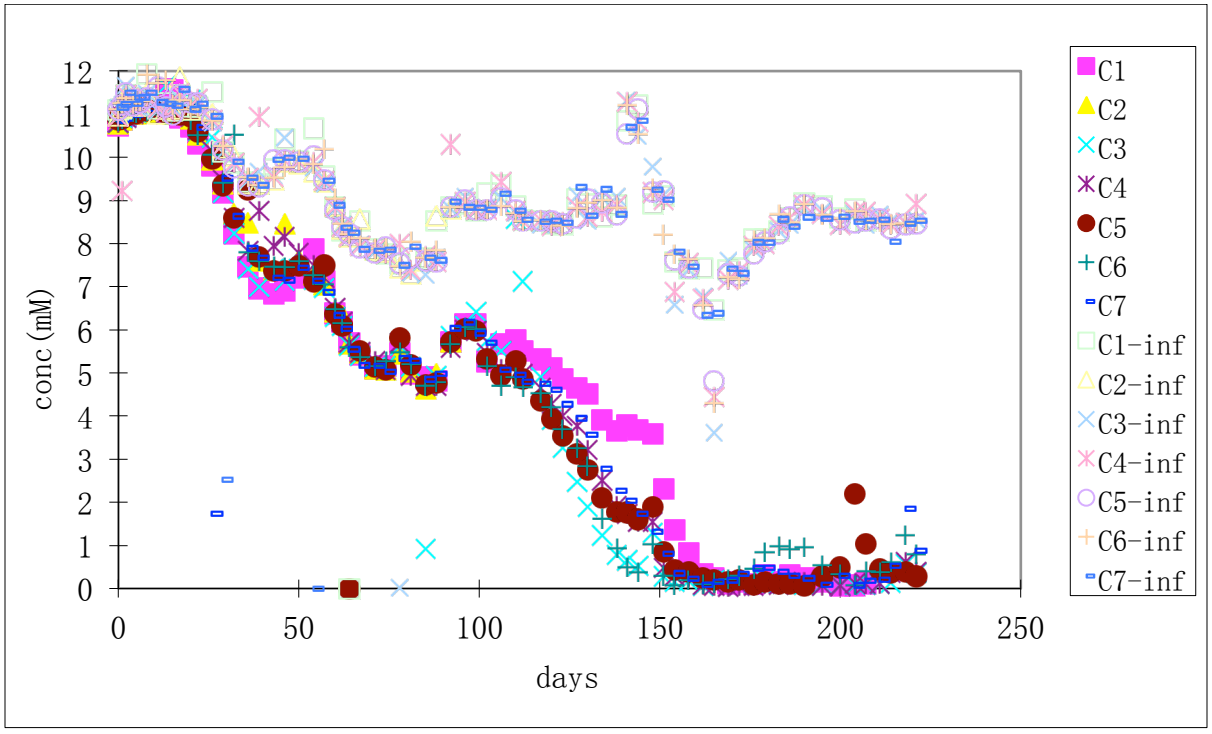

Figure 23. Influent and effluent sulfate concentration vs. time. Note: Decrease in influent concentration is due to variability in different batches of rifle groundwater.

Figure 17 shows that there is a small and gradual (seemingly linear) increase in pressure over time during the first 200+ days of biostimulation. Given the very slow flow rates, this does translate into a quantifiable change in permeability, but since the flow rates mimic those under Rifle conditions, changes in head should be similar here and in the field, and we are concluding that biostimulation with acetate does NOT affect the system's permeability in a detrimental manner; that is at least until methanogenesis becomes more dominant.

We do see a significant change in pressure along the longitudinal axis of the columns after about the first 220 days of biostimulation (see Figure 17). This corresponds to ~50 days after sulfate is completely reduced. Effluent analyses show that by this time methane is near solubility. Two gas-phase analyses for methane from different column effluents were conducted and yielded methane concentrations of 0.036M and 0.029M. Since pure methane at 1 atm. and 25 C has a concentration of ~0.04M, it looks as if the gas bubbles exiting the columns are mostly methane. Hence, we attribute the increase in backpressure to the formation and buildup of methane bubbles in the porous medium.

To determine changes in dispersivity and in overall porosity, bromide breakthrough experiments are being conducted at regular intervals using the fractional collection setup shown in Figure 16. Figure 24 shows breakthrough curves obtained for column #7 early and late into the biostimulation (day 26 and 211, respectively). Results indicate that over this time period, the dispersivity (seen by the skew of the curve) and the porosity (seen by the time to reach C/Co = 0.5) remained essentially unchanged. Additional breakthrough experiments are being performed right now and we expect that, based on these results, we will be able to estimate the volume of gas in the columns and link this to the changes in permeability.

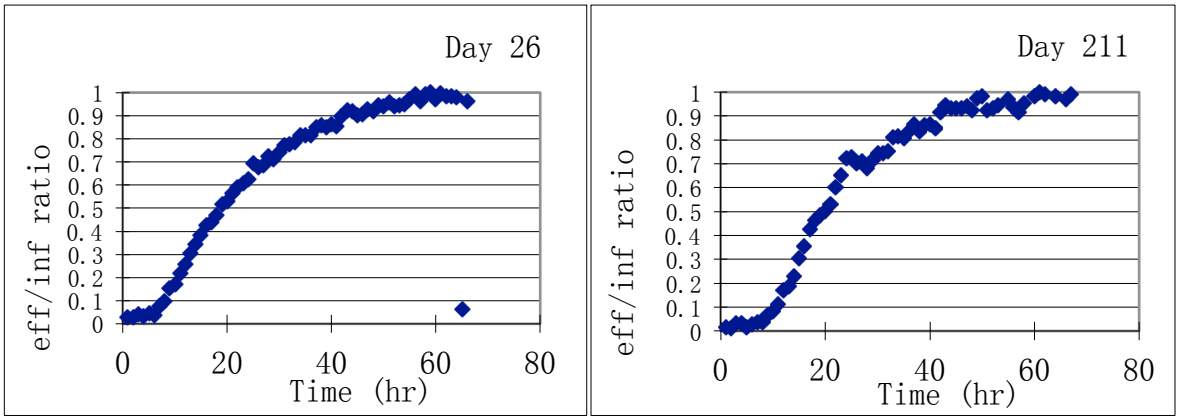

Figure 24. Bromide breakthrough at day 26 and 211 (Column 7)

Next Steps: Five columns are running right now. We will sacrifice one this month, given that we have not sacrificed any column since the gas phase methane production was first observed. With the other four columns, we will perform detailed analyses on the methane yield and do this while the acetate consumption keeps increasing. Projecting the trends in acetate consumption linearly (see Figure 20), we should be consuming all influent acetate within approximately three months. At that time we propose to sacrifice one more column, discontinue the supply of acetate, and track the behavior of the hydrology, microbiology, and geochemistry during the post stimulation period in the remaining three columns, which will be sacrificed at regular time intervals.

Since we did not expect the role of methanogenesis during the biostimulation of Rifle sediments, we did not monitor methane early on. Hence, we will start running two new columns to also track the methanogen numbers and methane production during the early times of the biostimulation (first 100 days).

Although this was not part of the initial goal, an important question we want to focus on now is what fraction of acetate goes toward methanogenesis and how does that change with time? We are also discussing taking effluent samples to analyze for planktonic methanogens. Sediment samples are being stored at -80 C for future microbiologic analyses (due to budgeting we have not sent them out).

Key findings to date: Although Rifle field experiments focusing on planktonic organisms have not reported significant presence of Archaea, our results seem to indicate that Archaea (in this case mathanogens) might be a dominant organism during biostimulation if one takes into account attached growth. Under Rifle flow conditions, and with acetate as the electron donor, permeability changes are expected to be negligible, at least until separate-phase methane builds up.

Subtask La Quinta (F-1 and F-1A; Bi-monthly sampling of background wells in years 1-3 for protein expression, gene expression, PLFA and TRFLP; Active Field experiments for assessing the rate of natural bioreduction of uranium)

The Rifle IFRC is investigating the extent to which regions of elevated subsurface microbial activity influence the fate and transport of uranium in the subsurface. Such zones of natural bioreduction are now viewed in terms of their role as net sources or sinks for uranium, an understanding of which will be critical in the decision-making process regarding long-term management of legacy sites where such features are known to occur (e.g. the Hanford 300 Area in addition to the Rifle site). The plume persistence aspects of this Subtask have been shifted to Subtask F-11 and are reported under that subheading (see below). Progress on the "La Quinta "experiments has been slowed due to unusually high runoff in the Colorado River during the spring of 2011 and the need to focus available funds on the "Best Western" field experiment. However, we have been able to make progress on analysis of hydrologic tests conducted late in 2010 and those results are reported here.

Hydrologic Characterization of Plot D

Slug tests, a constant-rate discharge pumping test, and EBF surveys were performed in selected Plot D wells in November 2010. Slug tests and EBF surveys were performed in wells LQ-107, LQ-114, LQ-115, LQ-116, and LQ-117 and a constant-rate discharge test was performed in well LQ-107.

Slug-Test Analyses. Analysis of the slug-test results indicates a homogeneous formation, over-damped (exponential decay) test response for all five wells tested. Assuming an anisotropic ratio of 0.1, hydraulic conductivity at the Plot D wells ranged from 0.634 to 3.82 m/day, with an average of 1.98 m/day. A comparison of hydraulic conductivity between the Plot D wells is presented in Figure 25.

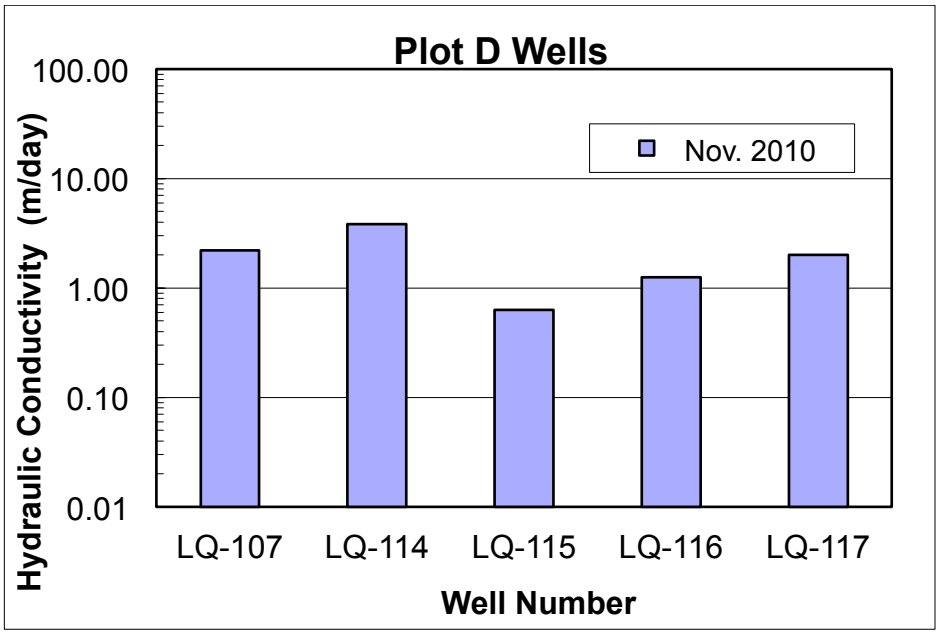

Figure 25. Comparison of Hydraulic Conductivity between the Plot D Wells.

Constant-Rate Discharge Test Analyses. An eight-hour constant-rate discharge pumping test followed by a recovery test was performed in well LQ-107 on November 11-12, 2010. Pressure transducers were used to measure drawdown and recovery in the pumping well and in the four observation wells with radial distances ranging from 1.03 to 2.04 m from the pumping well. The average discharge rate during the pumping test was 3.80 L/min. Recovery was monitored in the pumping and observation wells for a period of approximately two times the pumping duration after the pump was turned off. The drawdown responses in the Plot D wells during the constant-rate discharge test will be analyzed in fiscal year 2012.

Electromagnetic Borehole Flowmeter Survey Analyses. The dynamic (i.e., pump-induced) EBF survey results were used to characterize the vertical distribution of inferred hydraulic conductivity at the Plot D wells. The vertical wellbore flow measurements and the composite value of hydraulic conductivity estimated from the slug tests were used to calculate the vertical distribution of hydraulic conductivity at each well location. An example of a profile of the vertical distribution of hydraulic conductivity at a selected Plot D well, compared to the composite value of hydraulic conductivity calculated from the slug-test results, is shown in Figure 26.

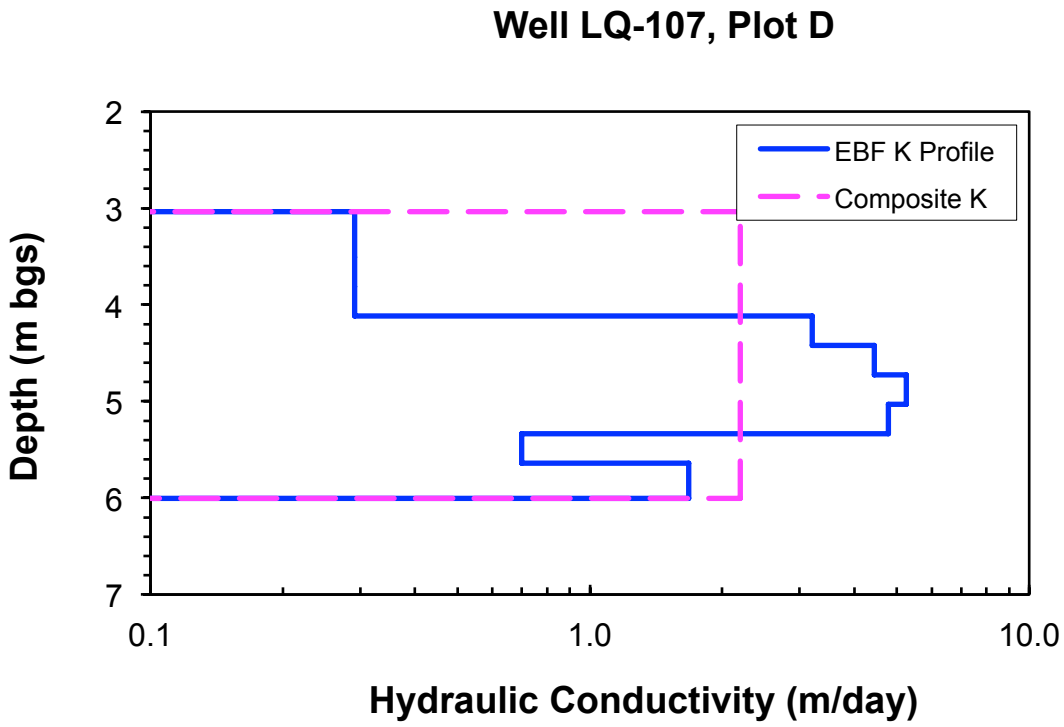

Figure 26. Example of Vertical Distribution of Hydraulic Conductivity Compared to the Composite Hydraulic Conductivity for a Selected Plot D Well.

Subtask Super 8 (F-8; Combined biostimulation/sorption experiment)

The overarching objectives of the Super 8 field experiment were threefold: (1) replication and extension of the "Little Rusty" [2008] uranium desorption experiment; (2) quantification of uranium mobility during acetate amendment under conditions of varying alkalinity and where microbial iron reduction is the dominant metabolic process; (3) assessing the extent to which uranium speciation impacts thermodynamic controls on enzymatic uranium reduction. Research activities associated with the LBNL SFA research program (Evolution Challenge) were integrated into the Super 8 experimental plan, as were other related SBR-funded projects (Dr. Jill Banfield and Dr. Luis Comolli; UCB/LBNL; Dr. Derek Lovely; UMASS). Experimental field activities that were part of the SLAC SFA (Dr. John Bargar; SLAC) were also integrated into the Super 8 Experiment. Here we report selected microbiological results on groundwater samples collected during the Super 8 experiment.

Hydrologic Characterization of Plot C before and after Super 8 Experiment. Slug tests, constant-rate pumping tests, and electromagnetic borehole flowmeter (EBF) surveys were conducted in Plot C wells before and after the Super-8 injection experiment in 2010 and the data analysis completed in 2011. Slug tests and EBF Surveys were performed in selected background wells, acetate injection wells, bicarbonate injection wells, and monitoring wells. Eight-hour constant-rate pumping tests were conducted in one monitoring well (CD-11) downgradient of the bicarbonate injection wells.

Slug-Test Analyses. Analysis of the slug-test results indicates a heterogeneous formation, over-damped (exponential decay) type test response for the CA bicarbonate injection wells and the CG acetate injection wells before and after the Super 8 experiment. The slug-test responses in these wells indicate a high-

permeability filter pack (i.e., disturbed, artificially imposed condition referred to as the inner zone) near the wellbore relative to the aquifer formation permeability immediately surrounding the wellbore's sand-pack/disturbed region (i.e., referred to as the outer zone). The slug-test responses indicating a high-permeability filter pack reflect a developed zone near the wellbore as a result of a large well-screen slot size (i.e., 20 slot size) at these well locations. An example of a heterogeneous formation, over-damped slug-test response on a semi-log plot is shown in Figure 27.

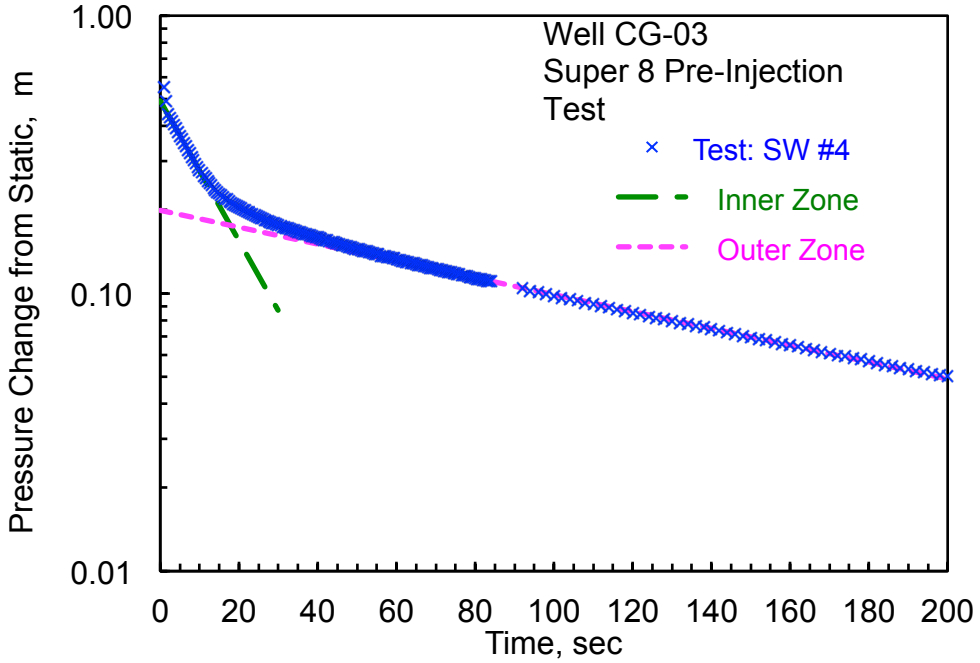

Figure 27. Example of a Slug-Test Semi-Log Plot Showing a Heterogeneous Formation/Over-Damped Response.

Analysis of the slug-test results for the CD monitoring and CU background wells generally indicate a homogeneous formation, over-damped (exponential decay) test response before and after the Super 8 experiment. These wells were constructed with 10 slot size well screens. As a result, the permeability of the filter pack material adjacent to the wellbore is similar to the permeability of the aquifer formation immediately surrounding the wellbore's filter pack. An example of a homogeneous formation, over-damped slug-test response on a semi-log plot is shown in Figure 28.

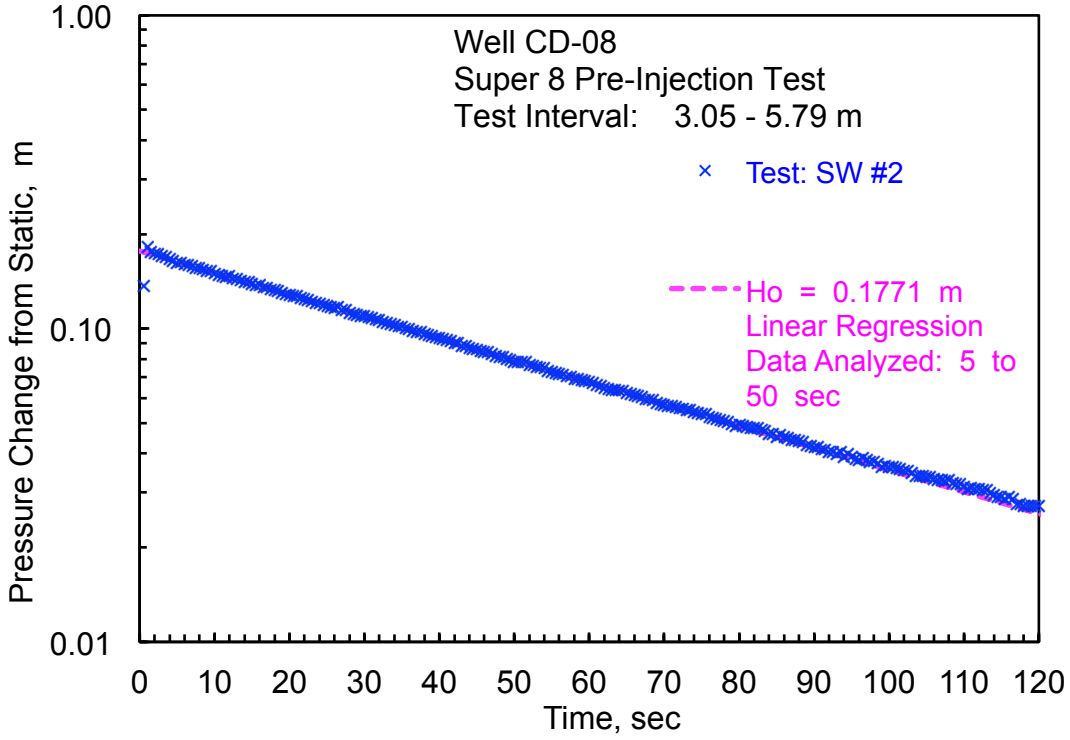

Figure 28. Example of a Slug-Test Semi-Log Plot Showing a Homogeneous Formation/Over Damped Response.

A comparison of hydraulic conductivity between the pre- and post-experiment results along the line of the CA bicarbonate injection wells and CG acetate injection wells is shown in Figures 29 and 30, respectively. The average pre- and post-experiment values of hydraulic conductivity for each of these groups of wells are summarized in Table 6. Because hydraulic conductivity is sensitive to vertical anisotropy due to a relatively thin, unconfined aquifer at Rifle, a vertical anisotropy ratio (i.e., K_v/K_h) of 0.1 was used for the slug-test analyses. The slug-test results indicate little variability (i.e., <1 log cycle) in hydraulic conductivity in both the inner (i.e., disturbed, artificially imposed condition near the wellbore) and outer zones (i.e., aquifer formation immediately surrounding the inner zone) for most of the CA and CG wells tested. However, the exceptions are the inner zones at acetate injection wells CG-04 and CG-05, which show a reduction in K of approximately one log cycle from 43.3 to 5.4 m/day and from 180 to 10.2 m/day, respectively. This corresponds with a reduction in K of less than one log cycle for the outer zones at these well locations, with reductions in K from 4.5 to 3.0 m/day and from 21.6 to 5.3 m/day, respectively. Comparison of pre- and post-experiment hydraulic conductivity results for the CD downgradient monitoring and CU background wells indicate little variability with a range of less than one log cycle (Table 6). Maps of the Super 8 pre- and post-experiment spatial distribution of hydraulic conductivity for Plot C are shown in Figures 31 and 32, respectively.

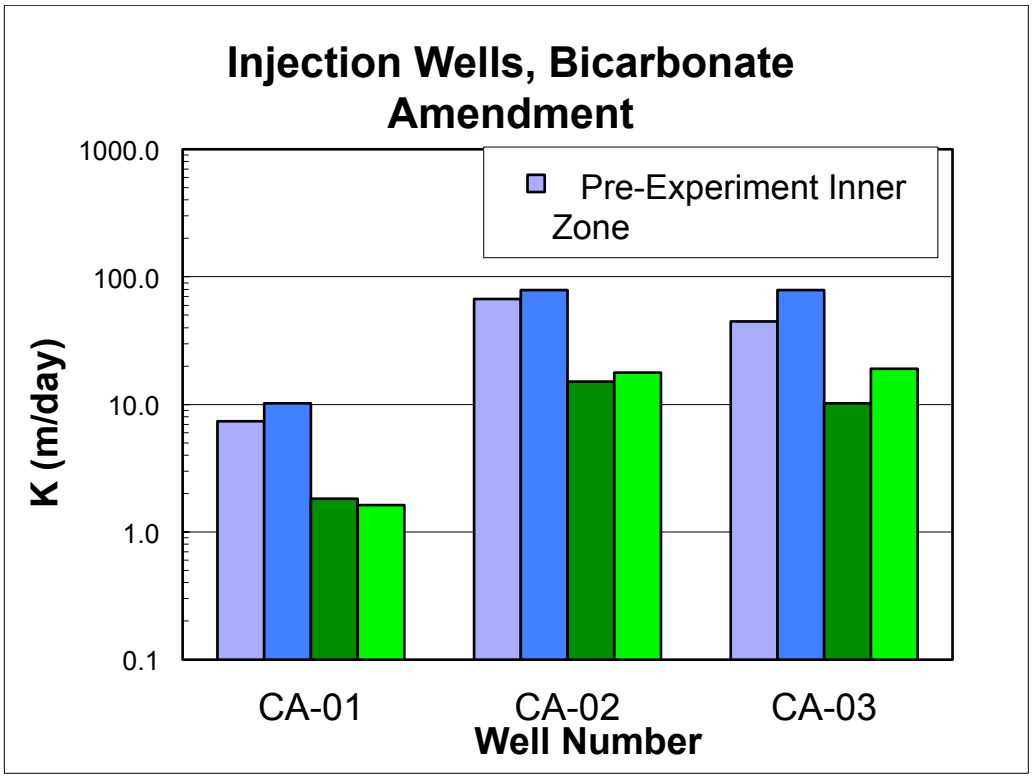

Figure 29. Variability of K at the Bicarbonate Injection Wells.

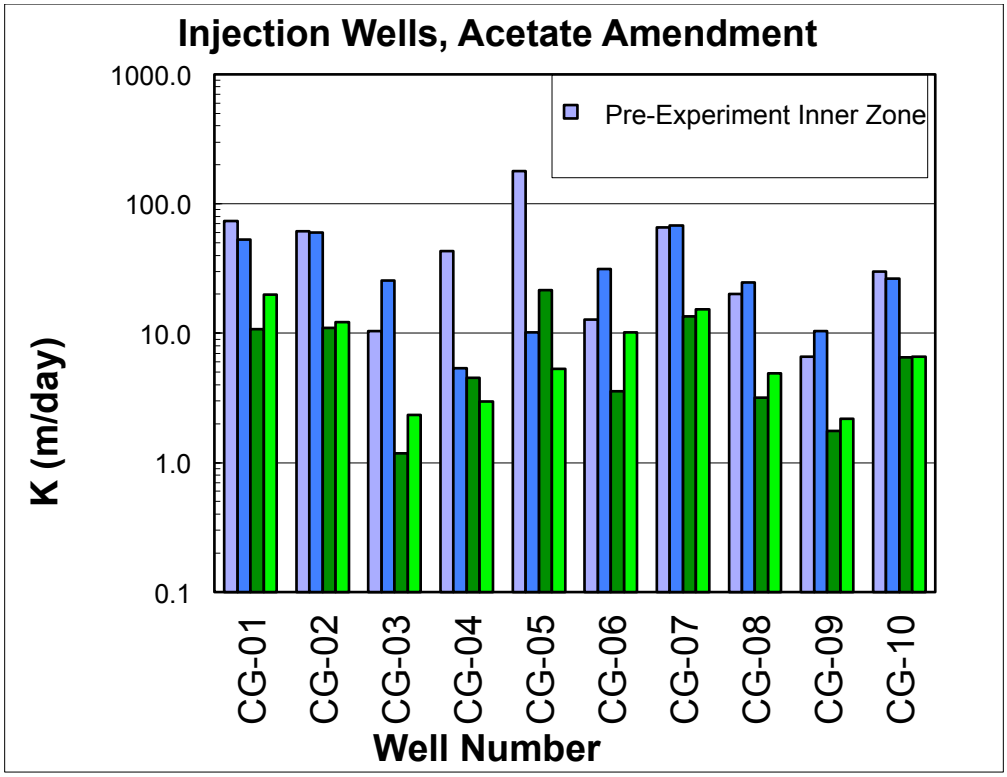

Figure 30. Variability of K at the Acetate Injection Wells.

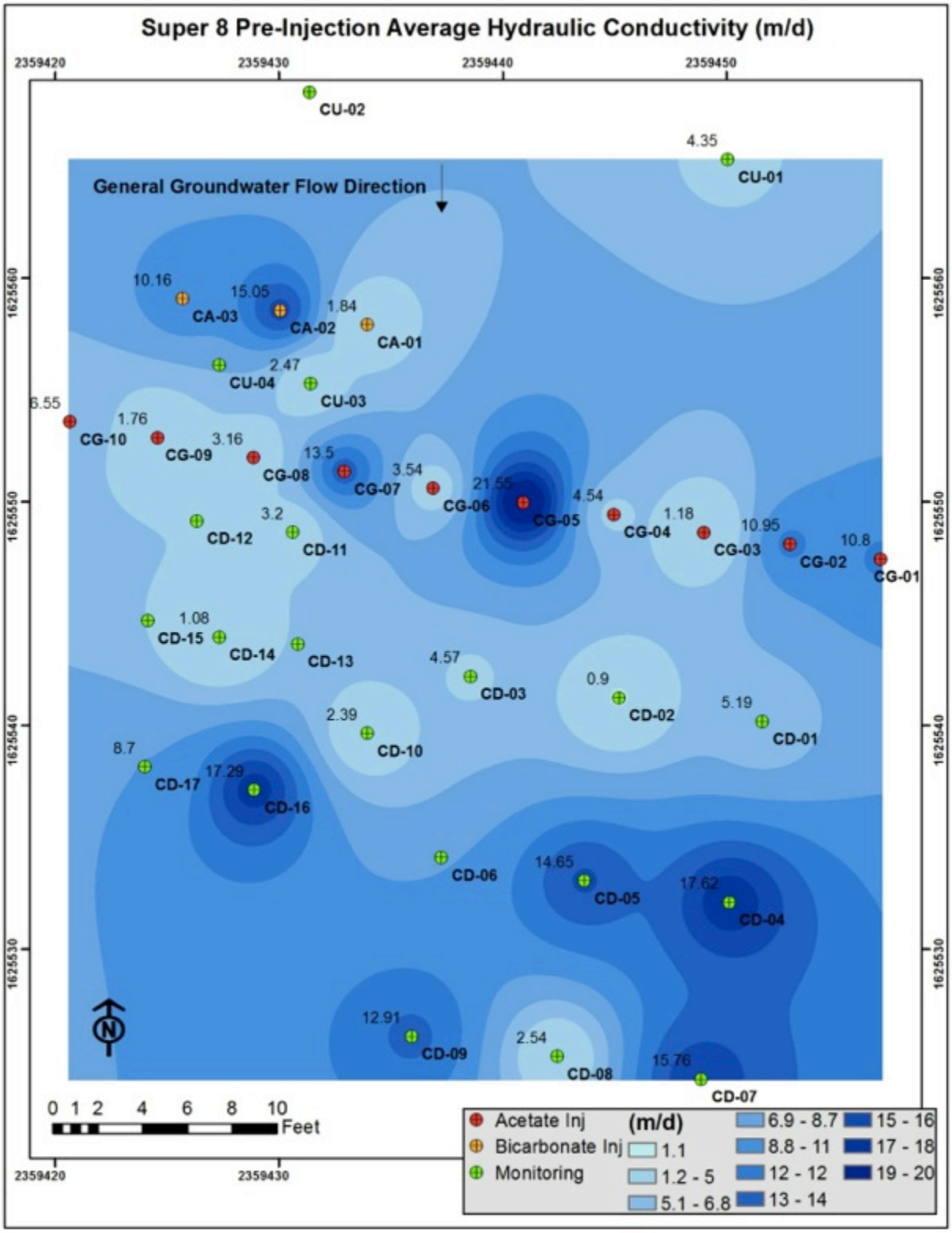

Figure 31. Super 8 Pre-Experiment Spatial Distribution of Hydraulic Conductivity.

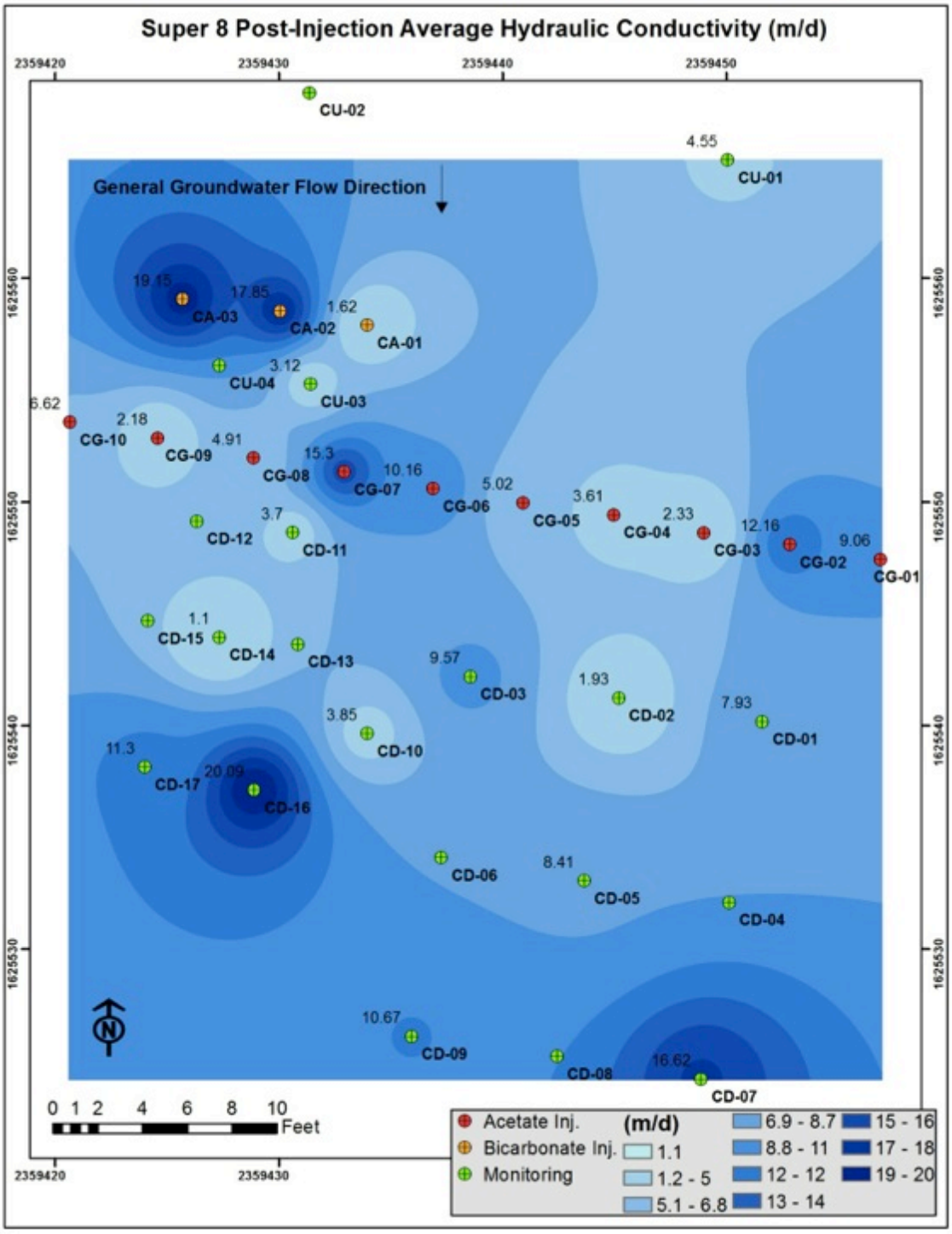

Figure 32. Super 8 Post-Experiment Spatial Distribution of Hydraulic Conductivity.

Table 6. Average Super 8 Pre- and Post-Experiment Values for Hydraulic Conductivity

	Average Pre-Experiment K (m/day)	Average Post-Experiment K (m/day)
Inner Zone - Bicarbonate Injection (CA) Wells	39.9	55.8
Outer Zone - Bicarbonate Injection (CA) Wells	9.02	12.9
Inner Zone - Acetate Injection (CG) Wells	50.4	31.5
Outer Zone - Acetate Injection (CG) Wells	7.75	8.18
Background (CU)/Monitoring (CD) Wells	5.29	5.91

Constant-Rate Discharge Test Analyses. An eight-hour constant-rate discharge pump test was performed in well CD-11 before and after the Super 8 experiment. Drawdown and recovery were measured manually in the pumping well and in 14 observation wells with radial distances ranging from 1.09 to 3.52 m from the pumping well. The average discharge rates during the pre- and post-experiment pumping tests were 4.93 and 3.90 L/min, respectively. Drawdown and recovery were measured with a pressure transducer in the pumping well and a few selected observation wells. For each of these tests, recovery was monitored in the pumping and observation wells for a period of approximately two times the pumping duration after the pump was turned off.

Preliminary analyses of the constant-rate discharge tests indicate that infinite-acting radial flow conditions were just approached near the end of the pumping tests. Based on the areal distance-drawdown analysis method, hydraulic conductivity was estimated to be 8.9 and 8.4 m/day for the pre- and post-experimental pumping tests, respectively. A specific yield of ~20% was estimated for both of these pumping tests. An initial comparison of the normalized drawdown response (i.e., drawdown divided by discharge rate) in the pumping well between the pre- and post-experiment pumping tests has been made. The pumping and recovery data analyses will be completed in fiscal year 2012.

Electromagnetic Borehole Flowmeter Survey Analyses. The dynamic (i.e., pump-induced) EBF survey results were used to characterize the vertical distribution of inferred hydraulic conductivity at the Plot C wells. The vertical wellbore flow measurements and the composite value of hydraulic conductivity estimated from the slug tests were used to calculate the vertical distribution of hydraulic conductivity at each well location. These EBF profile calculations can be used to compare the vertical distribution of hydraulic conductivity before and after the Super 8 experiment. An example of a comparison between the pre- and post-experiment vertical distribution of hydraulic conductivity at a selected Plot C well is shown in Figure 33.

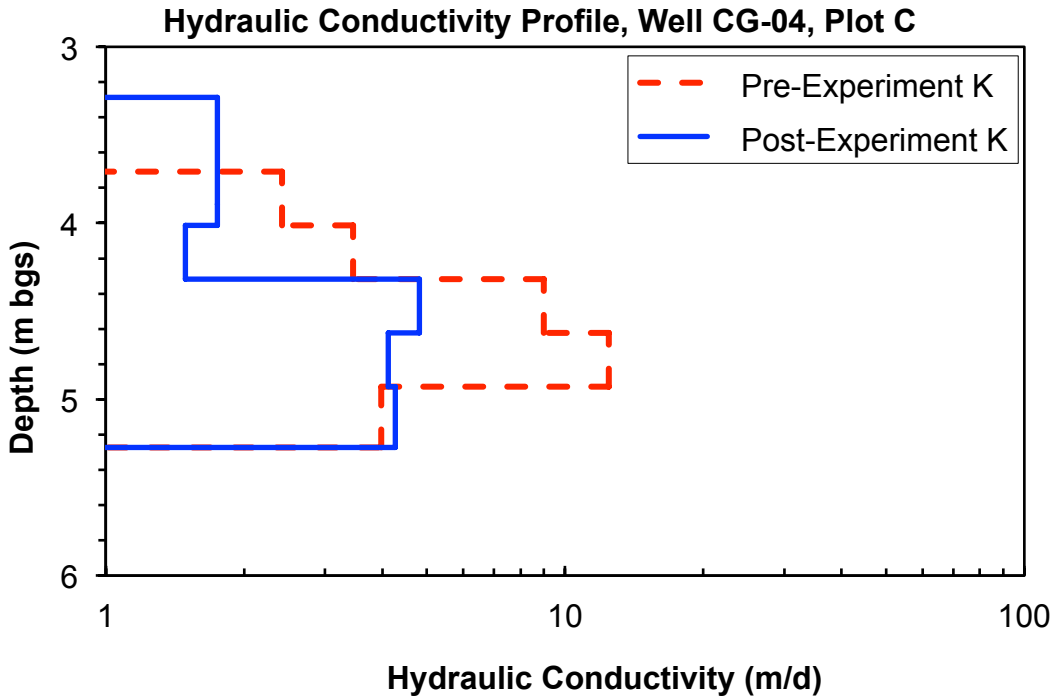

Figure 33. Comparison between the Pre- and Post-Experiment Vertical Distribution of Hydraulic Conductivity at a Selected Plot C Well.

Super 8 Microbial Samples. In the acetate-only amendment part of the "Super 8" field experiment, a temporal series of planktonic biomass samples were recovered from downgradient well CD01 over the period of dominant Fe(III) reduction (Figure 34; Wilkins et al., in prep.). Proteins and peptides were extracted from this biomass, and analyzed using 2D-LC-MS/MS at PNNL. The resulting data has initially been searched against predicted peptides from the *Geobacter bemidjiensis* genome. 16S rRNA EMIRGE analysis of the same biomass suggested that strains closely related to *G. bemidjiensis* (>98%) were the dominant member (20%) during the biostimulation process.

These results reveal that the activity of indigenous bacterial strains similar to *G. bemidjiensis* is rapidly stimulated upon the arrival of acetate in CD01. At sampling time point #2, occurring 6 days after the start of carbon addition, over 400 proteins were detected, and this value increased to ~1200 after 9 days of acetate amendment (Figure 34C). Both numbers of detected proteins and protein abundances (as determined via NSAF calculations) fluctuated over the period of dominant Fe(III) reduction; it is currently unknown what may have caused the large decrease in protein detection between samples #3 and #4, but the up-regulation of proteins involved in polyketide biosynthesis in sample #4 suggests that the *Geobacter* population may have been responding to some external environmental or biological stress.

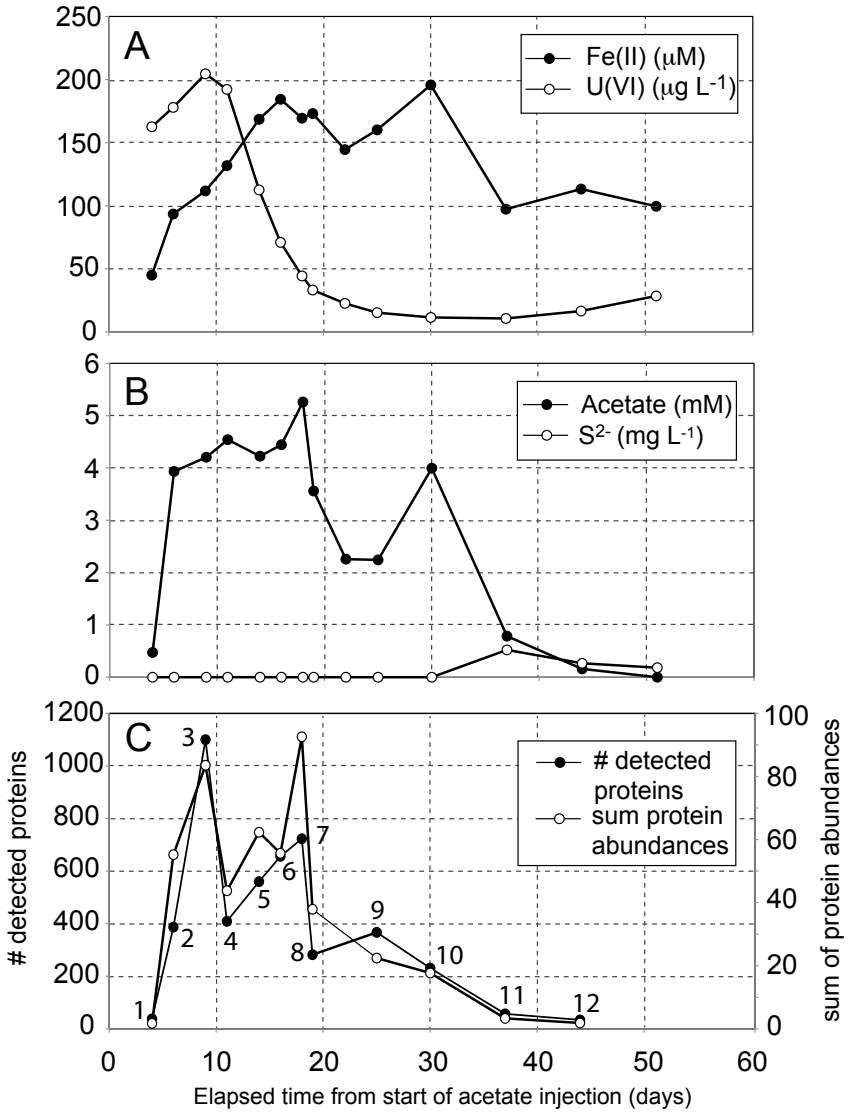

Figure 34. (A) Fe(II) and U(VI), and (B) Acetate and sulfide concentrations at time points where planktonic biomass samples for global shotgun proteomic analyses were recovered. Twelve of the fourteen samples were successfully processed, and temporal shifts in numbers of detected proteins, and protein abundances, and reported in (C). Mass spectrometry data was searched against a database consisting of predicted peptides from the *Geobacter bemidjiensis* genome. Values by the data points refer to the sample number.

Acetate utilized by *Geobacter* strains is directed to either biosynthetic pathways or respiration. The relative proportion of carbon being directed into each of these processes can be calculated by determining a ratio from spectral counts assigned to acetyl-CoA transferase (that converts acetate to acetyl-CoA for respiration) and pyruvate ferredoxin oxidoreductases (that converts acetyl-CoA to pyruvate for biosynthesis) (Figure 35). These data support the current hypothesis that following the arrival of acetate in the aquifer, cell proliferation occurs that requires relatively high levels of biosynthesis. At a certain point however, limiting conditions may reduce the rate of biosynthesis, while cell respiration continues. The plot in Figure 35 illustrates the shift in the calculated ratio. The highest ratio value (indicating greater

abundance of a protein involved in respiration relative to an enzyme involved in biosynthesis) occurs at a point where U(VI) concentrations are approaching their lowest levels (between days 20 – 25).

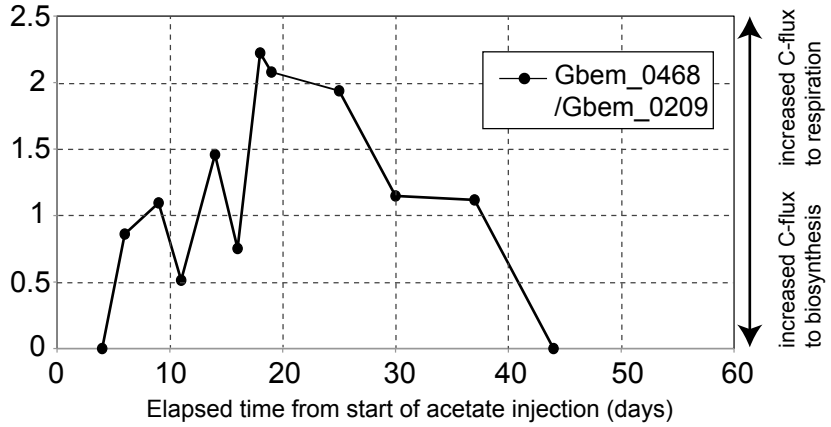

Figure 35. The temporal shift in the ratio of spectral counts assigned to the Geobacter acetyl-CoA transferase (Gbem_0468) / pyruvate ferredoxin oxidoreductase (PFOR) (Gbem_0209). The acetyl-CoA transferase converts acetate to acetyl-CoA for respiration, while the PFOR enzyme converts acetyl-CoA to pyruvate for biosynthesis. By comparing the ratio of these protein abundances, temporal shifts in carbon flux to respiration and biosynthesis can be inferred. Here, relatively more C flux is directed to biosynthesis over the first 15 days, relative to later time points. This corresponds to a period when acetate is entering the region around well CD01 and stimulating biomass growth.

Ongoing research efforts include a metagenomic sampling focused on two time points, one during peak iron reduction and one at the transition into sulfate reduction (as defined by the onset of measurable sulfide production). Preliminary 16S rRNA based community analysis of the planktonic community revealed filtration imparts selectivity on the planktonic community, with Firmicutes confined to the 1.2 μm filter and Candidate Division bacteria enriched on 0.2 μm filter. Ongoing community genomic efforts will characterize the communities on both filters in order to reconstruct genomes that may have been excluded from earlier community characterizations, which focused exclusively on the 0.2 μm bacterial community. Of particular interest, is the opportunity to reconstruct genomic and proteomic information for candidate division organism TG-1. This bacterium increases in abundance from 5% up to 20% of the community on the 0.2 μm filter, equaling *G. bemidjiensis* in dominance during later biostimulation time points. Genome reconstruction of organisms other than *G. bemidjiensis* will also be used to query existing field proteomic data from 2010. Protegenomic results from detailed time course of microbiological samples shown in Figure 34C will be integrated with the geochemistry data and used to inform reactive transport modeling of the "Super 8" experiment (see section on Modeling and Interpretation).

We also performed proteomics measurements and groundwater filters and sediment samples from the "Super 8" experiment. For a subset of the samples, proteomes were measured at ORNL on 28 sediment samples and 6 groundwater samples. For the sediment samples, the amount of proteome coverage is highly dependent on sample type, with maximum protein IDs at ~420 proteins and minimal IDs at ~70 proteins from non-treated background (Table 7).

Table 7. Proteomes Measured on Sediment and Groundwater Samples

Sample Name	Proteins	Peptides	Spectra	Trypsin SpCount
ColumnSed_Bkgrd	72	232	1350	678
ColumnSed_C1_2_AO_T1	373	894	3245	1009
ColumnSed_C1_5_AO_T2	397	1001	2566	474
ColumnSed_C1_7_AO_T4	157	338	1041	288
ColumnSed_C2_6_LacFe_T2	265	536	1062	190
ColumnSed_C3_3_Lac_SO4_T1	190	424	877	176
ColumnSed_C3_5_LacFe_T1	417	910	2108	512
ColumnSed_C5_5_AO_T4	194	401	920	195

Although coverage from these sediment samples is lower than the groundwater samples, this is typical of natural soil/sediment samples. However, we are still able to achieve deep enough coverage to see interesting proteins functions and should be able to track these proteins over all different treatment types in the 28 field samples. Figure 36 highlights one such protein - Phasin from *Dechloromonas aromatic*. Phasins (or granule-associate proteins) are surface proteins found covering polyhydroxyalkanoate (PHA) storage granules in bacteria. Polyhydroxyalkanoates are linear polyesters produced by bacterial fermentation of sugar or lipids for the purpose of storing carbon and energy, and are accumulated as intracellular granules by many bacteria under unfavorable conditions, enhancing their fitness and stress resistance. Thus we have found a biomarker for physiological response of this microbe in the Rifle field sediments, as one example of our ability to monitor the physiological response of the community during the field study. For both the groundwater and sediment samples, we are analyzing the MS/MS datasets with a number of different builds of metagenome/isolate databases as discussed above. All the data is posted on this website for the entire Rifle group.
https://compbio.ornl.gov/mspipeline/ersp_rifle/Field_Soil_2010/status.html

U Daro_RCB:637681894 11 31 57.8% 187 19045 6.9 Daro_3422 "Phasin" [637000088 "Dechloromonas aromatica RCB"]

	Filename	XCorr	DeltCN	Obs_mono_m/z	Cal_mono_m/z	PPM	Delta_amu	Ion%	#	Sequence
*	ColumnSed_C3_5_092010_LacFe_T1_OrbiXL_Run1_122811_03.07371.07371.3	5.3437	0.3753	1857.9762	1857.9801	-2.0760	-0.0039	51.4%	1	K.ATVDSLLSVANAALASAER.I
*	ColumnSed_C3_5_092010_LacFe_T1_OrbiXL_Run1_122811_03.07376.07376.2	5.581	0.4892	1857.9787	1857.9801	-0.7597	-0.0014	69.4%	6	K.ATVDSLLSVANAALASAER.I
	ColumnSed_C3_5_092010_LacFe_T1_OrbiXL_Run1_122811_05.03866.03866.2	3.2109	0.1145	1055.6086	1055.6092	-0.5758	-0.0006	94.4%	7	R.IAALNLNTAR.S
*	ColumnSed_C3_5_092010_LacFe_T1_OrbiXL_Run1_122811_03.03128.03128.2	3.1305	0.3994	1120.5594	1120.5617	-2.0266	-0.0023	80.0%	2	R.SVLEDSVSGTK.A
*	ColumnSed_C3_5_092010_LacFe_T1_OrbiXL_Run1_122811_03.03130.03130.1	1.9719	0.4203	1120.5602	1120.5617	-1.3146	-0.0015	55.0%	1	R.SVLEDSVSGTK.A
*	ColumnSed_C3_5_092010_LacFe_T1_OrbiXL_Run1_122811_05.05238.05238.2	3.6118	0.4489	1673.9222	1673.9205	1.0400	0.0017	68.8%	1	R.SVLEDSVSGTKALLGAK.D
*	ColumnSed_C3_5_092010_LacFe_T1_OrbiXL_Run1_122811_04.03879.03879.2	3.4792	0.386	1170.6596	1170.6613	-1.4832	-0.0017	70.0%	1	K.QVADLLDKAAK.S
*	ColumnSed_C3_5_092010_LacFe_T1_OrbiXL_Run1_122811_03.03144.03144.2	4.607	0.5975	1241.6590	1241.6621	-2.4953	-0.0031	80.8%	3	K.SAPAGSDVAVAAVK.S
*	ColumnSed_C3_5_092010_LacFe_T1_OrbiXL_Run1_122811_03.04694.04694.2	4.7445	0.5604	1505.7452	1505.7479	-1.8009	-0.0027	75.0%	1	K.SAIAAANSAFDNLNK.A
*	ColumnSed_C3_5_092010_LacFe_T1_OrbiXL_Run1_122811_07.04610.04610.2	5.7958	0.5947	1775.9155	1775.9171	-0.8797	-0.0016	73.5%	7	K.SAIAAANSAFDNLNKAAK.Q
*	ColumnSed_C3_5_092010_LacFe_T1_OrbiXL_Run1_122811_03.04661.04661.2	5.7612	0.658	1899.9908	1899.9907	0.0615	0.0001	77.8%	1	K.QVAEITEANVAAATNATVK.A

Figure 36. Phasin protein functions

During the Super 8 experiment, we also conducted the following sets of *in situ* column experiments:

- Acetate-only Sediment Columns (six time points, iron and sulfate reduction). A total of 6 temporal column samples were collected during acetate stimulation through iron and sulfate reduction. All columns were run in duplicate, resulting in a total of 12 samples. Samples have been processed for geochemistry and proteomics (ORNL). DNA was extracted and EMIRGE 16S rRNA amplicon sequencing was performed using Illumina technology, following tests of this novel method facilitating phylogenetic analysis (Miller *et al*., in prep.). A total of 13 samples (duplicate of six time points, and a background) were submitted to UCD in January 2012 for

community genomics. Results from the EMIRGE 16S amplicon and the proteogenomics analyses will be presented in subsequent reports.

- 2010 Lactate Perturbation Sediment Columns. This experiment was conducted in parallel to the acetate only column experiment (above). The impact of a disturbance, switching the electron donor from acetate to lactate, was monitored on iron and sulfate reducing communities. The impact on the community trajectory was monitored 1 and 4 weeks after the electron donor switch to assess the resistance and resilience of these communities to changes in their electron donor. To date, samples have been processed for geochemistry and proteomics (ORNL). DNA was extracted and EMIRGE 16S rRNA amplicon sequencing was performed. Metagenomics is planned for late 2012 pending results from the sequencing of acetate-only sediment columns (above).

The above *in situ* column experiments will provide key information on the metabolic status of sediment-attached first-stimulation microbial communities. The lactate-perturbation columns will provide novel data on the impact of a change in electron donor to the community structure and function and will also provide insight into the overall metabolic potential of the subsurface in microaerophylic alluvial aquifers.

Subtask Best Western (F-9; Combined biostimulation/sorption experiment Phase II)

Contributors to this section include Kenneth H. Williams, Alison Montgomery, Mark Robbins, Mark Conrad, Jennifer Druhan, Craig Ulrich, Joern Larsen, April van Hise [all LBNL]; Scott Waichler [PNNL]; Adrian Flores-Orozco and Andreas Kemna [Univ. of Bonn]; Val Stucker and Jim Ranville [Colorado School of Mines]; the Rifle IFRC Field Team [multi-institutional].

The "Best Western" field experiment, was aimed at understanding metabolic pathways under conditions of a second stimulation by electron donor amendment and the impact of prolonged bicarbonate injection on metal oxyanion (U, As, V, Se, Mo) mobility. Research activities associated with the Science Focus Area (SFA) research programs of LBNL (geophysical monitoring and sulfur/calcium/strontium isotope systematics) and SLAC (in-well spectroscopic columns) were integrated into the experimental plan. In addition, experimental activities of collaborating University-led, SBR funded projects were included, notably

- Dr. Jill Banfield and Dr. Luis Comolli (UCB/LBNL): CryoTEM imaging of size-dependent fractions of planktonic biomass
- Dr. Clara Chan (Univ. Delaware): Isolation and imaging of iron and sulfur oxidizing microorganisms
- Dr. Kirk Hatfield (Univ. Florida): Quantification of uranium and vanadium fluxes associated with prolonged bicarbonate addition
- Dr. Kristina Keating (Rutgers Univ.): Changes in nuclear magnetic resonance and magnetic susceptibility properties as impacted by changes in Fe-bearing minerals during biostimulation
- Dr. Derek Lovely (UMASS): Arsenic respiratory/detoxification pathways; Eukaryotic predation/grazing
- Dr. Craig Lundstrom and Dr. Tom Johnson (Univ. Illinois): Quantification of $^{238}U/^{235}U$ fractionation associated with reductive immobilization of uranium and enhanced abiotic uranium desorption
- Dr. Brian Mailloux and Dr. Jim Ranville (Barnard College and Colorado School of Mines): Quantification and modeling of arsenic speciation associated with elevated As fluxes during biostimulation

The overarching objectives of the "Best Western" field experiment were threefold: (1) acquisition of temporally dense, size-dependent proteogenomic data at a single location under conditions of a second stimulation; (2) replication and extension of the "Little Rusty" [2008] and "Super 8" [2010] uranium (U) desorption experiments but designed to enable direct comparison of desorption associated with acetate amendment (and associated reductive U immobilization) with desorption associated soley with abiotic bicarbonate amendment; (3) quantification of speciation-dependent arsenic release accompanying prolonged sulfate reducing conditions and the concomitant microbial response.

A variety of experimental approaches developed during the Super 8 experiment (2010) were again used to address the research objectives, including introduction of conservative and non-conservative amendments (e.g. sodium acetate, sodium bicarbonate, sodium bromide, D_2O, etc.), bulk groundwater sampling for geochemical and microbial constituents, deployment of in-well columns and passive flux meters, geophysical and hydrological wellbore testing, and cross-borehole electrical resistivity/spectral induced polarization monitoring.

Modification of Experimental Plot C for "Best Western." Installed in June 2010, Plot C was originally comprised of 34 wells (Figure 37). It was modified during drilling activities in July 2011 by installing two additional wells (CU05 and CD18), which straddle the injection gallery. The wells were installed for both the collection of sediments (CU05) used for preparation of the "Best Western" composite material (SLAC SFA in-well columns) and to allow for cross-borehole geophysical measurements across the injection zone (LBNL SFA activity).

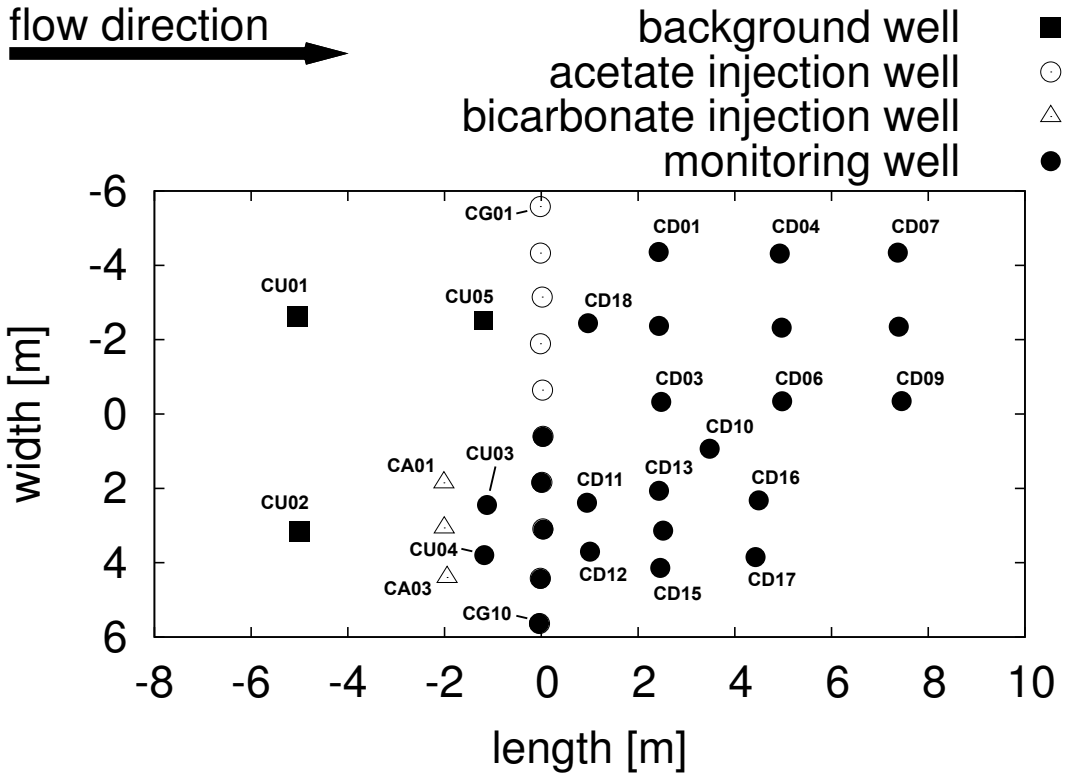

Figure 37. Well layout within Plot C, site of the "Best Western" [2011-12] field experiment, indicating the location of two new wells drilled in 2011 (CU05 and CD18).

As with the "Super 8" experiment, the prefix "C" denotes a location within Plot C, with wells denoted "CG" used for injection of sodium acetate and sodium bromide, wells denoted "CU" and "CD" used up- and downgradient monitoring, respectively, and wells denoted "CA" used for injection of sodium bicarbonate and D_2O. The spatial arrangement of all wells within Plot C is shown in Figure 37, with linear wellbore transects (e.g. between CD01, CD04, and CD11) oriented 190 degrees azimuthal from north, the approximate groundwater flow direction during a portion of the "Best Western" experiment.

Subsurface hydrologic context. The groundwater flow direction varies as a function of Colorado River stage, with the both the maximum discharge and length of duration in 2011 exceeding all years since 1986-87. In anticipation of runoff conditions, water levels measurements were made both within Plot C, as well as within the other experimental plots (Plots A, B, and D, see Figure 2) spanning much of the Old Rifle floodplain. As river stage increases following the onset of runoff, groundwater levels rise, with a corresponding impact on both hydraulic gradient and flow direction. The aggregate effect is a rotation of groundwater flow direction from a predominantly north-south orientation (180 degrees azimuthal from north) towards the northwest. The change in gradient and groundwater flow direction within Plot C over the September 2010 to September 2011 interval is shown in Figure 38.

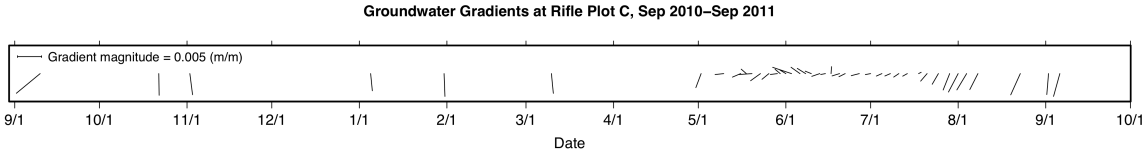

Figure 38. Hydraulic gradient (vector length) and groundwater flow direction (vector orientation) within Plot C over the September 2010 to September 2011 time period as calculated using water elevation in selected wells.

The change in gradient and groundwater flow direction within all four experimental plots over the May-September 2011 interval is shown in Figure 39. As can be see, greater variability in gradient and flow direction is observed in Plot D, which is the location closest to the river and perhaps most influenced by rapidly fluctuating discharge conditions, which vary diurnally due to variations in temperature and snowmelt. Similar trends in gradient and flow direction were observed at the three plots located farther from the river (Plots A-C) as a function of runoff, with a relatively short-lived excursion towards the northwest at the onset of runoff rapidly rotating back towards the southeast as runoff peaks and wanes. With increasing time, groundwater flow directions return to a quasi-basal flow near the beginning of the "Best Western" experiment, varying slightly from 190 to 180 degrees over the 90+ day length of the injection period. Water levels in a subset of wells (CG01-CG05, CA01-CA03, CU01, CD02, CD09, CD10-11, CD14, CD16-17) were monitored during the course of the "Best Western" experiment using pressure transducers placed at the bottom of each well. Water levels were corroborated through hand-measured values in all available wells at various time points during the experiment.

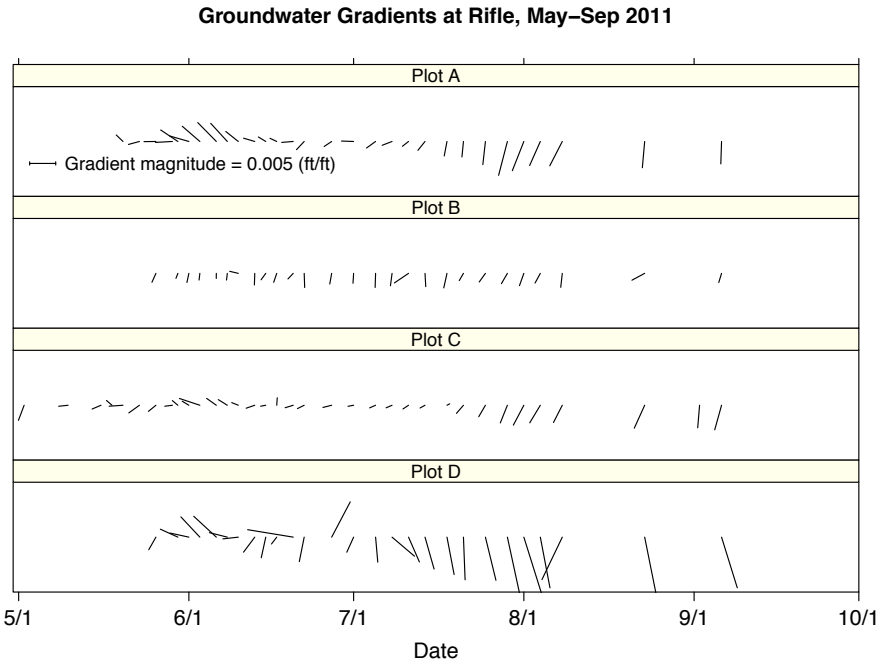

Figure 39. Hydraulic gradient (vector length) and groundwater flow direction (vector orientation) within Plots A-D over the May to September 2011 time period as calculated using depth to water elevations in selected wells.

Experimental Design and Timeline. The "Best Western" field experiment was designed to compare uranium and metal oxyanion (e.g. As, V, Mo, Se) dynamics associated with prolonged acetate amendment with regions exposed to elevated alkalinity (through NaHCO3 injection) in the absence of stimulated microbial activity. Accomplishing these objectives required groundwater amendments to be introduced at spatially distinct locations and over temporally distinct intervals (Table 8). Plot C was configured to allow introduction of NaHCO3 to an isolated portion of the aquifer (CA01-CA03), such that the impact of elevated alkalinity on metal oxyanion mobility was spatially segregated from that impacted by acetate injection (wells CG01-CG05; see Figure 37). Delineating the spatial distribution of the two injectates within Plot C was accomplished through the use of distinct conservative tracers: D2O (bicarbonate injection) and bromide (acetate injection).

Table 8: Injection parameters used for the "Best Western" experiment. *Concentrations stated are those in the injection tanks rather than groundwater concentrations following injection dilution after injection in well bores.

Injection activity	Injection wells	Date [2011]	Duration [days]	Injected volume [L]	Reagent concentration* [mM]	Isotope enrichment* [‰]
CH_3COONa NaBr	CG01-CG05	23-Aug to 3-Nov	72	4,200	150 [CH_3COO^-] 20 [Br^-]	n.a.
$NaHCO_3$ D_2O	CA01-CA03	31-Aug to 2-Dec	94	36,000	50 [HCO_3^-]	400 [^2H]

In order to prepare injectates for the "Best Western" Experiment, groundwater from a background location (well #655) was pumped into two separate injection vessels: a high-density polyethylene (HDPE) tank for the NaHCO3/D2O injectate, and a stainless steel tank for the CH3COONa/NaBr injectate. The HDPE tank (18,000L) was amended with NaHCO3 (50mM; Fisher Scientific) and D_2O (enrichment of tank groundwater by 400‰; dD of tank water ~280‰; Cambridge Isotope Laboratories, Inc.). Following addition of the reagents, the tank contents were circulated for 2 days to enhance mixing and reagent dissolution. The HDPE tank was capped and sealed with silicon caulk (to the extent possible), with the headspace continually flushed with CO_2 (100%) over the injection period. Regular measurement of tank contents indicated relatively stable values of pH (7.4±0.2; similar to site groundwater) and fluid conductivity (5200±300µS/cm; ca. two-fold greater than Plot C groundwater). Residual precipitate was visible in the bottom of the tank following the injection period; it was not removed prior to filling the second 18,000L tank. The stainless steel tank (2200L) was amended with $CH_3COONa \cdot 3H_2O$ (150mM; Sigma Aldrich) and NaBr (20mM; Sigma Aldrich) while sparging with N_2 to minimize oxygenation; circulation of each tank for one day prior to injection of each of the two tanks was used to enhance mixing of reagents. The tank remained sealed under an N_2 headspace throughout the injection period.

Both injectates were introduced to the aquifer using boreholes oriented roughly orthogonal to groundwater flow direction and spaced at 1.5 m intervals (see Figure 37). Tank contents were introduced to each injection well at two depths (3.5 and 5.5 m bgs) at rates of 180L $well^{-1}$ day^{-1} (bicarbonate tank; 3 wells) and 16L $well^{-1}$ day^{-1} (acetate tank; 10 wells). Cross-well mixing was used to disperse the injectate across the width of the injection zone, with peristaltic pumps circulating fluids (0.7 L min^{-1}) between adjacent wells through HDPE tubing. For both injectates, fluids from two wells (e.g. CA01 and CA03) were withdrawn from a depth of 6 m and injected simultaneously into an adjacent well (e.g. CA02) at a depth of 4 m to create head differences between adjacent wells; water level elevations were monitored at 15-minute intervals in all injection wells using pressure transducers, with data uploaded digitally to Rifle IFRC database. Pump directions were generally changed daily, such that individual wells served alternately as extraction and injection wells. The injection parameters and the wells used to introduce the various amendments are included in Table 8**.**

Collection and analysis of groundwater samples. *Geochemistry*: Pumped groundwater samples (12L purge volume) were obtained from monitoring wells located up and downgradient from the injection wells at roughly 2-day intervals (see Figure 37). Samples for anion and total inorganic carbon (TIC) analysis were filtered (PTFE; 0.45µm) and stored in refrigerated, no-headspace HDPE and glass vials, respectively, until analysis. Acetate, bromide, chloride, sulfate, and thiosulfate were measured using an ion chromatograph (ICS-2100, Dionex, CA) equipped with an AS18 column. TIC values (consisting of carbon derived from carbonates, hydrogen carbonates, and dissolved carbon dioxide) were determined following phosphoric acid addition while sparging and quantification of evolved CO_2 analyzer (TOC-VCSH, Shimadzu, Corp.). Samples for cation analysis (including uranium) were filtered (PTFE; 0.45µm) and acidified (0.2mL 12N HNO_3 per 20mL sample), with concentrations determined using ion coupled plasma mass spectrometry (ICP-MS) (Elan DRCII ICP-MS, Perkin Elmer, Inc.). Following analysis, residual aliquots (ca. 18mL) of the filtered, acid-preserved samples from CU01, CD01, CD04, CD14, and CD13-5 were shipped to the University of Illinois for $^{238}U/^{235}U$ isotopic analysis. Ferrous iron and aqueous sulfide concentrations were determined immediately upon sampling using the 1,10-Phenanthroline and Methylene Blue colorimetric methods, respectively (Hach Company). Samples for $d^{34}S$-sulfate and $d^{34}S$ -sulfide analysis were filtered (PTFE; 0.45µm) and preserved using 0.8M $BaCl_2$ and 1M CH_3COOZn, respectively; analysis was performed off-site at the University of California, Berkeley. Samples for water isotope analysis were filtered (PTFE; 0.45µm), added to gas-tight analytical vials (MicroLiter Analytical Supplies, Inc.), and stored at 4°C until analysis using Los Gatos Instrument's LWIA-24d Liquid Water Isotope Analytical instrument.

Samples for arsenic speciation analysis were collected from three wells exposed to acetate (CD01, CD02, CD04), one well exposed to elevated alkalinity (CD14), and one background/upgradient location (CU01). All samples were filtered (PTFE; 0.45µm) into cryogenic storage vials (2mL) and immediately flash-frozen in liquid nitrogen; duplicate samples were collected (Colorado School of Mines; Vassar College) and stored in the on-site -80°C freezer until shipment (via overnight courier) to the respective institutions on dry ice.

Groundwater quality parameters including pH, dissolved oxygen, temperature, electrical/fluid conductivity (EC), and oxidation-reduction potential (ORP) were measured continuously at 15-minute intervals in wells CD16 and LQ108 (ca. 10-m downgradient from Plot C) using multi-parameter probes (YSI, Inc.). The pH and EC of all sampled groundwaters were quantified prior to sample preservation using appropriate probes (Thermo Scientific, Inc.) calibrated at regular intervals throughout the experiment.

Proteogenomics/CryoTEM imaging: Serial groundwater filtration of planktonic biomass from well CD01 occurred before, during, and after acetate addition, with three filter sizes (1.2, 0.2, and 0.1µm) used to isolate size-dependent fractions within the stimulated (and post-stimulation) microbial community. Filtration of 100-200L of groundwater was typical, although smaller volumes were collected during peak sulfate reduction due to precipitate accumulation and filter clogging. Filters were placed in Mylar bags, sealed, frozen in liquid nitrogen, and stored at -80°C until shipment to the University of California, Berkeley (UCB) for extraction and processing; residual filter material was subsequently sent from UCB to PNNL for proteomic analysis. Aliquots of unfiltered CD01 groundwater were collected at identical time points during the first ca. 21 days of acetate amendment and flash-frozen in liquid nitrogen for eventual cryoTEM imaging.

Biogeochemistry Results. *Groundwater quality parameters and conservative tracer breakthrough:* While not a true conservative tracer, the spatiotemporal breakthrough of electrically conductive fluids within Plot C illustrates the differential impact of the tandem injections (acetate and bicarbonate) on total dissolved solids concentrations within the aquifer (Figure 40). The higher injection rates from the bicarbonate tank as compared to the acetate tank resulted in a greater flux of dissolved ions (Na^+ and HCO_3^-) per unit time and a correspondingly greater increase in total dissolved solids, hence a larger increase in EC. Furthermore, injection of non-conservative ionic species, such as acetate, which are metabolized and removed from solution, yields progressively smaller increases in EC with distance from the injection region; this effect is evident along the flow transect from CD01 to CD04 to CD07 (Figure 40). The breakthrough of electrically conductive fluids indicates a groundwater flow direction of 175-180° azimuthal from north. Breakthrough of conductive fluids entering the aquifer at wells CA01-CA03 (see Figure 37) appears to be impacting groundwater at CD06 and CD10, with the effect lessened with distance towards CD08 and CD09 – locations where the inferred flow direction would be expected to increase EC values with time. Whether the absence of an elevated EC breakthrough at CD08 and CD09 results from local variations in alluvial hydrological properties, the impact of Wasatch surface topography, or both remains to be determined. Analysis of dD data from these locations will help constrain the extent of injectate delivery from the bicarbonate tank in this region. All of the multi-level sampling wells in Plot C (CD06, CD12, CD13, and CD15) were impacted to some degree by the bicarbonate injection. Relatively modest differences in ionic strength/EC were observed as a function of depth at these locations (Figure 41) suggesting that the injected fluids were vertically using the cross-well mixing approach, as desired.

Irrespective of injectate (acetate or bicarbonate), pH values were generally between 7 and 7.7 (Figure 42), consistent with the range (7-7.5) observed in two of the upgradient monitoring wells (CU01 and CU02). The most rapid excursions in pH (to higher values) were associated with the onset of sulfate reduction

(details below) in wells impacted by acetate injection, such as CD01 and CD18, which began around 20-September-2011.

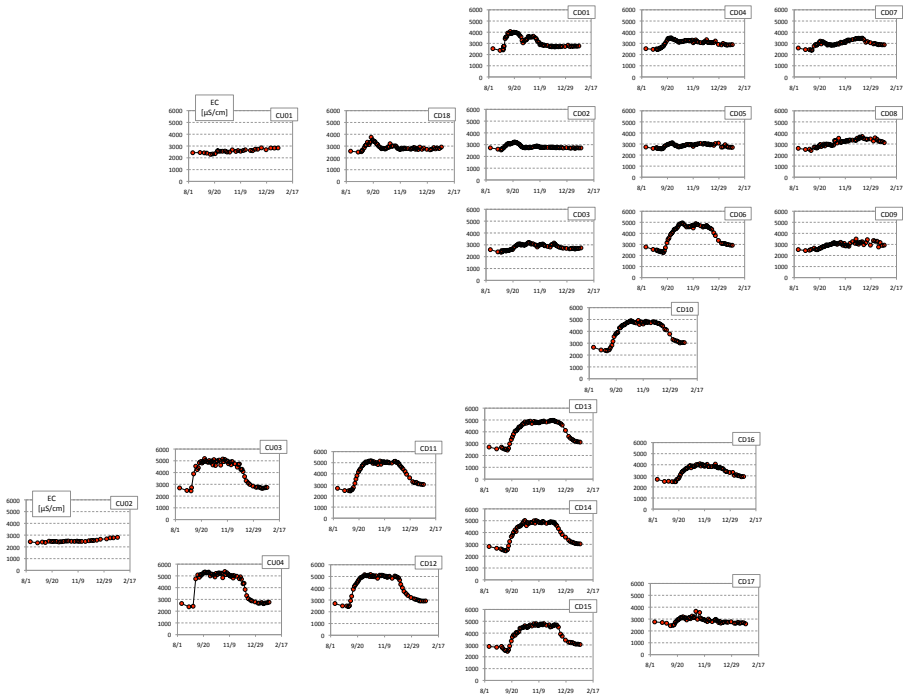

Figure 40. Change in fluid electrical conductivity (EC) at up- and downgradient well locations during the "Best Western" experiment, which spanned the 2011 and 2012 calendar years. The relative layout of the wells and the location of the wells used to inject sodium acetate/bromide (CG01-CG05) and sodium bicarbonate (CA01-CA03) is indicated in Figure 37.

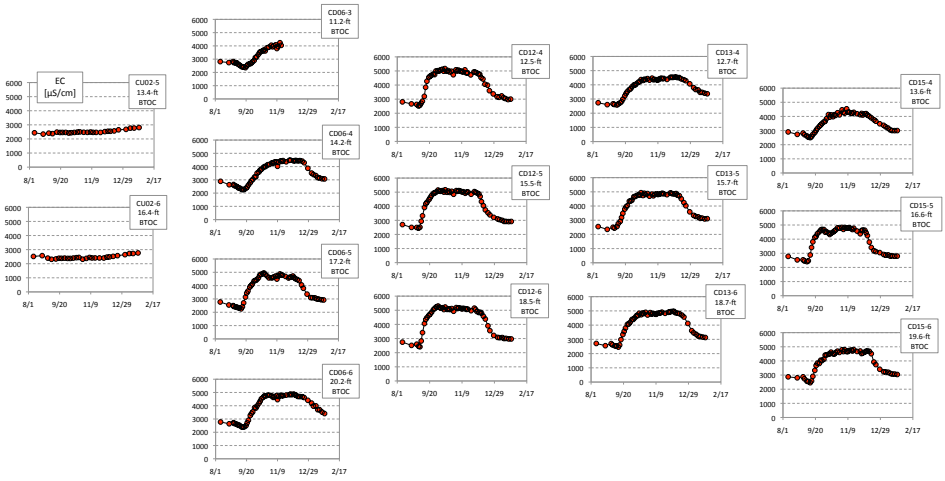

Figure 41: Change in fluid electrical conductivity (EC) at up- and downgradient multi-level sampling well locations during the "Best Western" experiment, which spanned the 2011 and 2012 calendar years. The depth below top of casing (BTOC) for each sampling port is indicated on each plot; for comparison between wells, sampling depths are plotted according to their relative position BTOC. The relative layout of the wells and the location of the wells used to inject sodium acetate/bromide (CG01-CG05) and sodium bicarbonate (CA01-CA03) is indicated in Figure 37.

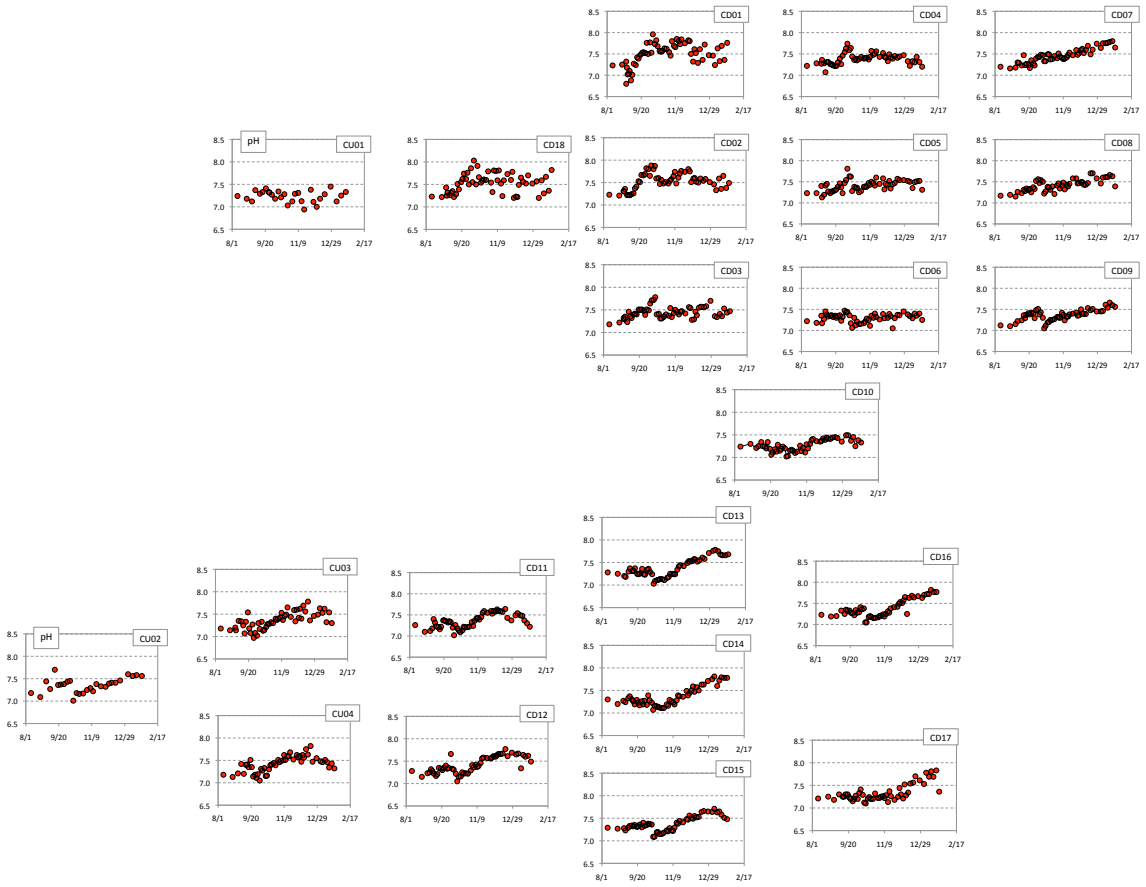

Figure 42. Change in fluid pH at up- and downgradient well locations during the "Best Western" experiment, which spanned the 2011 and 2012 calendar years. The relative layout of the wells and the location of the wells used to inject sodium acetate/bromide (CG01-CG05) and sodium bicarbonate (CA01-CA03) is indicated in Figure 37.

Bromide breakthrough at locations downgradient from the injection wells (CG01-CG05) similarly suggest a groundwater water flow direction of 175-180°, with only limited breakthrough observed along the western edge of the impacted region (e.g. CD03-CD06-CD09). Given the absence of bromide in CD01-CD17, only wells downgradient from the region of injection are shown (Figure 43). Given the injection tank concentration of 20mM and an expected dilution factor of 1:10 based on injection rate, the maximum concentration of bromide observed at CD01 (ca. 3mM) suggest either preferential flow and/or non-uniform injection rates into each of the five injection wells; periodic quantification of acetate and bromide concentrations in each of the five injection wells during amendment generally found the greatest concentrations in CG01 and CG02, with lower concentrations in CG04 and CG05 (data not shown). This observation suggests that comparisons of conservative tracer breakthrough from year to year may be confounded by differences in injection rates due to clogged injection tubing, degraded peristaltic pump injection tubing, or other experimental factors that are difficult/impossible to replicate precisely on an annual basis. Furthermore, installation of new wellbores (or collapsed coring locations) between annual experiments within the same flow cell appears capable of impacting breakthrough patterns; following the installation of CD18 in July 2011, bromide breakthrough patterns at wells downgradient (e.g. CD05) were retarded relative to their 2010 patterns (data not shown). Clearly, care must be taken when quantitatively comparing changes in breakthrough patterns from year to year and attribution of such changes to definitive causes (e.g. pore-scale biogeochemical changes, such as mineral precipitation and pore throat occlusion).

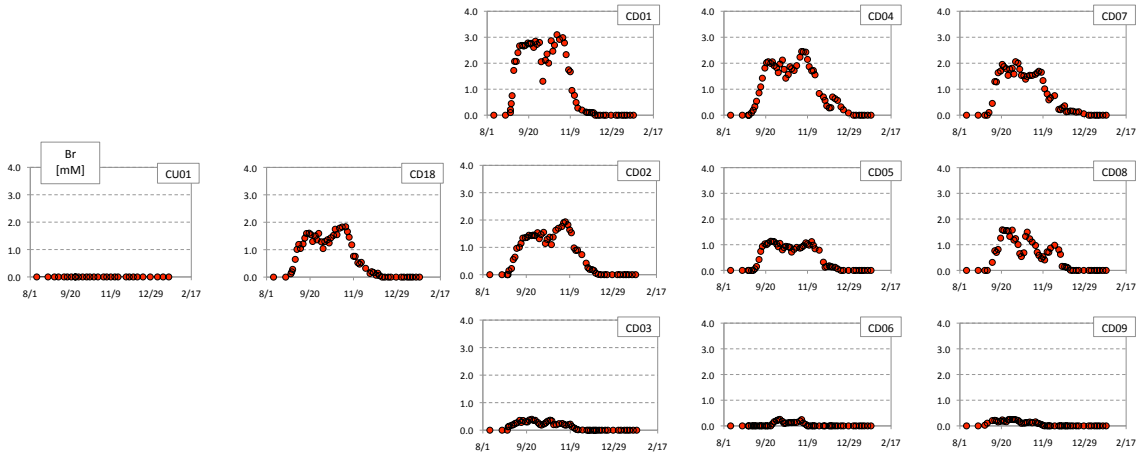

Figure 43: Change in bromide concentration at well locations up- and downgradient from injection wells CG01-CG05 during the "Best Western" experiment, which spanned the 2011 and 2012 calendar years. The relative layout of the wells is indicated in Figure 37.

Acetate injection: As a way of replicating the "Big Rusty" [2008] acetate-amendment experiment in Plot A and to enable a greater temporal resolution of proteogenomic changes accompanying biostimulation, acetate injection occurred over a period of 72-days. As noted, size-resolved proteogenomic sampling of groundwater from CD01 occurred before, during, and after acetate amendment, which was delivered to wells within Plot C in much the same manner as bromide (Figure 44). Specifically, the highest concentrations of acetate were observed at CD01 and along the CD01-CD04-CD07 wellbore transect. At no point during the injection period did acetate concentrations become limiting due to complete oxidation. The low value inflection in acetate concentrations observed at most locations corresponds to the 2-day interval between the first and second tanks when injection was halted due to tank re-filling and mixing.

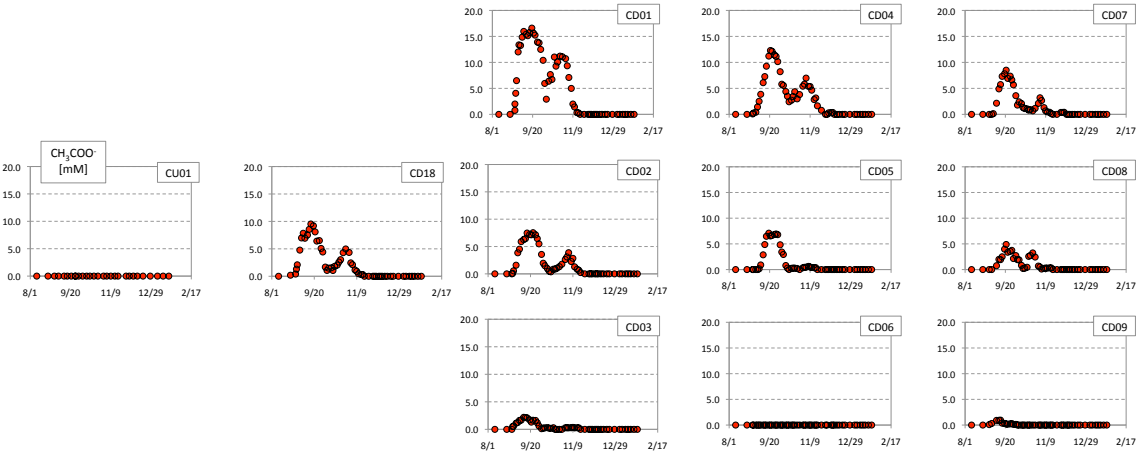

Figure 44: Change in acetate concentration at well locations up- and downgradient from injection wells CG01-CG05 during the "Best Western" experiment, which spanned the 2011 and 2012 calendar years. The relative layout of the wells is indicated in Figure 37.

Early breakthrough of acetate corresponded to an initial increase in Fe(II) concentrations (Figure 45), presumably related to the onset of microbial iron reduction and stimulation of metal reducing bacteria, such as members of the *Geobacteraceae*, as observed during previous experiments at the site. Additionally, elevated Fe(II) concentration may partially result from the onset of microbial sulfate reduction and the abiotic reduction of Fe(III) minerals by aqueous sulfide. As observed repeatedly at the

site, removal of sulfate (Figure 46) from groundwater tied to the activity of sulfate reducing bacteria is non-stoichiometric with respect to the amount of aqueous sulfide produced (Figure 47). This presumably results from the multiple sinks for aqueous sulfide within the aquifer, including precipitation of metal sulfides (e.g. FeS) and reduction of ferric oxide minerals, yielding Fe(II), elemental sulfur, and (perhaps) polysulfide and thiosulfate. For the first time, concentrations of thiosulfate were quantified during acetate amendment at Rifle, with production patterns mimicking those of aqueous sulfide, albeit at lower absolute concentration (Figure 48).

Dissolved gas measurements were made during and after the amendment period in four wells (CU01, CD01, CD04, and CD18); however, due to instrument problems, dissolved gas analysis only began near the end of the injection period (18-November-2011) when acetate concentrations were nearing their minima (see Figure 44). Concentrations of dissolved CH_4, CO_3, CO, and H_2 at well CD04 over the interval from 18-November-2011 to 01-January-2012 are shown in Figure 49. Although acetate levels fell below detection at CD04 by 28-November-2011, groundwater CH_4 concentrations persisted at levels ranging from 10-100µM, falling from a maximum value of ca. 150µM on 23-November-2011. Methane concentrations at CD01 were generally lower than those at CD01; however, the presence of CH_4 in groundwater indicates the onset of methanogenesis during "Best Western" and the inferred presence of Archaeal biomarkers in the proteogenomic samples; analysis of these samples is ongoing.

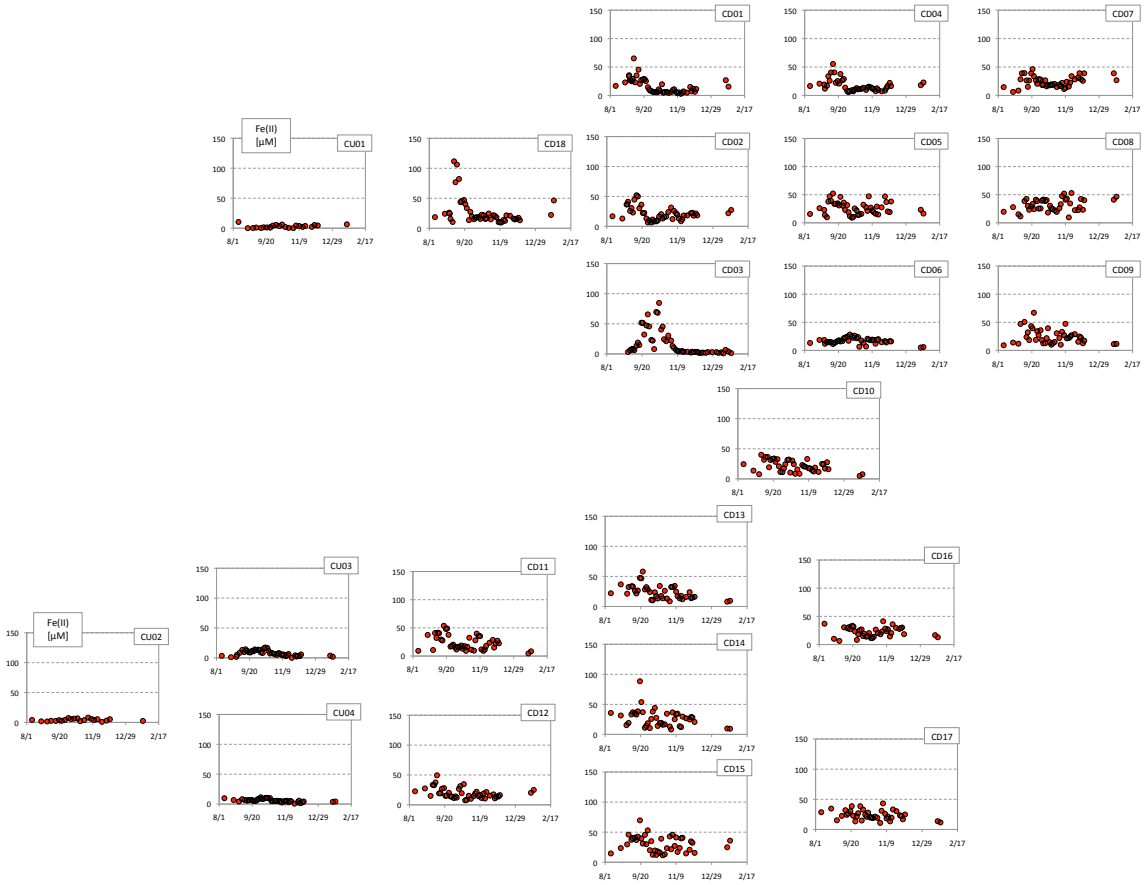

Figure 45: Change in ferrous iron concentration [Fe(II)] at up- and downgradient well locations during the "Best Western" experiment, which spanned the 2011 and 2012 calendar years. The relative layout of the wells and the location of the wells used to inject sodium acetate/bromide (CG01-CG05) and sodium bicarbonate (CA01-CA03) is indicated in Figure 37.

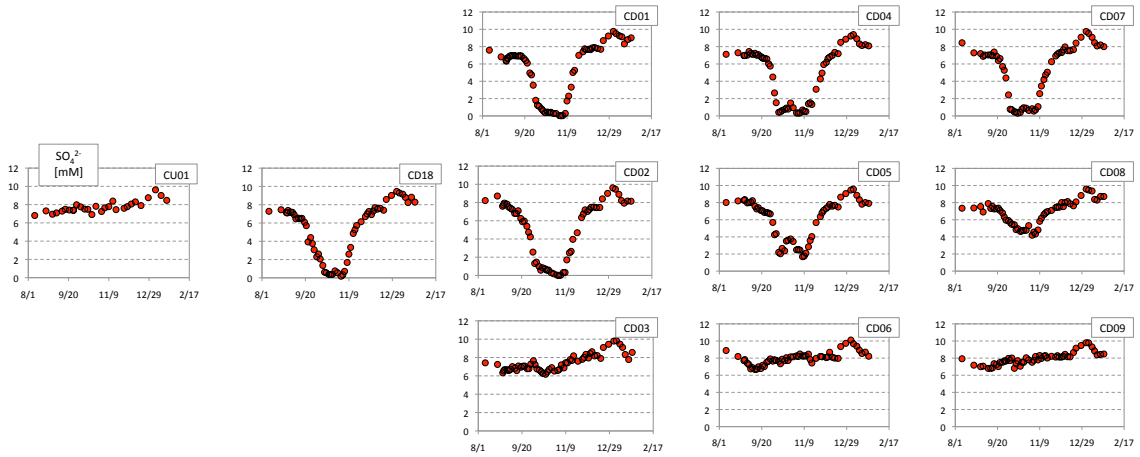

Figure 46: Change in sulfate concentration at well locations up- and downgradient from injection wells CG01-CG05 during the "Best Western" experiment, which spanned the 2011 and 2012 calendar years. The relative layout of the wells is indicated in Figure 37.

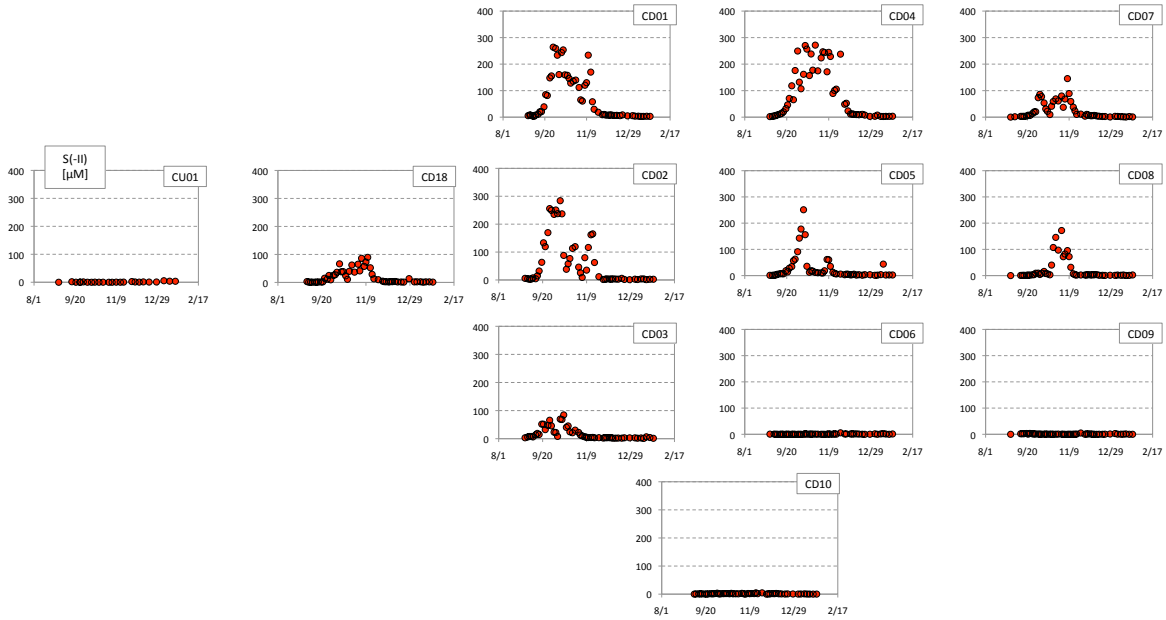

Figure 47: Change in aqueous sulfide concentration [S(-II)] at well locations up- and downgradient from injection wells CG01-CG05 during the "Best Western" experiment, which spanned the 2011 and 2012 calendar years. The relative layout of the wells is indicated in Figure 37.

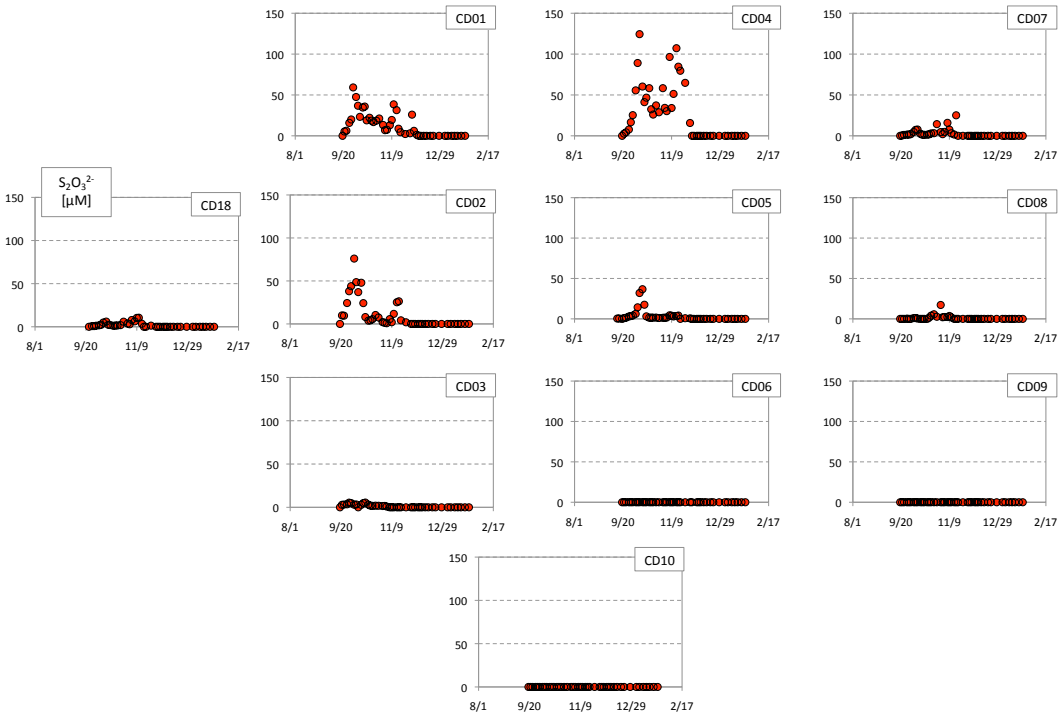

Figure 48: Change in thiosulfate concentration at well locations up- and downgradient from injection wells CG01-CG05 during the "Best Western" experiment, which spanned the 2011 and 2012 calendar years. The relative layout of the wells is indicated in Figure 37.

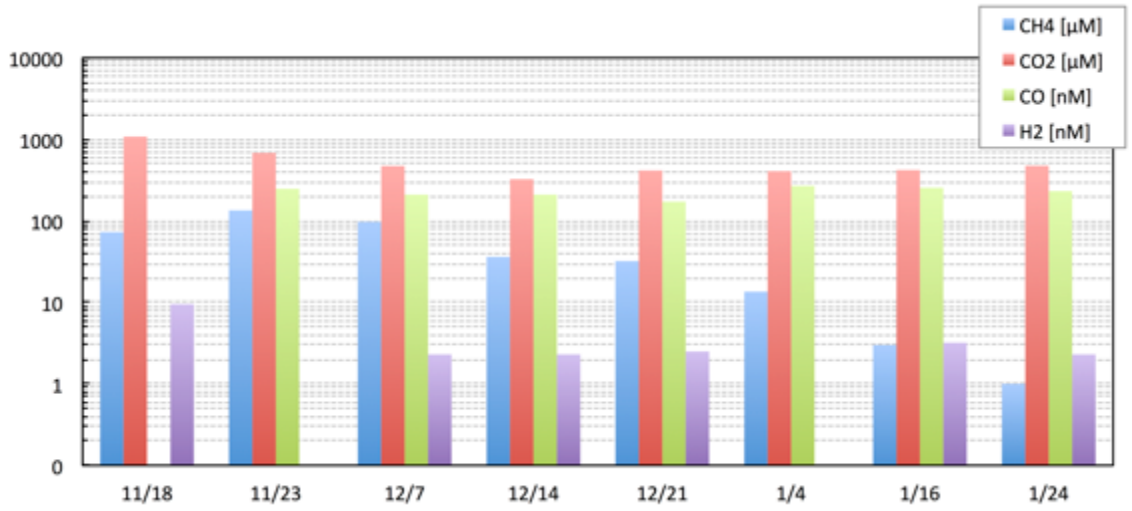

Figure 49: Change in select dissolved gas concentrations at well CD04 during the latter part of the "Best Western" acetate-injection and dates after acetate concentrations fell below detection on 28-November-2011.

Arsenic dynamics: Comparing the behavior of arsenic in groundwater under various geochemical conditions accompanying biostimulation (e.g. iron vs. sulfate reduction) was a principle objective of the "Best Western" experiment. More specifically, associating changes in total dissolved arsenic with specific changes in arsenic speciation was performed in conjunction with Dr. Jim Ranville and Valerie Stucker (Colorado School of Mines) as part of their DOE-funded project on coupled arsenic and uranium dynamics with Dr. Brian Mailloux (Barnard College) and Dr. Alison Keimowitz (Vassar College). Ion chromatography coupled to inductively coupled plasma – mass spectrometry was investigated as a method to determine the aqueous arsenic speciation. As observed repeatedly at Rifle, dissolved arsenic concentrations increase only modestly during periods of iron reduction, followed by larger increases once sulfate reduction becomes the dominant metabolic pathway and aqueous sulfide concentrations increase; data from CD01 illustrate the relationship between total dissolved arsenic (max. 600ppb or 8µM) and other aqueous constituents during "Best Western" (Figure 50). In contrast, upgradient locations (e.g. CU01) exhibit relatively stable levels of arsenic (ca. 130ppb or 1.7µM; data not shown), with more than 90% present as arsenate and only a small amount of arsenite. Associated with the elevated release of arsenic at CD01 during sulfate reduction, four additional arsenic species are present. The vast bulk of these species are thioarsenic compounds (mono-, di-, tri-, and tetrathioarsenate), suggesting a strong correlation between arsenic release, thioarsenic speciation, and elevated sulfide concentrations. Interestingly, locations immediately downgradient of CD01 (CD04 and CD07) exhibited much lower increases in total dissolved arsenic with time, even though aqueous sulfide concentrations were similar to those observed at CD01. This observation suggests that advection of arsenic-laden groundwaters may be spatially limited, with arsenic released at one location (e.g. CD01) being titrated from solution over distances of less than 2.5m through a variety of processes, including adsorption and precipitation as arsenic sulfides. Additional pH-Eh controls on arsenic speciation and solubility need to be examined, given the elevated pH values observed at CD01 during the period of maximum release (7.5-8) as compared to those at CD04 and CD07 (7.0-7.5; see Figure 42).

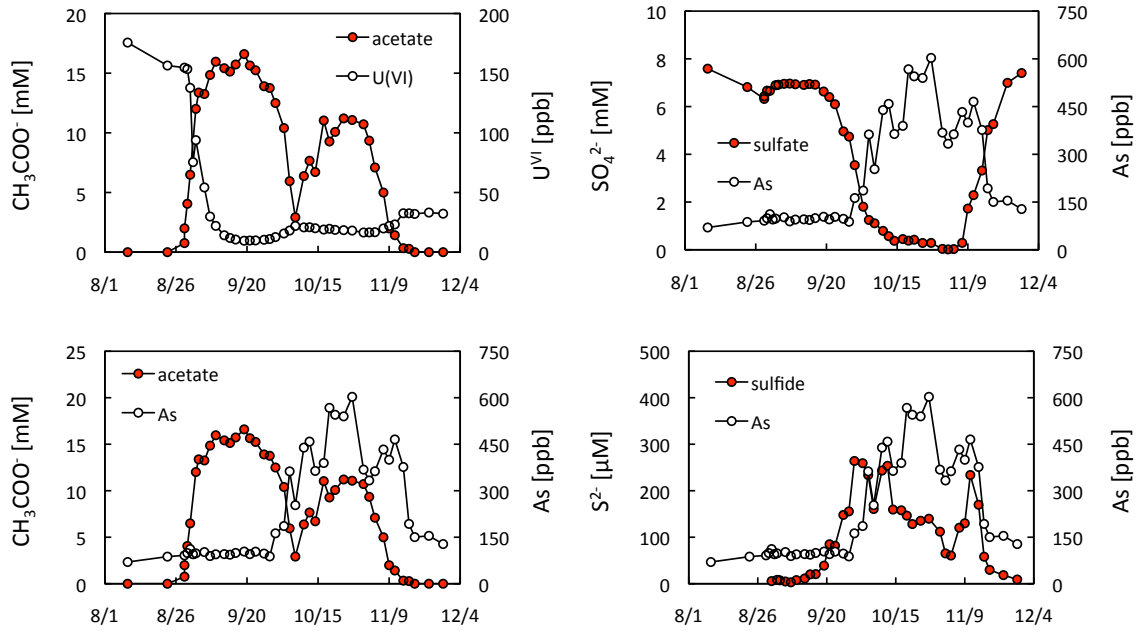

Figure 50: Change in total dissolved arsenic at well CD01 as compared to a variety of aqueous constituents (uranium, acetate, sulfate, and aqueous sulfide) during the "Best Western" experiment.

Bicarbonate injection: The length of sodium bicarbonate injection during "Best Western" exceeded all previous such injections at Rifle, enabling refinement of multi-rate mass transfer models describing uranium (U) desorption from diffusion-limited domains, such as those associated with fine-grained sediments. Additionally, bicarbonate injection during "Best Western" was not associated with spatially overlapping acetate injection, as occurred during the "Super 8" experiment. Rather, the bicarbonate-induced desorption of U and other metal oxyanions was allowed to proceed to its maximum extent over the course of 92 days. As observed during "Super 8," the most labile fraction of U desorbed rapidly, with U concentrations increasing by two- to four-fold within 7-10 days of bicarbonate reaching a given well location. Data from CD14 are shown in Figure 51, with other locations exhibiting similar desorption trends and both larger and smaller peak U concentrations. Uranium desorption continued over the 92-day injection period, albeit at progressively lower rates.

The temporal behavior of other metal oxyanions of interest (vanadium, arsenic, and molybdenum) associated with the bicarbonate flush is also shown in Figure 51, as are comparative data from a biostimulated location (CD01). While rates of vanadium (V) and molybdenum (Mo) desorption at CD14 are initially slower than those for U, concentrations of both metals continue to increase for most of the injection period. It is not yet known whether desorption of V and Mo occurs primarily as a result of the formation of soluble metal-carbonato species (i.e., as with Ca-U-CO3 species) or whether exchange with HCO_3^- ions displaces formerly sorbed V and Mo oxyanions. Unlike either U or V, temporal trends for Mo at CD14 exhibit a bimodal pattern, perhaps indicative of two distinct sorption reservoirs. Ion exchange (by Na^+) may also impact Fe(II) dynamics within the bicarbonate-impacted portion of the flow cell, with small but quantifiable increases in Fe(II) accompanying injection of sodium bicarbonate (see Figure 45). Persistence of Fe(II) during bicarbonate injection indicated that the injected fluids remained largely un-impacted by molecular oxygen while in the 18,000L tank, otherwise titration of Fe(II) following introduction of oxidized injectate would have been expected.

Of particular note is the difference in arsenic behavior between biostimulated and bicarbonate-amended locations (Figure 51). In contrast to the dramatic increase in arsenic concentration accompanying sulfidogenesis, relatively modest increases in dissolved arsenic were observed at CD14 as a result of the bicarbonate injection; arsenic concentrations at CD14 roughly doubled from initial values of ca. 40ppb during the injection period. As with V and Mo, it is not yet known whether this increase in concentration is primarily related to ion exchange or some other process. Temporal changes in Mo concentrations varied between biostimulated and bicarbonate-impacted locations, with Mo levels falling in conjunction with the onset of sulfate reduction. Given that molybdate and sulfate are structural analogues, removal of Mo from groundwater (as molybdate) likely occurred in conjunction with sulfate respiration by sulfate reducing bacteria (SRB). Prior to starting acetate injection during "Best Western," vanadium concentrations at CD01 remained significantly below their pre-stimulation levels in 2010, the first year that acetate-amendment occurred in Plot C. Before starting biostimulation as part of "Super 8," background vanadium concentrations at CD01 were ca. 2300ppb or 48μM, falling rapidly to very low levels (10-20ppb or 0.1-0.4μM) as a result of just 23 days of acetate amendment (data not shown). While having rebounded slightly by the beginning of "Best Western," vanadium levels remained very low (ca. 70ppb or 0.9μM) relative to their initial, un-stimulated values. Fluctuations in vanadium values at CD01 during acetate amendment (Figure 51) are most likely tied to the same processes impacting vanadium desorption at CD14. Where rates of desorption exceed rates of reductive immobilization, vanadium concentrations would be expected to increase. Such an effect may have occurred at CD01 once acetate oxidation coupled to sulfate reduction began to generate large quantities of 'biogenic' alkalinity (as bicarbonate).

While beyond the scope of "Best Western" or other field activities at Rifle, results presented in Figure 51 may offer some insight into the relative merits of competing uranium remediation approaches at sites like Rifle where a variety of redox-sensitive metals and metalloids may be present. For the tenth consecutive

season, acetate amendment resulted in rapid and highly effective removal of uranium from groundwater at multiple downgradient locations. Removal of uranium persists so long as acetate delivery is maintained; however, other deleterious side effects can accompany prolonged acetate injection, such as enhanced release of arsenic to groundwater. Were it possible to minimize the extent of sulfate reduction, uranium (and vanadium) bioreduction might be maintained in a way that minimizes arsenic release by preventing the formation of highly mobile thioarsenic species. Thus far, lab and field experiments have been unable to forestall the activity of SRB so long as sulfate is present and suggesting that sulfidogenesis is unavoidable outcome of organic carbon additions to the Rifle subsurface. Alternative uranium remediation techniques, such as bicarbonate flushing, also provide methods to decrease uranium concentrations without the negative impact on arsenic contamination.

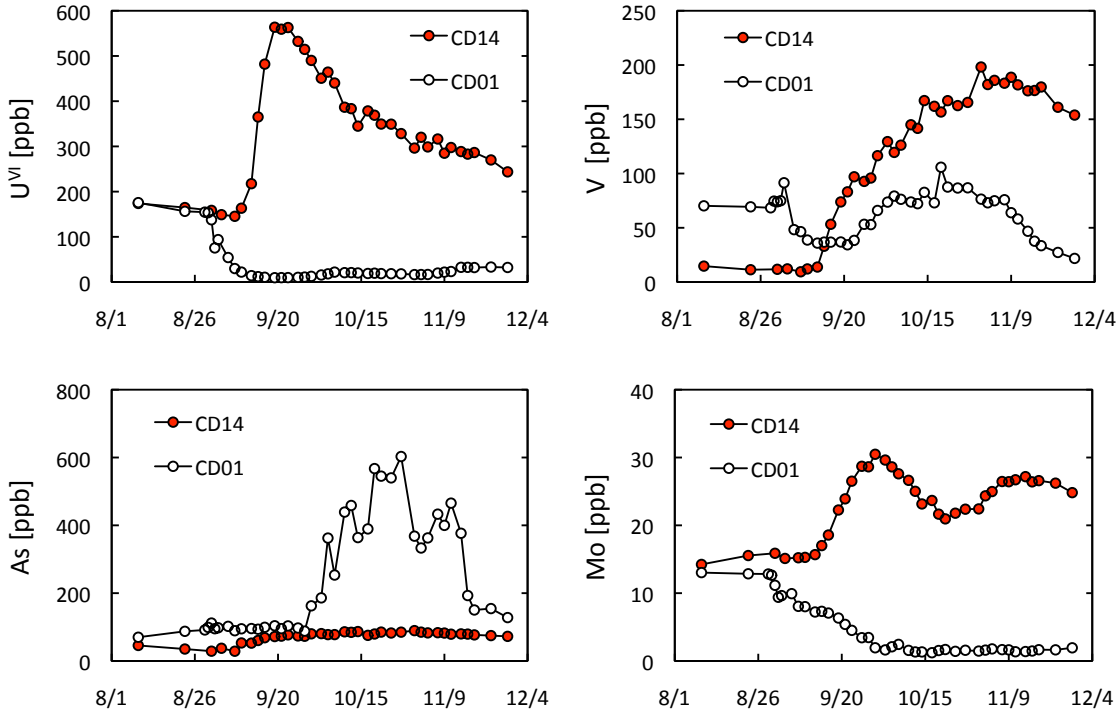

Figure 51: Comparison of temporal changes in uranium, vanadium, arsenic, and molybdenum concentrations at wells CD01 (acetate-impacted) and CD14 (bicarbonate-impacted) during the "Best Western" experiment.

Geophysical Monitoring. The spectral induced polarization (SIP) geophysical method – also referred to as complex conductivity – involves acquisition of voltage magnitude and phase data using a network of electrodes located at the ground surface or in boreholes. Previous experiments at the Rifle IFRC site have shown the SIP method to be a useful means for monitoring the *in situ* activity of subsurface microorganisms and the end products of their metabolism, especially under conditions where their activity is stimulated through organic carbon addition (i.e., biostimulation). Geophysical data acquisition during "Best Western" was focused primarily on decoupling the underlying mechanisms responsible for generating anomalous complex conductivity signatures associated with such activity. Specifically, we sought to separate the contribution of purely abiotic processes, such as ion exchange associated with introduction of exchangeable ions (e.g. Na^{+}) and carbonate mineral precipitation, from biologically mediated processes (e.g. biomineral formation) on complex conductivity signatures.

SIP data were collected using casing-affixed Cu^0 electrodes along two wellbore transects oriented roughly parallel to groundwater flow direction: CG02-CD01-CD04-CD07 (acetate amendment) and CA01-CG07-CD13-CD16 (bicarbonate amendment). Data were acquired at multiple time points before, during, and after the amendment experiments using a Zonge GDP-32(II) and a modified dipole-dipole acquisition scheme. SIP data were inverted using CRTomo, which utilizes an algorithm that solves directly for conductivity magnitude and phase by consequent adoption of complex calculus, with the region of interest represented as a two-dimensional distribution of magnitude and phase values. Following inversion, magnitude and phase data were converted to their complex notation (i.e., the real and imaginary components of conductivity, Figure 52). The real component (σ') accounts for ohmic conduction (i.e., that associated with energy loss and dominated by ionic/electrolyte conduction within the pore space), whereas the imaginary component (σ") is related to polarization (i.e., energy storage or charge separation) related to accumulation of charge and/or charge transfer reactions along the fluid-mineral interface. Increases in σ" have been shown to be sensitive to regions of (semi)conductive mineral precipitation (e.g. FeS) and concomitant increases in electroactive ion concentration, such as Fe(II), in the vicinity of such mineral accumulation. In contrast, increases in σ' are primarily related to changes in the ionic strength of the pore fluids, which allows the method to be used to delineate the spatiotemporal distribution of conductive injectates. Data acquired during "Best Western" represents the first spectral data (i.e., multi-frequency data; 0.0625-128Hz) collected between borehole/subsurface electrodes at Rifle, with the intent of improving the spatial resolution as compared to previous SIP datasets where electrode coverage was limited to the ground surface.

As presented in Figure 52, changes in both σ' and σ" accompanied acetate amendment along the CG02-CD01-CD04-CD07 transect. Data acquired prior to starting acetate injection (31-August-2011) revealed a conductivity (σ') profile typical of the Rifle subsurface, with lower conductivity values characteristic of the (un)saturated alluvium from 2-6m underlain by the more conductive, partially saturated silt- and mudstones of the Wasatch Formation. At a later time point (17-October-2011), elevated conductivity values were observed throughout the wellbore transect as a result of acetate/bromide injection; σ' increases were greatest within a relatively thin layer (ca. 4m below ground surface) located between CD01 and CD04. Little change in σ' as a function of frequency was observed at either time point, with variations in σ' being generally uniform from low (0.06Hz) to high (16Hz) frequency. In contrast, large changes in σ" were observed as a function of frequency between the two time points; higher frequency data appear to constrain the anomalous σ" to a more restricted vicinity nearest the injections wellbores (here CG02), as compared to lower frequency data, where the σ" is more diffuse. Based on previous field SIP experiments at Rifle and laboratory SIP experiments using acetate-stimulated Rifle sediments, the large increases in σ" on 17-October-2011 (ca. 50-days after acetate injection began) are related to the precipitation and accumulation of iron monosulfides associated with concurrent iron and sulfate reduction. For the first time, SIP data collection appears to have constrained the location of this precipitation front with a high degree of resolution and without the need for post-injection sediment recovery. Such data will be used as part of the LBNL SFA program to constrain precipitation locations within reactive transport models describing biogeochemical processes during "Best Western."

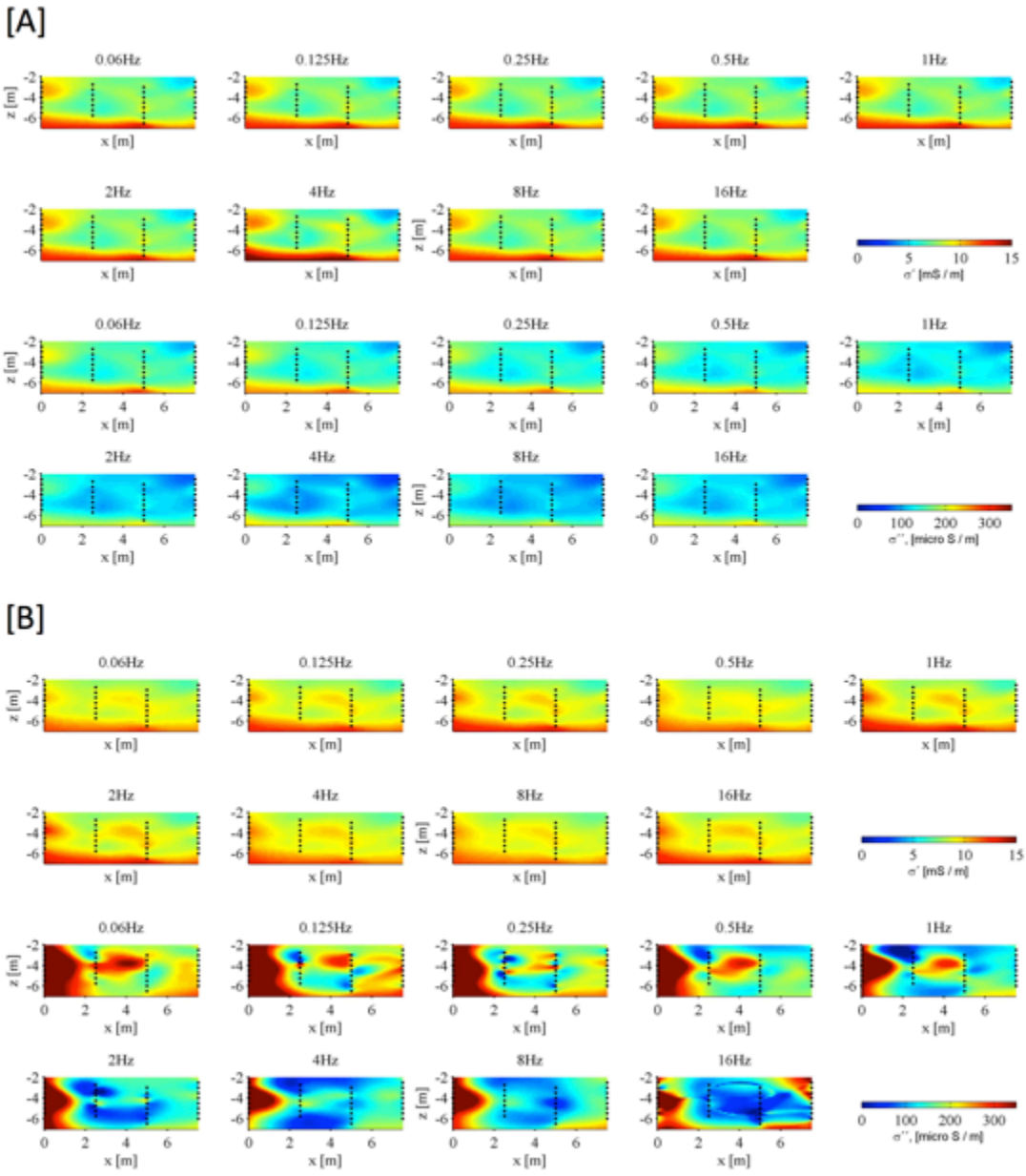

Figure 52: Change in the real (σ') and imaginary (σ") components of conductivity along the CG02-CD01-CD04-CD07 transect, which was located downgradient of acetate amendment; wellbores and electrode locations denoted by vertical dashed lines. Data were collected [A] prior to acetate amendment (31-August-2011) and [B] ca. 50-days after injection began (17-October-2011).

In contrast to regions exposed acetate amendment, changes in σ" associated with the bicarbonate injection were less definitive (Figure 53). Where increases in σ" occurred, they occurred in close proximity to regions of pre-existing σ" anomalies, with such 'baseline' anomalies likely the result of silt- and clay-rich sediments. Although laboratory data have shown a correlation between σ" increases and carbonate

mineral precipitation – something that could have occurred in association with bicarbonate injection – the effect may also be explained by significant ion exchange occurring during the injection. Specifically, large quantities (ca. 50mM) of Na^+ ions displace those of Ca^{2+} and Mg^{2+} that occupy clay mineral surfaces and balance the net negative surface charge of the clays. Exchange of a less mobile, more strongly bound ion (Ca^{2+}) with a more mobile ion (Na^+) might be expected to result in greater polarization – manifest as an increase in σ" – due to the greater charge separation that can occur for the more weakly bound ion (Na^+) under an applied field. Laboratory experiments designed to confirm the ion exchange mediated polarization process are currently underway using Rifle sediments. Similar to the change in σ' values with time observed along the acetate-impacted transect, large increases in σ' were observed along the CA01-CG07-CD13-CD16 transect. Consistent with the larger increases in EC observed within the bicarbonate-impacted portion of the flow cell (see Figure 40), increases in σ' observed in this region were also much larger. In general, increases in σ' were vertically uniform, corroborating the vertical EC profiles discussed earlier.

Comparison of the spectral response observed between the two regions (acetate vs. bicarbonate) is facilitated by averaging the change in the phase response (i.e. the offset between the applied and measured voltage) for one or more regions of the two-dimensional panels presented in Figures 52 and 53. The phase response (a direct measure of polarization magnitude) may then be plotted as a function of frequency at a variety of time points for data collected along the two transects, with the results constituting the characteristic spectral response of sediments exposed to acetate or bicarbonate injection. Two very different patterns result (Figure 54) when looking at the average spectral response of sediments within the first 2m of the injection boreholes (CG02 and CA01 for the acetate- and bicarbonate- impacted panels, respectively). Whereas the spectral response of sediments downgradient from CA01 is largely replicable with time, the response downgradient from CG02 varies dramatically with time. Indeed, it appears that diagnostic SIP signatures exist for each of the two processes, perhaps allowing for discrimination of such processes where they occur in tandem. Development of a suite of diagnostic indicators (e.g. hydrological, isotopic, geophysical) is a stated objective of LBNL's SFA program under the Evolution Challenge, and this differential SIP response joins fractionation of $^{34}S\text{-}SO_4^{2-}$ associated with even small levels of microbial sulfate reduction as a definitive diagnostic indicator of specific subsurface biogeochemical processes.

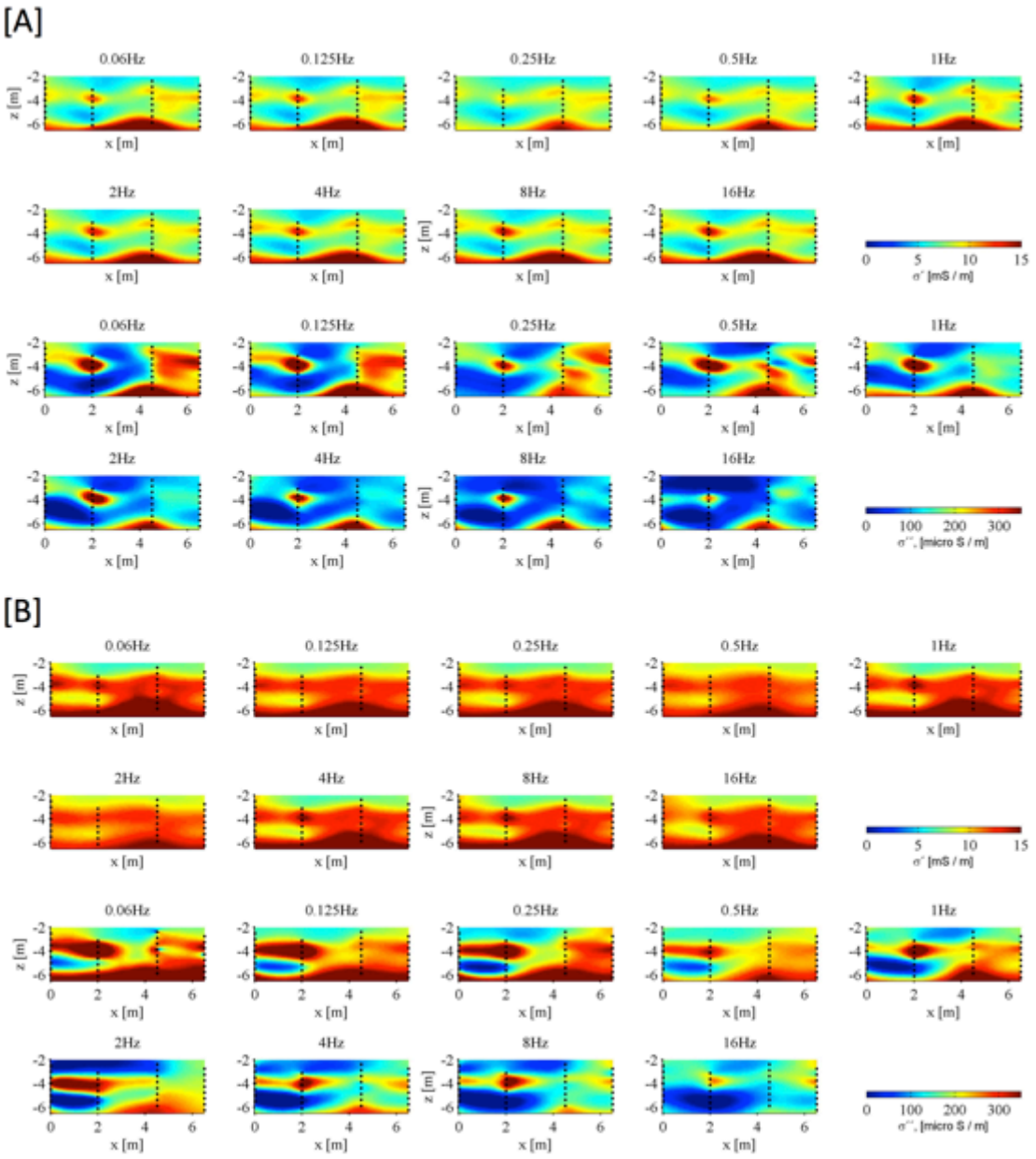

Figure 53: Change in the real (σ') and imaginary (σ") components of conductivity along the CA01-CG07-CD13-CD16 transect, which was located downgradient of bicarbonate amendment; wellbores and electrode locations denoted by vertical dashed lines. Data were collected [A] prior to acetate amendment (31-August-2011) and [B] ca. 50-days after injection began (17-October-2011).

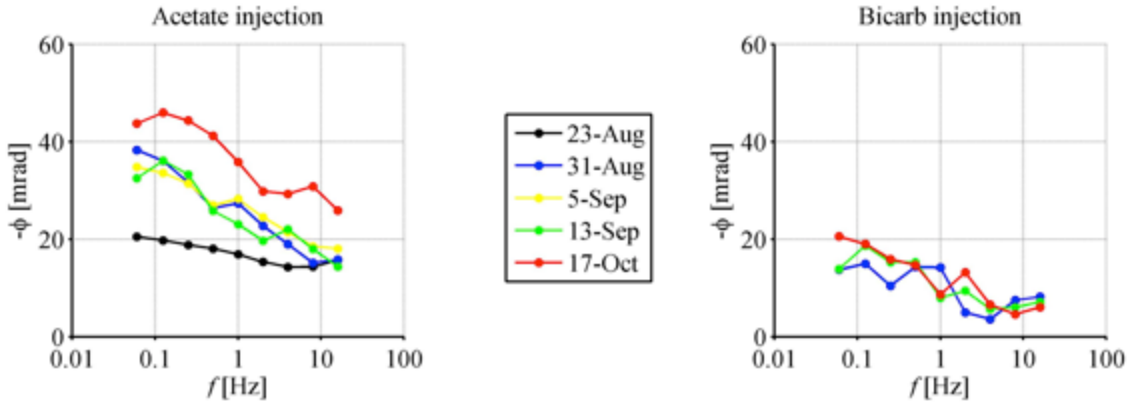

Figure 54: Change in the characteristic spectral response of sediments within 2m of the acetate (left) and bicarbonate (right) injection zones at multiple time points over the course of injection. Sulfate reduction, accumulation of aqueous sulfide, and titration of Fe(II) from groundwater (as FeS) was ongoing along the acetate-impacted transect between 13-September and 17-October, as indicated in Figures 45-47.

Microbiology. During the "Best Western" experiment, a follow-up series of samples were recovered from the same well that "Super 8" biomass samples had been collected (Well CD-01, Figure 55). To date, DNA has been extracted from all filters and we intend to submit 10 time points (2 from 2010 and 8 from 2011) for community sequencing. This sequencing will include all filters (1.2, 0.2, and 0.1 μm) for each time point in order to minimize size bias and capture the overall diversity of the planktonic biomass. Metagenomic reconstructions will underpin both community proteomic and transcriptomic efforts planned for Spring 2012. These samples were obtained with a number of aims:

1. To investigate potential "memory effects" within the microbial community following primary biostimulation that may affect the response of the bacterial population to secondary carbon amendment.
2. To obtain enriched biomass containing putative "nano" microorganisms that may represent Candidate Divisions previously reconstructed in an analogous secondary biostimulation experiment in 2008. In addition to 1.2 and 0.2 filters, we added a third 0.1 um filters to capture any 'nano'-biomass. This data will allow more targeted characterization of the physiology of these uncultivated organisms using transcriptomic and proteomic data based on metagenomic reconstructions.
    a. Preliminary data from 2011 using Cryo-EM (Figure 56) and clone library analysis (Figure 57) confirmed the presence of small OD1 and OP11 bacteria were present in the aquifer.
3. To obtain the first temporal microbiological dataset from the same well over two periods of acetate amendment. We have collected biomass samples not only spanning two years (2010 and 2011), but also from a well with biomass collection past the onset of methane production during secondary stimulation, to begin to elucidate organic carbon turnover and cycling in the aquifer from a proteogenomic perspective.

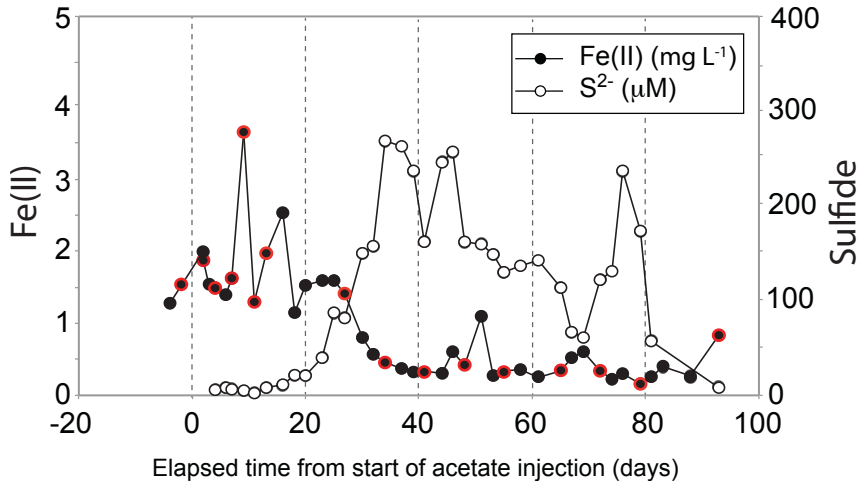

Figure 55. Fe(II) and sulfide geochemistry for well CD01 during the period of acetate amendment of the 2011 biostimulation experiment. Red circles indicate time points where planktonic biomass for metagenomics, transcriptomics, and proteomics was collected on a series of filters (1.2 μm, 0.2 μm, and 0.1 μm).

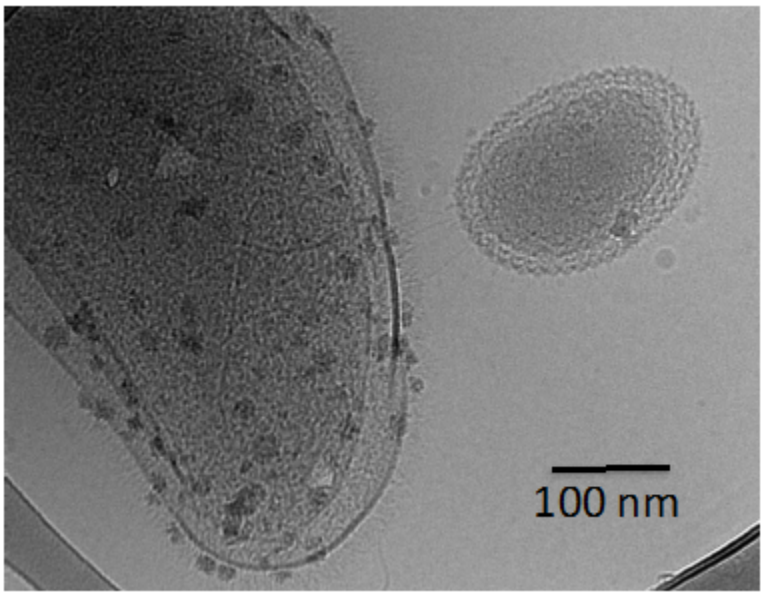

Figure 56. 'Nano' bacteria are visualized during secondary stimulation (B. Luef). Cryogenic transmission electron microscopy (cryo-TEM) with 2D projection collected on biostimulated groundwater (09/03/2011) during iron reduction. This *in situ* imaging captured a ~250 nm bacterium with an s-layer containing cell envelope (right) along side a larger (>1 μm) bacterial cell with nano-particle aggregates attached to the outer membrane (left).

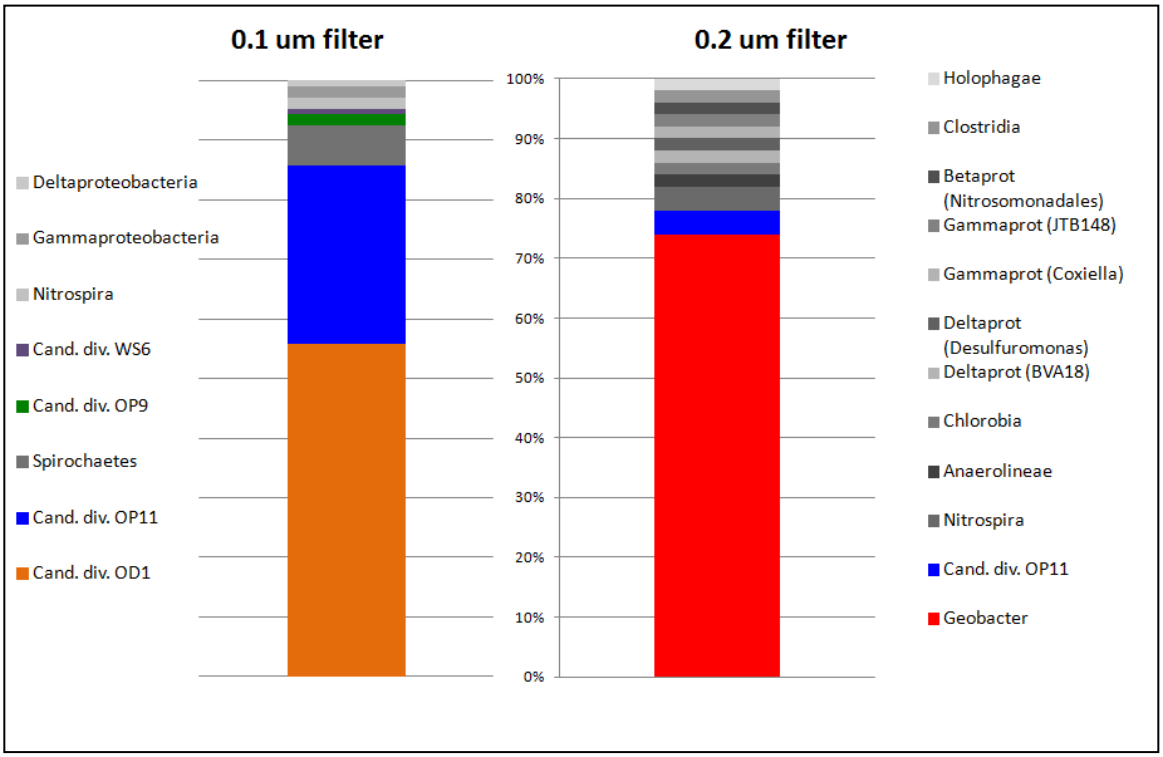

Figure 57. Clone library analysis of the 09/03/11 groundwater community confirmed that reconstructed 2008 secondary stimulation genomes from the Candidate Division OD1 and OP11 bacteria are present in the Rifle aquifer in secondary stimulation during 2011. The enrichment of the Candidate Divisions on the 0.1 μm (not 0.2 μm) filter confirms the small cell size predicted from the genome size obtained by 2008 metagenomic efforts.

Initial results clearly show the relationship between microbe size and preponderance of species present in the planktonic phase, at least during a second stimulation such as "Best Western." Proteogenomics studies planned for 2012 will enable us to clearly establish community and metabolic changes that occurred as the "Best Western" experiment proceeded. These results will be integrated with the geochemistry results described above.

Subtask F-11 Uranium plume dynamics

This subtask was initiated in 2010 as a preliminary response to the observed persistence of the uranium groundwater plume and the need for a scientific assessment of the sources of uranium in groundwater at the Rifle IFRC. Underlying this subtask are four hypotheses to explain the persistence of the U(VI) plume (Figure 58):

A. Downward flux of U from the vadose zone that is entrained into the aquifer during times of high water table associated with high runoff in the Colorado River
B. Mobilization of reduced U from naturally bioreduced zones
C. Slow oxidation of U(IV) dispersed through the saturated zone
D. Influx of natural background U(VI) from upgradient groundwater recharge

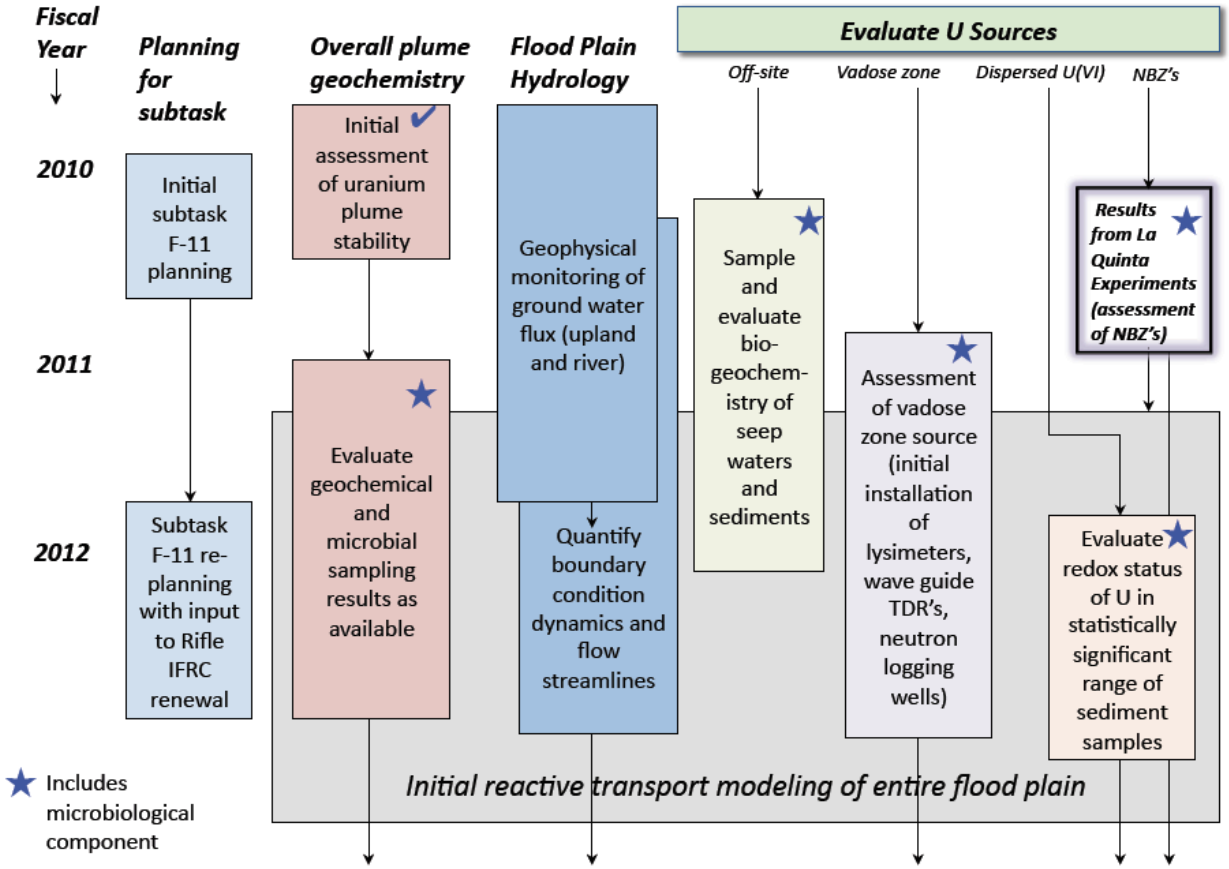

Figure 58. Activities map of Subtask F-11 "Uranium Plume Dynamics."

Here we report on selected activities in Subtask F-11, focusing on determining if the vadose zone is a significant source of U at Rifle and on determining if in-well flow may be impacting U concentration measurements in wellbores. Significant progress was made in these areas, demonstrating that even under conditions of extended water table rise, U concentrations do not increase in the upper parts of the aquifer as has been observed at the Hanford Site (300 Area IFRC). We take this as strong evidence that the vadoze zone is not a dominant source of U that is capable of sustaining the U plume there. Electromagnetic Borehole Flowmeter (EBF) Passive Surveys at the site indicate the in-well flows are not significant at Rifle even under conditions of extreme water table rise. Again this contrasts with high in-well flows at the Hanford 300 Area IFRC where those flows have been shown to confound U concentrations measurements.

Measurement of U concentrations in pumped vs. bailed samples during water table rise. Ongoing monitoring of selected wells across the Rifle floodplain for a range of constituents provided an opportunity to compare U concentrations at the top of the water table with those measured after standard slow-purge sampling during water table rise. Figure 59 shows the wells we monitor every two weeks and Figure 60 shows the unusual extent of water table rise during spring runoff, 2011.

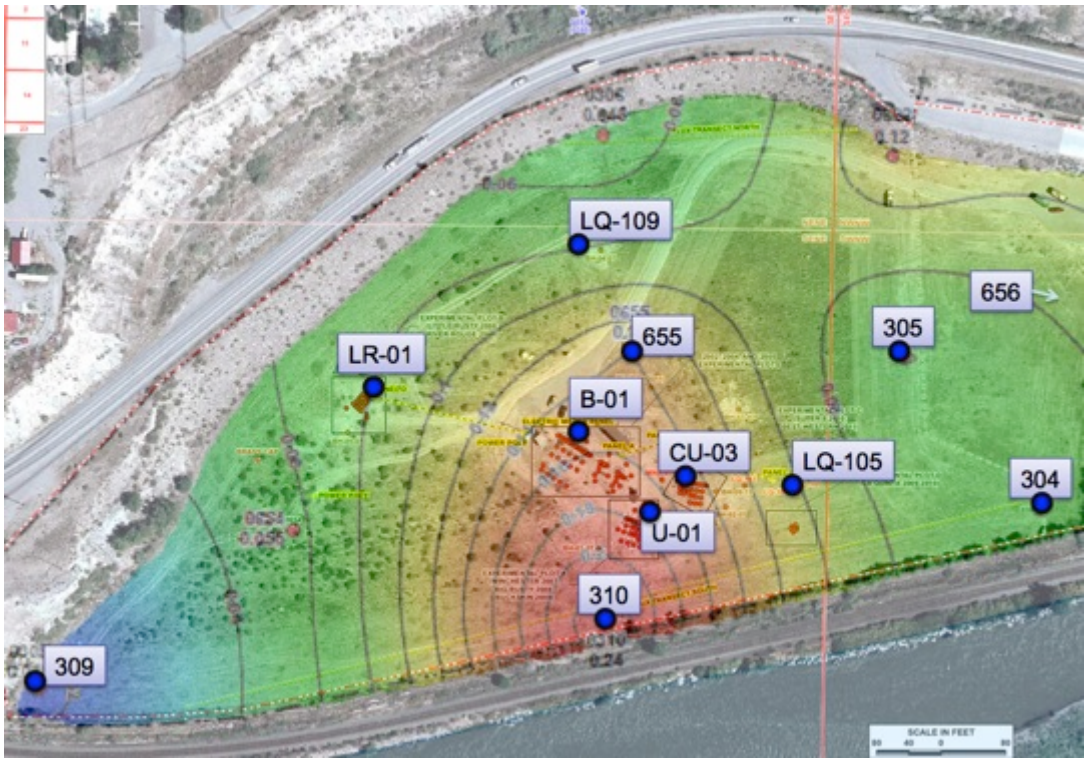

Figure 59. Well sampled every two weeks and used for comparison of pumped vs. bailed samples.

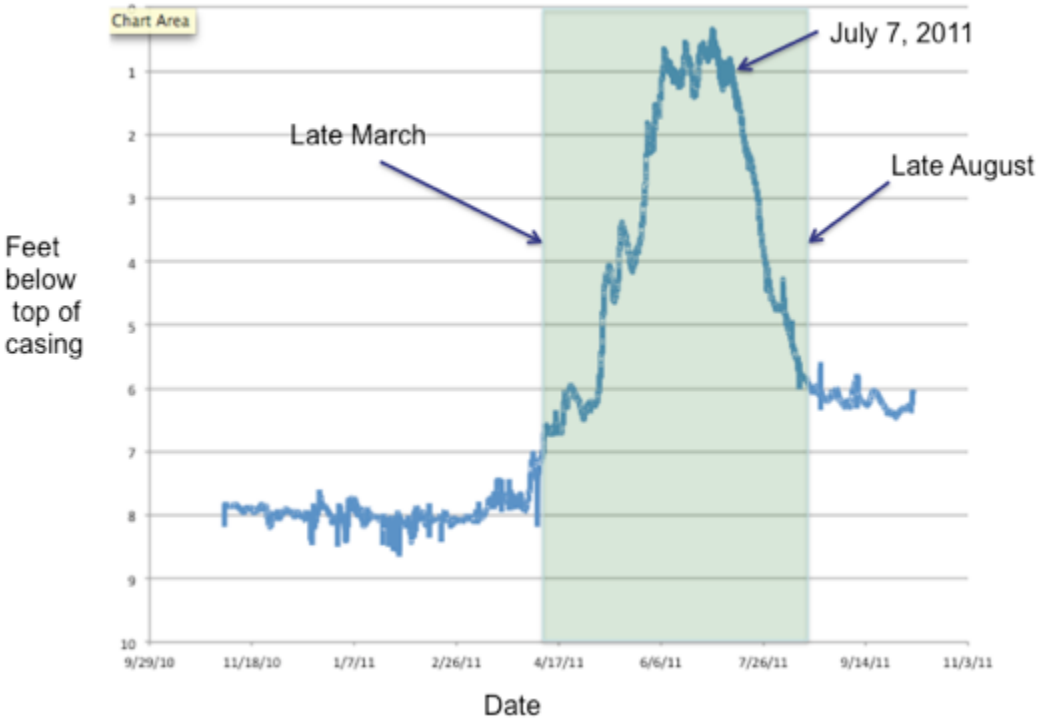

Figure 60: Water level in the Colorado River adjacent to the Rifle IFRC, Spring 2011. Light green panel shows the duration of rising and falling water table depicted in subsequent figures.

Figure 61 shows changes in U concentration in pumped samples collected during the rise and fall of the water table. Note that some wells increase in concentration while others decrease with no consistent change upward as would be expected if the vadose zone were the source of U that sustains the Rifle U plume. In fact, of the twelve wells monitored, only two of them show consistent increase over the time period of water table rise and fall. Most of the wells stay relatively constant while three of them decrease significantly during part of the time period of interest. We interpret the decrease in U concentration as an indication of dilution by water with relatively low U flowing into the area of a given well.

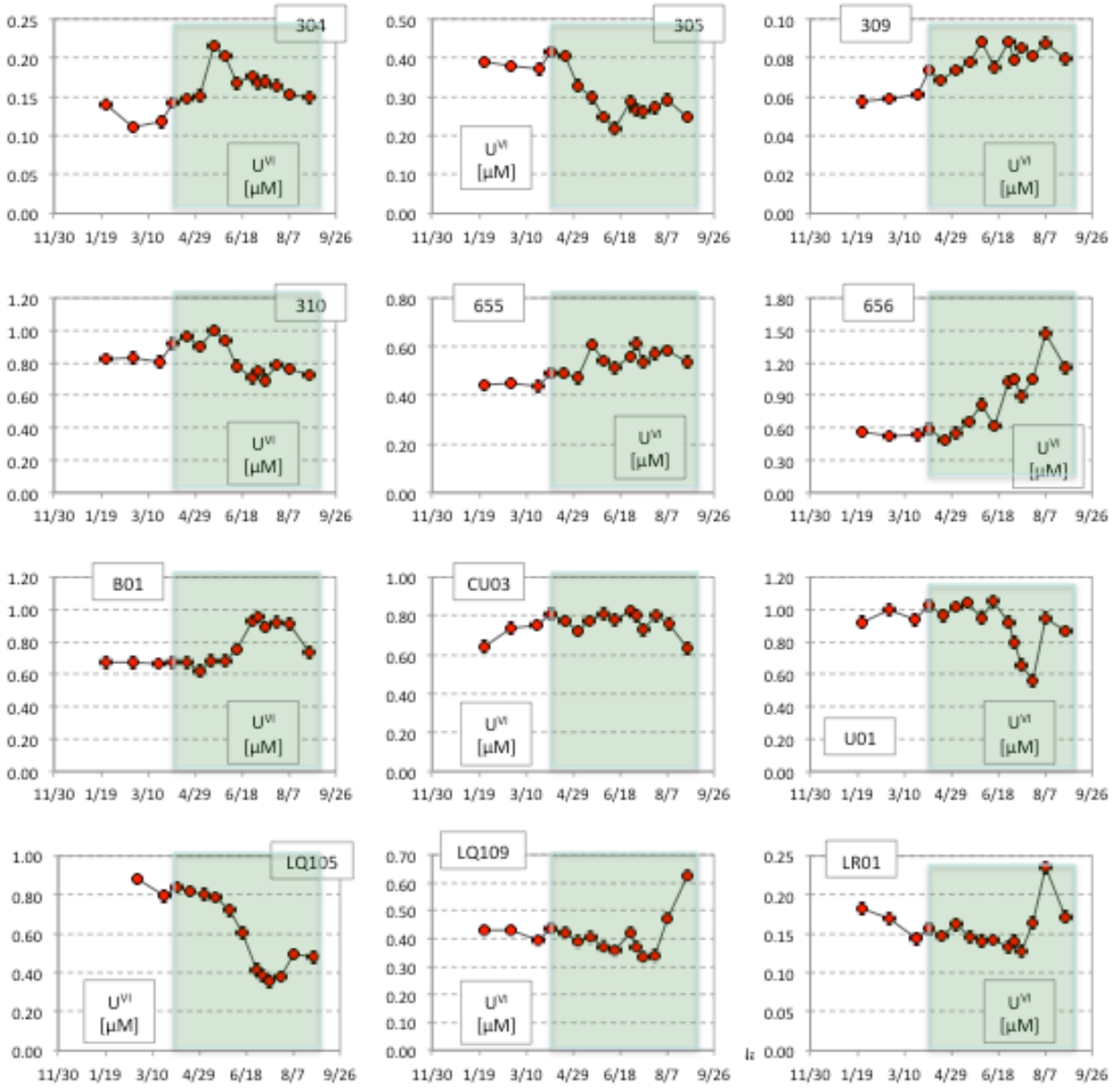

Figure 61. Change in U concentration before, during, and after spring runoff 2011.

In order to better assess the role of the vadose zone as a possible U source, we collected both pumped and bailed samples on July 7, 2011 from all twelve wells shown in Figure 61. Bailed samples were collected at the top of the water table in each well. Pumped samples were collected in the normal fashion from a tube at mid-aquifer depth, using slow purge after the bailed samples were collected. Results are shown in Figure 62. Only two of the twelve wells exhibit greater U concentration in bailed samples than in pumped samples and those differences are relatively minor. All other wells are either nearly the same for bailed versus pumped samples or the pumped samples have higher U concentrations. These results suggest that the vadose zone is not a significant source of U at the Rifle IFRC.

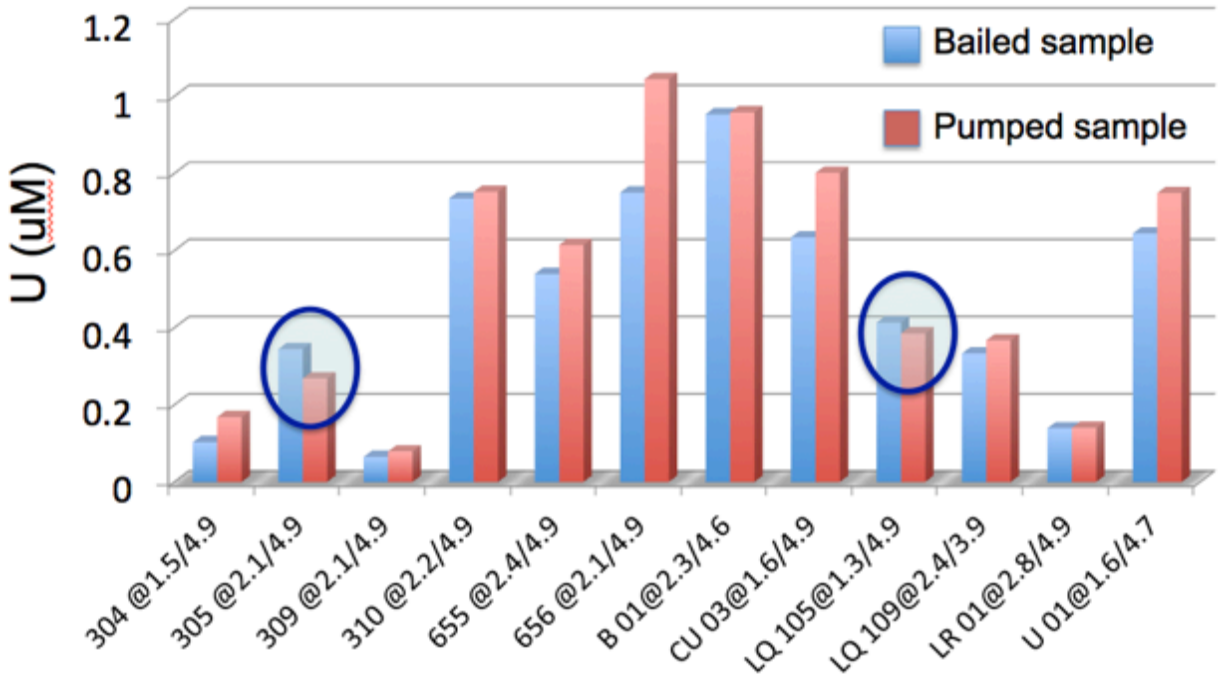

Figure 62. Comparison of pumped versus bailed samples. Numbers after the @ symbol indicate the depth of sample collection for bailed/pumped samples in meters.

Electromagnetic Borehole Flowmeter (EBF) Passive Surveys. In order to better assess the impact of rise and fall of the water table at Rifle on uranium concentration measurements, we conducted passive EBF surveys in selected wells. Specifically, on June 7-9, 2011, a series of passive (i.e., ambient) EBF surveys were conducted in selected wells during the period of high stream-flow peak runoff to assess vertical wellbore flow under high water-table conditions at the Rifle IFRC site (Figure 63). The high stream-flow peak runoff during 2011 was higher than normal for the Colorado River (stream-flow data can be found at http://waterdata.usgs.gov/nwis). A dynamic river boundary, such as the Colorado River, and associated high water-table levels during high spring runoff conditions has the potential to affect the ambient vertical flow in the wellbores and impact the distribution of hydro-chemical constituents in the aquifer as a result of mixing or exchange of groundwater within the well screens (Vermeul et al. 2010; Newcomer et al. 2010). Passive EBF surveys were conducted in 14 wells in experimental plots A, B, C, and D. The wells surveyed included D-04 and D-10 in Plot A; LR-03 and LR-04 in Plot B; CA-01, CD-04, CD-11, CD-16, CD-17, CG-01, and CG-10 in Plot C; and LQ-107, LQ-114, and LQ-117 in Plot D.

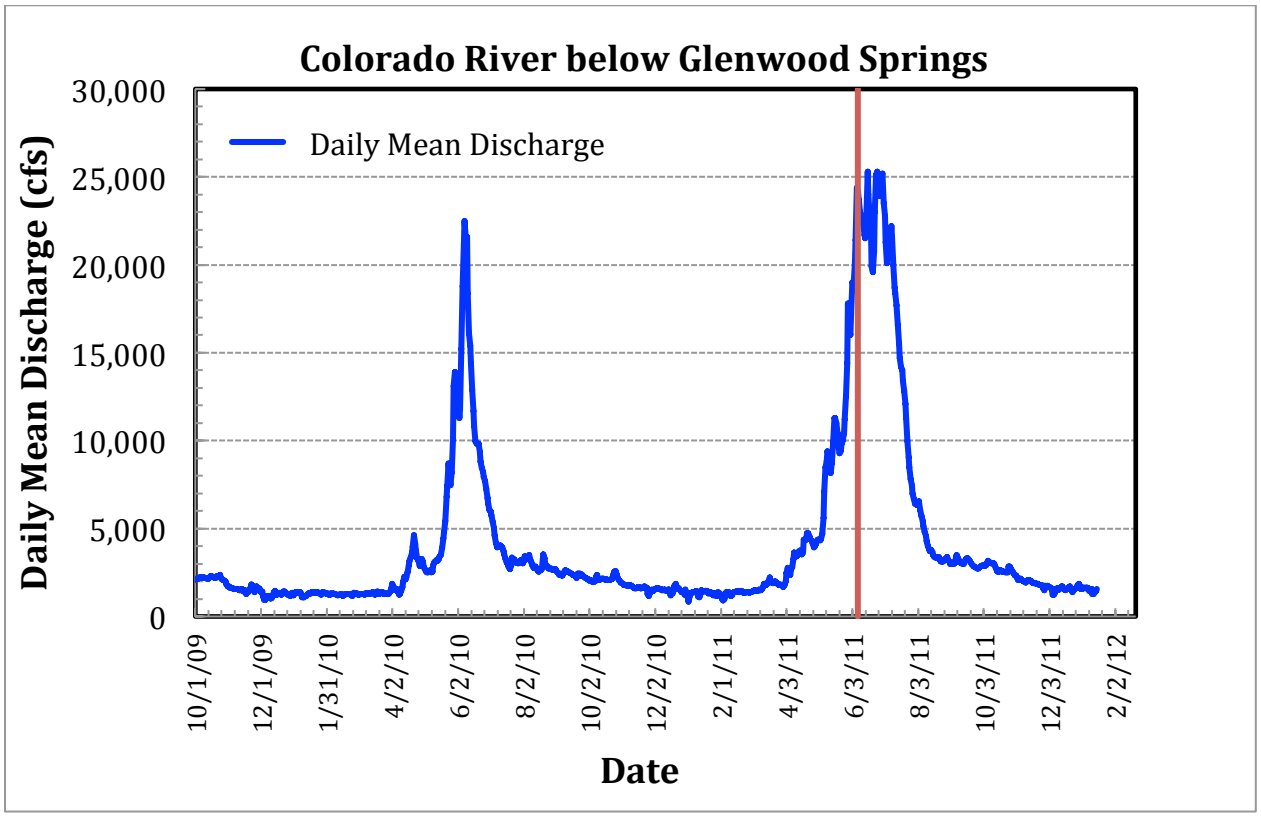

Figure 63. Timing of June 2011 EBF Passive Surveys Compared to Colorado River Daily Mean Discharge Over the Past Two Years.

The maximum ambient vertical wellbore flow measured during high stream-flow runoff conditions in June 2011 ranged between -0.18 LPM (downward flow) to +0.22 LPM (upward flow). This compares to a range of -0.44 to +0.25 LPM measured in selected Rifle wells during low stream-flow conditions in September – December in recent years (i.e., 2007-2010). The highest measured vertical wellbore flows occurred during low stream-flow runoff at the Plot D wells, the closest wells to the river shore. Vertical wellbore flow comparisons between high and low stream-flow conditions for selected wells in each of the plots are presented in Figures 64-67. These low, comparable ambient wellbore flow ranges indicate that seasonal fluctuations in the Colorado River stream flows have low impact on vertical wellbore flows within the well screens at the Rifle plots.

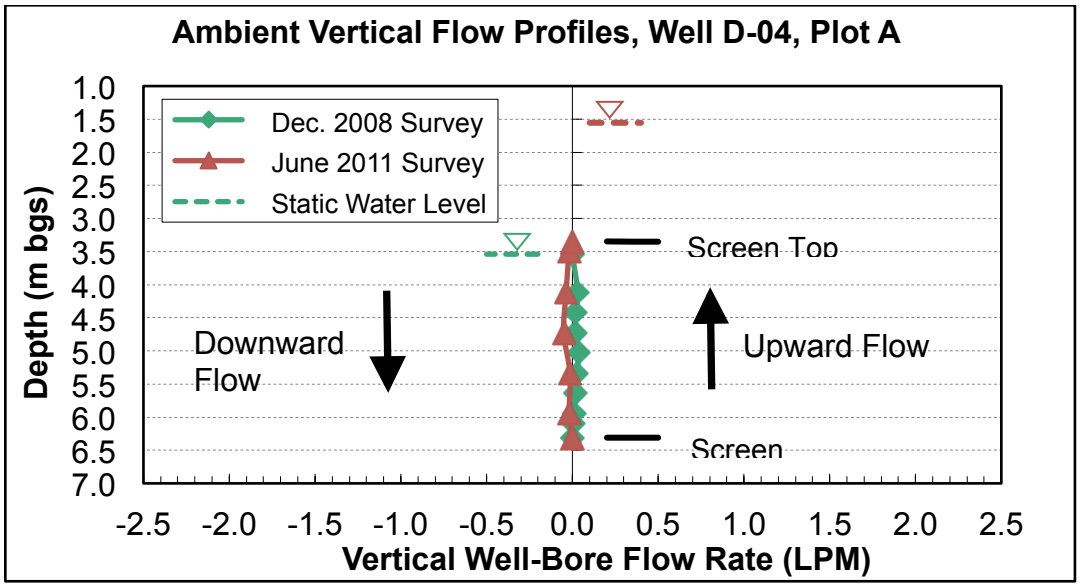

Figure 64. Example of Passive EBF Surveys at Plot A During High (June 2011) and Low (December 2008) Colorado River Discharge.

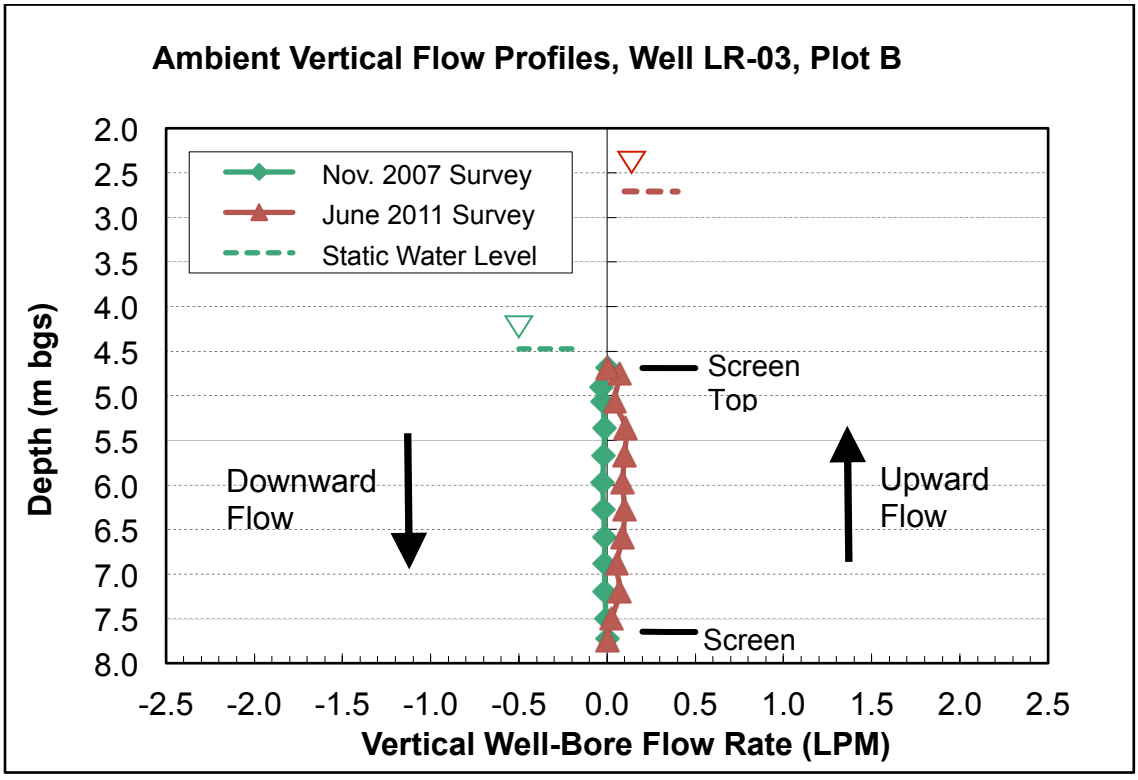

Figure 65. Example of Passive EBF Surveys at Plot B During High (June 2011) and Low (November 2007) Colorado River Discharge.

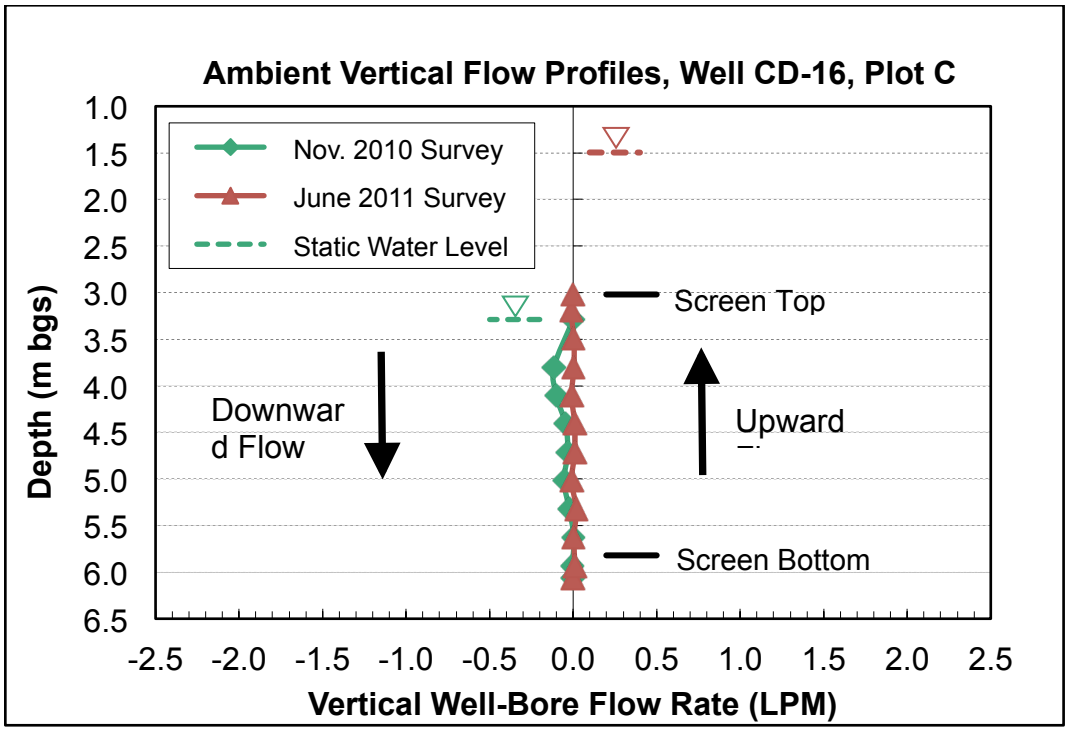

Figure 66. Example of Passive EBF Surveys at Plot C During High (June 2011) and Low (November 2010) Colorado River Discharge.

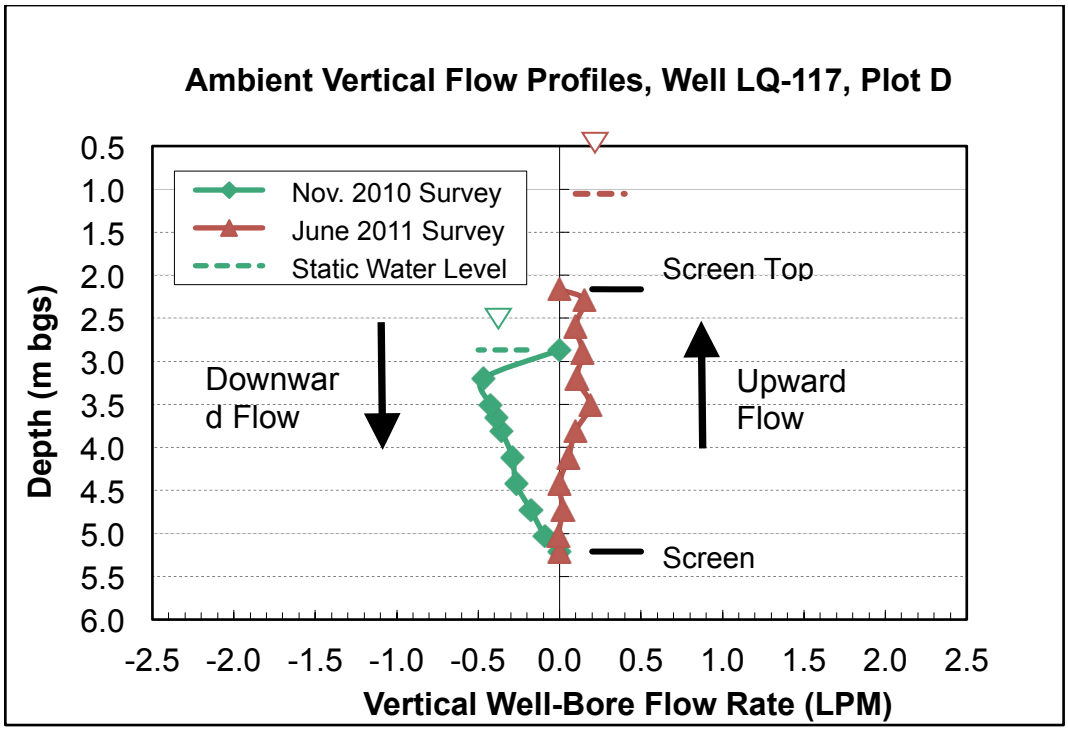

Figure 67. Example of Passive EBF Surveys at Plot D During High (June 2011) and Low (November 2010) Colorado River Discharge.

During 2011, we also continued assessment and sampling of springs on the north side of Highway 6. The results changed our conceptual model for the groundwater system north of the site. There are apparently two mains sources of water recharging the groundwater system, both of them anthropogenic. First, irrigation water from Rifle Gap is used to irrigate the Rifle Cemetery and apparently recharges part of the older alluvial aquifer upgradient from the Rifle IFRC site. Second, discharged Colorado River water from the City of Rifle domestic water treatment plant recharges the part of the older alluvial aquifer on the east side of the drainage that bifurcates the site. Both of these sources apparently desorb U(VI) from older alluvial aquifer sediments, ending up with ~twice the drinking water standard (MCL) for U just before entering the Rifle IFRC site. Details of flux and concentrations to the Rifle IFRC site are not known and we are developing plans to assess both. The potential of an offsite source of U is of great importance to DOE-LM as they assess natural attenuation at the site.

During 2011 we also initiated more extensive sampling for H, O, and S isotopes in groundwater and surface water in and around the Rifle floodplain. We are still analyzing these results and they will be reported during 2012. Broadly, these results are expected to allow us to further distinguish the sources and mixing of groundwater on the floodplain, enabling quantification of the contribution of off-site U to the Rifle uranium plume.

As part of this effort, Peter Nico (LBNL) and Brandy Stewart/Brent Peyton (Montana State University) are continuing to analyze seep sediment materials across a reductive gradient just to the north of Highway 6 (across the road from the site). They are examining both the biogeochemistry and the microbiology of the seep sediments as an analogue to subsurface naturally reduced zones (NRZ's) and will report their results at the annual PI for the SBR Program, including analysis of reductively immobilized U in the sediments using light source spectroscopy.

Data Management

The data management for the Rifle IFRC is implemented through Zend Framework web application which is hosted on a dedicated Linux (Ubuntu 11.04) server located in the Sky Research Data Center (located in Ashland, Oregon). The server is a HP Proliant DL360 G5 dual core (3 GHz Intel Xeon) with 16 GB Memory and about 3TB of fast disk. Data from this server is backed up nightly to tape. The web application is accessible through http://www.rifleifrc.org. Zend Server (a custom LAMP stack) is used as the web server software.

The websites are optimized for rapid access, with typical page load times of < 1 second (analyzed using YSlow). Extensive use is made of Javascript and CSS, which is loaded from content distribution networks and cached clientside for speed optimization. Much of the content accessible through the site (such as weather, site cameras and 3rd party data) is provided from other locations on the web through a range of different mechanisms (both push and pull). Extensive use is made of the Google Maps API (V3) to provide both a lightweight map selector and spatial information. User password management is done through the phpBB forum software. User authorization can be set at the individual menu level or on the overall site level, and allows for multiple levels of authorization granularity. Data visualization and graphing is done through JPGRAPH (a PHP graphing library) and through VisIt (LLNL 2005) which is used to generate on demand server side 3D visualizations and animations which are provided to users as links through email. The basic architecture of the Rifle data management application is identical to that used for the 300 Area IFRC. This synergy allows for optimization of resources. On November 29, 2011 the status and capabilities of the Rifle IFRC database was presented to both DOE Office of Science program managers and an external review committee.

Capability Overview. During 2009 and 2010 the basic Rifle IFRC data management architecture was put in place. In 2011 the focus was on enhancing functionality, and on ensuring that data collected by the project participants is rapidly submitted to the website. Functionality enhancements will be continuing in 2012. A comprehensive sample and result model was put in place, and import of results into this is underway. This will allow joint visualization and analysis of results. Some other capabilities (Figure 68) include:

- Tools used by the project PI to verify that users have read the appropriate site documents
- User controlled upload and editing of data packages. Data packages provide a first cut approach toward data curation, and ensure that data is at least available in initial format
- User controllable QR code generation for field labels allowing for tracking and metadata capture for field samplers
- User controllable generation of visualizations of modeling results

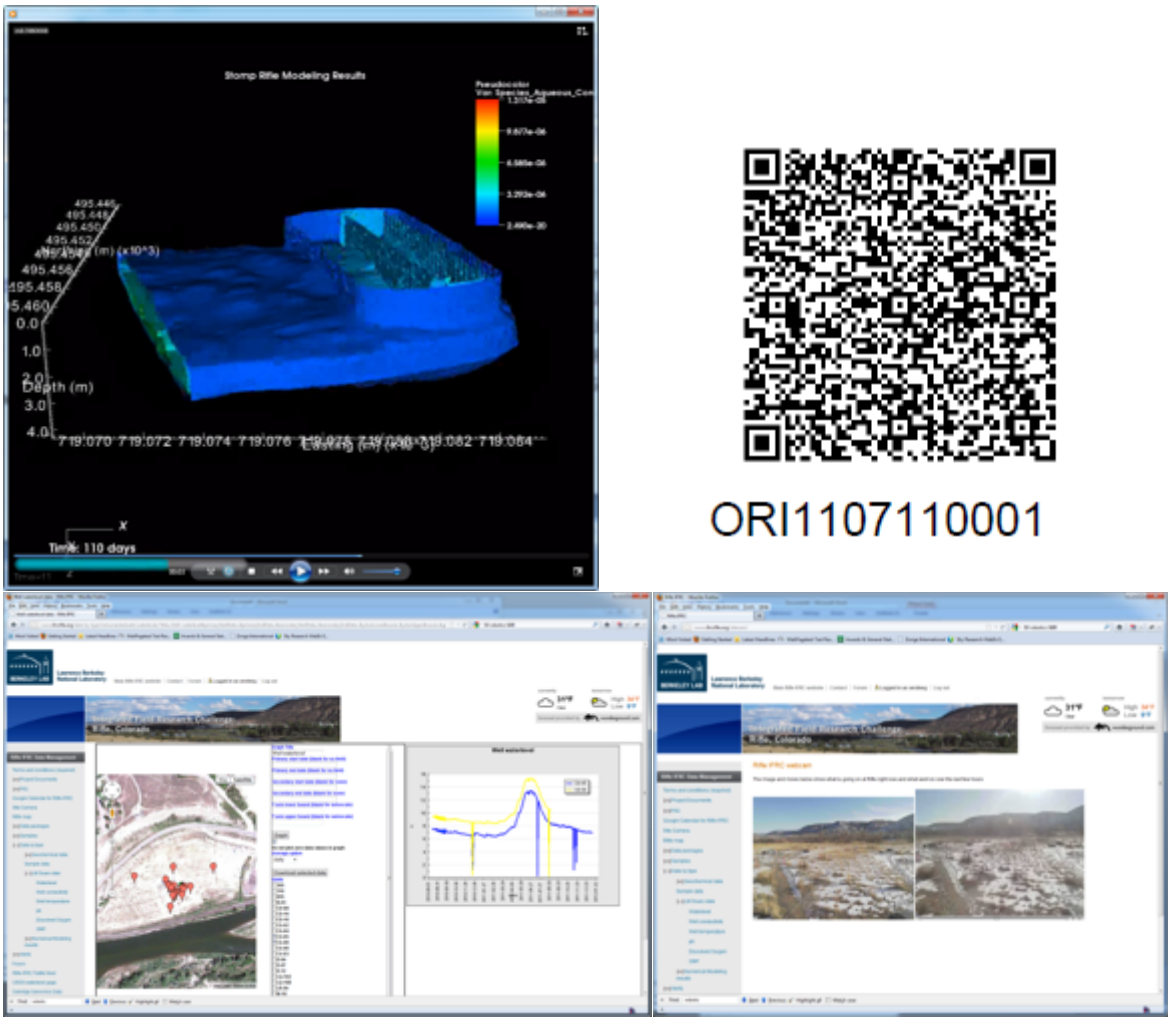

Figure 68. Top left: on demand generated visualization of STOMP modeling results. For this, the LBNL Visualization package VISIT is being used. Users require specific visualizations, which are generated from the modeling files (~10 GB, located serverside). An email with modeling results is sent to the requester. Top right: On demand generated QR codes allows users to label and track field samples. Bottom left: Users have direct access to SOARS data. This data is ingested hourly from the DOE LM system, and is directly available for download and graphing. Bottom right: Rifle IFRC sitecam and automatic movie provides access to site conditions.

Modeling and Interpretation

Rifle IFRC modeling is tasked with developing a predictive understanding of the processes, properties, and conditions controlling natural and engineered uranium bioremediation. To this end, mathematical models have been developed to address three-dimensional variably saturated flow through physically and chemically heterogeneous sediments, as well as the interaction of biologically-mediated reaction products with the subsurface geochemical environment. In particular, uranium mobility is very sensitive to many water chemistry components that are impacted (1) directly by the terminal electron accepting process (TEAP) reactions induced by acetate biostimulation and (2) indirectly by subsidiary reactions involving the biologically-mediated reaction products. Considerable effort has gone into incorporating reactions for aqueous and surface complexation [U(VI), Fe(II)], cation exchange (Ca++, Mg++, Na+, K+), mineral precipitation and dissolution (calcite, siderite, goethite, iron sulfide), and TEAPs [Fe(III), U(VI), sulfate] that link the observed uranium behaviors to changes in pH, Eh, alkalinity, and calcium. For example, uranium surface complexation is directly affected by the large amount of bicarbonate produced by the acetate-oxidizing microorganisms but also indirectly by changes in the pH from mineral reactions induced by sulfide. The current reaction network addresses two functional acetate-oxidizing microbial groups (Fe(III)-reducing bacteria and sulfate-reducing bacteria), four biologically-mediated TEAPs (phyllosilicate Fe(III), poorly crystalline iron Fe(III), U(VI), sulfate), seven minerals, and 102 biogeochemical species. The modeling also addresses site-specific issues such as the continuous influx of actionable levels of U(VI) into the treatment zone, seasonal water table variation, spatially variable physical (hydraulic conductivity, porosity) and geochemical (reactive surface area) material properties, and competition for the acetate electron donor by sulfate reducing bacteria. A September 2011 journal article published in the Journal of Contaminant Hydrology, "Variably saturated flow and multicomponent biogeochemical reactive transport modeling of a uranium bioremediation field experiment" summarizes the modeling capability and application to the 2008 "Big Rusty" field experiment (Yabusaki et al., 2011).

In 2011, we built on this base subsurface flow and reactive transport modeling capability by focusing on the mechanistic, predictive and quantitative understanding of the bacteria that catalyze bioreduction in the Rifle aquifer. The approach is a multiscale integration of three recent technological advancements: 1) groundwater proteomic analyses (Callister et al., 2010; Wilkins et al., 2009) that can identify genome-specific peptides by matching liquid chromatography-tandem mass spectrometry spectra to peptides predicted from the metagenome of the groundwater sample; 2) "*in silico*" models of cell-scale physiological metabolic pathways for key microbial species (Mahadevan et al., 2011) that include hundreds of intra-cellular and environmental exchange reactions that can be linked to species-specific peptides; and 3) massively parallel processing multifluid flow and biogeochemical reactive transport subsurface simulators that address highly detailed coupled processes and properties, including the genome-scale *in silico* models.

The modeling task first incorporated and tested *in silico* metabolic models in 2008. In this case, a table lookup version of the Mahadevan et al. (2006) *Geobacter sulfurreducens in silico model* replaced the Fe(III) TEAP reactions and rate laws in the 1-D reactive transport simulation of the 2007 Winchester experiment. There were two issues with its use. The first issue was the computational burden of solving more than 600 reactions with a constraint-based flux balance approach for every time step in every grid cell. This represented an order of magnitude increase in computational time over previous non-*in silico* model simulations, which did not bode well for multidimensional simulations. The second issue was that we could not assess whether the predicted activities of the individual metabolic pathways were correct. While each of the intracellular reactions is annotated with specific *G. sulfurreducens* genes and proteins, the lack of detailed field proteomic data left no effective means to assess and validate the large number of detailed process reactions.

In 2009, the eSTOMP massively parallel processing multifluid flow and biogeochemical reactive transport subsurface simulator enabled the first three-dimensional, coupled variably-saturated flow and

biogeochemical reactive transport modeling of the Rifle Site. Simulations that were taking several weeks on desktop computers were now completed in a few hours. Most importantly, the reaction-dominated computations were highly scalable, meaning there was no longer a computational barrier to including *in silico* reaction models into eSTOMP.

Advancements in groundwater and sediment sampling and sequencing of DNA and proteins have now made it possible to determine a wide range of metabolic process activities by their association with genes, proteins, and peptides for specific microorganism species in groundwater samples (Callister et al., 2010; Wilkins et al., 2009). Furthermore, the level of activity for each process can be related to the abundance of genome- and reaction-specific proteins. Since activity between cells from the same genome can vary in time and space depending on biogeochemical conditions, the monitoring of the proteomic data can provide highly detailed feedback on the evolving magnitude (and direction) of intracellular reactions that comprise the metabolic pathways for the microorganisms of interest. We used three planktonic biomass samples collected on days 5 (Arthur), 7 (Cristobal), and 10 (Dolly) from well D-04 during the 2008 "Big Rusty" field experiment. Following protein extraction, 2D protein identification technology (MudPIT) was used to generate mass spectra that was matched against predicted peptides of *Geobacter metallireducens*.

Key progress made in 2011 was the integration of the Sun et al. (2009) *Geobacter metallireducens in silico* model into the eSTOMP coupled process subsurface simulator. The *in silico* model mechanistically represents 697 intracellular and 51 environmental exchange reactions. The system of reactions is driven by external fluxes of acetate, Fe(III), and ammonium uptake from the eSTOMP reactive transport routines. The flux balance approach assumes intracellular reactions rapidly equilibrate to extracellular changes. This allows the system of physico-chemically constrained reaction fluxes to be solved using a linear programming approach (CPLEX) optimized for maximum biomass growth. Calculated mass fluxes (e.g., Fe(II), biomass, bicarbonate, H+, NH4+) are scaled by gdw of biomass, which then become source terms in eSTOMP. The incorporation of the unabridged *in silico* model specification into a large-scale subsurface flow and reactive transport simulator is unprecedented and requires supercomputing resources to address the modeled complexity. Computational effort in eSTOMP has increased tenfold with the inclusion of the *in silic*o model. This particular application to the 2008 "Big Rusty" field experiment was run with 1024 cores on the massively parallel EMSL Chinook computer.

At this time, 180 of the 637 *G. metallireducens* genes detected in planktonic biomass samples from the 2008 "Big Rusty" field experiment have been associated with *in silico* model reactions. Figure 69 compares the number of predicted *in silico* model reactions in specific COG (clusters of orthologous groups) categories with the number of proteins detected in those same categories. While there are COGs with proteomic activity that are not represented by *in silico* model predicted reactions, the model does appear to match the field proteomics for the metabolic pathways related to respiration (i.e., central metabolism) particularly well.

One example of a respiration pathway is the TCA cycle. Figure 70 compares heat maps representing the in silico model predicted fluxes for specific reactions in the TCA cycle and the abundance of detected proteins associated with those same reactions. In general, the greatest protein abundances (e.g., acetyl-CoA transferase, citrate synthase) consistently match the highest *in silico* model reaction fluxes. Although proteomic activity was detected for a small number of reaction pathways that were predicted to be inactive, there is good agreement for which reactions are active that often extends to their relative magnitude. In a few of the reactions (e.g., Acetyl-CoA hydrolase/transferase), even the progressive increase in reaction activity over the three proteomic samples at 5 (Arthur), 7 (Cristobal), and 10 (Dolly) days is also in agreement.

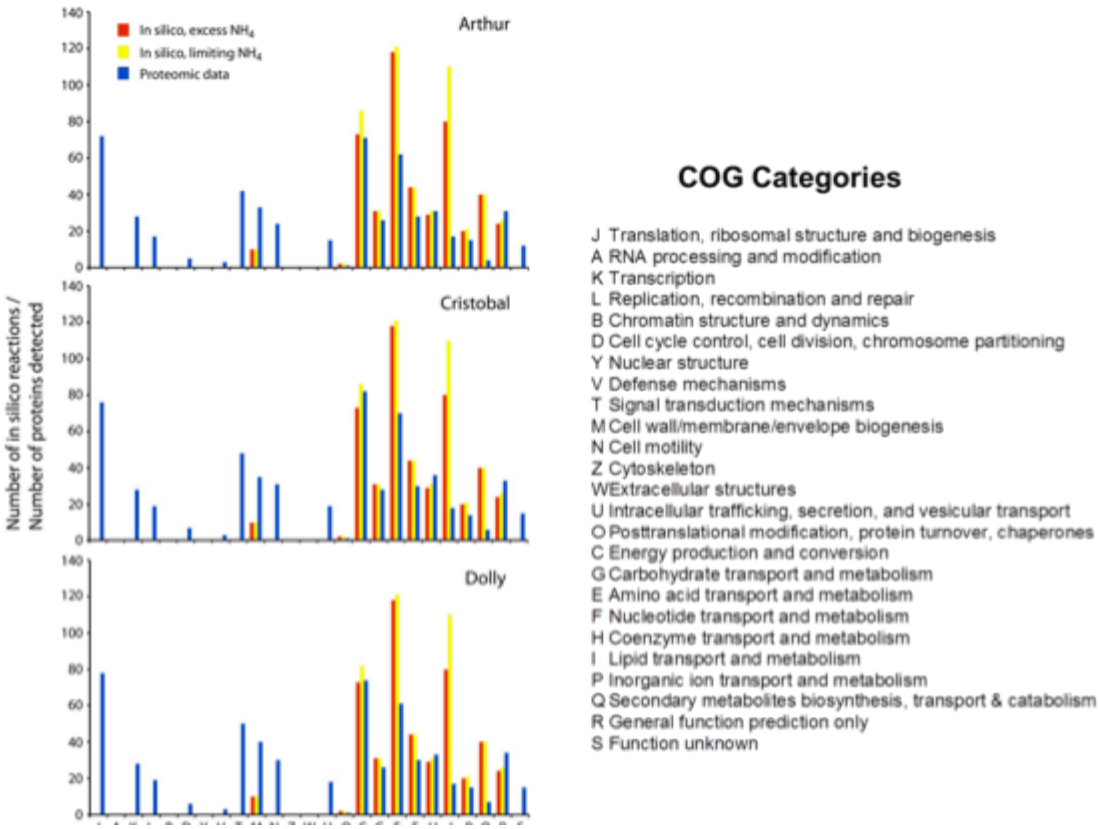

Figure 69. Comparison of the number of predicted *in silico* model reactions in specific COG (clusters of orthologous groups) categories with the number of proteins detected in those same categories.

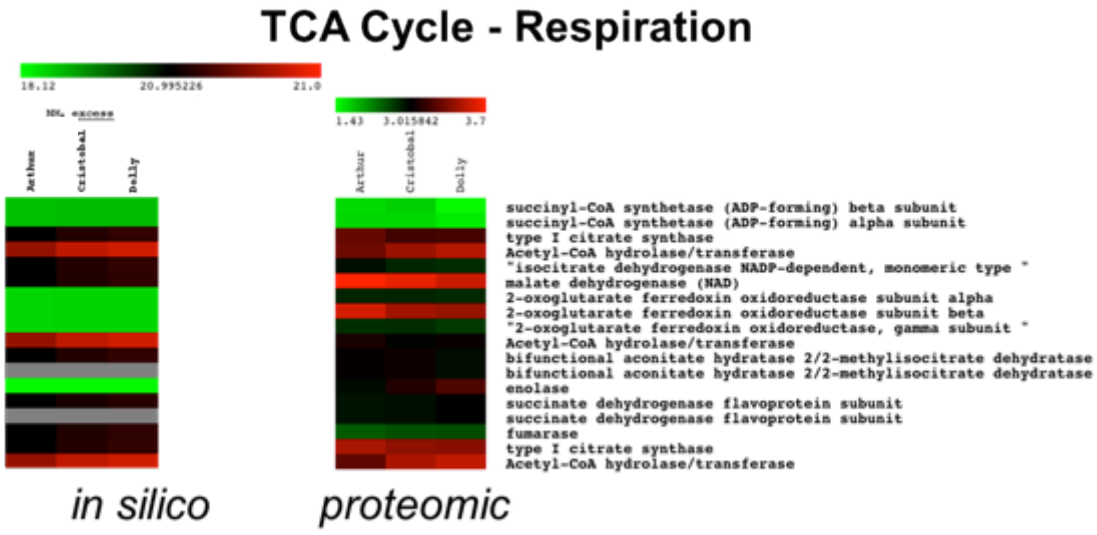

Figure 70. Comparison of heat maps representing the in silico model predicted fluxes for specific reactions in the TCA cycle and the abundance of detected proteins associated with those same reactions.

Geobacter species have the ability to fix nitrogen, which can be a competitive advantage when ammonium is limiting. Nitrogen fixation, however, is an energetically expensive pathway that *Geobacter sp.* will employ only if ammonium concentrations are limiting. The limiting ammonium concentration has been reported by Mouser et al. (2009) to be 5 μM, which should generally not come into play at the Rifle site. Furthermore, there is no evidence for depletion of ammonium during biostimulation. Thus, it was quite surprising that *G. metallireducens* proteins associated with nitrogen fixation were identified in all three proteomic samples with abundances that grew for 3 of the 4 detected nitrogenase enzymes. Figure 71 compares the protein abundance heat map with the predicted absence of reaction fluxes supporting nitrogen fixation under the assumption of excess ammonium. To test the nitrogen fixation pathway, we employed an ammonium uptake rate consistent with a concentration of 0.5 uM, which allowed both nitrogen fixation as well as ammonium uptake. The predicted reaction flux heat map trends track the field proteomics data, including the increasing protein abundances over time. However, the predicted cofactor biosynthesis proteins were not detected in the proteomic datasets. This result suggests the general opportunity to improve the model using observed proteome expression. In this case, decreasing the initial ammonium concentration at least for selected nodes would improve model response. Alternatively, we could adjust in *in silico* model behavior to include a threshold value for ammonium triggering of the nitrogen fixation pathway.

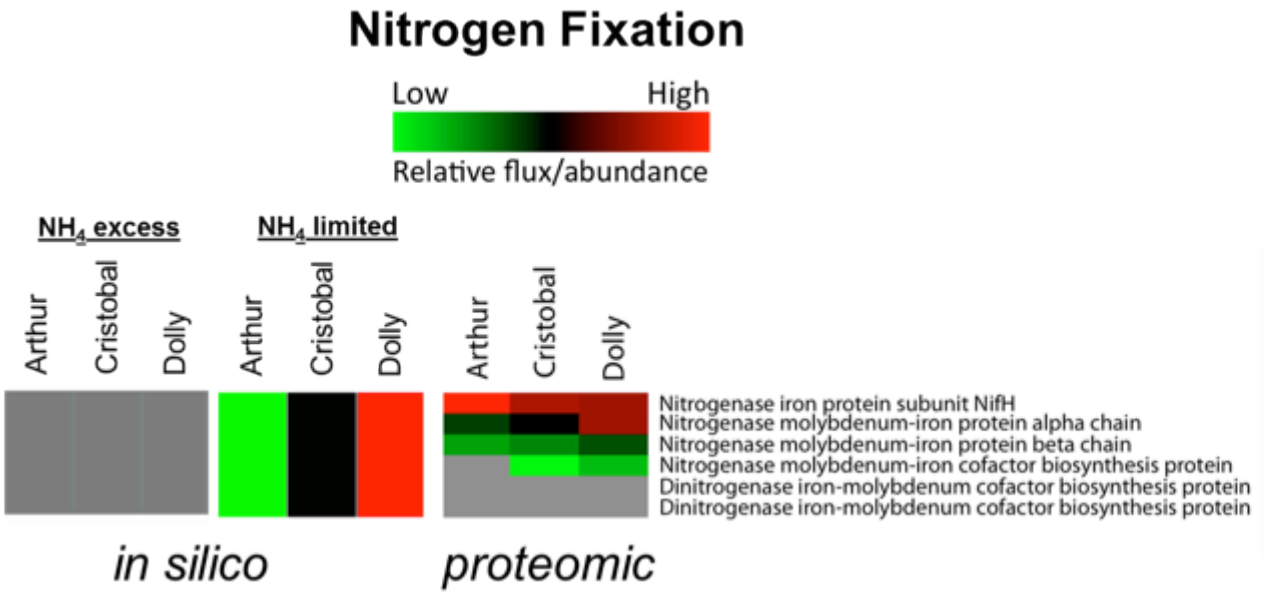

Figure 71. Comparison of the protein abundance heat map with the predicted absence of reaction fluxes supporting nitrogen fixation under the assumption of excess ammonium.

For the 2008 "Big Rusty" simulation with eSTOMP, the *G. metallireducens in silico* modeling results are very similar to our previous approach using standard Fe(III) TEAP reactions with a dual monod rate law with thermodynamic constraints. This is because acetate is the principal driver for the modeled biological activity, the same monod electron donor term is used for acetate uptake, and the apparent stoichiometry from the *in silico* model for Ac : Fe(III) : HCO3- is very close: 1:8:2 vs 1: 7.2 :1.8. Since both modeling results compare well with respect to observed behaviors, this is an encouraging sign for the *in silico* model, which was not specifically designed for the Rifle experimental conditions.

In summary, the *G. metallireducens in silico* model does particularly well predicting central metabolism pathways as indicated by protein abundance associated with the TCA cycle and acetate activation. The highest predicted reaction fluxes are associated with the highest protein abundances, acetyl-CoA transferase and citrate synthase. In particular, the predicted reaction fluxes match detected proteins that suggest gluconeogenesis over glycolysis pathways. While nitrogenase activity (for fixing nitrogen) is stimulated when ammonium concentrations are limiting in the model, there is a lack of feedback to other genes/proteins associated with this regulation.

We already know that acetate electron donor concentrations introduced at injection wells will become spatially and temporally variable due to preferential flow and downgradient mixing processes, as well as consumption (i.e., oxidation) by metal and sulfate reducing bacteria. The assessment of the *Geobacter metallireducens in silico* model under a range of concentrations for electron donors, terminal electron acceptors, nutrients, and biomass can be considered the first step in refining (1) the model, (2) our understanding of *Geobacter* physiology, and (3) our conceptualization of nutrient (e.g., ammonium) availability. We will now focus on simulation of the 2010 and 2011 biostimulation experiments where the analysis of more planktonic biomass samples over longer time periods for a wider range of conditions will provide new knowledge and a rigorous test of the *in silico* models. *In silico* models are under development for other important microorganisms (e.g., *Desulfobacterales*) and we anticipate future simulations that will include multiple interacting *in silico* models requiring even higher levels of computational performance. Increasing availability of metagenomic data from the Rifle site will allow a wider range of important organisms to be considered with varying degrees of proteomically annotated physiology. Since it is probable that many of these organisms may not be available for experimentation in pure culture, alternatives to fully specified genome-scale *in silico* models will be explored. Ultimately, the field proteome, metagenome, and biogeochemistry will provide a basis for refining mechanistic genome-specific metabolic models beyond the initial foundation from pure culture microcosm/chemostat experiments.

Selected Collaborator Research Activities

SLAC-SFA Collaborative experiments: Speciation and stability of uranium in reduced sediments. J.R. Bargar (SLAC), lead

The SLAC-SFA program is conducting experiments at the Rifle IFRC to characterize the speciation of uranium occurring in reduced field sediments and the stability of these forms of uranium. This work is focused in three areas: (i) characterizing the chemical and physical forms of U(IV) products obtained following acetate-stimulated bioreduction in the Old Rifle aquifer, (ii) characterizing the oxidation rates and mechanisms of well characterized forms of U(IV) believed to be important in aquifers, with emphasis on biogenic uraninite and monomeric complexes of U(IV) bound to biomass and magnetite, and (iii) characterizing the fate of U(VI) adsorbed to or incorporated in Fe(III)-(oxyhydr)oxides under iron reducing conditions. The Old Rifle site is an ideal location for the proposed work because of the extensive knowledge about geochemical and microbiological dynamics at this site, the ability to temporally separate dominantly metal- and sulfate- reducing conditions, the availability of wells exhibiting contrasting DO and Fe(II) concentrations, and the availability of research infrastructure. Results during the past year are summarized below.

Products of U(VI) bioreduction in aquifers. J.R. Bargar, J. Lezama-Pacheco, N. Janot, and J.E. Stubbs (SLAC); E. Suvorova and R. Bernier-Latmani (EPFL); J. Cerrato, L.Y. Blue, and D.E. Giammar (WUStL); K.M. Campbell (USGS), K.H. Williams (LBNL); and P.E. Long (LBNL)

The stability of bioreduced U(IV) in aquifers is fundamentally linked to its molecular-scale structure and composition. Laboratory research utilizing pure microbial cultures has demonstrated that bacteria can rapidly precipitate uraninite. These observations have led to the use of biologically mediated uraninite precipitation to account for U(VI) removal in biogeochemical transport models. However, recent pure culture and sediment microcosm studies have altered the confidence in this general paradigm by demonstrating that monomeric forms of bioreduced U(IV) can be obtained under a wide range of conditions. We posit that non-uraninite forms of U(IV) are more susceptible to chemical transformations, oxidation, and remobilization in aquifers because solid-phase dissolution is not required in order to release uranium. If correct, this behavior would have important implications for the remobilization of reduced uranium during the post-stimulation phase of a bioreduction experiment, as well as for the release of U(IV) from naturally reduced sediments over time. It would favor the use of aquifer management techniques that could promote the conversion of monomeric U(IV) to uraninite in-situ, or the direct precipitation of uraninite.

A question highlighted by this discussion is, what U(IV) products are produced in field sediments that have been artificially or naturally bioreduced? To date, no published studies have comprehensively assessed the speciation of *field bioreduced* uranium in whole sediments and linked it to sediment geochemistry (*i.e.*, studying all particle sizes and elemental associations present in sediments). This dearth of information is due in large part to significant experimental challenges, which include the dilute concentrations of uranium in field sediments (often below spectroscopic detection limits), the inaccessibility of the subsurface, and the expense of drilling to recover samples. In 2009, in collaboration with the Rifle IFRC, we developed a novel *in-situ* method that provides direct access to the biogeochemical conditions in the Old Rifle aquifer using sediment columns emplaced in wells. This approach allowed us to assess the speciation of uranium in bioreduced field sediments. The success of the demonstration project led us to conduct subsequent experiments in 2010, to address differences in U(IV) biomineralization occurring under iron- and sulfate-reducing conditions, and in 2011 to temporally resolve processes occurring during the Fe reduction stage – and examine the impact of post-stimulation aging on U(IV) speciation and stability. Each experiment requires approximately one year in the field,

and subsequently, extensive use of synchrotron-based x-ray absorption spectroscopy (XAS) and x-ray microprobe (XRM) measurements interspersed with scanning and transmission electron microscopy (SEM and TEM) characterization. This approach, coupled with sediment extractions, can provide a holistic view of sediment grain coating mineralogy, and its relationship to uranium speciation and behavior. Such information provides the scientific basis for physically accurate models of reduced uranium behavior in reduced aquifers.

2009 in-situ column demonstration project in Old Rifle "Buckskin" acetate biostimulation experiment: In-well sediment column experiments were initiated in July 2009 in conjunction with the "Buckskin" acetate-stimulated bioremediation experiment (in the Winchester gallery) led by Ken Williams of the Rifle IFRC team. Fresh moist sediments were harvested from adjacent boreholes, loaded into columns under anaerobic conditions, and installed into wells P-101 and P-102 on the same day in the Winchester flow cell. Groundwater was drawn through the columns and amended with 5 mM acetate for 90 days to simulate conditions in the center of the acetate plume and with 10 μM U(VI) to accumulate sufficient uranium for spectroscopic analysis. XAS analyses of harvested sediments show that uranium is present as U(IV).

In 2011, we completed SEM-EDS (energy dispersive spectroscopy) and focused ion beam (FIB)-TEM analyses from our 2009 experiment (which ended in Nov 2010) sediments, which led us to reevaluate our EXAFS fitting model. XRM, SEM-EDS, and TEM-EDS analyses show that U, Fe, and S co-accumulated in grain coatings during the bioreduction experiment. Fe and S atomic percentages are highly correlated and typically show a stoichiometric ratio of 1:1, implicating FeS as a primary mineralogic component of the coatings (Figure 72). Microprobe Fe K-edge XAS and selected area electron diffraction (SAED) measurements confirm that FeS is a present in the sulfidic coatings. Clone library analyses completed in 2011 show the dominance of *Desulfobacter,* which increased in abundance throughout the experiment. Analysis of 100 pages of SEM-EDS data from petrographic thin sections were analyzed in 2011 to assess the spatial relationship between U, Fe, and S in the coatings at the sub-coating spatial scale, *i.e.*, a few hundred nm to a few microns. At this spatial scale, the local atomic percent of uranium was found to be uncorrelated with either Fe or S in the majority of locations examined (Figure 72). This observation led to two important conclusions: (i) that uranium is not chemically bound to the sulfidic phases. This conclusion is explained as follows: Our expectation is that reduction of U(VI) by FeS and its subsequent binding to FeS surfaces or structural incorporation into FeS should generate elemental correlations between U and Fe or U and S. In the absence of such a correlation, it is not possible to demonstrate that U(VI) is directly reduced by FeS, especially since enzymatic U(VI) reduction pathways were also available. If one concludes that U(IV) dominantly was not bound to FeS in the grain coatings, then it is likely that "direct" reduction by microbial enzymes was the dominant U(VI) reduction pathway. (ii) Our prior extended x-ray absorption fine structure (EXAFS) fitting model, which had assumed surface complexation of U(IV) on FeS, could not be justified in light of the newer EDS analyses. We subsequently reanalyzed the XAS data and found it to be consistent with a dominant component of U(IV) associated with biomass, and including a smaller component of biogenic uraninite being present. Overall, these results paint a complex new biogeochemical picture in which grain coatings are an essential component. The coatings, likely created by biofilm communities, are sites of active biomineralization of U(IV) and iron sulfides.

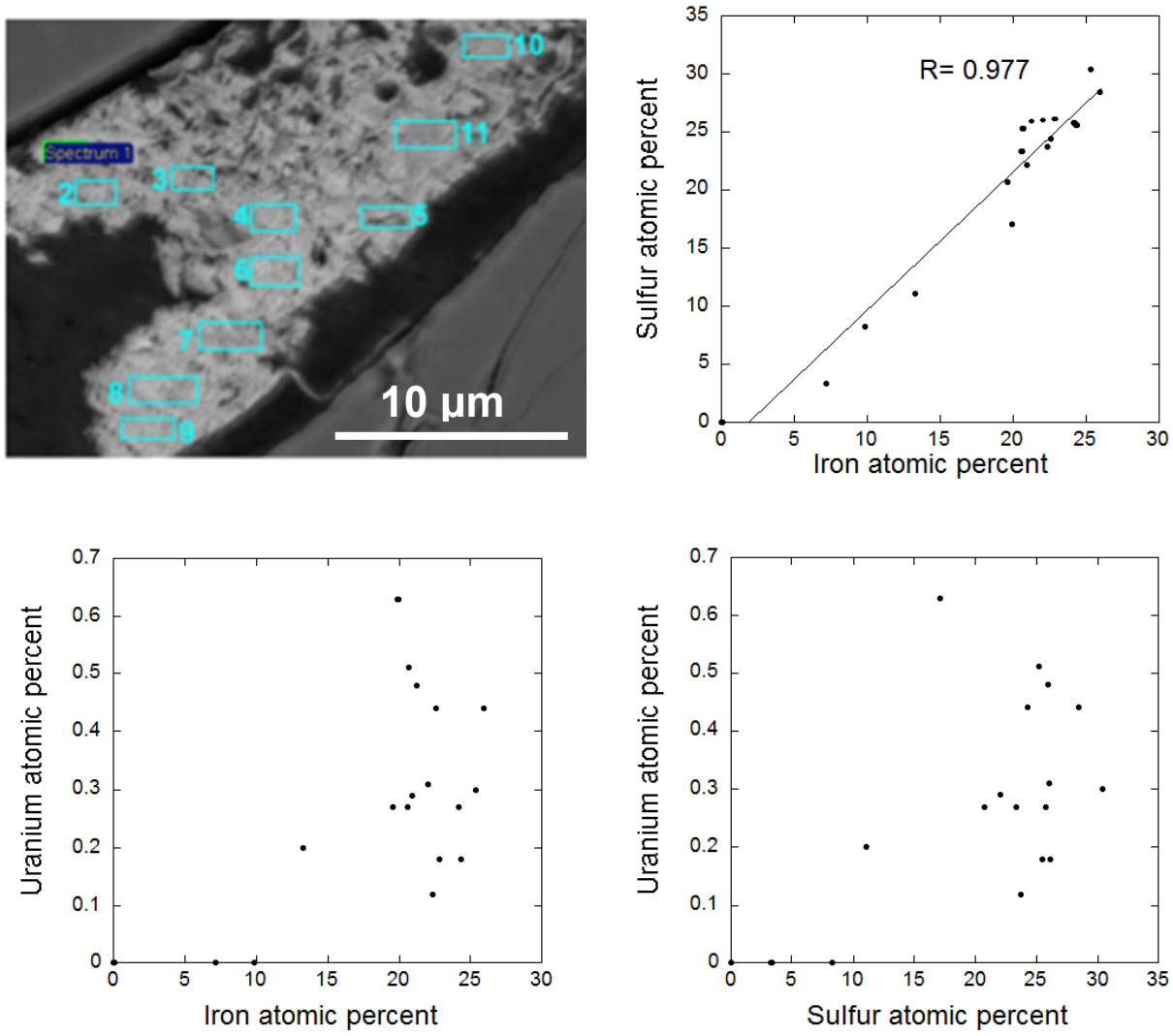

Figure 72. Back-scattered electron scanning electron micrograph of a sulfide-rich U-bearing portion of grain "t9". Rectangular boxes on SEM micrograph provide locations of EDS measurements. Scatter plots show EDS-derived atomic percents of U, Fe, and S present at different locations in and around the sulfidic crack filling. R is the correlation coefficient for the specific plot.

The formation of coatings containing biomass and reduced U and FeS has numerous important implications for uranium behavior. Biomass encapsulating U(IV) dramatically retards U(IV) oxidation (Cambell *et al.*, *ES&T*, 2011; see also results in the next section). The abundance of FeS proximal to U(IV) is expected to provide a further buffer against oxidation. Moreover, the ability of coatings to grow continuously provides a mechanism for mineral surface area to be effectively renewed during bioremediation. This growing "surface area" can sequester U(IV) in zones of relatively good fluid flow, reducing the dependence of uranium attenuation on slow uranium diffusion into tertiary pore spaces. Overall, this work constitutes a transformative shift in how we think about U(VI) bioreduction in sediments. A manuscript from this study is being submitted at the time of writing.

2010 "Super 8" in-situ column experiment: While successful in its initial objectives, the 2009 *in-situ* field experiment did not attempt to investigate differences in U(IV) speciation under iron and sulfate reduction conditions. Geochemical conditions vary strongly between these two biogeochemical regimes. In particular, concentrations of Fe(II) are relatively high whereas H_2S is low during iron reduction. Under sulfate-reducing conditions these concentration profiles become inverted. These trends are important because Fe(II) and H_2S are highly reactive species that can reduce U(VI) and react with other solutes (including one-another) to create other secondary minerals and mineral coatings that also can react with U(VI) or U(IV). Bicarbonate alkalinity can peak at four-fold higher values during sulfate reduction as compared to iron reduction, modifying the overall U(VI) redox potential and reduction kinetics, as well as the pool of reducible U(VI) species. Previous laboratory research by our group and others indicates that a surprising variety of U(IV) products can be produced by biological U(VI) reduction. It is therefore reasonable to posit that the dominant U(IV) species produced in field sediments under iron reducing conditions may be compositionally and structurally different from that formed under sulfate-reducing conditions. We further expect the uranium reduced under iron- and sulfate-reducing conditions will have different stabilities with respect to oxidation by O_2 and potential solid-phase oxidants. The 2010 "Super 8" *in-situ* column acetate biostimulation experiment was designed to compare U(IV) bioreduction products obtained under these two contrasting regimes. This experiment concluded in November 2011. A detailed description of the "Super 8" experiment is provided in the 2010 Rifle annual report.

In 2011, we performed XAS, XRM and SEM measurements on sediments harvested in the fall 2010 phase of the "Super 8" experiment. These results already have led to two significant discoveries. First, XRM and SEM-EDS measurements reveal major difference in the sediment geochemistry between the two sets of conditions. Sediments exposed only to Fe reducing conditions do not exhibit grain coatings, and uranium cannot be detected in XRM and SEM-EDS measurements of these samples (Figure 73). These observations suggest that the U(IV) accumulated in the iron-reduced sediments is spread out among the sediment grains. In contrast, columns in which U amendment was initiated after the onset of sulfate-reducing conditions exhibit sulfide-rich grain coatings also enriched in U similar to those observed in the 2009 experiment. FeS is present as judged by SEM-EDS measured Fe:S stoichiometric ratios of 1:1. As observed in the 2009 study, U generally is not correlated with Fe or S on the scale of a few microns within the coatings. The second major observation is somewhat surprising; U L_{II}-edge EXAFS are similar in all sediments regardless of biogeochemical regime, and specifically are consistent with U(IV) bound to biomass. These observations suggest that U(IV) bioreduction mechanisms are dominant and similar under all conditions observed. Further analyses are underway, including metagenomic analyses of sediments by the Banfield group.

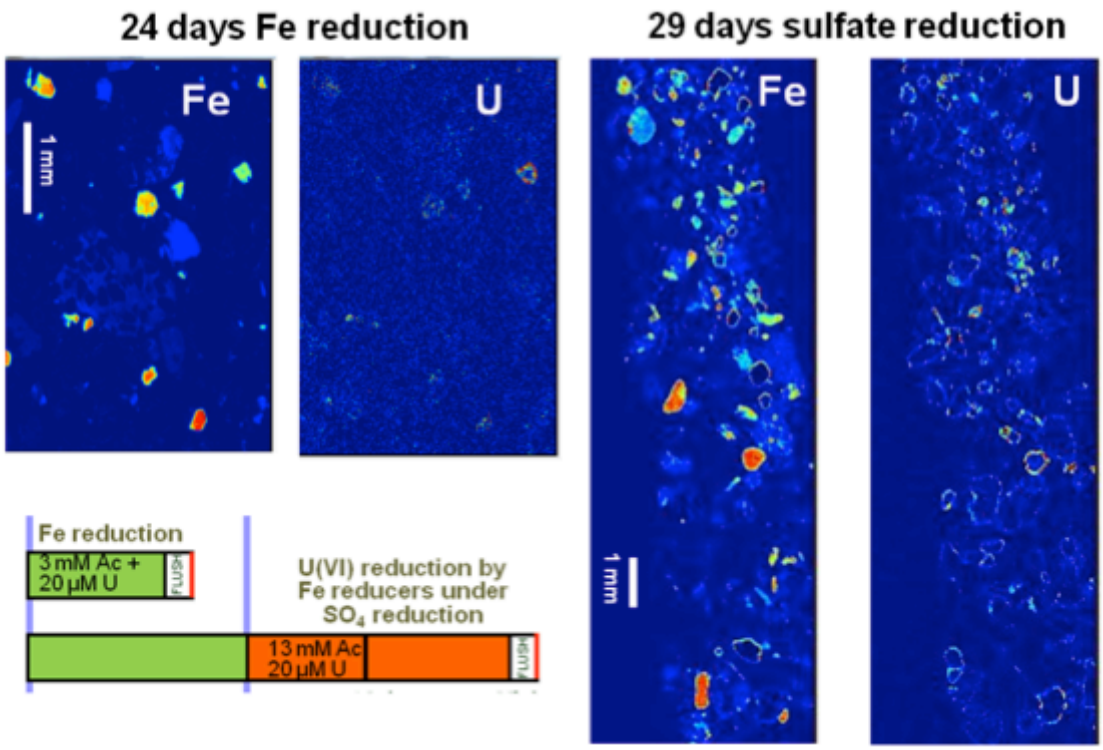

Figure 73. XRM measurements showing Fe and U distributions in column sediments exposed to iron-reducing conditions (left) and sulfate-reducing conditions (right). Under iron-reducing conditions, U is present at or below the detection limit. Under sulfate-reducing conditions, FeS-rich coatings form in which uranium is concentrated. The inset on the lower left illustrates the general time of amendment experiments in the iron and sulfate reducing columns. Sulfate reducing columns were eluted with acetate-amended groundwater as of the Super8 experiment for 37 days in order to encourage onset of sulfate reducing conditions prior to starting uranium amendment.

2011 "Best Western" in-situ column experiment: During the fall 2011 "Best Western" experiment, we installed *in-situ* columns in experimental plot C to temporally resolve the abundance and molecular-scale speciation of U(IV) species formed under iron reducing conditions and to follow their transformations with time during subsequent changing aquifer conditions. Columns were harvested on 3-day intervals during the Fe-reduction phase. A subset of columns remains in the aquifer to probe the impact of rebounding aquifer conditions on U(IV) and will be harvested through the winter, spring, and summer 2012. Harvested column sediments are being analyzed using a suite of techniques including x-ray absorption spectroscopy, x-ray microscopy, electron microscopy, and elemental extractions for Fe and S species. These experiments will help to establish conceptual reaction models to describe U(IV) complexes that occur in the aquifer during biostimulation and their fate after biostimulation ceases.

Stability of U(IV) in aquifers. J.R. Bargar, J. Lezama, and J. Stubbs (SLAC); D. Alessi, and R. Bernier-Latmani (EPFL); J. Cerrato, L.Y. Blue, and D.E. Giammar (WUStL), and P.E. Long (PNNL).

These experiments are designed to address the question, *what are the rates and mechanisms of oxidation and re-release of naturally or artificially reduced uranium in the field?* Our experiments in the Old Rifle aquifer have focused on two forms of reduced uranium: (i) biogenic nano-uraninite, and (ii) monomeric U(IV) bound to bacterial biomass and to biogenic magnetite. These forms of U(IV) are potentially important in reduced sediments. Our goal is to compare U(IV) loss rates obtained in the field to rates obtained in laboratory experiments using relatively simple media to understand the chemical factors controlling U(IV) release to aquifers under *bona-fide* subsurface conditions. Trace elements present in groundwater can have a profound effect on the stability of U(IV). For example, dissolved silicate is known to retard uraninite dissolution rates by 100-fold, and we have found that 1 mM Mn^{2+} can retard biogenic uraninite dissolution by 1,000-fold. Both of these ions (any many others) occur in Rifle groundwater. Laboratory experiments do not account for the full complement of trace or major ions in groundwater, nor the time-dependent variation that arises from the complex interactions of subsurface processes. Thus, experiments in aquifers provide important information that informs biogeochemical reactive transport models.

Biogenic nano-uraninite: Biogenic nano-uraninite produced by *Shewanella* sp. CO-9 (an isolate from the Rifle site) was installed in oxic and suboxic wells at the Rifle site in July 2009, and harvested in Oct 2009, April 2010, and April 2011. A paper from the first 3-month period was published in 2011 in *ES&T* (Cambell *et al.*, *ES&T*, 2011). This study provided two important conclusions: (i) over the time scale of the experiment, the intrinsic dissolution rate of biogenic uraninite in Rifle wells is consistent with published literature values from laboratory studies. However, (ii) modest diffusional barriers can lead to 100-fold retardation of the overall oxidation rates. The presence of bacterial biomass further retarded uraninite oxidation rates. This study highlights the importance of diffusion barriers in stabilizing U(IV) in sediments. It can further be concluded that fine-grained naturally reduced zone sediments in diffusional contact with the aquifer should stably host U(IV) for tens or hundreds of years.

Monomeric U(IV) complexes bound to biomass and biogenic magnetite: As compared to uraninite, monomeric U(IV) complexes are likely to be more labile, more easily oxidized, and therefore less stable in the environment. In this field project, monomeric U(IV) species were produced by reducing aqueous U(VI) in two systems with environmental relevance: (1) *Shewanella* sp. CO-9 (an isolate from the Rifle site), and (2) magnetite of biogenic origin that had been surface-loaded with phosphate. These laboratory-produced materials were uniformly embedded in polyacrylamide and agarose gels which were deployed at the Old Rifle site in wells B-02 (oxic to suboxic conditions) and P-103 (anoxic to suboxic conditions). Several experimental difficulties were encountered during this experimental program, which prolonged the experimental period. One important lesson learned was that polyacrylimide gels are relatively unsuitable hosts for monomeric U(IV) species, which are easily oxidized during the polymerization step. Subsequently, agarose gels were used to encapsulate monomeric U(IV) for deployment in Rifle wells. The use of un-gelled samples also was discontinued during this experimental period because gel-free samples (originally designed for the biogenic uraninite experiments) were deemed to be unnecessary for XAS analysis. Gel pucks remain solid throughout the experiment and thus can be retained in slotted tubes (slit dimensions smaller than gels) without membranes – a major advantage as the membranes were found to impose diffusional barriers on experimentally observed rates. Gel pucks also contain less uranium than the un-gelled samples, and this change to the experimental approach allowed the amount of uranium be used to be substantially reduced. Un-deployed control samples and the Rifle-deployed samples are being analyzed using U L_{III}-edge X-ray absorption spectroscopy (XAS) to determine possible changes in uranium speciation.

Uranium losses after 1 month of deployment are illustrated in Figure 74, measured by drying followed by digestion. In both wells, approximately 90% of the initial uranium was lost from the phosphate-sorbed magnetite gels. More than 80% of monomeric U(IV) was lost from biomass gels in well P-103, and nearly 35% from those in well B-02. This last result is somewhat surprising, because well B-02 is more oxic than well P-103. This observation suggests that dissolved oxygen is not the only parameter controlling uranium release. Also included in the figure are data from gels containing biogenic uraninite deployed for 4 months (Campbell *et al.*, 2011). Despite the 4-fold increase in deployment time, the uraninite-containing gels release markedly less uranium, supporting the relative stability of biogenic uraninite as compared to monomeric U(IV) species.

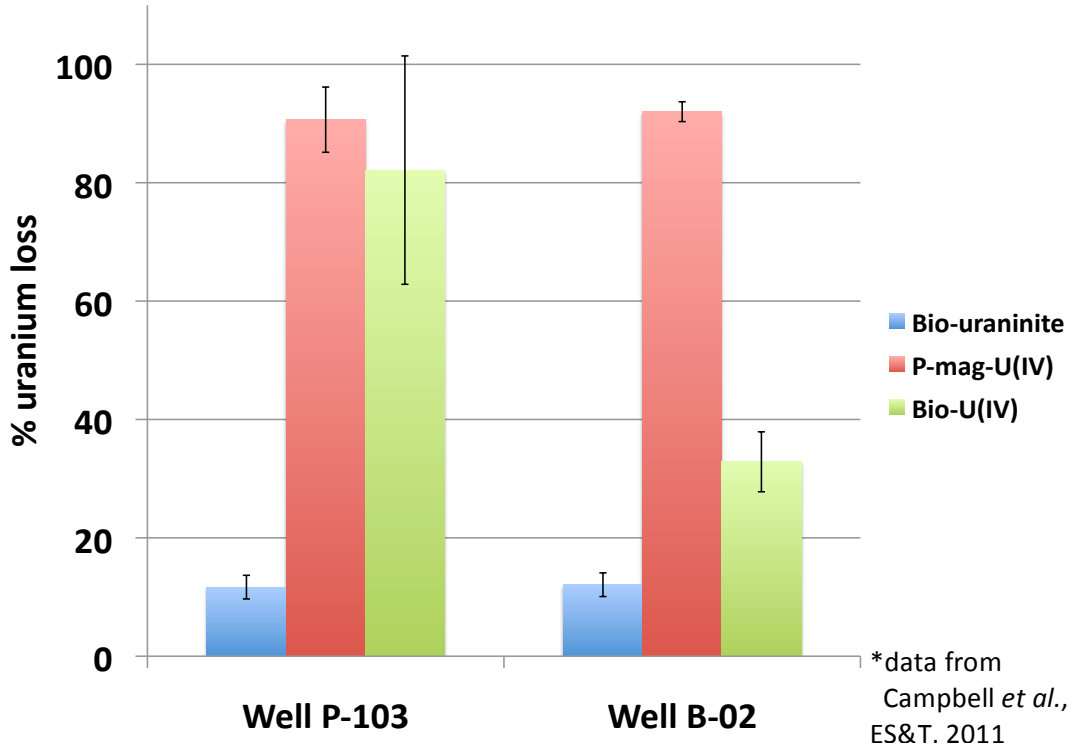

Figure 74. Uranium release from agarose gel pucks installed in wells P-103 and B-02 for one month.

Spatial Relationships of Uranium Sequestration Pathways Arising from Interactions Between Uranium and Iron Biogeochemistry. M. Massey, and S. Fendorf (Stanford), J.R. Bargar and J. Lezama (SLAC); K.H. Williams (PNNL); and P.E. Long (PNNL).

The Old Rifle IFRC site is an excellent location to address the question, "how do uranium-Fe(II)-Fe oxide interactions differ across advective and diffusive transport paths *in aquifers*?" Interactions between U(VI) and Fe(II) in the presence of Fe (oxyhydr)oxides can lead to three principal sequestration mechanisms: adsorption of U(VI) onto Fe (oxyhydr)oxides; reduction of U(VI) to U(IV) solids by Fe(II); and, incorporation of U(V/VI) into Fe (oxyhydr)oxides. Our objective is to generate biogeochemical gradients across Fe-oxide-coated sand medium that would lead to spatially distinct differences in the operative sequestration mechanisms. Laboratory studies are currently underway to characterize the mechanisms of U incorporation into Fe oxides, and the controls on this pathway versus reduction and adsorption; these experiments at the Old Rifle IFRC site will help to place those mechanisms into a spatial and

environmental context by examining the interactions between Rifle groundwater, Fe oxides, and U under the two different flow regimes.

Diffusion experiments (Figure 75) were installed in well P-101 during fall 2011 to study the behavior of U(VI) adsorbed to ferrihydrite under field conditions where Fe(II) is naturally abundant (100 to 150 μM concentration) and can drive U(VI) and Fe(III). Similar experiments performed in 2010 showed that sequestration pathways were distributed spatially across the gradient created by Fe(II) and other solutes diffusing into the porous medium. The 2010 experiment was the first observation of U incorporation into Fe oxides in a field setting. The 2011 experiment is being conducted in order to replicate the 2010 results and increase understanding of the sustainability of these sequestration pathways over extended timescales. Incorporation of U(VI) into Fe oxides can enhance the attenuation of uranium in contaminated aquifers. This research is informing our understanding of how and where Fe(II)-Fe oxides interactions sequester or reduce U(VI) in aquifers.

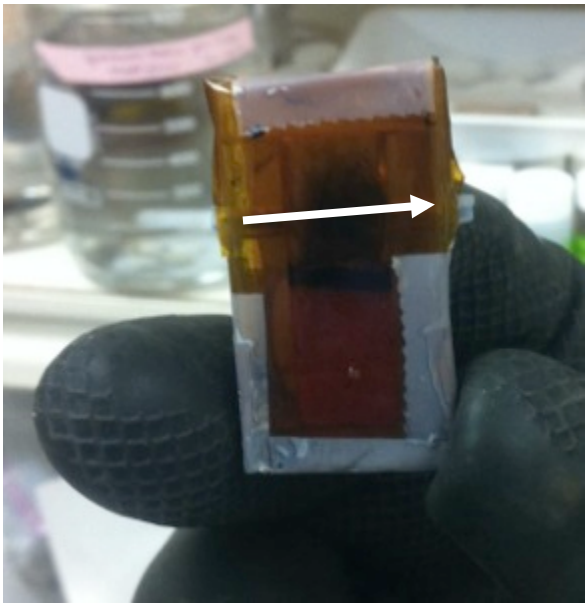

Figure 75. Photo of the reactor harvested from well P-101 in Dec, 2011. Flow proceeds through one end of the reactor as illustrated by the arrow. Diffusion gradients are created down into the ferrihydrite aggregate, simulating gradients in fine-grained sediments that abut higher-permeability flow paths. The black line in the middle of the picture is an area where ferrihydrite in contact with the flow path was reduced. Below this, ferrihydrite still exhibits a red (oxidized) color.

Vanadium Reduction and Microbial Characterization. (Alexis Yelton, Jill Banfield, Birgit Luef, UC Berkeley).

A V-reducing bacterium was isolated from Rifle groundwater on acetate and vanadate as a sole electron acceptor (Yelton *et al*., in prep.). Identification of the 16S ribosomal RNA sequence of this isolate indicated that it was in the *Betaproteobacterium* class in the genus *Simplicispira*. We refer to it as *Simplicispira* str. BDI for "bioreduction and detoxification *in situ*." High-density cell suspensions of this isolate were capable of reduction of up to 5 mM vanadate over the course of six days (Figure 76).

We sequenced the genome of the isolate using Illumina sequencing technology and created an automatic assembly of the resulting sequence with the Velvet software. The genome was approximately 4.2 Mb in length with a 65% GC content (Table 9). This high GC content is consistent with the genomes of other *Comamonadaceae* organisms. Manual curation of the assembly is ongoing. Genes of interest include anaerobic respiration genes: a large number of cytochrome genes (13 multi-heme c-type cytochrome genes) and denitrification genes (20 denitrification genes; napABDGH, nirNT, norB, nosZ). We showed growth of str. BDI on nitrate in the laboratory, confirming this function. The genome also contained a number of heavy metal-resistance genes (21 heavy metal-associated genes and 9 copper resistance genes). We infer that these resistance genes may help str. BDI survive in the contaminated aquifer at Rifle. We also note Type II secretion and conjugation genes, suggesting an evolutionary strategy based on adaptability through plasmid exchange, and flagellar genes that indicate the importance of motility to this organism in a low nutrient environment with unevenly dispersed energy sources. Cryo-EM imaging of str. BDI (Figure 77) confirmed the existence of flagella and two component systems for this isolate.

Str. BDI appears to be ubiquitous in the Rifle sediment. A 16S rRNA gene sequence with > 97% nt ID with BDI has been found in DNA data from in-well column samples taken during Fe-reduction and unstimulated sediments in 2010 (K. Wrighton and K. Handley, unpublished data). Relative abundance from this EMIRGE data indicated relatively more BDI 16S rRNA genes in the background sample as compared to the Fe reduction sample (7% vs. 4-5%). SSU similar to BD1 were also found in samples taken during sulfate reduction at a lower abundance (1.7%). Currently 16S rRNA amplicon data from V and acetate-stimulated in-well columns is being analyzed.

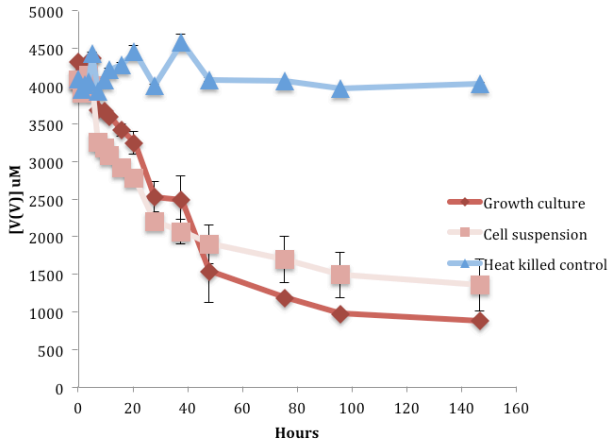

Figure 76. Vanadate reduction of Str. BDI in high-density cell suspension.

Table 9. General genome features of str. BDI

Number of contigs > 1 kb	234
Total length of contigs > 1 kb	4,217,881
Average contig length	18,025
Average coverage	263
GC content	65%
N50	32,693

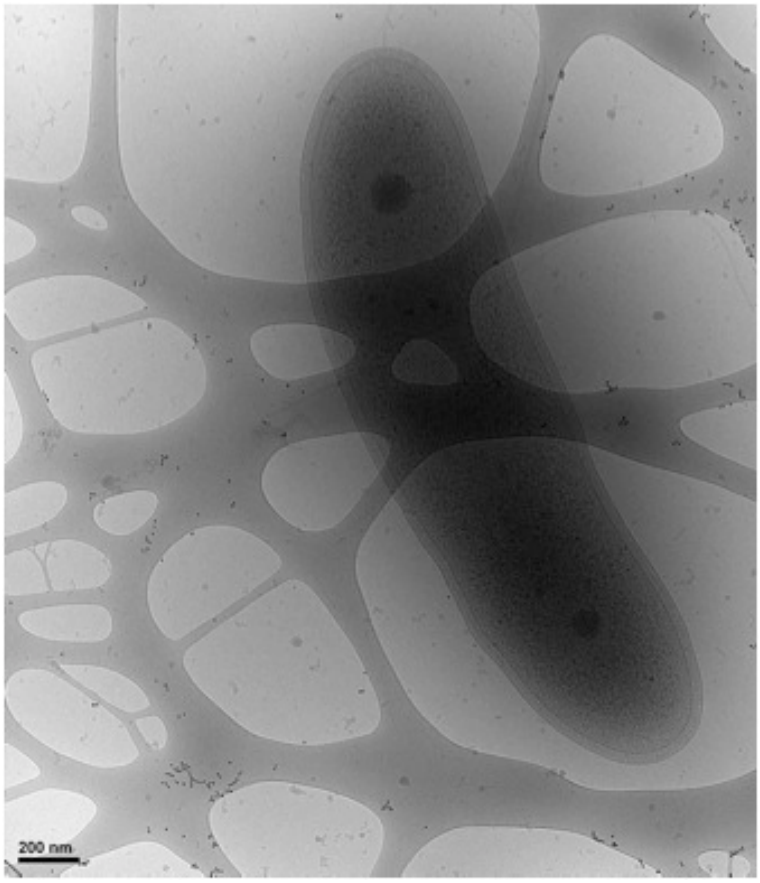

Figure 77. Cryo-EM micrograph of str. BDI grown on nitrate and acetate.

3D reconstruction of biological organization and mineralization in sediment attached biofilms during uranium bioremediation. Jill Banfield, Department of Earth and Planetary Science, University of California, Berkeley (PI); Luis Comolli, Life Science Divison, LBNL, Steven Singer, Physical and Life Sciences Directorate, LBNL, Birgit Luef, LBNL.

This collaborative project has participated in specialized field sampling for microscopy as part of both the "Super 8" and "Best Western" Experiments. This project has also provided cryoEM for other Rifle IFRC related experiments including Janet Leavitt/Steve Cabaniss (redox status uranium sorbed to cells) and Roberto Orellana/Janet Leavitt/Derek Lovley (redox status of uranium in contact with *Geobacter* with and without pilin genes). The key results of from CryoEM samples collected from the "Super 8" and "Best Western" Experiments are summarized below.

Iron-reducing bacteria accumulate ferric oxyhydroxide nanoparticle aggregates. We characterized groundwater planktonic FeRB from the uranium-contaminated aquifer sampled during *in situ* acetate amendment at the Department of Energy's Rifle Integrated Field Research Challenge site in Rifle, Colorado, USA. The "Super 8" field experiment was conducted during August and September 2010. Our work differs from prior ultrastructural characterization efforts targeting natural subsurface microbial consortia in that samples were cryo-plunged directly on site immediately after sampling. This step minimizes post-collection alteration including cell damage. Cells and cell-associated minerals were analyzed using 2D and 3D cryo-TEM, high resolution TEM (HRTEM), energy dispersive spectroscopy

(EDS) and scanning transmission X-ray microscopy (STXM). In addition, confocal laser scanning microscopy (CLSM) was performed on cells labeled with a *Geobacter*-specific fluorescence *in situ* hybridization (FISH) probe. This combination of microscopy and spectroscopy tools provided insight into the structure and composition of minerals associated with FeRB and uncovered a mechanism by which *Geobacter* may obtain energy during planktonic growth. Cryo-TEM 2D projections of *Geobacter* cells with nanoparticle aggregates attached to the outer membrane show that the number and size of nano-aggregates covering the surface of individual cells varied greatly (see Figure 56 for an example of attached nanoaggregates). Some cells exhibited very few small nano-aggregates, whereas others were almost entirely covered. Cells varied in both size and shape as observed by cryo-TEM. They were cocci-, comma- or rod-shaped. 3D reconstruction of a nano-aggregate decorated *Geobacter* cells enable us to take a single slice through the center of a tomographic reconstruction of a *Geobacter* cell in grey scale or to show 3D volume rendering of nano-aggregates attached to the cell wall in orange (images not shown). Energy dispersive X-ray spectra from nano-aggregates attached to a bacterium enable us to define the most abundant elements in the aggregates (Fe, O, Ca, V, and Si; Figure 78).

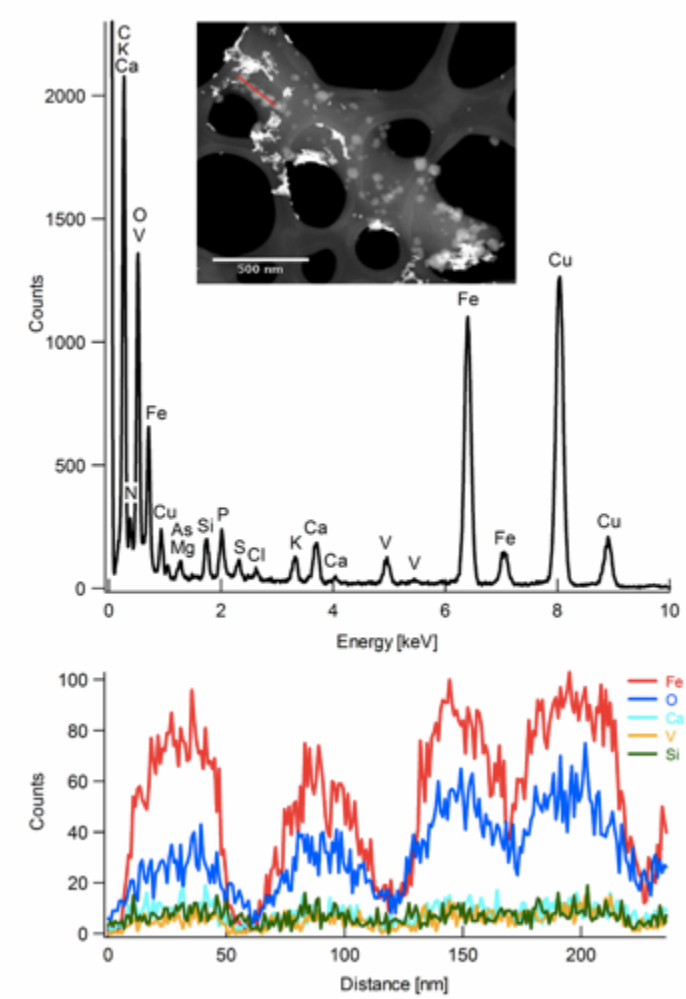

Figure 78. (A) TEM image of a bacterium with nano-aggregates attached to its cell surface. Red line indicates region of the line scan. (B) X-ray EDS sum spectrum of the nano-aggregates. Enhanced Cu and C peaks derived from the carbon coated formvar Cu-grids used for sample preparation. (C) EDS line scans of the 5 most abundant elements Fe, O, Ca, V and Si within the nano-aggregates (line scan location shown in red on A.

Scanning Transmission X-ray Microscopy (STXM) analysis of a cell exhibiting nano-aggregates results in an image recorded at Fe L_3-edge (709.5eV) and elemental distribution maps. Fe $L_{2,3}$ NEXAFS spectra from selected areas shown in the STXM image show the relative abundance of C, Ca, Fe, V, and combined C and Fe. For clarity, spectra from the diffuse and aggregate #2 areas were multiplied by a factor of 15 and 2 respectively, and all spectra were shifted vertically. Fe standards, confirmed by XRD are shown for comparison, include Fe(II) carbonate (siderite), Fe(III) oxyhydroxide (ferrihydrite) and mixed valent magnetite (Fe_3O_4). Vertical dashed lines are located at 707.8eV and 709.5eV. Fe $L_{2,3}$ NEXAFS spectra collected on the cell surface attached nano-aggregates show that the redox state of Fe was mixed valent Fe(II)-Fe(III) with variable proportions of Fe(II) and Fe(III) from one aggregate to another. These results suggest that *Geobacter* may use the nano-aggregates as redox capacitors, but research on their function is still in progress. Their persistence over two biostimulation experiments at the Rifle IFRC ("Super 8" and "Best Western") indicate their significance over a range of biogeochemical parameters and under actual subsurface conditions.

Previous research demonstrates that during initial *in situ* biostimulation with acetate, planktonic microbial population in the subsurface are dominated by *Geobacter sp.* (e.g. Wilkins et al. 2009 among many others; see Geobacter.org). We therefore hypothesize that microbes with nano-aggregates on their cell surfaces collected during the "Super 8" experiment and examined with our cryoTEM techniques were indeed *Geobacter sp*. To directly test this hypothesis, we combined fluorescent *in situ* hybridization (FISH) with TEM imaging of cryo-preserved samples. Epifluorescence images of planktonic cells on a TEM grid are positively labeled with *Geobacter* probe (Geo3 B). TEM 2D projections of these same *Geobacter* cells clearly exhibit aggregates of nanoparticles attached to the outer membrane (Figure 79). This unequivocally demonstrates that the nano-aggregates are formed by *Geobacter sp*. The aspect ratio of the *Geobacter* cells imaged by TEM is different than that in Figure 56 or Figure 80 due to thawing required prior to the FISH process.

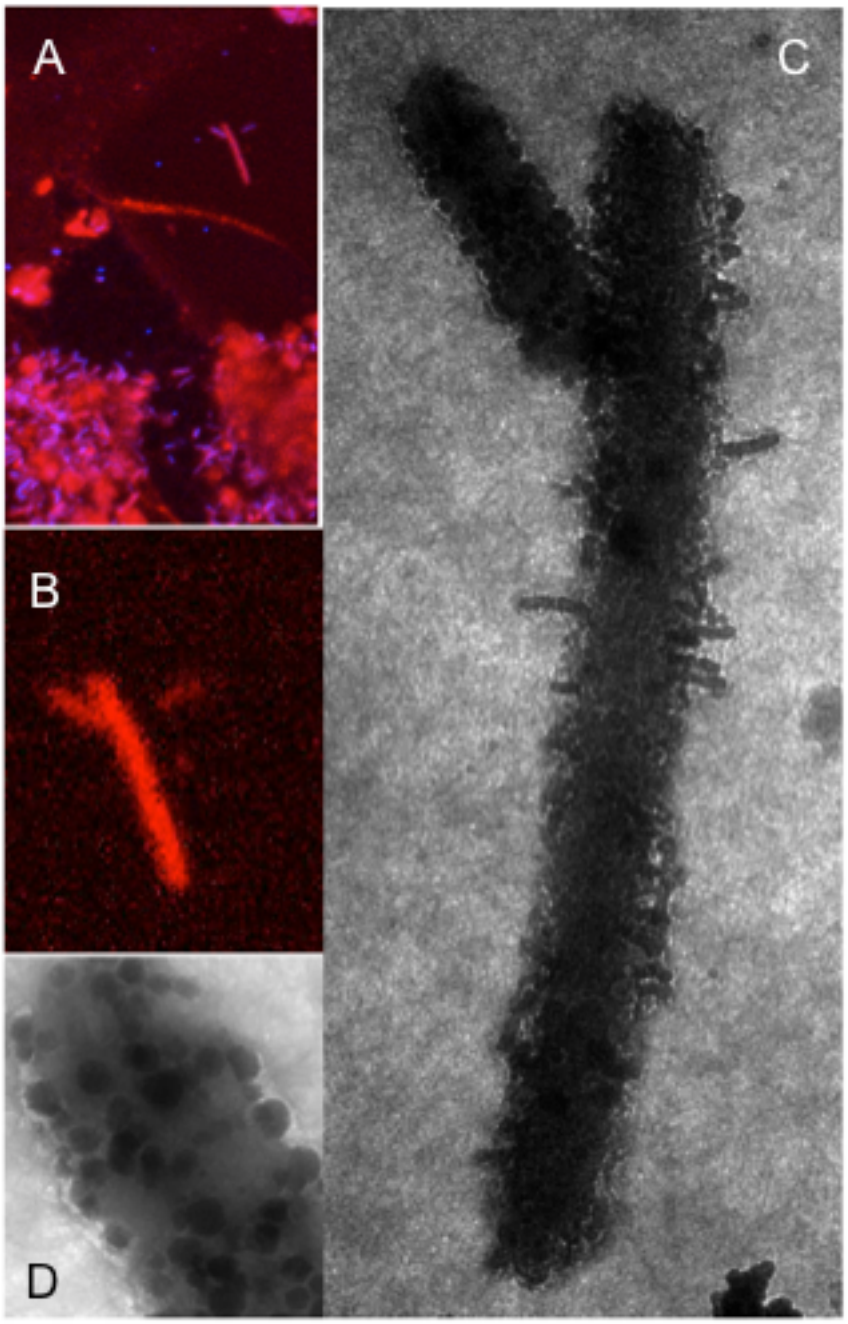

Figure 79. Correlative FISH and cryo-TEM image analysis. A) Epifluorescence image of planktonic cells on a TEM grid positively labeled with *Geobacter* probe (Geo3 B) in red; DAPI in blue. (B) Close up of positively labeled with *Geobacter* cells in red. (C) TEM 2D projection of the same *Geobacter* cells with aggregates of nanoparticles attached to the outer membrane imaged after FISH labeling. (D) Close up of nano-aggregates attached to the outer membrane.

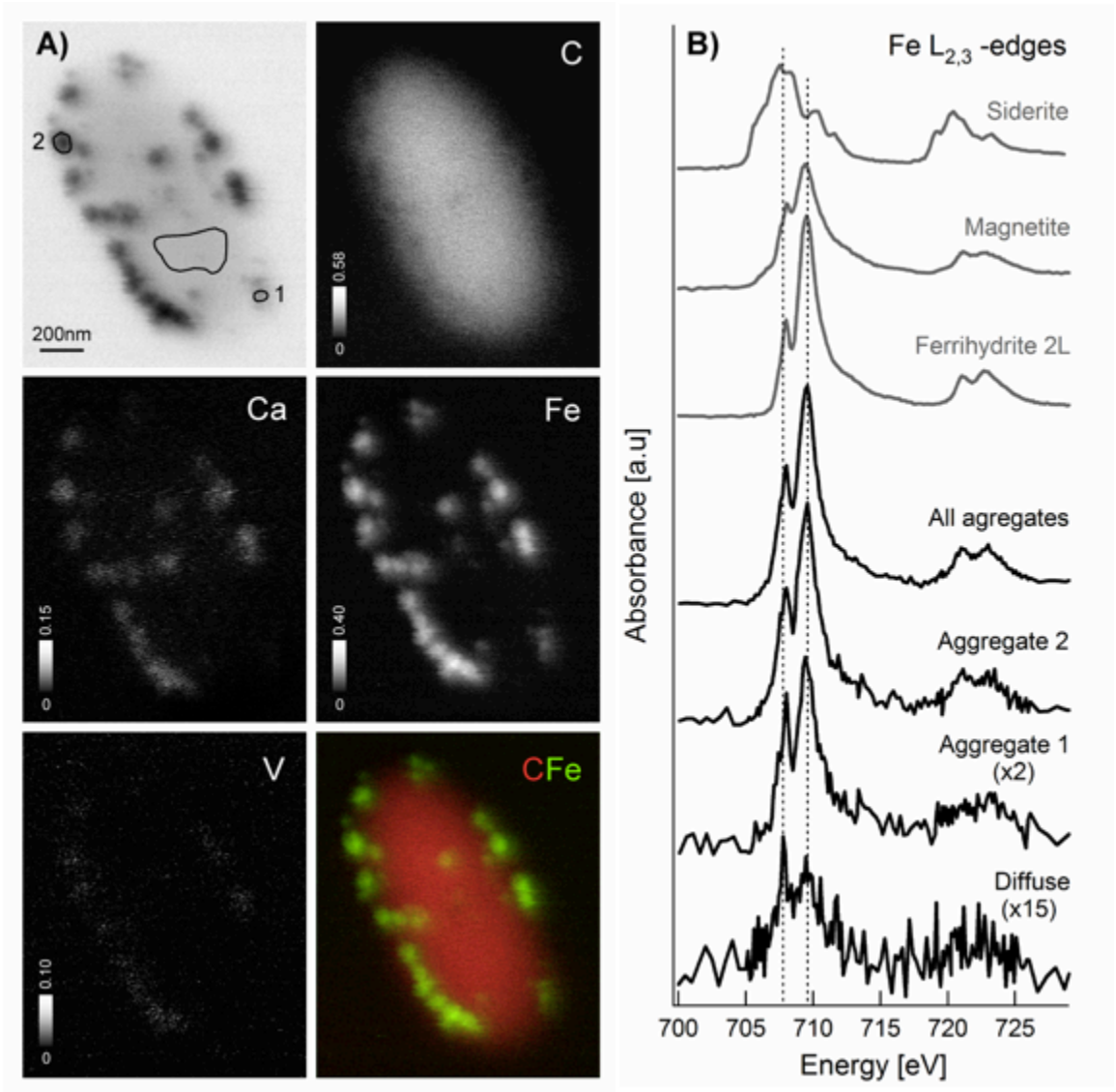

Figure 80. STXM analysis of a cell exhibiting nano-aggregates. (A) STXM image recorded at Fe L_3-edge (709.5eV) and elemental distribution maps. Intensity scale bars are in optical density unit. (B) Fe $L_{2,3}$ NEXAFS spectra from selected areas pointed out in the STXM image (data collection and analysis S. C. Fakra at the Advanced Light Source, Lawrence Berkeley National Laboratory).

Extensive two-dimensional and three-dimensional cryo-TEM data were acquired from the groundwater samples described above. Three-dimensional reconstructions from tilt series of nano-organisms prove their median size (150, short axis to 250 nm, long axis) is at or below previously estimated lower size limit for life (250 ±50 nm, Steering Group for the Workshop on Size Limits of Very Small Microorganisms, National Research Council 1999). Unique space optimization strategies are suggested by their 3D architecture (Figure 81). Specifically, the inside of the cell exhibits an apparent compactness unusual for microorganisms. There are also few ribosomes visible and a lack of contrast variations. Analysis of these images is still in progress.

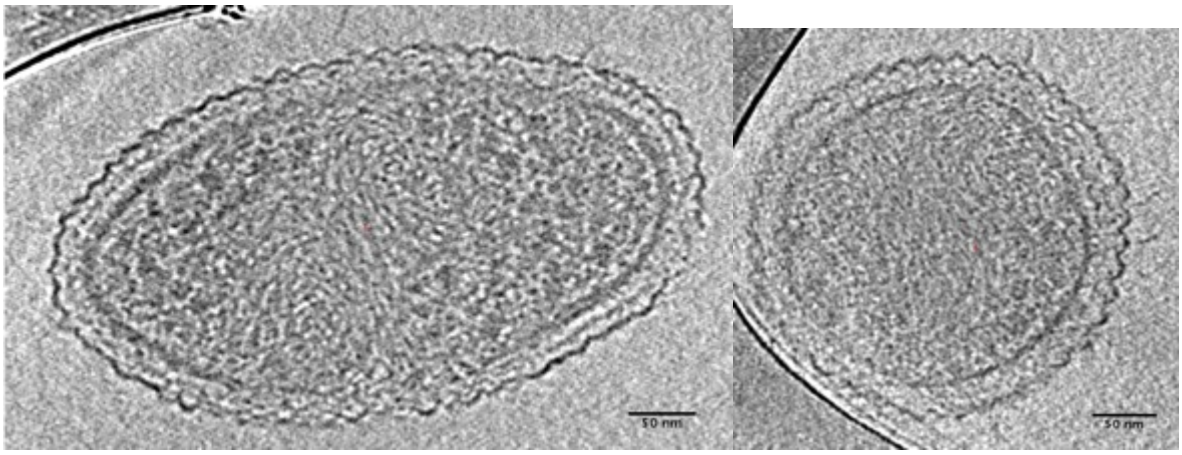

Figure 81. Nanobacteria in groundwater samples collected during the "Best Western" experiment (Well CD-01, Sept 3 and Sept 5, 2011) imaged by cryo-TEM.

Viruses are also present in groundwater samples from both the "Super 8" and "Best Western" experiments. Cryo-TEM images of viruses from Rifle ground water samples demonstrate their ubiquitous presence consistent with assembled genomes from sequencing of groundwater samples (see earlier section on the "Big Rusty" Experiment). Figure 82 shows typical imaging results for viruses (well CD-O1, "Super 8" experiment).

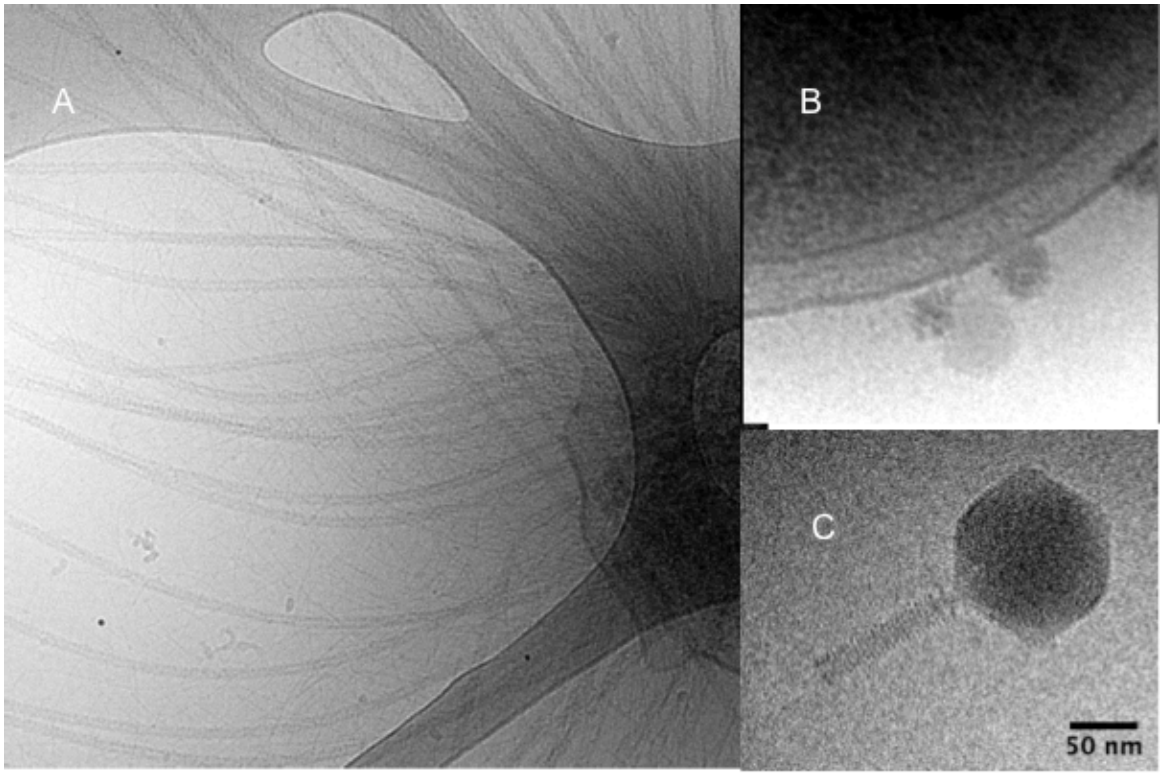

Figure 82. Cryo-TEM images of viruses from Rifle ground water samples, well CD-O1, "Super 8" biostimulation experiment. A). Rod-shape viruses being released from an infected cell. B). Bacteriphage penetrating a bacterium cell wall, adjacent to nano-aggregates. A bacteriophage of the same morphology as in B) free in suspension.

Development of U isotope fractionation as an indicator of U(VI) reduction. C. C. Lundstrom, T. M. Johnson, R. A. Sanford, A. E. Shiel, A. Basu (University of Illinois at Urbana–Champaign); Kenneth H. Williams and Philip E. Long (LBNL).

The UIUC group is evaluating U isotopes as an indicator of U(VI) reduction in uranium plumes. This work aims to increase understanding of U reduction in the controlled field setting at the IFRC Rifle site. Several questions must be answered in the development of U isotopes as a new tool for understanding U immobilization in the subsurface. In the past year, we have started to address several questions: (1) Are there confounding processes that complicate efforts to use $^{238}U/^{235}U$ as an indicator of U(VI) reduction (e.g., adsorption, mixing of distinct U from different flow paths)? (2) Is the U isotopic fractionation factor for U(VI) reduction constant or does it vary? (3) Can reoxidation be detected using $^{238}U/^{235}U$? (4) How do effective fractionation factors for field experiments compare to intrinsic fractionation factors for laboratory microbial experiments? (5) What are the fractionation factors for relevant microbial reductions of U(VI)?

Sample U isotopic compositions were determined by multi-collector inductively coupled plasma mass spectrometry (Nu Plasma, Nu Instruments Ltd.) using a double spike technique (^{233}U–^{236}U) by a method modified after Bopp et al. (2010). Uranium isotopic compositions are reported in the typical delta notation ($\delta^{238}U$) relative to the U isotopic standard CRM 112-A. A closed system Rayleigh distillation model was used to extract the magnitude of the isotopic fractionation. This is quantitatively expressed as the isotopic fractionation factor ε, where $\varepsilon = (\alpha\text{-}1) \times 10^3$ (±2SE) and $\alpha = {}^{238}U/^{235}U_{product}/{}^{238}U/^{235}U_{reactant}$.

Variability in U isotopic composition across the Rifle floodplain. Rifle floodplain samples exhibit limited but significant variation in U concentration and isotopic composition (Figure 83). The three surface waters collected north of the site are characterized by mean U concentration and $\delta^{238}U$ of 37 ppb and -0.12‰, respectively. The remaining floodplain samples from the site exhibited U concentration ranging from 44.5–327 ppb and $\delta^{238}U$ from -0.19 to 0.24‰. The total variation, 0.44‰, is greater than the long-term error, 0.09‰ (2× root mean square error between measurements of full sample duplicates; n=16). Among floodplain samples, as the U concentration increases, a corresponding increase is observed in the $\delta^{238}U$ value. This relationship is attributed to mixing between background U coming into the site with remaining contaminant U from historical U mill operations.

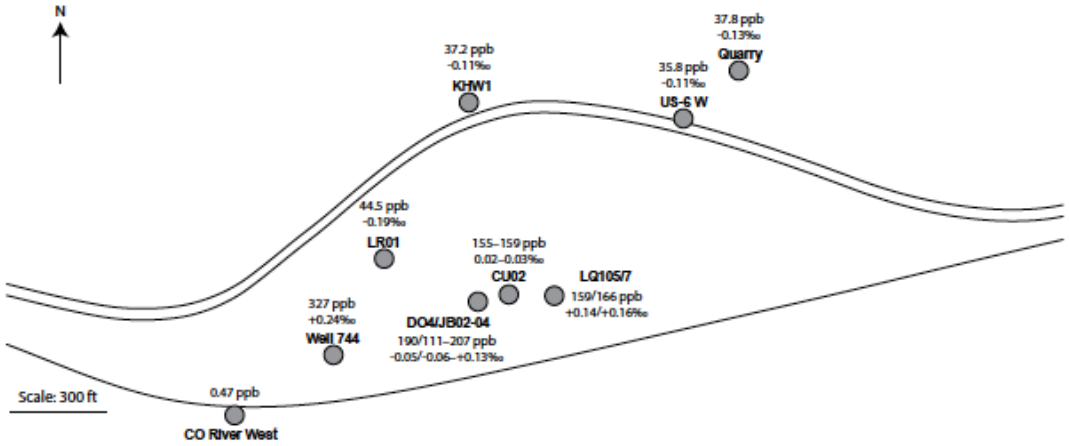

Figure 83. Rifle floodplain U(VI) concentration and $\delta^{238}U$ results.

Evaluating adsorption as a source of U isotopic fractionation. Groundwater samples from the 2010–2011 experiment (Plot C) were used to evaluate adsorption as a source of U isotopic fractionation. In this experiment, bicarbonate was injected to desorb U from aquifer solids. Samples were collected from the downgradient well, CU-03. Preinjection groundwater had a [U(VI)] of ~150 ppb. During the injection the concentration reached a high of 300 ppb before dropping to 70 ppb and then returning to preinjection levels. Although laboratory experiments have found preferential adsorption of ^{235}U to Mn oxyhydroxides ($\Delta^{238}U = 0.22\pm0.09‰$) (Brennecka et al, 2011), field experiments at the IFRC Rifle site revealed non-significant U isotopic fractionation (Figure 84) is associated with adsorption and desorption of U(VI) from aquifer solids (Laubach et al., 2011).

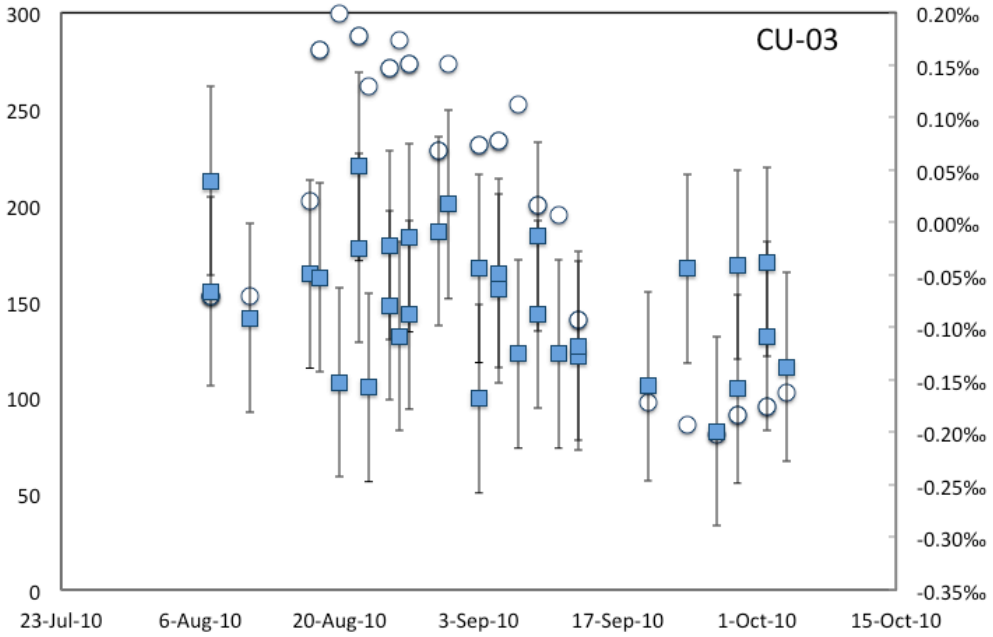

Figure 84. Plot of U(VI) concentration (circles) and $\delta^{238}U$ (squares) vs. date for CU-03 groundwater samples.

Uranium isotope fractionation associated with field biostimulation experiments. Previous work (Bopp et al., 2010) has shown large shifts in $\delta^{238}U$ accompany U(VI) bioreduction ($\Delta^{238}U = 1.05‰$). A more detailed study to increase confidence in the use of $\delta^{238}U$ as an indicator of U(VI) reduction is underway as we seek to apply this method to bioremediation experiments in which groundwater is treated with acetate only or both acetate and bicarbonate. In addition, this data set gives us, for the first time, $\delta^{238}U$ measurements during rebound of U(VI) concentrations as reduction wanes. This is particularly important as the long-term success of this remediation technique depends on the stability of sequestered U(IV).

We have measured groundwater $\delta^{238}U$ for two wells downgradient of the injection gallery; one of the wells (CD-01) was amended with acetate and the other (CD-14) with both acetate and bicarbonate (Figure 85). Preinjection values for the two wells are identical to those upgradient, within the uncertainties. For CD-01, the acetate injection upgradient led to a dramatic drop in U(VI) concentration (from 165 to 10.6 ppb) and $\delta^{238}U$ (from 0.03 to -1.32‰), resulting from the preferential removal of ^{238}U as reduced U(IV). An excursion to greater $\delta^{238}U$ values during the period when U(VI) concentration was at a minimum may

be related to a contribution of relatively heavy U from nano-colloidal U(IV) in the filtered groundwater. After the amendment ceased, the groundwater U(VI) concentration and $\delta^{238}U$ returned to approximately preinjection values. Lack of an increase of $\delta^{238}U$ above preinjection values is consistent with advection of U(VI) from upgradient, rather than reoxidation of U(IV), as the primary source.

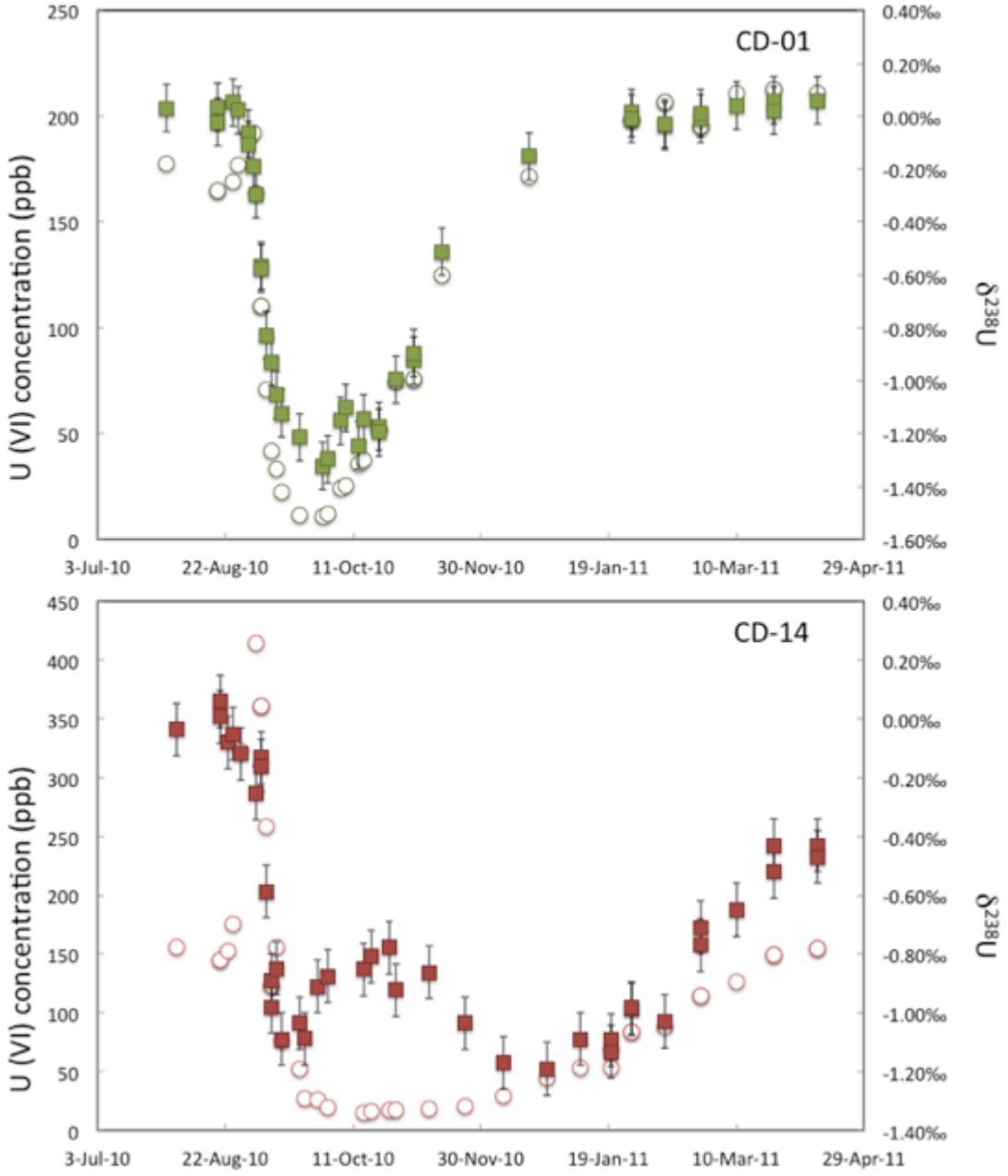

Figure 85. Plot of U(VI) concentration (circles) and $\delta^{238}U$ (squares) vs. date for CD-01 (above) and CD-14 (below) groundwater samples.

For CD-14, a large increase in the U(VI) concentration was induced by the bicarbonate injection (up to 415 ppb), while no change was observed in $\delta^{238}U$. This is in agreement with previous Rifle field

experiments that revealed the absence of significant U isotope fractionation with adsorption–desorption of U(VI) (Laubach et al., 2010). The acetate injection led to a dramatic decrease in the U(VI) concentration and $\delta^{238}U$ values (to 15 ppb and -1.19‰). The recovery of U(VI) concentration and $\delta^{238}U$ is much slower for CD-14. Despite the return of U(VI) concentration to preinjection values by the end of the field season, sustained U isotope fractionation (-0.43‰) is observed.

Similar shifts in isotopic composition are observed for the 2010–2011 and the 2009 (Bopp et al., 2010) biostimulation experiments ($\Delta^{238}U$ = 1.35‰ and 1.05‰, respectively), with ε values for the acetate-amendment induced concentration drop that are within error (0.44±0.09‰ and 0.46±0.11‰, respectively). These ε values are approximately half the intrinsic ε values determined from laboratory microbial experiments (~1‰) for nutrient limited electron-donor poor conditions. This difference may be due to heterogeneity effects or to a difference in reduction mechanism.

Microbial U reduction (laboratory experiments). Microbial reduction of U(VI) in the subsurface induces U isotopic fractionation, although the controlling factors and the degree of variability of the isotopic fractionation are not yet well-understood. The primary objectives of the microbial study are to determine (1) the variability of the isotopic fractionation factors (ε) with different metabolic pathways and (2) whether ε values are highest under nutrient limiting, electron-donor poor conditions such as those observed in natural environments. We experimentally determined ε values for U(VI) reduction by a metabolically diverse group of microorganism including two strains of *Geobacter sulfurreducens* (PCA and Criddle), *Anaeromyxobacter dehalogenans* strain FRCW, *A. dehalogenans* strain FRC-R5 and *Desulfitobacterium* Viet1.

We measured the ε values for each bacterial species in duplicate batch incubation experiments amended with U(VI) and 0.5 mM electron-donor at 30 °C. We demonstrated that all strains tested during this investigating induce significant isotopic fractionation during U(VI) reduction. The ε values obtained for U(VI) reductions by *G. sulfurreducens* strains PCA and Criddle were 0.68‰ and 0.95‰, respectively. The ε values for *A. dehalogenans* strain FRCW, *A. dehalogenans* strain FRC-R5 and *Desulfitobacterium* Viet1 were 0.75‰, 0.98‰ and 0.84‰, respectively. These results indicate that the isotopic fractionation factors vary with metabolic pathway. We observed a systematic relationship between the cell-specific reduction rate and the isotopic fractionation factors. The ε values increase with decreasing cell-specific reduction rate, suggesting that cell-specific reduction rates are good indicators of the magnitude of microbial U isotopic fractionation. Our data also suggest that ε tends to reach highest values (~1‰) under nutrient limited electron-donor poor conditions. The results of the microbial study reinforce the use of U isotopes as an indicator of microbial U(VI) reduction and can be used to help interpret the U isotope data for the IFRC Rifle site.

Research Plans: Next 12 Months

Subtask Big Rusty (F-5, F-7)

Analysis of metagenomes for selected samples from the Big Rusty Experiment is nearly complete with submittal of manuscripts planned for the first half of 2012.

Subtask La Quinta (F-1, F-2)

"La Quinta" research will continue to focus on conservative and reactive tracer experiments, and *in situ* column experiments. This experimental plot has been designed to track water geochemistry and microbiology in and out of naturally reduced zones (NRZ's) to determine if they are currently sinks or sources for uranium and ascertain the rate of natural bioreduction of U(VI). Completion of non-reactive tracer experiments at the experimental plot has been delayed for a number of reasons, notably the extended runoff in the Colorado River in the spring of 2011. However, our analysis of the geochemistry of samples from "La Quinta" continues and we anticipate submittal of a manuscript for review in the first quarter of 2012. Our ability to conduct non-reactive and reactive tracer tests in the "La Quinta" experimental plot in FY-2012 and FY-2013 will be limited by funding.

Subtask Buckskin (F-7A; Post-biostimulation monitoring, including in situ columns)

Results from bioreduced columns operated *in situ* in downgradient and upgradient wells (and described above will be submitted for publication during the first quarter of 2012. Analysis of the proteogenomics of the initial *in situ* column from the "Buckskin" experiment will also be submitted for publication during the first quarter of 2012.

Subtask Super 8 (F-8; Combined biostimulation/sorption experiment)

Analysis of the extensive data set from the Super 8 experiment continues. Development of manuscripts on Super 8 biogeochemistry, and analysis and publication of a variety of other data sets, including proteogenomic data will occur over the next 6 to 9 months. Reactive transport modeling will be particularly fruitful during 2012 with completion of the 3D model for the experimental plot expected early in 2012. Results are expected to further constraint key rate and thermodynamic parameters, providing global information for modeling uranium bioreduction and desorption processes in a range of environments.

Subtask Best Western (F-9; Combined biostimulation/sorption experiment)

Analysis of the "Best Western" Experiment is under way. We anticipate important results on biotic vs. abiotic bicarbonate sources and on proteogenomics of sulfate reduction and methanogenesis. Submittal of publications is expected late in 2012 or early in 2013.

Subtask Uranium Plume Dynamics (F-11; Quantifying mechanisms, processes, and sources that sustain the uranium plume at the Rifle IFRC)

In this subtask, we will continue to collect selected data in various parts of the floodplain to initiate efforts to quantify the U mechanisms, processes, and sources that sustain the plume. These activities include monitoring selected wells during water table rise and fall, geophysical imaging of groundwater flux near the Colorado River, and proximal to the upland edge of the floodplain, and monitoring the biogeochemistry of the seeps north of Highway 6. We will also continue to examine floodplain hydrology in response to changes in discharge of the Colorado River based a newly instrumented stilling well

upriver from the site. These activities are all budget constrained, but we plan to submit manuscript on data a collected in 2011 and 2012 early in 2013.

A key part of this subtask is assessing the metabolic potential of the Rifle IFRC alluvial aquifer. Initial samples for this effort have been collected and will be processed early in 2012. We expect initial results in mid-2012 with submittal of publication for review in late 2012 or early 2013.

Subtask The Hampton Experiment (F-12; Tracer test to assess U adsorption, U desorption, and U isotope exchange kinetics)

The Rifle IFRC continues to consider a tracer test that would be conducted at Experimental Plot B. The concept of the experiment is to inject groundwater from one of the wells upgradient from Experimental Plot C into the injection wells at Experimental Plot B. The conditions of the Experimental Plot C re are chemically different than at plot B (higher U, greater alkalinity). Br and U isotopes would be added to the groundwater prior to the injection. The goals of the experiment are to examine the ability of the reactive transport model that we are completing for the "Little Rusty" Experiment (U desorption under high alkalinity) to describe the results of a new tracer test. In the previous experiment, we only had U desorption, which was kinetically controlled (described in the RTM with mass transfer). In The Hampton, we would have U adsorption kinetics at first (because of higher U in the injected water), followed by U desorption as the experiment ended. Plus, with the U isotope added, we would have non-stimulated U isotopic exchange kinetics, plus adsorption and desorption of the isotope. The experiment will provide crucial additional information to support our reactive transport modeling.

Subtask River Rouge II Experiment (F-13; Tracer test under biotic Fe-reduction conditions)

The River Rouge II Experiment is planned as a short-duration tracer test in which U behavior under conditions of significant soluble Fe(II) associated with prior bioreduction experiments exists in groundwater. The experiment will enable us to understand the sorption behavior of U under such conditions. Both the River Rouge II and The Hampton experiments are still being scheduled and planned and are subject resource constraints due to our reduced budget in FY-2012.

Subtask Comfort Experiment (F-14; In situ reoxidation rates for U(IV) under conditions of oxygen amendment.

The Comfort Experiment would take advantage of the presence of U(IV) in the subsurface from the bioreduction associated with the "Super 8" and "Best Western" experiments. The experiment is still being designed and planned but likely would be performed during the August and September 2012. Currently we have field data on U(IV) oxidation rates are limited to in-well bioreduced U(IV) experiments. These provide bounding results, but do not represent rates of U(IV) bioreduced on sediments. Due to our extensive date on U isotopic fractionation associated with U(VI) bioreduction, we can now separate U from desorption from U derived from reoxidation. As for other experiments planned for 2012, the Comfort Experiment is subject to resource constraints due to our reduced budget for FY-2012.

Data Management

In 2012 the key data management objective is to integrate the Rifle database with the genomic and metagenomic databases to provide users access to all data related to specific samples. Another objective is to enhance sample and result tracking, and provide smart phone apps for field data collection, as well as continue to develop basic client or server side data processing. For this, we will be exploring existing solutions such as World Wind.

Outreach Activities

Rifle IFRC participants continued to be active in professional societies, organizing and chairing sessions and presenting numerous abstracts at professional meetings during 2011 (see list of published abstracts). Several of the abstracts and presentations were invited, including international meetings. For example, Peter Jaffe, Phil Long and others organized a highly successful session on bioreductive immobilization of metals and radionuclides at the Fall AGU meeting in December 2011. The session was entitled "Bioreductive Immobilization and Remediation of Metals and Radionuclides: Mechanisms, Models, and Sustainability". Conveners included P R Jaffe, Princeton Univ; P E Long, Lawrence Berkeley National Laboratory; L Li, Pennsylvania State Univ; L N'Guessan, ExxonMobil, D. Wellman, PNNL, and Justin Marble, U.S. DOE. There were ~50 abstracts submitted to session.

As another example, Jim Davis gave an invited presentation at the Goldschmidt Conference August 14-19, 2011 in Prague, Czech Republic. Jim's presentation was entitled "A Coupled Ion Exchange, Surface Complexation, Calcite Dissolution, and Mass Transfer Model to Describe Uranium(VI) Desorption and Reactive Transport at the Rifle (USA) Field Site" was well received by an international audience.

In other outreach activities, Steve Yabusaki, Yilin Fang, Scott Waichler, and Phil Long continued their work with the Nuclear Regulatory Commission to apply and extend bioremediation models developed for the Rifle IFRC to uranium contamination in alluvial aquifers and Uranium *In Situ* Recovery (ISR) sites. This work continues to demonstrate the currency and importance of the Rifle IFRC in providing the scientific basis for meeting the global clean up challenge for uranium-contaminated sites.

The Rifle IFRC continues to attract and benefit from new collaborators (see list at the beginning of this document). The Rifle IFRC will continue to add new collaborators as long as they 1) provide the highest quality science that is relevant to project objectives, 2) can be effectively and safely integrated into planned field or laboratory experiments, and 3) collaborate with the Rifle IFRC team on publication of results. As a practical matter, we are likely close to a natural maximum number of collaborators on the project. As current collaborators complete their research and the research focus of the Rifle IFRC shifts, new collaborators will be added.

Working in conjunction with the Garfield County Public Library (GCPL) system, Dr. Kenneth H. Williams supported a proposal to the American Library Association (ALA) to sponsor the exhibition "Discover Earth: A Century of Change" for eight weeks in 2012-2013 at the Rifle, CO branch library (details at www.ala.org/offices/ppo/programming/discoverearth). Underwritten by the National Science Foundation, the proposal was successful, and the GCPL was one of only ten libraries countrywide selected to host the exhibition. The Discover Earth exhibition will focus on local earth science topics—such as weather, water cycle, and ecosystem changes—as well as a global view of the changing planet. The primary message of the exhibition is that the global environment changes – and is changed by – the local environment of the exhibition-hosts' communities. As part of the Rifle IFRC's commitment to the proposal, Dr. Williams will be presenting a seminar for the local community at the Rifle library on July 12th, 2012 entitled "Mines, Mills, and Monitoring: A History of Uranium Mining and Processing in Garfield County" with a focus on DOE's ongoing research activities at the Rifle IFRC site.

Challenges/Opportunities/Concerns

Challenges

We have made excellent progress interpreting new metagenome data by combining new tool development conducted in parallel by the Banfield Laboratory, in part funded by the KBase Program, with deep sequencing and data analysis to assemble nearly complete genomes as described above. However, we are significantly challenged as we enter the 6th year of the project and we begin to get very deep key metagenomes for background sediment sample thanks to our 1 terabase of sequencing provided by the CSP. We will meet this challenge by prioritization of reduced funding for FY-2012, focusing on ***field personnel, metagenome data collection, tool development and data analysis***. We have achieved acceleration of genome assembly and interpretation of key samples, and we will need to ensure that resource allocations enable both successful sample collection and interpretation of genomic data in conjunction will crucial environmental parameters. Success continues to require careful management of resources to ensure balanced data collection and analysis for floodplain wide samples, enabling a fundamental understanding of the metabolic potential of the subsurface, including controls on carbon cycling.

Database management and data integration also continue to be a challenge for the project. We have successfully developed key data structures and continue to add data structures that incorporate a wide array of microbiological data. While we have made significant strides in implementing this approach, the database management effort (indeed, the entire project) is budget-limited. We will address the database challenge by continuing to develop the necessary database structures and ingesting project data broadly. However, these efforts will likely lag behind actual data collection and analysis without an increase in support. We are encouraged that BER is tackling the database management problem on a broad basis and are anxious to support that process, including integration with other projects facing similar issues such and ASCEM and the Critical Zone Obseratories.

Opportunities

Opportunities to expand the scope and scientific impact of the Rifle IFRC continue to revolve around existing and new collaborations with SBR Investigators. As noted above, several new University lead-proposals are focused on the Rifle IFRC and further leverage the scientific outcomes of our field experiments. Two particularly important examples are funding of our CSP sequencing request (lead by Jill Banfield, UC Berkeley) and a Genomic Sciences project (lead by Barbara Methe, JCVI). We will take full advantage of having multiple sequencing efforts at the Rifle IFRC. The Banfield-lead research has been awarded a terabase of sequencing, the largest such award to date. The research will address the metabolic potential across the Rifle flood plain including conditions of varying saturation with rise and fall of the water table. This work thus has both a spatial and temporal component that is tightly coupled to both the fate of organic carbon and U at the site and to the development of novel strategies to first predict and then actually stimulate a desired metabolic function in the subsurface. The sequencing lead by Methe research will focus initially on a single location of naturally reduced sediment samples (near well P-103). Depending on the outcome of sequencing on the initial samples, it may be possible to assess the differences in the microbial community in two different types of naturally reduced sediments at Rifle. The two sequencing efforts will share data and insights providing full integration and optimal leveraging of the sequencing efforts.

We also are continuing to benefit by strong integration with the SLAC SFA and the LBNL Sustainable Systems SFA and by access to EMSL capabilities. Recognition that significant U(IV) exists naturally in the subsurface at the Rifle IFRC is credited in large part to spectroscopy done at SLAC and the SLAC

SFA 3-year proposal integrates fully with Rifle IFRC experiments using the subsurface at Rifle to ensure environmental relevance to SLAC SFA research. Similarly, a portion of the LBNL SFA is focused on Rifle IFRC and the move of the Rifle IFRC to LBNL further enhances the synergism and leveraging between the two projects that simply would not be possible otherwise. Co-PI's will also continue to request EMSL instrument time and support to conduct analyses that cannot readily be performed elsewhere. Key successes related to our SLAC collaboration include demonstrating that U(VI) sorbed to *Geobacter* cell surfaces is partly reduced by cells that are not actively respiring. This was unexpected and fundamentally modifies our views of biosorption of U in the subsurface.

The transition of the Rifle IFRC to LBNL has significantly enhanced integration with the LBNL Sustainable Systems SFA. Additional opportunity lies in new linkages and synergy as we jointly develop exciting new research directions for both the Rifle IFRC and the Sustainable Systems SFA in the future.

Another key opportunity for 2012 continues to be enhanced understanding of carbon cycling in the shallow subsurface. We have made progress on factors governing cycling of recalcitrant organic carbon in the subsurface. Results are expected to have important relevance to the global carbon cycling in the shallow subsurface and its impact on CO_2 in the atmosphere, an area we expect to become the focus of future sampling and field experiments at the Rifle IFRC going forward. In addition, field experiments at the Rifle IFRC involving bicarbonate amendment to the subsurface provide fundamental science information on calcite precipitation kinetics under field conditions, one key to understanding reactions important to carbon sequestration in the deeper subsurface.

Environmental manipulation via carbon cycle management may well prove to be critical in order to respond to the growing pools of CO_2 and CH_4 in the atmosphere. The foundation for design of interference strategies, and a vital component of monitoring, strategy redesign, and outcome validation must be science. We cannot claim to have the science in place at this time because we barely have a sense of a scale of the biological diversity and complexity in terrestrial environments, such as soils and sediments, let alone methods to build and evaluate models. The Rifle site can meet this critical research need. **The site provides a rare opportunity to make focused use of new high-throughput sequencing and linked "omics" methodologies to enable understanding and management of terrestrial carbon cycle fluxes and dynamics.** The approach directly links to in-stride research on the metabolic potential of the subsurface at Rifle and will find broad application in areas such as response to permafrost thawing, biotechnology, and maintenance and enhancement of carbon pools sequestered in the subsurface in addition to the continued contribution to metals and radionuclide cycling and sequestration.

Concerns

Health and Safety was and continues to be the top concern of the Rifle IFRC in 2011 and going forward. The project has an excellent safety record, but we must remain vigilant to ensure the continued safe operation of the site. As part of the transition of the Rifle IFRC project to Lawrence Berkeley National Laboratory, we reviewed and updated all governing documents, including the Health and Safety Plan for the project. While we are confident that the revisions and updates will serve us well, it is crucial that we fully implement all safety protocols at the site and that we ensure that all individuals working at the site are cognizant of hazards and conduct themselves accordingly. It is particularly important that even under reduced budgets, we maintain full attention to safety at the site.

Publications

Rifle IFRC peer-reviewed journal articles published or accepted as of January 2012 (55 Total)

Baldwin, B.R., Peacock, A.D., Gan, Y.-D., Resch, C.T., Arntzen, E., Smithgall, A.N., Pfiffner, S.M., Freifeld, B.M., White, D.C., Long, P.E., 2009. In-Well Sediment Incubators to Evaluate Microbial Community Stability and Dynamics following Bioimmobilization of Uranium. Remediation Journal 19, 73-89.

[#]Barlett, M., Moon, H., Peacock, A., Hedrick, D., Williams, K., Long, P., Lovley, D., Jaffe, P., 2012. Uranium reduction and microbial community development in response to stimulation with different electron donors. Biodegradation 23, 1-12.

Bopp, C.J.I., Lundstrom, C.C., Johnson, T.M., Sanford, R.A., Long, P.E., Williams, K.H., 2010. Uranium 238U/235U Isotope Ratios as Indicators of Reduction: Results from an in situ Biostimulation Experiment at Rifle, Colorado, U.S.A. Environ. Sci. Technol. 44, 5927-5933.

Callister, S.J., Wilkins, M.J., Nicora, C.D., Williams, K.H., Banfield, J.F., Verberkmoes, N.C., Hettich, R.L., N'Guessan, L., Mouser, P.J., Elifantz, H., Smith, R.D., Lovley, D.R., Lipton, M.S., Long, P.E., 2010. Analysis of biostimulated microbial communities from two field experiments reveals temporal and spatial differences in proteome profiles. Environ. Sci. Technol. 44, 8897-8903.

[@]Campbell, K.M., Davis, J.A., Bargar, J., Giammar, D., Bernier-Latmani, R., Kukkadapu, R., Williams, K.H., Veramani, H., Ulrich, K.U., Stubbs, J., Yabusaki, S., Figueroa, L., Lesher, E., Wilkins, M.J., Peacock, A., Long, P.E., 2011a. Composition, stability, and measurement of reduced uranium phases for groundwater bioremediation at Old Rifle, CO. Applied Geochemistry 26, Supplement, S167-S169.

[@]Campbell, K.M., Veeramani, H., Ulrich, K.-U., Blue, L.Y., Giammar, D.E., Bernier-Latmani, R., Stubbs, J.E., Suvorova, E., Yabusaki, S., Lezama-Pacheco, J.S., Mehta, A., Long, P.E., Bargar, J.R., 2011b. Oxidative Dissolution of Biogenic Uraninite in Groundwater at Old Rifle, CO. Environmental Science & Technology 45, 8748-8754.

Chandler, D.P., Kukhtin, A., Mokhiber, R., Knickerbocker, C., Ogles, D., Rudy, G., Golova, J., Long, P.E., Peacock, A., 2010. Monitoring Microbial Community Structure and Dynamics during in situ U(VI) Bioremediation with a Field-Portable Microarray Analysis System. Environ. Sci. Technol. 44, 5516-5522.

*Chen, J.S., Hubbard, S.S., Williams, K.H., Pride, S., Li, L., Steefel, C., Slater, L., 2009. A state-space Bayesian framework for estimating biogeochemical transformations using time-lapse geophysical data. Water Resources Research 45, W08420, doi:08410.01029/02008WR007698.

*Commer, M., Newman, G., Williams, K.H., Hubbard, S.S., 2011. Three-dimensional spectral induced polarization data inversion for complex resistivity. Geophysics 76, 157-171.

^Dohnalkova, A.C., Marshall, M.J., Arey, B.W., Williams, K.H., Buck, E.C., Fredrickson, J.K., 2011. Imaging hydrated microbial extracellular polymers: Comparative analysis by electron microscopy. Applied and Environmental Microbiology 77, 1254-1262.

*Druhan, J.L., Conrad, M.E., Williams, K.H., N'Guessan, L., Long, P.E., Hubbard, S.S., 2008. Sulfur Isotopes as Indicators of Amended Bacterial Sulfate Reduction Processes Influencing Field Scale Uranium Bioremediation. Environ. Sci. Technol. 42, 7842-7849.

[#]Elifantz, H., N'Guessan, L.A., Mouser, P.J., Williams, K.H., Wilkins, M.J., Risso, C., Holmes, D.E., Long, P.E., Lovley, D.R., 2010. Expression of acetate permease-like (apl) genes in subsurface communities of Geobacter species under fluctuating acetate concentrations. FEMS Microbiology Ecology 73, 441-449.

*Englert, A., Hubbard, S.S., Williams, K.H., Li, L., Steefel, C.I., 2009. Feedbacks Between Hydrological Heterogeneity and Bioremediation Induced Biogeochemical Transformations. Environmental Science & Technology 43, 5197-5204.

Fang, Y., Yabusaki, S., Morrison, S., Amonette, J.P., Long, P., 2009. Multicomponent reactive transport modeling of uranium bioremediation field experiments. Geochim Cosmochim Acta 73, 6029-6051.

Flores Orozco, A.n., Williams, K.H., Long, P.E., Hubbard, S.S., Kemna, A., 2011. Using complex resistivity imaging to infer biogeochemical processes associated with bioremediation of an uranium-contaminated aquifer. J. Geophys. Res. 116, G03001.

Hedrick, D.B., Peacock, A.D., Long, P., White, D.C., 2008. Multiply methyl-branched fatty acids and diacids in the polar lipids of a microaerophilic subsurface microbial community. Lipids 43, 843-851.

Hedrick, D.B., Peacock, A.D., Lovley, D.R., Woodard, T.L., Nevin, K.P., Long, P.E., White, D.C., 2009. Polar lipid fatty acids, LPS-hydroxy fatty acids, and respiratory quinones of three Geobacter strains, and variation with electron acceptor. Journal of Industrial Microbiology & Biotechnology 36, 205-209.

[#]Holmes, D.E., O'Neil, R.A., Vrionis, H.A., N'Guessan, L.A., Ortiz-Bernad, I., Larrahando, M.J., Adams, L.A., Ward, J.E., Nicoll, J.S., Nevin, K.P., Chavan, M.A., Johnson, J.P., Long, P.E., Lovley, D.R., 2007. Subsurface clade of Geobacteraceae that predominates in a diversity of Fe(III)-reducing subsurface environments. ISME Journal 1, 663-677.

Hyun, S.P., Fox, P.M., Davis, J.A., Campbell, K.M., Hayes, K.F., Long, P.E., 2009. Surface complexation modeling of U(VI) adsorption by aquifer sediments from a former mill tailings site at Rifle, Colorado. Environ. Sci. Technol. 43, 9368-9373.

[@]Istok, J.D., Park, M., Michalsen, M., Spain, A.M., Krumholz, L.R., Liu, C., McKinley, J., Long, P., Roden, E., Peacock, A.D., Baldwin, B., 2010. A thermodynamically-based model for predicting microbial growth and community composition coupled to system geochemistry: Application to uranium bioreduction. Journal of Contaminant Hydrology 112, 1-14.

Kerkhof, L.J., Williams, K.H., Long, P.E., McGuinness, L.R., 2011b. Phase Preference by Active, Acetate-Utilizing Bacteria at the Rifle, CO Integrated Field Research Challenge Site. Environmental Science & Technology 45, 1250-1256.

[@]Klammler, H., Hatfield, K., Guimar,,es da Luz, J.A., Annable, M.D., Newman, M., Cho, J., Peacock, A., Stucker, V., Ranville, J., Cabaniss, S.A., Rao, P.S.C., 2012. Contaminant discharge and uncertainty estimates from passive flux meter measurements. Water Resour. Res. 48, W02512.

Komlos, J., Moon, H.S., Jaffé, P.R., 2008a. Effect of Sulfate on the Simultaneous Bioreduction of Iron and Uranium. Journal of Environmental Quality 37, 2058-2062.

Komlos, J., Peacock, A., Kukkadapu, R.K., Jaffé, P.R., 2008b. Long-Term Dynamics of Uranium Reduction/Reoxidation under Low Sulfate Conditions. Geochim Cosmochim Acta 72, 3603-3615.

Kukkadapu, R.K., Qafoku, N.P., Arey, B.W., Resch, C.T., Long, P.E., 2010. Effect of extent of natural subsurface bioreduction on Fe-mineralogy of subsurface sediments. Journal of Physics: Conference Series 217 012047.

*Li, L., Gawande, N., Kowalsky, M.B., Steefel, C.I., Hubbard, S.S., 2011. Physicochemical Heterogeneity Controls on Uranium Bioreduction Rates at the Field Scale. Environmental Science & Technology 45, 9959-9966.

*Li, L., Steefel, C.I., Kowalsky, M.B., Englert, A., Hubbard, S.S., 2010. Effects of physical and geochemical heterogeneities on mineral transformation and biomass accumulation during biostimulation experiments at Rifle, Colorado. Journal of Contaminant Hydrology 112, 45-63.

*Li, L., Steefel, C.I., Williams, K.H., Wilkins, M.J., Hubbard, S.S., 2009. Mineral Transformation and Biomass Accumulation Associated With Uranium Bioremediation at Rifle, Colorado. Environmental Science & Technology 43, 5429-5435.

[@]Liang, Y., Van Nostrand, J.D., N'Guessan, L.A., Peacock, A.D., Deng, Y., Long, P.E., Resch, C.T., Wu, L., He, Z., Li, G., Hazen, T.C., Lovley, D.R., Zhou, J., 2012. Microbial Functional Gene Diversity with a Shift of Subsurface Redox Condition during in situ Uranium Reduction. Applied and Environmental Microbiology In press.

[#]Mahadevan, R., Palsson, B.Ø., Lovley, D.R., 2011. In situ to in silico and back: elucidating the physiology and ecology of Geobacter spp. using genome-scale modelling. Nature Reviews Microbiology 9, 39-50.

[@]Melton, S.J., Yu, H., Williams, K.H., Morris, S.A., Long, P.E., Blake, D.A., 2009. Field-Based Detection and Monitoring of Uranium in Contaminated Groundwater using Two Immunosensors. Environmental Science & Technology 43, 6703-6709.

Miletto, M., Williams, K.H., N'Guessan, A.L., Lovley, D.R., 2011. Molecular Analysis of the Metabolic Rates of Discrete Subsurface Populations of Sulfate Reducers. Applied and Environmental Microbiology 77, 6502-6509.

Moon, H.S., McGuinness, L., Kukkadapu, R.K., Peacock, A.D., Komlos, J., Kerkhof, L.J., Long, P.E., Jaffe´, P.R., 2010. Microbial reduction of uranium under iron- and sulfate-reducing conditions: Effect of amended goethite on microbial community composition and dynamics. Water Research 44, 4015-4028.

[#]Mouser, P.J., Holmes, D.E., Perpetua, L.A., DiDonato, R., Postier, B., Liu, A., Lovley, D.R., 2009a. Quantifying Expression of Putative Oxidative Stress Response Genes in Geobacter species During In Situ Bioremediation of Uranium-Contaminated Groundwater: Comparison with Oxidative Stress Response in the Subsurface Isolate Geobacter uraniireducens. Journal of Microbial Ecology (ISME Journal) 3, 454-465.

Mouser, P.J., N'Guessan, A.L., Elifantz, H., Holmes, D.E., Williams, K.H., Wilkins, M.J., Long, P.E., Lovley, D.R., 2009b. Heterogeneity in ammonium availability at an in situ uranium bioremediation field site and its impact on community structure and the expression of nitrogen fixation and ammonium transporter genes during bioremediation. Environ. Sci. Technol. 43, 4386-4392.

N'Guessan, A.L., Elifantz, H., Nevin, K.P., Mouser, P.J., Methe, B., Woodard, T., Manley, K., Williams, K.H., Wilkins, M.J., Larsen, J., Long, P.E., Lovley, D.R., 2009. Molecular Analysis of Phosphate Limitation in Geobacteraceae During the Bioremediation of a Uranium-Contaminated Aquifer. ISME Journal 4, 253-266.

[#]N'Guessan, A.L., Moon, H.S., Peacock, A.D., Tan, H., Sinha, M., Long, P.E., Jaffé, P.R., 2010. Post-biostimulation microbial community structure changes that control the reoxidation of uranium. FEMS Microbiology Ecology 74, 184-195.

[#]N'Guessan, A.L., Vrionis, H.A., Resch, C.T., Long, P.E., Lovley, D.R., 2008. Sustained removal of uranium from contaminated groundwater following stimulation of dissimilatory metal reduction. Environ. Sci. Technol. 42, 2999-3004.

[#]O'Neil, R.A., Holmes, D.E., Coppi, M.V., Adams, L.A., Larrahondo, M.J., Ward, J.E., KP, N., Woodard, T.L., Vrionis, H.A., N'Guessan, A.L., Lovley, D.R., 2008. Gene transcript analysis of assimilatory iron limitation in Geobacteraceae during groundwater bioremediation. Environmental Microbiology 10, 1218-1230.

Peacock, A.D., Hedrick, D.B., Long, P.E., Nevin, K.P., Resch, C.T., Lovley, D.R., White, D.C., 2011. Field-scale uranium (VI) bioimmobilization monitored by lipid biomarkers and 13C-acetate incorporation. Remediation Journal 21, 85-106.

*Personna, Y., Ntarlagiannis, D., Slater, L., Yee, N., O'Brien, M., Hubbard, S., 2008. Spectral Induced Polarization Monitoring and Modeling of Microbial-Mediated Iron Sulfide Transformations. Journal of Geophysical Research 113, G02020, doi:02010.01029/02007JG000614.

Qafoku, N.P., Kukkadapu, R.K., Mckinley, J.P., Arey, B.W., Kelly, S.D., Wang, C., Resch, C.T., Long, P.E., 2009. Uranium in Framboidal Pyrite from a Naturally Bioreduced Alluvial Sediment. Environ. Sci. Technol. 43, 8528-8534.

Stucker, V., Ranville, J., Newman, M., Peacock, A., Cho, J., Hatfield, K., 2011. Evaluation and application of anion exchange resins to measure groundwater uranium flux at a former uranium mill site. Water Research 45, 4866-4876.

Wilkins, M.J., Callister, S.J., Miletto, M., Williams, K.H., Nicora, C.D., Lovley, D.R., Long, P.E., Lipton, M.S., 2011. Development of a biomarker for Geobacter activity and strain composition; Proteogenomic analysis of the citrate synthase protein during bioremediation of U(VI). Microbial Biotechnology 4, 55-63.

Wilkins, M.J., VerBerkmoes, N.C., Williams, K.H., Callister, S.J., Mouser, P.J., Elifantz, H., N'Guessan, L., Thomas, B.C., Nicora, C.D., Shah, M.B., Abraham, P., Lipton, M.S., Lovley, D.R., Hettich, R.L., Long, P.E., Banfield, J.F., 2009. Proteogenomic Monitoring of Geobacter Physiology during Stimulated Uranium Bioremediation. Applied and Environmental Microbiology 75, 6591-6599.

*Williams, K.H., Kemna, A., Wilkins, M.J., Druhan, J., Arntzen, E., N'Guessan, A.L., Long, P.E., Hubbard, S.S., Banfield, J.F., 2009. Geophysical Monitoring of Coupled Microbial and Geochemical Processes During Stimulated Subsurface Bioremediation. Environmental Science & Technology 43, 6717-6723.

Williams, K.H., Long, P.E., Davis, J.A., Steefel, C.I., Wilkins, M.J., N'Guessan, A.L., Yang, L., Newcomer, D., Spane, F.A., Kerkhof, L.J., McGuinness, L., Dayvault, R., Lovely, D.R., 2011. Acetate availability and its influence on sustainable bioremediation of uranium-contaminated groundwater. Geomicrobiology Journal 28, 519-539.

Williams, K.H., N'Guessan, A.L., Druhan, J., Long, P.E., Hubbard, S.S., Lovley, D.R., Banfield, J.F., 2010a. Electrodic voltages accompanying stimulated bioremediation of a uranium-contaminated aquifer. Journal of Geophysical Research Biogeosciences 115 G00G05.

Williams, K.H., Nevin, K.P., Franks, A., Long, P.E., Lovley, D.R., 2010b. An electrode-based approach for monitoring in situ microbial activity during subsurface bioremediation. Environ. Sci. Technol. 44, 47-54.

*Wu, Y., Hubbard, S.S., Williams, K.H., Ajo-Franklin, J., 2010. On the complex conductivity signatures of calcite precipitation. Journal of Geophysical Research Biogeosciences 115 G00G04.

Yabusaki, S.B., Fang, Y., Long, P.E., Resch, C.T., Peacock, A.D., Komlos, J., Jaffe, P.R., Morrison, S.J., Dayvault, R.D., White, D.C., Anderson, R.T., 2007. Uranium Removal from Groundwater via In situ Biostimulation: Field-Scale Modeling of Transport and Biological Processes. Journal of Contaminant Hydrology 93, 216-235.

Yabusaki, S.B., Fang, Y., Williams, K.H., Murray, C.J., Ward, A.L., Dayvault, R.D., Waichler, S.R., Newcomer, D.R., Spane, F.A., Long, P.E., 2011. Variably saturated flow and multicomponent biogeochemical reactive transport modeling of a uranium bioremediation field experiment. Journal of Contaminant Hydrology 126, 271-290.

[@]Yeh, G.-T., Gwo, J.-P., Siegel, M.D., Li, M.-H., Fang, Y., Zhang, F., Luo, W., Yabusaki, S.B., 2012. Innovative mathematical modeling in environmental remediation. Journal of Environmental Radioactivity In press.

[#]Yun, J., Ueki, T., Miletto, M., Lovley, D.R., 2011. Monitoring the Metabolic Status of Geobacter Species in Contaminated Groundwater by Quantifying Key Metabolic Proteins with Geobacter-Specific Antibodies. Applied and Environmental Microbiology 77, 4597-4602.

[#]Zhuang, K., Izallalen, M., Mouser, P., Richter, H., Risso, C., Mahadevan, R., Lovley, D.R., 2011. Genome-scale dynamic modeling of the competition between Rhodoferax and Geobacter in anoxic subsurface environments. ISME Journal 5, 305-316.

*Publications primarily supported by the Lawrence Berkeley National Laboratory (LBNL) Sustainable Systems Science Focus Area (SFA), with significant leveraging from, and through collaboration with, the Rifle IFRC.

[#]Publications primarily supported SBR Grants to Derek Lovley, University of Massachusetts in collaboration with the Rifle IFRC.

^Publication primarily supported by an EMSL Research and Capability Development Proposal and the DOE Subsurface Biogeochemical Research program (SBR) in collaboration with the Rifle IFRC and LBNL. The Environmental Molecular Sciences laboratory (EMSL), is a national scientific user facility sponsored by the U.S. DOE's Office of Biological and Environmental Research (OBER) and located at the Pacific Northwest National Laboratory (PNNL).

Rifle IFRC Book Chapter

Melton, S. J., Yu, H., Ali, M. F., Williams, K. H., Wilkins, M. J., Long, P. E., and Blake, D. A., 2008. Detection of hexavalent uranium with inline and field-portable immunosensors. In: Merkel, B. J. and Hasche-Berger, A. Eds.), *Uranium, Mining and Hydrogeology*. Springer-Verlag, Berlin

Published Abstracts

106 total abstracts published over the life of the project.

Antonopoulos, D.A., Ammar, A., Boyanov, M.I., Domanus, M.H., Long, P., Meyer, F., O'Loughlin, E.J., Sholto-Douglas, D., Skinner-Nemec, K., Williams, K.H., Kemner, K.M., 2009. Microbial Community Analyses of Iron-rich Mineral Suspensions Inoculated with Sediments from a Uranium Mill Tailings Site. American Society for Microbiology 109th General meeting, Philadelphia, PA, USA.

Antonopoulos, D.A., Bates, B.S., Boyanov, M.I., Brulc, J.M., Egholm, M., Garoutte, A., Harkins, T., Kwon, M., Long, P., Meyer, F., O'Loughlin, E.J., Osterberger, J., Simen, B.B., Skinner, K.A., Wilkening, J., Williams, K.H., Kemner, K.M., 2010. The Evolution of Microbial Communities Within Iron-rich Mineral Suspensions Inoculated with Sediments from an UMTRA Site. American Society for Microbiology, 110th Annual Meeting San Diego, CA May 23-27, 2010 N-1350/664, 115.

Bargar, J., Campbell, K., Veeramani, H., Suvorova, E., Bernier-Latmani, R., Stubbs, J.E., Lezama, J., Ulrich, K.-U., Blue, L.Y., Giammar, D.E., Long, P.E., Yabusaki, S., 2010a. Stability of BiogeochemicallyReduced Uranium Under in situ Conditions at the Old Rifle site. Long Term Serviellance and Maintenance Conference 2010 http://www.lm.doe.gov/ltsm_conference/Presentations.htm, Wednesday, 17 October 2010, PM Concurrent Session.

Bargar, J., Campbell, K.M., Veeramani, H., Ulrich, K., Long, P.E., Williams, K.H., Bernier-Latmani, R., Giammar, D., 2009a. Mechanisms of Biogenic Uraninite Corrosion in Groundwater at the Rifle IFRC site Eos Trans. AGU, Fall Meet. Suppl. 90, Abstract H33L-07.

Bargar, J., Williams, K.H., Campbell, K.M., Long, P.E., Stubbs, J.E., Blue, L., Suvorova, E., Lezama-Pacheco, J., Bernier-Latmani, R., Giammar, D., 2010b. Whole-sediment speciation of U(IV) in acetate-bioreduced aquifer sediments at the Rifle, CO, IFRC site. Abstract presented at 2010 Fall Meeting, AGU, San Francisco, Calif., 13-17 Dec. Abstract B54A-03.

Bargar, J., Williams, K.H., Campbell, K.M., Stubbs, J.E., Suvorova, E., Lezama-Pacheco, J.S., Alessi, D., Stylo, M., Handley, K.M., Bernier-Latmani;, R., Cerrato, J., Davis, J.A., Fox, P.M., Giammar, D., Long, P.E., 2011a. Progress in understanding uranium(IV) speciation and dynamics in biologically reduced sediments: Research at molecular to centimeter scales by the SLAC SFA program (Invited). Presented at the 2011 Fall Meeting, AGU, San Francisco, Calif., 5-9 Dec. Abstract H23I-02.

Bargar, J.R., Bernier-Latmani, R., Campbell, K.M., Giammar, D.E., Long, P.E., Ulrich, K.-U., Veeramani, H., 2009b. Rates and Mechanisms of Biogenic Uraninite Corrosion in Groundwater at the Rifle IFRC Site. Migration '09: 12th International Conference on the Chemistry and Migration Behaviour of Actinides and Fission Products in the Geosphere, Kennewick, Washington, USA Abstract No: PB4-7, 112.

Bargar, J.R., Campbell, K.M., Ulrich, K.-U., Veeramani, H., Giammar, D.E., Bernier-Latmani, R., Long, P.E., 2009c. Corrosion of Biogenic Uraninite: Molecular- and Intermediate-scale Measurements. Geological Society of America Abstracts with Programs, 2009 Portland GSA Annual Meeting (18-21 October 2009) Paper No. 64-8. 41, 189.

BARGAR, J.R., CAMPBELL, K.M., VEERAMANI, H., STUBBS, J.E., LEZAMA-PACHECO, J.S., SUVOROVA, E., ULRICH, K.-U., BLUE, L.Y., BERNIER-LATMANI, R., GIAMMAR, D.E., YABUSAKI, S.B., LONG, P.E., 2010c. Reactivity of nano-biogenic uraninite in the subsurface: Dissolution rates and mechanisms. Geochim Cosmochim Acta 74, A52.

BARGAR, J.R., STUBBS, J.E., SUVOROVA, E.I., WILLIAMS, K.H., CAMPBELL, K.M., LEZAMA-PACHECO, J.S., CERRATO, J.M., STYLO, M.A., ALESSI, D.S., WEBB, S.M., BERNIER-LATMANI, R., GIAMMAR, D.E., DAVIS, J.A., FOX, P., LONG, P.E., 2011b. Speciation and dynamics of biologically reduced U(IV) in the Old Rifle, CO, aquifer. Mineralogical Magazine, Goldschmidt Conference Abstract 75, 484.

Barlett, M.A., Lovley, D.R., 2009. Interactions between Iron-reducing and Sulfate-reducing Bacteria during in situ Bioremediation of Uranium-contaminated Groundwater. American Society for Microbiology 109th General meeting, Philadelphia, PA, USA.

Bopp, C.J.I., Lundstrom, C.C., Johnson, T.M., Williams, K.H., Wilkins, M.J., N'Guessan, A.L., Long, P.E., 2009. 238U/235U Isotope Ratios as Tracers of Uranium Reduction: In Situ Experiments at Rifle, CO. Geological Society of America Abstracts with Programs, 2009 Portland GSA Annual Meeting (18-21 October 2009) Paper No. 264-7. 41, 683.

Bush, R., 2010. Old Rifle Title I Processing Site, Rifle, Colorado: What Are They Doing on My Site? Long Term Serviellance and Maintenance Conference 2010 http://www.lm.doe.gov/ltsm_conference/Presentations.htm, Wednesday, 17 October 2010, PM Concurrent Session.

Callister, S.J., Long, P.E., McCue, L., Monroe, M.E., Nicora, C.D., Norbeck, A.D., Smith, R.D., Banfield, J.F., Wilkins, M.J., Lovley, D.R., Elefantz, H., N'Guessan, L., Holmes, D.E., Mouser, P., Scheffrahn, R.H., Hugenholtz, P., Williams, K.H., Warnecke, F., Lipton, M.S., 2008. A Meta-Proteome Evaluation of Two Diverse Microbial Communities - One Involved in Uranium (VI) Reduction and the Other in Ligno-Cellulose Degradation. American Society for Microbiology 108th General Meeting: Boston, MA, June 1- 5, 2008 N-287/0606.

Campbell, K.M., Bargar, J., Veeramani, H., Bernier-Latmani, R., Giammar, D., Blue, L., Williams, K.H., Davis, J.A., 2009. Composition and stability of U(IV) phases at Rifle, CO. Eos Trans. AGU, Fall Meet. Suppl. 90, Abstract H34A-02.

Campbell, K.M., Davis, J.A., Fuller, C.C., 2008a. Uranium(IV) oxidation during anoxic chemical extractions of natural sediment: Importance of Fe(III). Eos Trans. AGU 89, Fall Meet. Suppl., Abstract B13E-06.Campbell, K.M., Qafoku, N.P., Kukkadapu, R., Williams, K.H., Lesher, E., Figueroa, L., Peacock, A., Wilkins, M.J., Davis, J.A., Icenhower, J., Long, P.E., 2008b. Characterizing the extent and role of natural subsurface bioreduction in a uranium-contaminated aquifer. Goldschmidt Conference Abstracts 2008, A133.

Campbell, K.M., Williams, K H, Lesher, E, Davis, J A; Long, P E, 2007. A Comparison of Naturally-Occurring and Artificially Stimulated Uranium(VI) Bioreduction in Sediment from a Field-scale Experiment in Rifle, CO. Eos Trans. AGU 88 (52), Fall Meeting Supplement, Abstract B32A-05.

Chen, J., Hubbard, S.S., Williams, K.H., Tuglus, C., Flores-Orozco, A., Kemna, A., 2010. A Hierarchical Bayesian Model for Estimating Remediation-induced Biogeochemical Transformations Using Spectral Induced Polarization Data: Development and Application to the Contaminated DOE Rifle (CO) Site. Abstract presented at 2010 Fall Meeting, AGU, San Francisco, Calif., 13-17 Dec. Abstract H11E-0847.

Chen, J., Pullman, S., Hubbard, S.S., Peterson, J., 2009. A Web Interface for Software of Stochastic Inversion of Spectral Induced Polarization Data. Eos Trans. AGU, Fall Meet. Suppl. 90, Abstract NS31B-1168.

Cho, J., Newman, M.A., Stucker, V., Peacock, A., Ranville, J., Cabaniss, S., Hatfield, K., Annable, M.D., Klammler, H., Perminova, I.V., 2010. Characterizing In Situ Uranium and Groundwater Flux. Abstract presented at 2010 Fall Meeting, AGU, San Francisco, Calif., 13-17 Dec. Abstract H53C-1058.

Chourey, K., VerBerkmoes, N., Dill, B., Shah, M., Wilkins, M., Long, P., Williams, K., Jansson, J., Brodie, E., Chavarria, K., Tom, L., Handley, K., Banfield, J., Hettich, R., 2010. Novel Protocols for Proteogenomic Characterizations of Soil Microbial Communities. American Society for Microbiology, 110th Annual Meeting San Diego, CA May 23-27, 2010 N-1341/655 114.

Chourey, K., Verberkmoes, N., Lefsrud, M., Abraham, P., Shah, M., Holmes, D., Lovley, D., Wilkins, M., Williams, K., Banfield, J., Long, P., Wickham, G., Thompson, D., Hettich, R., 2008. Metaproteomics of Subsurface Microbial Communities from Metal-Contaminated Environmental Sites. American Society for Microbiology 108th General Meeting: Boston, MA, June 1- 5, 2008 N-335/0253.

Chourey, K., VerBerkmoes, N., Shah, M., Lovley, D., Wilkins, M., Williams, K., Banfield, J., Long, P., Wickham, G., Thompson, D., Hettich, R., 2009. Metaproteomics of Metal-Contaminated Soil and Groundwater Microbial Communities. American Society for Microbiology 109th General meeting, Philadelphia, PA, USA.

CONRAD, M.E., WILLIAMS, K.H., BILL, M., GUPTA, M., BERMAN, E., DAVIS, J.A., LONG, P.E., 2011. THE EFFECT OF BICARBONATE GENERATED FROM MICROBIAL OXIDATION OF ACETATE DURING BIOSTIMULATION OF URANIUM REDUCTION AT THE OLD RIFLE UMTRA SITE. Geological Society of America Abstracts with Programs 43, 231.

Dar, S.A., Tan, H., Williams, K.H., Jaffe, P., Lovley, D.R., 2010. Geobacter Species and Sulfate Reducing Bacteria Are Primarily Attached to Sediments During the Sulfate Reduction Phase of in situ Bioremediation of Uranium-contaminated Groundwater. American Society for Microbiology, 110th Annual Meeting San Diego, CA May 23-27, 2010. N-1351/665 115.

DAVIS, J.A., HAY, M., FOX, P.M., WILLIAMS, K.H., 2011. A coupled ion exchange, surface complexation, calcite dissolution, and mass transfer model to describe uranium(VI) desorption and reactive transport at the Rifle (USA) field site. Mineralogical Magazine, Goldschmidt Conference Abstract 75, 729.

Draper, K., Ward, A.L., Yabusaki, S., Murray, C.J., Greenwood, J., 2009. Abundances of Natural Radionuclides (40K, 238U, 232Th) in Hanford and Rifle Integrated Field Research Challenge Site Sediments and the Application to the Estimation of Grain Size Distributions. Eos Trans. AGU, Fall Meet. Suppl. 90, Abstract H33B-0872.

DRUHAN, J.L., CONRAD, M.E., WILLIAMS, K.H., DEPAOLO, D.J., 2010a. Permeability reduction, calcium and sulfur isotope fractionation during uranium bioremediation. Geochim Cosmochim Acta 74, A247.

Druhan, J.L., Conrad, M.E., Williams, K.H., Steefel, C., Depaolo, D.J., 2010b. Sulfur isotope fractionation as an early indicator of microbial sulfate reduction under conditions of stimulated subsurface metal bioremediation. Abstract presented at 2010 Fall Meeting, AGU, San Francisco, Calif., 13-17 Dec. Abstract B54A-04.

Druhan, J.L., Conrad, M E, Williams, K H, N'Guessan, L, Long, P E, Hubbard, S S, 2007. Sulfur Isotopes as Indicators of Bacterial Sulfate Reduction Processes Influencing Field Scale Uranium Bioremediation. Eos Trans. AGU 88 (52), Fall Meeting Supplement, Abstract H13G-1668.

Elifantz, H., N'Guessan, L.A., Mouser, P.J., Williams, K.H., Wilkins, M.J., Ward, J.E., Long, P.E., Lovley, D.R., 2008. Quantifying Gene Transcripts to Diagnose Acetate Limitation in Geobacter Species during in situ Bioremediation of Uranium-Contaminated Groundwater. American Society for Microbiology 108th General Meeting, Boston, MA, June 1-5, 2008 Q-528/0312.

Englert, A., Hubbard, S.S., Li, L., Kowalsky, M.B., Williams, K.H., Spane, F., Newcomer, D., Long, P., Steefel, C., 2008. Evidence of Flow Rerouting Caused by Bioremediation-Induced Clogging at the Uranium Contaminated DOE Integrated Field Challenge Site, Rifle, Colorado. Eos Trans. AGU 89, Fall Meet. Suppl., Abstract H51K-04.

Englert, A., Kowalsky, M; Li, L; Long, P; Hubbard, S, 2007. Characterization of Transient Transport Behavior During Biostimulation Field Experiments Using Novel Breakthrough Analysis Approaches. Eos Trans. AGU 88 (52), Fall Meeting Supplement, Abstract H21C-0707.

FANG, Y., YABUSAKI, S., WILKINS, M.J., LONG, P.E., 2011. EVALUATION OF AN IN SILICO GEOBACTER METALLIREDUCENS MODEL USING PROTEOMIC DATA FROM A FIELD BIOSTIMULATION EXPERIMENT. Geological Society of America Abstracts with Programs 43, 229.

Fang, Y., Yabusaki, S.B., 2008. Multicomponent modeling of in situ uranium bioremediation: Findings and challenges. Goldschmidt Conference Abstracts 2008, A255.

Figueroa, L., Hartmann, J., Lesher, E., Ranville, J., Honeyman, B., Campbell, K., Williams, K., Davis, J., Long, P., 2009. The Role of Dissolved and Particulate Organic Carbon in Biostimulated Uranium Attenuation. Migration '09: 12th International Conference on the Chemistry and Migration Behaviour of Actinides and Fission Products in the Geosphere, Kennewick, Washington, USA Absract No: PB4-9, 113.

Flores-Orozco, A., Williams, K.H., Kemna, A., 2008. Application of a Spectral Induced Polarization Data Error Model for Field Scale Biogeophysical Monitoring. Eos Trans. AGU 89, Fall Meet. Suppl., Abstract H33G-1112.

Flores-Orozco, A., Williams, K.H., Kemna, A., Campbell, K.M., Kukkadapu, R.K., Peacock, A., Long, P.E., 2009. Delineating subsurface zones of natural bioreduction using the complex resistivity method Eos Trans. AGU, Fall Meet. Suppl. 90, Abstract H53B-0923.

Fox, P.M., Davis, J.A., Bargar, J., Williams, K.H., Singer, D.M., Long, P., 2011. Quantitative Analysis of Uranium Accumulation on Sediments during Field-scale Biostimulation under Variable Bicarbonate Concentrations at the Rifle IFRC Site. Presented at the 2011 Fall Meeting, AGU, San Francisco, Calif., 5-9 Dec. Abstract H24A-05.

FOX, P.M., DAVIS, J.A., KUKKADAPU, R., 2010. Fe(II) uptake and transformation on uranium contaminated sediment from the Rifle IFRC field site. Geochim Cosmochim Acta 74, A302.

Fox, P.M., Hyun, S.P., Davis, J.A., Hayes, K., Dayvault, R., Williams, K.H., Long, P.E., 2008. Uranium Desorption From Contaminated Sediments at the USDOE IFC Research Site in Rifle, CO: From Batch to Field. Eos Trans. AGU 89, Fall Meet. Suppl. Abstract H31B-0868.

Garg, S., Mahadevan, R., Scheibe, T., Fang, Y., Long, P., Lovley, D., 2008. An integrated model of G. sulfurreducens for investigating bioremediation of U(VI) in subsurface sediments. Computational Methods in Water Resources XVII International Conference, San Francisco, California, July 6-10, 2008.

Giammar, D.E., Ulrich, K.-U., Ilton, E.S., Veeramani, H., Sharp, J.O., Bernier-Latmani, R., Schofield, E.J., Bargar, J.R., 2009. Geochemical Factors Controlling The Equilibrium Solubility And Dissolution Rate Of Biogenic Uraninite. Migration '09: 12th International Conference on the Chemistry and Migration Behaviour of Actinides and Fission Products in the Geosphere, Kennewick, Washington, USA Abstract No: B4-1, 40.

Gupta, M., Williams, K.H., Berman, E.S., Conrad, M.E., 2010. Hydrological Tracer Studies at a DOE IFRC Site in Rifle, Colorado. Abstract presented at 2010 Fall Meeting, AGU, San Francisco, Calif., 13-17 Dec. Abstract H23E-1269.

HANDLEY, K.M., WRIGHTON, K.C., WILKINS, M.J., WILLIAMS, K.H., VERBERKMOES, N.C., THOMAS, B.C., SHARON, I., HETTICH, R., LONG, P.E., BANFIELD, J.F., 2011. PROTEOGENOMICS: UNDERSTANDING MICROBIAL COMMUNITY FUNCTION DURING URANIUM BIOREMEDIATION. Geological Society of America Abstracts with Programs 43, 230.

Holmes, D.E., Perpetua, L.A., Chavan, M.A., Lovley, D.R., 2008. Microarray Analysis of Growth of Geobacter uraniireducens on Sediment Fe(III) Oxides. American Society for Microbiology 108th General Meeting: Boston, MA, June 1- 5, 2008 N-326/0244.

Hubbard, S.S., Wu, Y., Chen, J., Franklin, J.B.A., Li, L., Tuglus, C., Williams, K.H., 2009. Assessing Feedbacks between Remediation-Induced Biogeochemical Transformations and Flow Characteristics using Multi-Scale Geophysical Approaches. Eos Trans. AGU, Fall Meet. Suppl. 90, Abstract H53J-02.

Hyun, S., Campbell, K M, Hayes, K F, Davis, J A, 2007. Experimental Study of U(VI) Release Kinetics from Aquifer Sediments from a Former Uranium Mill Tailings Site (Rifle, Colorado, USA). Eos Trans. AGU 88 (52), Fall Meeting Supplement, Abstract H23D-1630.

Hyun, S., Davis, J.A., Hayes, K.F., 2010. Kinetics of Abiotic Uranium(VI) Reduction by Sulfide. Abstract presented at 2010 Fall Meeting, AGU, San Francisco, Calif., 13-17 Dec. Abstract B51C-0378.

Hyun, S.P., Fox, P.M., Hayes, K.F., Davis, J.A., 2009. Surface complexation modeling of U(VI) adsorption by an aquifer sediment from a former mill-tailings site at Rifle, Colorado. 237th American Chemical Society National Meeting, Salt Lake City, UT, March 22-26, 2009, GEOC-0055. .

Jaffe, P.R., Banfield, J.F., Elbishlawi, H., Kerkhof, L., Komlos, J., Kukkadapu, R.K., Long, P.E., Mcguinness, L., Moon, H.S., Peacock, A.D., Wilkins, M.D., Williams, K.H., 2008a. Microbial, geochemical, and physical responses to biostimulation for U(VI) reduction in soil columns. Goldschmidt Conference Abstracts 2008, A421.

Jaffe, P.R., ElBishlawi, H, Hettich, R L, Kerkhof, L, Komlos, J, Kukkadapu, R P, Lipton, M S, Long, P E, McGuinness, L, Moon, H, Peacock, A D, VerBerkmoes, N C, Williams, K H, 2007. Evolution of the Microbial Community Structure and Iron Reduction Rate in a Column Biostimulation Experiment During the Transition From Iron to Sulfate Reduction. Eos Trans. AGU 88 (52), Fall Meeting Supplement, Abstract B33A-0855.

Jaffe, P.R., Kerkhoff, L., Komlos, J., Kukkadapu, R.K., Long, P.E., McGuinness, L., Moon, H.S., 2008b. The Effect of Iron and Sulfate Levels on the Transition from Iron to Sulfate Reduction during Biostimulation. Eos Trans. AGU 89, Fall Meet. Suppl., Abstract B13E-05.

Jaffe, P.R., Long, P.E., Moon, H., N'Guessan, L., Peacock, A., Sinha, M., Tan, H., Traub, D., Williams, K.H., 2010. Post-Biostimulation Biogenic U(IV) Stability and Microbial Community Structure that Affects its Dynamics. Abstract presented at 2010 Fall Meeting, AGU, San Francisco, Calif., 13-17 Dec. Abstract B54A-02.

Jaffe, P.R., Tan, H., Kerkhof, L., McGuinness, L., Peacock, A., Long, P.E., 2011. C-13 Stable Isotope Probing of Biostimulation Experiments to Identify Acetate Utilizers. Presented at the 2011 Fall Meeting, AGU, San Francisco, Calif., 5-9 Dec. Abstract H21A-1061.

Kerkhof, L., McGuinness, L., Williams, K., Wilkins, M.J., Peacock, A., Long, P., 2008. Stable Isotope Probing of Acetate-Utilizing Bacteria in the Subsurface at the Rifle, CO Integrated Field Challenge Site. American Society for Microbiology 108th General Meeting, Boston, MA, June 1-5, 2008 N-338/0256.

Kukkadapu, R., 2008. The Role of Biotransformed Iron Minerals in Attenuation of Soluble Radionuclides in Contaminated Aquifers. The 5th International Nassau-Argonne Mössbauer Symposium, Advanced Photon Source, Argonne National Laboratory, Argonne, IL (May 2008).

Kukkadapu, R., 2009. Effect of Fe-mineral (oxide and clays) reductive biotransformations on remediation of radioactive metals from contaminated aquifers. Annual Meeting of the Clay Minerals Group of The Mineralogical Society of United Kingdom. The Newcastle University, U.K. Advances in Clay Science for Future Geological, Environmental and Industrial Applications, Newcastle University, UK, December 14-16, 2009 9.

Kukkadapu, R., Fox, P.M., Davis, J., 2011. Nature and Reactivity of Sediment-Associated Spiked Fe(II) Toward Abiotic Uranium Reduction. Presented at the 2011 Fall Meeting, AGU, San Francisco, Calif., 5-9 Dec. Abstract H21A-1054.

Kukkadapu, R., Qafoku, N., McKinley, J., Arey, B., Long, P., 2008a. Uranium Association with Soil Fe-minerals. 236th American Chemical Society National Meeting & Exposition, Philadelphia, PA, USA.

Kukkadapu, R.K., McKinley, J.P., Arey, B.W., Qafoku, N.P., Kelly, S.D., Wang, C., Long, P.E., 2009. Fe-Mineralogy of the Rifle Alluvial Sediments: Implications for in situ Bioremediation and Long Term Behavior of U(VI). Migration ’09: 12th International Conference on the Chemistry and Migration Behaviour of Actinides and Fission Products in the Geosphere, Kennewick, Washington, USA Abstract No: PB4-11, 114-115.

Kukkadapu, R.K., Qafoku, N.P., McKinley, J.P., Arey, B.W., Kelly, S.D., Campbell, K.M., Resch, C.R., Wang, C., Williams, K.H., Wilkins, M.J., Long, P.E., 2008b. Uranium Association With Framboidal Pyrite and Magnetite-like Phases in Alluvial Sediments. Eos Trans. AGU 89, Fall Meet. Suppl., Abstract B11B-0346.

LAUBACH, P., JOHNSON, T., LUNDSTROM, C., WILLIAMS, K.H., LONG, P., 2011. FIELD-SCALE DETERMINATION OF URANIUM ISOTOPE FRACTIONATION INDUCED BY U(VI) ADSORPTION AND DESORPTION: THE SUPER 8 EXPERIMENT AT DOE'S RIFLE, COLORADO SITE. Geological Society of America Abstracts with Programs 43, 231.

Leavitt, J., Cabaniss, S., Howe, K., Comolli, L., Long, P., Stucker, V., 2011. Sorption of U(VI) to G. uraniireducens and A. palmae under Old Rifle Conditions. Presented at the 2011 Fall Meeting, AGU, San Francisco, Calif., 5-9 Dec. Abstract H21A-1045.

LEZAMA PACHECO, J.S., BARGAR, J.R., BERNIER-LATMANI, R., SUVOROVA, E.I., WILLIAMS, K.H., LONG, P.E., GIAMMAR, D.E., DAVIS, J.A., STUBBS, J.E., 2011. SPECTROSCOPIC INSIGHTS ON U(IV) SPECIES IN BIOLOGICALLY REDUCED SEDIMENTS AT THE OLD RIFLE AQUIFER. Geological Society of America Abstracts with Programs 43, 230.

Lezama-Pacheco, J.S., Bargar, J., Stubbs, J., Bernier-Latmani, R., Suvorova, E., Williams, K.H., Davis, J.A., Fox, P.M., Giammar, D., Cerrato, J., Long, P., 2011. Speciation of uranium in biologically reduced sediments during iron and sulfate reduction in the Old Rifle Aquifer. Presented at the 2011 Fall Meeting, AGU, San Francisco, Calif., 5-9 Dec. Abstract V22B-07.

Li, L., Gawande, N., Kowalsky, M.B., Steefel, C., Hubbard, S.S., 2011. Field Scale Controls of Uranium Bioreduction Efficacy: the Role of Physico-chemical Heterogeneity. Presented at the 2011 Fall Meeting, AGU, San Francisco, Calif., 5-9 Dec. Abstract H21A-1068.

Li, L., Steefel, C.I., Kowalsky, M.B., Englert, A.L., Hubbard, S.S., 2008a. Effects of Physical and Chemical Heterogeneities on Biogeochemical Processes Associated With Uranium Bioremediation at Rifle, Colorado. Eos Trans. AGU 89, Fall Meet. Suppl., Abstract H24B-02.

Li, L., Steefel, C.I., Williams, K.H., Wilkins, M., Englert, A.L., Hubbard, S.S., 2008b. Solid Phase Transformation And Biomass Accumulation During Uranium Bioremediation At Rifle, Colorado. Computational Methods in Water Resources XVII International Conference, San Francisco, California, July 6-10, 2008.

Li, L., Steefel, C I; Kowalsky, M B, 2007. Biogeochemical Reaction Kinetics Associated With Uranium Bioremediation at Multiple Scales. Eos Trans. AGU 88 (52), Fall Meeting Supplement, Abstract H32D-03.

Liang, Y., Nostrand, J.D.V., Peacock, A.D., Long, P.E., Wu, L., He, Z., Li, G., Zhou, J., 2008. Microarray-Based Functional Analysis of Microbial Communities for In-Situ Uranium under Sulfate-Reducing vs. Fe-reducing Conditions. American Society for Microbiology 108th General Meeting: Boston, MA, June 1- 5, 2008 N-278/0588.

Long, P., 2010. Bioremediation of Subsurface Aquifers (Invited). Society for General Microbiology NT05 (web address: https://http://www.sgm.ac.uk/meetings/past.cfm.

Long, P., Banfield, J., Chandler, D., Davis, J., Dayvault, R., Hettich, B., Hubbard, S., Jaffe, P., Kerkhof, L., Kukkadapu, R., Lipton, M., Lovley, D., N'Guessan, L., Peacock, A., Spane, F., VerBerkmoes, N., Williams, K., Yabusaki, S., Team, I.S., 2009a. Biostabilization of Uranium in an Alluvial Aquifer: Overview of Results from Field-scale Electron Donor Amendments. Migration '09: 12th International Conference on the Chemistry and Migration Behaviour of Actinides and Fission Products in the Geosphere, Kennewick, Washington, USA Abstract No: B4-4, 43.

Long, P., Williams, K., Banfield, J., Bush, R., Campbell, K., Chandler, D., Davis, J., Dayvault, R., Englert, A., Fang, Y., Fox, P., Hettich, R., Holmes, D., Hubbard, S., Jaffe, P., Kerkhof, L., Kukkadapu, R., Li, L., Lipton, M., Lovley, D., Morris, S., Morrison, S., Newcomer, D., N'Guessan, A.L., Peacock, A., Hyun, S., Qafoku, N., Resch, C.T., Spane, F., Steefel, C., VerBerkmoes, N., Yabusaki, S., Yelton, P., 2008a. In Situ Bioreduction of Uranium in an Alluvial Aquifer: Overview of Results from the Integrated Field-Scale Subsurface Research Challenge Site (IFC) at Rifle, Colorado. Eos Trans. AGU 89, Fall Meet. Suppl., Abstract H53E-1116.

Long, P.E., 2008. Field-scale bioreduction of U(VI) to U(IV) in an alluvial aquifer: Evidence for microbially mediated precipitation of Uranium under both natural and biostimulated conditions. Goldschmidt Conference Abstracts 2008, A568.

Long, P.E., Banfield, J, Bush, R, Campbell, K, Chandler, D P, Davis, J A, Dayvault, R, Druhan, J, Elifantz, H, Englert, A, Hettich, R L, Holmes, D, Hubbard, S, Icenhower, J, Jaffe, P R, Kerkhof, L J, Kukkadapu, R K, Lesher, E, Lipton, M, Lovley, D, Morris, S, Morrison, S, Mouser, Newcomer, D, N'Guessan, L, Peacock, A, Qafoku, N, Resch, C T, Spane, F, Spaulding, B, Steefel, C, Verberkmoes, N, Wilkins, M, Williams, K H, Yabusaki, S B, 2007. The Integrated Field-Scale Subsurface Research Challenge Site (IFC) at Rifle, Colorado: Preliminary Results on Microbiological, Geochemical and Hydrologic Processes Controlling Iron Reduction and Uranium Mobility. Eos Trans. AGU 88 (52), Fall Meeting Supplement, Abstract B24D-04.

Long, P.E., Rifle-IFRC-Science-Team, 2010. Rifle IFRC overview and summary of progress to date. Long Term Serviellance and Maintenance Conference 2010 http://www.lm.doe.gov/ltsm_conference/Presentations.htm, Wednesday, 17 October 2010, PM Concurrent Session.

Long, P.E., Williams, K.H., Davis, J.A., Banfield, J.F., Bargar, J., Lovley, D.R., Hatfield, K., Wilkins, M.J., Yabusaki, S., Murray, C.J., Jaffe, P.R., Team, R.I.S., 2011a. Progress Toward Understanding of Coupled Microbiology, Biogeochemistry, and Hydrogeology Controls on Subsurface Mobility of Uranium (Invited). Presented at the 2011 Fall Meeting, AGU, San Francisco, Calif., 5-9 Dec. Abstract V22B-01.

LONG, P.E., WILLIAMS, K.H., PEACOCK, A.D., BARGAR, J.R., BUSH, R.P., DAVIS, J.A., FOX, P.M., HATFIELD, K., NEWMAN, M.A., CAMPBELL, K.M., 2011b. UNPREDICTED PERSISTENCE OF A URANIUM PLUME AT A FORMER MILL TAILINGS SITE IN RIFLE, COLORADO: EVIDENCE FOR MULTIPLE SOURCES OF URANIUM. Geological Society of America Abstracts with Programs 43, 230.

Long, P.E., Williams, K.H., Yabusaki, S., N'Guessan, A.L., Peacock, A., Flores-Orozco, A., Kemna, A., Lovley, D.R., 2009b. Natural and Accelerated in situ Bioremediation of Metals and Radionuclides: Progress in Mechanistic Understanding and Monitoring Methods. Eos Trans. AGU, Fall Meet. Suppl. 90, Abstract H21H-03.

Long, P.E., Williams, K.H., Yabusaki, S., Peacock, A., Bargar, J., Wilkins, M., Davis, J.A., Fox, P.M., Dayvault, R., Rifle-IFRC-Science-Team, 2010. Biogeochemical Dynamics in a Shallow Alluvial Aquifer: Impact on Uranium and Other Redox-sensitive Contaminants Over Time and Space (Invited). Abstract presented at 2010 Fall Meeting, AGU, San Francisco, Calif., 13-17 Dec. Abstract B53A-01.

Long, P.E., Williams, K.H., Yabusaki, S.B., Fang, Y., N'Guessan, A.L., Wellman, D.M., Steefel, C.I., Li, L., Deutsch, W.J., 2008b. In Situ Bioremediation of Metals and Radionuclides: Results from Field-scale Experiments and Future Prospects. Eos Trans. AGU 89, Fall Meet. Suppl., Abstract H41L-04.

McGuinness, L., Moon, H., Jaffe, P., Long, P., Kerkhof, L., 2009. Profiling Microbial Populations in Sediment Column Experiments during Iron, Uranium, and Sulfate Reduction. American Society for Microbiology 109th General meeting, Philadelphia, PA, USA.

Methé, B.A., Deboy, R., Goll, J., Geimer, M., Brami, D., Lovley, D.R., 2010. Metatranscriptomic Analyses of a Subsurface Environment Undergoing in situ Uranium Bioremediation. American Society for Microbiology, 110th Annual Meeting San Diego, CA May 23-27, 2010 R-2925/983, 199.

Methé, B.A., Deboy, R., Ren, Q., McCorrison, J., Holmes, D., Lovley, D.R., 2009. Metagenomic and Metatranscriptomic Analysis of In Situ Uranium Bioremediation American Society for Microbiology 109th General meeting, Philadelphia, PA, USA.

Miletto, M., N'Guessan, L.A., Williams, K.H., Long, P.E., Lovley, D.R., 2009. Phylogenetic Analysis and Quantification of Dissimilatory (Bi)Sulfite Reductase Genes and Transcripts during In situ Bioremediation of Uranium-Contaminated Groundwater. American Society for Microbiology 109th General meeting, Philadelphia, PA, USA.

Moon, H., McGuiness, L., Kukkadapu, R.K., Peacock, A., Komlos, J., Kerkhof, L., Long, P.E., Jaffe, P.R., 2009. Effect of 57Fe-goethite Amendment on Microbial Community Composition and Dynamics During the Transition from Iron to Sulfate Reduction Eos Trans. AGU, Fall Meet. Suppl. 90, Abstract H31B-0787.

Moses, W.W., O'Neil, J.P., Boutchko, R., Nico, P.S., Druhan, J.L., Vandehey, N.T., 2010. Radiotracer Imaging of Sediment Columns. Abstract presented at 2010 Fall Meeting, AGU, San Francisco, Calif., 13-17 Dec. Abstract B51C-0364.

Mouser, P., 2010. Quantifying Temporal Autocorrelations for the Expression of Geobacter species mRNA Gene Transcripts at Variable Ammonium Levels during in situ U(VI) Bioremediation. Abstract presented at 2010 Fall Meeting, AGU, San Francisco, Calif., 13-17 Dec. Abstract B51B-0350.

Mouser, P.J., N'Guessan, A., Elifantz, H., Williams, K.H., Wilkins, M., Long, P.E., Lovley, D.R., 2008. Influence of Ammonium Availability on Expression of Genes for Nitrogen Fixation and Ammonium Uptake during Bioremediation of a U(VI)-Contaminated Aquifer: Implications for U(VI) Removal and the Metabolic State of Subsurface Geobacteraceae. American Society for Microbiology 108th General Meeting, Boston, MA, June 1-5, 2008 Q-526/0310.

Mouser, P.J., Wilkins, M.J., Williams, K.H., Smith, D.F., Paša-Tolić, L., 2011. Molecular-Scale Characterization of Natural Organic Matter From A Uranium Contaminated Aquifer and its Utilization by Native Microbial Communities. Presented at the 2011 Fall Meeting, AGU, San Francisco, Calif., 5-9 Dec. Abstract H21A-1062.

Murray, C.J., Yabusaki, S.B., Fang, Y., Waichler, S.R., Bott, Y.-J., Ward, A., Long, P., 2010. Coupled-Process Modeling Of In Situ Uranium Bioremediation Near Rifle, Colorado. Geological Society of America Abstracts with Programs, Denver Annual Meeting, 31 October –3 November 2010. 42, 41 Paper 49-42.

N'Guessan, A., Williams, K.H., Yabusaki, S., Long, P.E., Lovley, D., 2008a. Biogeochemical Differences of Pilot-Scale Bioremediation Treatment Plots Undergoing Iron Reduction or Sulfate Reduction in a Uranium-Contaminated Aquifer. 236th American Chemical Society National Meeting & Exposition, Philadelphia, PA, USA.

N'Guessan, L., Elifantz, H., Mouser, P., Nevin, K., Manley, K., Williams, K., Wilkins, M., Long, P., Lovley, D., 2008b. Molecular Analysis of Phosphate Limitation in Geobacter Species during Bioremediation of a Uranium-Contaminated Aquifer. American Society for Microbiology 108th General Meeting: Boston, MA, June 1- 5, 2008 Q-525/0309.

N'Guessan, A.L., Qafoku, N.P., Kukkadapu, R., Wang, Z., Williams, K.H., Peacock, A., Yabusaki, S., Long, P.E., 2009a. Biogeochemical Characterization of Processes Governing the Fate and Transport of Uranium in Naturally Reduced and Biostimulated Sediment. Migration '09: 12th International Conference on the Chemistry and Migration Behaviour of Actinides and Fission Products in the Geosphere, Kennewick, Washington, USA Abstract No: PB4-12, 115-116.

N'Guessan, L.A., Qafoku, N.P., Williams, K.H., Peacock, A.D., Long, P.E., 2009b. Comparative Microbial Community Characterization of Naturally Reduced and Biostimulated Sediment with a High Uranium Retaining Capacity. American Society for Microbiology 109th General meeting, Philadelphia, PA, USA.

Newman, M.A., Peacock, A., Hatfield, K., Stucker, V., Cho, J., Klammler, H., Ranville, J.F., Cabaniss, S., Annable, M.D., Perminova, I., 2011a. Passive methods for quantifying the In Situ Flux of Water, Uranium, and Microbial Biomass. Presented at the 2011 Fall Meeting, AGU, San Francisco, Calif., 5-9 Dec. Abstract H21A-1077.

NEWMAN, M.A., STUCKER, V., CHO, J., PEACOCK, A., KLAMMLER, H., HATFIELD, K., RANVILLE, J., CABANISS, S., LEAVITT, J., ANNABLE, M., 2011b. QUANTIFYING THE IN SITU FLUX OF WATER, URANIUM, AND MICROBIAL BIOMASS. Geological Society of America Abstracts with Programs 43, 230.

Ntarlagiannis, D., Slater, L.D., Williams, K.H., Hubbard, S.S., Wu, Y., 2010a. Investigating the effect of electro-active ion concentration on spectral induced polarization signatures arising from biomineralization pathways. Abstract presented at 2010 Fall Meeting, AGU, San Francisco, Calif., 13-17 Dec. Abstract NS31B-1401.

NTARLAGIANNIS, D., WILLIAMS, K., SLATER, L., HUBBARD, S., WU, Y., 2010b. Investigating the effect of electroactive ion concentration on induced polarization signatures arising from biomineral formation. Geochim Cosmochim Acta 74, A767.

O'Loughlin, E.J., Boyanov, M., Kwon, M., Long, P.E., Williams, K.H., Kemner, K.M., 2009. Effects of microbial activity and electron shuttles on the reduction of U(VI) under Fe(III)- and sulfate-reducing conditions Eos Trans. AGU, Fall Meet. Suppl. 90, Abstract H31B-0788.

O'LOUGHLIN, E.J., BOYANOV, M.I., KWON, M.J., LONG, P.E., WILLIAMS, K.H., KEMNER, K.M., 2011. Effects of microbial activity and electron shuttles on the reduction of U(VI) under sulfidogenic conditions. Mineralogical Magazine, Goldschmidt Conference Abstract 75, 1556.

Peacock, A.D., Long, P.E., N'Guessan, L., Williams, K.H., Chandler, D., 2011. Monitoring Subsurface Microbial Biomass, Community Composition and Physiological Status during Biological Uranium Reduction with Acetate Addition using Lipid Analysis, DNA Arrays and q-PCR. Presented at the 2011 Fall Meeting, AGU, San Francisco, Calif., 5-9 Dec. Abstract H21A-1067

Qafoku, N., Gartman, B., Murray, C., Arey, B., Kukkadapu, R.K., Resch, C.T., Ward, A.L., Draper, K., Williams, K., Long, P., 2011a. Mineralogical and solid phase physical and geochemical controls on U mobility in the sediments from Rifle, CO. Presented at the 2011 Fall Meeting, AGU, San Francisco, Calif., 5-9 Dec. H21A-1066.

Qafoku, N., Kukkadapu, R.K., Long, P.E., 2010. Unraveling the soil system complex behavior: Mineral and migrating fluids interactive processes and reactions (Invited). Soil Science Society of America Annual Meeting, Long Beach, CA, October 31 - November 3, 2010 S02 Soil Chemistry.

QAFOKU, N.P., GARTMAN, B., KUKKADAPU, R.K., AREY, B., MURRAY, C.J., RESCH, C.T., WILLIAMS, K., LONG, P.E., 2011b. CHARACTERIZATION OF U CONTAMINATION AND SOLID PHASE MINERALOGY AND GEOCHEMISTRY IN THE RIFLE SUBSURFACE SEDIMENTS. Geological Society of America Abstracts with Programs 43, 231.

Qafoku, N.P., Kukkadapu, R., McKinley, J., Arey, B., Kelly, S.D., Campbell, K.M., Resch, C.T., Wang, C., Williams, K.H., Wilkins, M.J., Long, P.E., 2009. Mineralogical control on U(VI) attenuation in the contaminated sediments from Rifle, CO. 237th American Chemical Society National Meeting, Salt Lake City, UT, March 22-26, 2009, GEOC-0055. Presented March 24, 2009, in the symposium "Metal and Metaloid Speciation and Adsorption", in Honor of James O. Leckie.

Scheibe, T.D., Mahadevan, R., Fang, Y., Garg, S., Long, P.E., Lovley, D.M., 2008. Integration of Genome-Scale Metabolic Models of Iron-Reducing Bacteria With Subsurface Flow and Geochemical Reactive Transport Models. Eos Trans. AGU 89, Fall Meet. Suppl., Abstract B11B-0356.

Smith, R.W., Fujita, Y., Ginn, T.R., Hubbard, S.S., Dafflon, B., Delwiche, M., Gebrehiwet, T., Henriksen, J.R., Peterson, J., Taylor, J.L., 2011. Microbially Induced Calcite Precipitation for Subsurface Immobilization of Contaminants Presented at the 2011 Fall Meeting, AGU, San Francisco, Calif., 5-9 Dec. Abstract H21A-1051.

Steefel, C.I., Williams, K.H., Li, L., Davis, J.A., 2008. Modeling of thermodynamic and kinetic controls on complex biogeochemical reaction networks. Goldschmidt Conference Abstracts 2008, A893.

Strycharz, S., Peacock, A., Williams, K.H., N'Guessan, L., Lovley, D.R., 2009. Geobacter Species Are Predominately Planktonic during Growth in Uranium-Contaminated Subsurface Sediments. American Society for Microbiology 109th General meeting, Philadelphia, PA, USA.

Stucker, V., Ranville, J.F., Giloteaux, L., Williams, K.H., 2011. Impacts of acetate biostimulation for uranium bioreduction on aqueous arsenic geochemistry. Presented at the 2011 Fall Meeting, AGU, San Francisco, Calif., 5-9 Dec. Abstract H21A-1065.

Tarrell, A.N., Haas, A., Revil, A., Figueroa, L.A., Rodriguez, D., SmartGeo, 2010. Near-Real-Time Geophysical and Biological Monitoring of Bioremediation Methods at a Uranium Mill Tailings Site in Rifle, Colorado. Abstract presented at 2010 Fall Meeting, AGU, San Francisco, Calif., 13-17 Dec. Abstract H24E-06.

Tuglus, C., Chen, J., Hubbard, A., Hubbard, S., 2009a. Hierarchical Bayesian Model of Geochemical and Geophysical Elements of In-Situ Remediation. SAMSI Space-time Analysis for Environmental Mapping, Epidemiology and Climate Change Opening Workshop Durham, N.C., September 13-16, 2009.

Tuglus, C., Chen, J., Hubbard, S.S., 2009b. Hierarchical Bayesian Model for Estimating the Spatiotemporal Distribution of Geochemical Processes Associated with In-Situ Remediation Using Geophysical Datatsets. Eos Trans. AGU, Fall Meet. Suppl., 90, Abstract H53B-0918.

Walsh, D., Turner, P., Frid, I., Shelby, R., Grunewald, E.D., Magnuson, E., Butler, J.J., Johnson, C.D., Cannia, J.C., Woodward, D.A., Williams, K.H., Lane, J.W., 2010. Field Demonstration of Slim-hole Borehole Nuclear Magnetic Resonance (NMR) Logging Tool for Groundwater Investigations. Abstract presented at 2010 Fall Meeting, AGU, San Francisco, Calif., 13-17 Dec. Abstract NS23A-1455.

Wilkins, M.J., Williams, K.H., VerBerkmoes, N.C., Hettich, R.L., Lipton, M.S., Long, P.E., Banfield, J.F., 2008. Proteogenomic Analysis of Geobacter Populations in a low Nutrient Contaminated Aquifer Under Stimulated Conditions. Eos Trans. AGU 89, Fall Meet. Suppl., Abstract B33C-0445.

Wilkins, M.J., Williams, K H, Verberkmoes, N C, Hettich, R L, Lipton, M S, Long, P E, Banfield, J F, 2007. Environmental Proteomic Analysis in a Contaminated Aquifer: From Column to Field-Scale. Eos Trans. AGU 88 (52), Fall Meeting Supplement, Abstract B11C-0618.

Willams, K.H., 2010. Prospecting for natural attenuation:Coupled geophysical-biogeochemical studies at DOE's Rifle, CO IFRC site. Long Term Serviellance and Maintenance Conference 2010 http://www.lm.doe.gov/ltsm_conference/Presentations.htm, Wednesday, 17 October 2010, PM Concurrent Session.

Williams, K.H., Franks, A., Nevin, K.P., Wilkins, M.J., Elifantz, H., Mouser, P.J., N'Guessan, L., Long, P.E., Lovley, D.R., 2008. Electrode-Based Approaches for Monitoring the in Situ Activity of Geobacter species during Bioremediation of Uranium-Contaminated Groundwater. American Society for Microbiology 108th General Meeting, Boston, MA, June 1-5, 2008 Q-294/0890.

Williams, K.H., Kemna, A, Wilkins, M, Druhan, J, Arntzen, E, N'Guessan, L, Long, P, Hubbard, S, Banfield, J, 2007. Geophysical monitoring of microbial activity during stimulated subsurface bioremediation. Eos Trans. AGU 88 (52), Fall Meeting Supplement, Abstract NS11C-0694.

WILLIAMS, K.H., N'GUESSAN, A.L., WILKINS, M.J., LONG, P.E., 2010. Formation of Selenium nanospheres accompanying bioremediation of a uranium-contaminated aquifer. Geochim Cosmochim Acta 74, A1133.

Williams, K.H., Nevin, K.P., Franks, A., Long, P.E., Lovley, D.R., 2009. Electrode-based Approaches for Monitoring and Stimulating the in situ Activity of Geobacter Species during the Bioremediation of Uranium-contaminated Groundwater. American Society for Microbiology 109th General meeting, Philadelphia, PA, USA.

WILLIAMS, K.H., WILKINS, M.J., DOHNALKOVA, A.C., DRUHAN, J.L., CONRAD, M.E., 2011. Characterization of elemental sulfur reducing bacteria using transmission electron microscopy and their impact on sulfur isotope fractionation. Mineralogical Magazine, Goldschmidt Conference Abstract 75, 2163.

Wrighton, K.C., Thomas, B., Miller, C.S., Sharon, I., Wilkins, M.J., VerBerkmoes, N.C., Handley, K.M., Lipton, M.S., Hettich, R.L., Williams, K.H., Long, P.E., Banfield, J.F., 2011. Recovery of community genomes to assess subsurface metabolic potential: exploiting the capacity of next generation sequencing-based metagenomics. Presented at the 2011 Fall Meeting, AGU, San Francisco, Calif., 5-9 Dec. Abstract H23I-04.

Wu, Y., Ajo-Franklin, J., Williams, K.H., Hubbard, S.S., Nico, P.S., 2008. Multi-scale Geophysical Signatures of Biogenic Calcite and FeS Precipitation Using Rifle as a Model Site. Eos Trans. AGU 89, Fall Meet. Suppl., Abstract H51M-07.

Wu, Y., Hubbard, S.S., Williams, K.H., Ajo, J.B., 2009. Complex conductivity signatures of CaCO3 precipitation and its mixture with FeS. Eos Trans. AGU, Fall Meet. Suppl. 90, Abstract H43C-1042.

Yabusaki, S., Fang, Y., Waichler, S., Murray, C., Ward, A., Newcomer, D., Spane, F., Long, P.E., Davis, J.A., Fox, P., Williams, K., Steefel, C., Rifle-IFRC-Science-Team, 2010a. Variably-Saturated Flow and Biogeochemical Reactive Transport at an In Situ Uranium Bioremediation Site (Invited). Soil Science Society of America Annual Meeting, Long Beach, CA, October 31 - November 3, 2010 S02 Soil Chemistry, 306 Symposium--Reactive Transport Modeling In Soils.

Yabusaki, S., Fang, Y., Waichler, S., Murray, C.J., Ward, A.L., Long, P.E., 2010b. Modeling In Situ Uranium Bioremediation at a Former Uranium Mill Tailings Site. Eos Trans. AGU 91, Abstract H41C-02.

Yabusaki, S., Fang, Y., Wilkins, M.J., Long, P., 2011. Using proteomic data to assess a genome-scale "in silico" model of metal reducing bacteria in the simulation of field-scale uranium bioremediation. Presented at the 2011 Fall Meeting, AGU, San Francisco, Calif., 5-9 Dec. Abstract H21A-1063.

Yabusaki, S., Long, P., Fang, Y., Lipton, M., Banfield, J., Hettich, R., VerBerkmoes, N., Kerkhof, L., Lovley, D., Chandler, D., Peacock, A., 2008. A path forward for biogeochemical reactive transport modeling of in situ uranium bioremediation. Computational Methods in Water Resources XVII International Conference, San Francisco, California, July 6-10, 2008.

Yabusaki, S.B., Fang, Y., Davis, J.A., Steefel, C.I., Long, P.E., 2009. Reactive Transport Modeling of In Situ Uranium Biostimulation Experiments at the Rifle IFRC. Migration ’09: 12th International Conference on the Chemistry and Migration Behaviour of Actinides and Fission Products in the Geosphere, Kennewick, Washington, USA Abstract No: C-4, 46.

ZACHARA, J., DAVIS, J.A., LONG, P.E., WILLIAMS, K.H., FRESHLEY, M., MCKINLEY, J.P., 2011. PERSISTENCE OF URANIUM GROUNDWATER PLUMES: CONTRASTING MECHANISMS AT TWO CONTAMINATED DOE SITES. Geological Society of America Abstracts with Programs 43, 230.

Zhao, J., Scheibe, T.D., Fang, Y., Lovley, D.R., Mahadevan, R., 2010. Systematic Investigation of Critical Parameters Involved in a Geobacter-mediated Bioremediation Model by Global Sensitivity Analysis. American Society for Microbiology, 110th Annual Meeting San Diego, CA May 23-27, 2010 Q-2334/747, 172.

References Cited

Handley KM, Williams KH, Miller CS, VerBerkmoes NC, Chourey K, Thomas BC, Sharon I, Wrighton KW, Hettich R, Long P, Banfield JF (in prep.) High augmentation of a subsurface carbon and energy pool establishes heterotroph-autotroph coupling interfaced via the TCA cycle.

Miller CS, Baker B, Thomas B, Singer SW, Banfield J (2011) *Genome biol*, http://genomebiology.com/2011/12/5/R44.

Miller CS, Handley KM, Wrighton KC, Thomas BC, Banfield JF (in prep.) Deep sequencing of full-length rRNA genes reveals dynamic population responses in rare members of a subsurface microbial community.

Wilkins MJ, Nicora CD, Wrighton KC, Williams KH, CS Miller, KM Handley, Giloteaux L, Montgomery A, Lovley DR, Banfield JF, Long PE, Lipton MS (in prep.) Proteomics inferred temporal shifts in metabolism and physiology of a *Geobacter* population during subsurface biostimulation.

Wrighton KC, Thomas BC, Sharon I, Miller CS, Castelle C, VerBerkmoes NC, Wilkins MJ, Handley KM, Hettich RL, M Lipton MS, Williams KH, Long PE, and Banfield JF (in prep.) Proteogenomics reveals that fermentation is obligate for many "Candidate Division" Bacteria.

Yelton AP, Wrighton KC, Handley KM, Luef B, Butler RG, Banfield JF (in prep.) Isolation and genome sequencing of a novel vanadium-reducing *Simplicispira* sp. from a vanadium and uranium-contaminated aquifer.

References (From Davis section on abiotic U reduction)

Amirbahman, A., D. B. Kent, G. P. Curtis, and J. A. Davis (2006), Kinetics of sorption and abiotic oxidation of arsenic(III) by aquifer materials, *Geochimica et Cosmochimica Acta*, *70*(Journal Article), 533-547.

Bank, T. L., R. K. Kukkadapu, A. S. Madden, M. A. Ginder-Vogel, M. E. Baldwin, and P. M. Jardine (2008), Effects of gamma-sterilization on the physico-chemical properties of natural sediments, *Chemical Geology*, *251*(1-4), 1-7.

Behrends, T., and P. Van Cappellen (2005), Competition between enzymatic and abiotic reduction of uranium(VI) under iron reducing conditions, *Chemical Geology*, *220*(3-4), 315-327.

Boland, D. D., R. N. Collins, T. E. Payne, and T. D. Waite (2011), Effect of Amorphous Fe(III) Oxide Transformation on the Fe(II)-Mediated Reduction of U(VI), *Environ. Sci. Technol.*, *45*(4), 1327-1333.
Boyanov, M. I., E. J. O'Loughlin, E. E. Roden, J. B. Fein, and K. M. Kemner (2007), Adsorption of Fe(II) and U(VI) to carboxyl-functionalized microspheres: the influence of speciation on uranyl reduction by titration and XAFS, *Geochimica et Cosmochimica Acta*, *71*, 1898-1912.

Bopp, C.J., Lundstrom, C.C., Johnson, T.M., Sanford, R.A., Long, P.E. and K.H. Williams. (2010) Uranium $^{238}U/^{235}U$ Isotope ratios as indicators of reduction: Results from an in situ biostimulation experiment at Rifle Colorado, U.S.A. Environ. Sci. Technol. 44, 5927–5933.

Brennecka, G.A., Wasylenki, L.E., Bargar, J.R., Weyer, S. and A.D. Anbar. (2010) Uranium isotope fractionation during adsorption to Mn-oxyhydroxides. Environ. Sci. Technol. 45, 1370–1375.

Chakraborty, S., F. Favre, D. Banerjee, A. C. Scheinost, M. Mullet, J.-J. Ehrhardt, J. Brendle, L. c. Vidal, and L. Charlet (2010), U(VI) Sorption and Reduction by Fe(II) Sorbed on Montmorillonite, *Environmental Science & Technology*, *44*(10), 3779-3785.

Chiu, V. Q., and J. G. Hering (2000), Arsenic adsorption and oxidation at manganite surfaces. 1. Method for simultaneous determination of adsorbed and dissolved arsenic species, *Environmental Science & Technology*, *34*(10), 2029-2034.
Coston, J. A., C. C. Fuller, and J. A. Davis (1995), Pb2+ and Zn2+ adsorption by a natural aluminum- and iron-bearing surface coating on an aquifer sand, *Geochimica et Cosmochimica Acta*, *59*(17), 3535-3547.
Dixit, S., and J. G. Hering (2006), Sorption of Fe(II) and As(III) on goethite in single- and dual-sorbate systems, *Chemical Geology*, *228*(1-3), 6-15.

Du, X., B. Boonchayaanant, W.-M. Wu, S. Fendorf, J. Bargar, and C. S. Criddle (2011), Reduction of Uranium(VI) by Soluble Iron(II) Conforms with Thermodynamic Predictions, *Environmental Science & Technology*, null-null.

Fendorf, S. E., and R. J. Zasoski (1992), Chromium(III) oxidation by delta-MnO2. 1. Characterization, *Environmental Science & Technology*, *26*(Journal Article), 79-85.

Fox, P. M., J. A. Davis, and G. W. Luther III (2009), The kinetics of iodide oxidation by the manganese oxide mineral birnessite, *Geochim. Cosmochim. Acta*, *73*, 2850-2861.

Fox, P. M., D. B. Kent, and J. A. Davis (2010), Redox Transformations and Transport of Cesium and Iodine (−1, 0, +5) in Oxidizing and Reducing Zones of a Sand and Gravel Aquifer, *Environmental Science & Technology*, *44*(6), 1940-1946.

Gehin, A., J. M. Greneche, C. Tournassat, J. Brendle, D. G. Rancourt, and L. Charlet (2007), Reversible surface-sorption-induced electron-transfer oxidation of Fe(II) at reactive sites on a synthetic clay mineral, *Geochimica et Cosmochimica Acta*, *71*(Journal Article), 863-876.

Gorski, C. A., and M. M. Scherer (2009), Influence of magnetite stoichiometry on Fe^{II} uptake and nitrobenzene reduction, *Environ. Sci. Technol.*, *43*, 3675-3680.

Handler, R. M., B. L. Beard, C. M. Johnson, and M. M. Scherer (2009), Atom exchange between aqueous Fe(II) and goethite: An Fe isotope tracer study, *Environ. Sci. Technol.*, *2009*(43), 1102-1107.

Hansel, C. M., S. G. Benner, and S. Fendorf (2005), Competing Fe(II)-induced mineralization pathways of ferrihydrite, *Environ. Sci. Technol.*, *39*(18), 7147-7153.

Hyun, S. P., P. M. Fox, J. A. Davis, K. M. Campbell, K. F. Hayes, and P. E. Long (2009), Surface complexation modeling of U(VI) adsorption by aquifer sediments from a former mill tailings site at Rifle, Colorado, *Environ. Sci. Technol.*, *43*(24), 9368-9373.

Ilton, E. S., S. M. Heald, S. C. Smith, D. Elbert, and C. Liu (2006), Reduction of Uranyl in the Interlayer Region of Low Iron Micas under Anoxic and Aerobic Conditions, *Environmental Science & Technology*, *40*(16), 5003-5009.

Ilton, E. S., J.-F. o. Boily, E. C. Buck, F. N. Skomurski, K. M. Rosso, C. L. Cahill, J. R. Bargar, and A. R. Felmy (2009), Influence of Dynamical Conditions on the Reduction of UVI at the Magnetite−Solution Interface, *Environmental Science & Technology*, *44*(1), 170-176.

Jeon, B.-H., B. A. Dempsey, W. D. Burgos, and R. A. Royer (2001), Reactions of ferrous iron with hematite, *Colloids and Surfaces A: Physicochemical and Engineering Aspects*, *191*(1-2), 41-55.
Jeon, B.-H., B. A. Dempsey, W. D. Burgos, M. O. Barnett, and E. E. Roden (2005), Chemical reduction of U(VI) by Fe(II) at the solid-water interface using natural and synthetic Fe(III) oxides, *Environmental Science & Technology*, *39*(Journal Article), 5642-5649.
Jones, A. M., R. N. Collins, J. Rose, and T. D. Waite (2009), The effect of silica and natural organic matter on the Fe(II)-catalysed transformation and reactivity of Fe(III) minerals, *Geochim. Cosmochim. Acta*, *73*, 4409-4422.

Komlos, J., A. Peacock, R. K. Kukkadapu, and P. R. Jaffé (2008), Long-term dynamics of uranium reduction/reoxidation under low sulfate conditions, *Geochimica et Cosmochimica Acta*, *72*(15), 3603-3615.

Larese-Casanova, P., and M. M. Scherer (2006), Fe(II) Sorption on Hematite: New Insights Based on Spectroscopic Measurements, *Environmental Science & Technology*, *41*(2), 471-477.

Laubach et al. (2010) Field-scale determination of uranium isotope fractionation induced by U(VI) adsorption and desorption: The Super 8 experiment at DOE's Rifle, Colorado site. GSA Abstracts with Programs 42, 231.

Liger, E., L. Charlet, and P. Van Cappellen (1999), Surface catalysis of uranium(VI) reduction by iron(II), *Geochimica et Cosmochimica Acta*, *63*(19/20), 2939-2955.

O'Loughlin, E. J., S. D. Kelly, R. Cook, E., R. Csencsits, and K. M. Kemner (2003), Reduction of uranium(VI) by mixed Iron(II)/Iron(III) hydroxide (green rust): Formation of UO_2 nanoparticles, *Environ. Sci. Technol.*, *37*(4), 721-727.

Pedersen, H. D., D. Postma, R. Jakobsen, and O. Larsen (2005), Fast transformation of iron oxyhydroxides by the catalytic action of aqueous Fe(II), *Geochim. Cosmochim. Acta*, *69*(16), 3967-3977.
Postma, D. (1985), Concentration of Mn and separation from Fe in sediments--I. Kinetics and stoichiometry of the reaction between birnessite and dissolved Fe(II) at 10°C, *Geochimica et Cosmochimica Acta*, *49*(4), 1023-1033.

Scott, M. J., and J. J. Morgan (1995), Reactions at oxide surfaces. 1. Oxidation of As(III) by synthetic birnessite, *Environmental Science & Technology*, *29*(8), 1898-1905.

Stewart, B. D., P. S. Nico, and S. Fendorf (2009), Stability of uranium incorporated into Fe (hydr)oxides under fluctuating redox conditions, *Environ. Sci. Technol.*, *43*(13), 4922-4927.

Stookey, L. L. (1970), Ferrozine: A new spectrophotometric reagant for iron, *Anal. Chem.*, *42*(7), 779-781.

Taggart, J. E. (2002), Analytical methods for chemical analysis of geologic and other materials, *Open-File Report Rep. 02-223*, U. S. Geological Survey.

Williams, A. G. B., and M. M. Scherer (2004), Spectroscopic evidence for Fe(II)-Fe(III) electron transfer at the iron oxide-water interface, *Environmental Science & Technology*, *38*(Journal Article), 4782-4790.

Yee, N., S. Shaw, L. G. Benning, and T. H. Nguyen (2006), The rate of ferrihydrite transformation to goethite via the Fe(II) pathway, *American Mineralogist*, *91*, 92-96.

Zhang, S., D. B. Kent, D. C. Elbert, Z. Shi, J. A. Davis, and D. R. Veblen (2011), Mineralogy, morphology, and textural relationships in coatings on quartz grains in sediments in a quartz-sand aquifer, *Journal of Contaminant Hydrology*, *124*(1-4), 57-67.

Steering Group for the Workshop on Size Limits of Very Small Microorganisms, National Research Council (1999). Size Limits of Very Small Microorganisms: *Proceedings of a Workshop. National Academies Press:* Washington, D.C., http://www7.nationalacademies.org/ssb/nanomenu.html).